Histamine H-receptor agonists and antagonists

ter Laak, A.M.

1995

document version
Publisher's PDF, also known as Version of record

Histamine H_1-receptor Agonists and Antagonists

Molecular Modeling and Drug Design

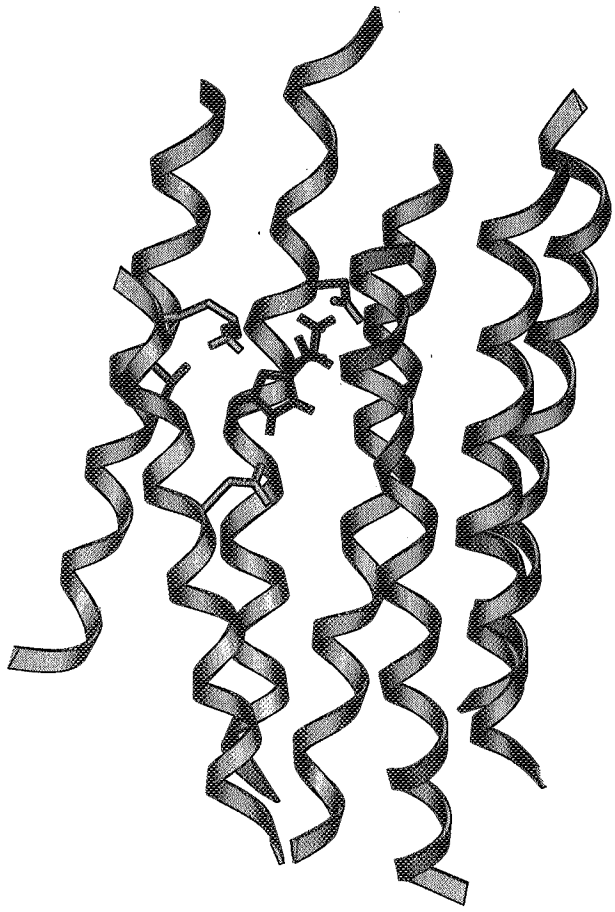

Ton ter Laak

Histamine H_1-receptor Agonists and Antagonists

Molecular Modeling and Drug Design

VRIJE UNIVERSITEIT

Histamine H1-receptor Agonists and Antagonists
Molecular Modeling and Drug Design

ACADEMISCH PROEFSCHRIFT

ter verkrijging van de graad van doctor aan
de Vrije Universiteit te Amsterdam,
op gezag van de rector magnificus
prof.dr E. Boeker,
in het openbaar te verdedigen
ten overstaan van de promotiecommissie
van de faculteit der scheikunde
op maandag 16 oktober 1995 te 13.45 uur
in het hoofdgebouw van de universiteit,
De Boelelaan 1105

door

Antonius Marinus ter Laak

geboren te Delft

Promotor	prof.dr H. Timmerman
Copromotor	dr G.M. Donné-Op den Kelder
Referent	prof.dr H. Wikström

The investigations described in this thesis were supported by a grant of the Netherlands Technology Foundation (STW/NWO) and performed at the Department of Pharmacochemistry, Vrije Universiteit, Amsterdam, The Netherlands. Part of the thesis work (Chapter 4) was performed at the Institut de Chimie Thérapeutique, École de Pharmacie, BEP, Lausanne, Switzerland. Part of the studies presented in Chapter 5 were performed at the Department of Pharmaceutical Chemistry, Faculty of Pharmacy, Utrecht University, Utrecht, The Netherlands.

Cover design: SETOR V.4.13.4, University of British Colombia (1995).

CONTENTS

CHAPTER 1

INTRODUCTION

Introduction

At the beginning of this century, not long after the first synthesis of 2-(imidazol-4-yl)ethylamine (Windaus and Vogt, 1907), this compound (histamine) was found to be vasoactive and a potent stimulator of smooth muscle contraction (Dale and Laidlow, 1910-1911). From then on, it became apparent that histamine has many more pharmacological actions and is released upon injurious stimulation of many human and animal tissues. Therefore, in early years, histamine was particularly seen as an important mediator in certain pathological conditions (i.e., injuries, allergic reactions).

Bovet and Staub (1937) were the first investigators to synthesize (weak) competitive inhibitors of the histamine response (i.e. piperoxan and thymoxyethyldiethylamine). The discovery of the first relatively potent H_1-antagonist with two aromatic rings (antergan, Halpern et al., 1942) was the initiation of an enormous step forward in the field of histamine research: within ten years, chemists around the world synthesized more than 5000 antihistaminic compounds (Bovet, 1959). Today many of these early compounds, which are now known as 'classical' histamine H_1-antagonists, are still used as therapeutic drugs (i.e., diphenhydramine, promethazine, chlorphenyramine, mepyramine and tripelenamine) in allergy and occasionally sleep disturbances.

Histamine receptor subtypes

It was recognized by Ash and Schild (1966) that some pharmacological actions of histamine (stimulation of gastric acid secretion and uterus contraction) were not antagonized by drugs such as diphenhydramine and mepyramine and that in various organs there were differences in the structure-activity relationships of histamine agonists. These findings led the authors to suggest the existence of a second subtype of histamine receptor. Soon thereafter, the histamine H_2-receptor was defined by Black et al. (1972), who synthesized and reported the first potent histamine antagonist of gastric acid secretion (the H_2-antagonist burimamide).

About ten years later, a third histamine receptor (H_3) was discovered by the group of

Schwartz (Arrang et al., 1983). This histamine H_3-receptor, located on nerve endings in the central nervous system (CNS) and characterized as a histamine autoreceptor, appears to play a regulatory role in neurotransmission both in central and peripheral neuronal systems. Since the discovery of, respectively, the H_2- and H_3-receptor, many selective and potent ligands have been synthesized for these receptors and tested for potential use as pharmacological tools and/or as drugs. These histamine H_2- and H_3-ligands are, in general, structurally quite different from those binding at H_1-receptors (for detailed reviews: Casy et al., 1978; Cooper et al., 1990; Leurs et al., 1995).

Therapeutic use of histamine H_1-antagonists

'Antihistamines' or 'antihistaminics' are still commonly used terms for antagonists of the histamine H_1-receptor, since they were the first histamine antagonists discovered. It was shown by Riley and West in 1953 that substantial amounts of histamine are stored in, and can be released by mast cells, present in various body tissues. Exposure to antigen, which binds and activates IgE-type antibodies on mast cells, may cause a massive release of histamine by these cells (i.e., in the lungs, skin or eyes). Histamine release may then be involved in various effects of an allergic reaction, i.e. bronchoconstriction, vasodilation, progress of the allergic reaction (increased vasopermeability, stimulation of prostaglandin production) and even, in case of high systemic histamine concentrations, anaphylactic shock.

Since the unwanted pharmacological action of histamine is often associated with degranulation of mast cells, the therapeutic use of antihistamines is, in theory, indicated for pathological conditions which display type I hypersensitivity reactions (urticaria, allergic rhinitis, conjunctivitis, hay fever, asthma and anaphylactic shock).

Indeed, upon their introduction in the 1940s, inhaled or parental antihistamines appeared to offer protection against certain allergic reactions, i.e. against bronchoconstriction caused by inhaled allergen or exercise challenge. Histamine H_1-antagonists appeared, however, relatively ineffective upon oral administration, especially in the treatment of asthma (Rafferty and Holgate, 1988). In contrast to what was expected, the success of antihistamines as anti-allergic drugs with a broad application was not established.

Two reasons can be given for the relatively poor success of classical antihistamines: firstly, many allergic mediators other than histamine, i.e. eicasonoids (prostaglandins, thromboxanes, leukotrienes) and platelet activating factor (PAF), play a role in allergic reactions and may in some cases surpass the role of histamine. Secondly, classical antihistamines are known for displaying CNS and other side effects (sedation, dizziness, sleepiness, dry mouth, accomodation and gastrointestinal problems). These side effects, especially sedation, do not

allow the use of substantial high dosages needed for the treatment of asthma and have always been a serious drawback for the therapeutic use of classical histamine H_1-antagonists. As a consequence, the clinical use of classical compounds is limited to conditions such as urticaria, allergic rhinitis and conjunctivitis.

In the 1980s, new antihistamines such as astemizole and terfenadine, which lack sedative side effects were introduced (Nicholson, 1982). Since then, more 'non-sedating' antihistamines have become available (i.e. loratadine, temelastine, epinastine, acrivastine, mequitazine and cetirizine). Many studies have indicated that the lack of central effects of most of these non-sedating antihistamines can be attributed to their low ability to reach the brain (Laduron et al., 1982; Barnett et al., 1984; Sorkin and Heel, 1985; Calcutt et al., 1987; Fügner et al., 1988). However, it has also been reported that H_1-receptor subtypes may exist, and that some antihistamines are probably 'non-sedating' because they have higher affinity for peripheral (versus central) H_1-receptors (Uzan, 1979; Ahn and Barnett, 1986).

Scope of this thesis

In summary, the mechanisms responsible for the non-sedating profile of the modern antihistamines were unclear in the early ninetees and are subject of study in this thesis. The investigations described in this thesis aim at developing possibilities for the rational design and development of new H_1-antagonists devoid of sedative effects.

Originally our studies aimed at exploring presumed differences between central and peripheral subtypes of the histamine H_1-receptor (Barbe, 1983; Ahn and Barnett, 1986). However, in Chapter 3 we reach the conclusion that 'non-sedating' antihistamines probably lack central side effects because they are unable to penetrate the blood brain barrier. Consequently, the course of the investigations changed and diverged into two directions.

The first section of this thesis describes studies performed to identify factors playing a role in the incidence of central side effects of H_1-antagonists (SECTION I).

The second section focuses on the 3-dimensional structural requirements for potent histamine H_1-antagonists using different molecular modeling techniques (pharmacophore building, H_1-receptor homology building and receptor ligand docking) (SECTION II). An important spin-off of these modeling studies - but partly beside the scope of this thesis - is also included in Section II and involves an extensive modeling study on the histamine H_1-agonist binding site (Chapter 9).

Section I

The research described in section I of this thesis aims at a better understanding of the factors which determine the incidence of side effects evoked by antihistamines. Receptor heterogeneity between peripheral and central H_1-receptors, as suggested in literature, is investigated and described in Chapter 3.

Further investigations are focused on molecular properties of antihistaminic drugs which can be expected to influence passage across the blood-brain barrier (BBB). In Chapter 4, lipophilicity parameters (such as log P_{oct}, log $D_{oct,7.4}$, Δlog P and Λ_{alkane}) are determined for a series of structurally different sedating and non-sedating H_1-antagonists. A tentative qualititative model for the design of non-sedating H_1-antagonists is presented. In Chapter 5, the H_1-antagonist binding to human serum albumin (HSA) and total serum protein of a small series of antihistamines is presented, and the relation between serum protein binding and physicochemical parameters (and/or CNS properties) is discussed. For a more detailed introduction to Section I, the reader is referred to Chapter 2 which gives an overview of strategies aiming at the rational design of non-sedating H_1-antagonists.

Section II

For the rational design of new non-sedating H_1-antagonists, not only knowledge of the optimal physicochemical properties is required (Section I), but it is also useful to establish the structural and conformational requirements for potent and selective histamine H_1-antagonists. In recent years, more and more H_1-antagonists, which only partly resemble the molecular structure of typical classical antihistamines, have been reported (i.e., loratadine, epinastine, cetirizine, terfenadine); some are structurally quite different from classsical H_1-antagonists (i.e. temelastine, levocabastine, cicletanide, astemizole). A review of the quantitative structure-activity relationships (QSAR) and molecular modeling studies performed by the early ninetees on - mostly classical - histamine H_1-antagonists is given in Chapter 6.

Many of the published modeling studies on histamine H_1-antagonists use the relatively rigid and potent H_1-antagonist cyproheptadine as template molecule (Chapter 6). However, the major drawback of these studies is that only a limited number of generally flexible H_1-antagonists is considered in these models and that the direction of the acidic proton with respect to the basic nitrogen present in all classical H_1-antagonists, is not taken into account. In Chapter 7, a new modeling approach is presented, also using cyproheptadine as template molecule, but now with an aspartate residue from the H_1-receptor protein included in the model. This strategy yields a pharmacophore which accomodates all known (semi-)rigid H_1-antagonists and contains stereoselectivity properties.

3-Dimensional properties important for optimal drug-receptor interactions are further investiged by docking H_1-antagonists into a 3-dimensional model of the histamine H_1-receptor. Chapter 8 describes homology building of the histamine H_1-receptor, a G-protein coupled receptor (GPCR), using bacteriorhodopsin (not a GPCR) as a template. Although such an approach is useful to discover possibly important interaction sites within the receptor, GPCR models based on bacteriorhodopsin are relatively crude and, as discussed in Chapter 8, should be interpreted with care.

In the case of histamine *H_1-antagonists* which, beside a common basic nitrogen atom and at least one aromatic ring, have no clearly defined interaction sites, identification of complementary amino acid residues in the H_1-receptor is complicated. This appeared to be more successful for histamine *H_1-agonists*, which are known to interact with the receptor via well-defined hydrogen bonds. Modeling studies in combination with results from site-directed mutagenesis strongly suggest the existence of different binding sites for subclasses of histamine H_1-agonists and reveal the amino acid residues essential for the binding of (and receptor stimulation by) the endogenous H_1-agonist histamine (Lys^{200}, Asn^{207}, Asp^{116}) (Chapter 9). The modeling studies in which H_1-agonists and H_1-antagonists are docked into H_1-receptor protein models suggest the aspartate residue in transmembrane domain III (Asp^{116}) to be involved in receptor stimulation by aminergic agonists.

SECTION I

STUDIES TOWARDS THE RATIONAL DESIGN OF NON-SEDATING HISTAMINE H_1-ANTAGONISTS

CHAPTER 2

RATIONAL DESIGN OF NON-SEDATING HISTAMINE H1-ANTAGONISTS

A SHORT INTRODUCTION TO SECTION I

Non-sedating histamine H1-antagonists

During the 1980s, the therapeutic potential for antihistaminic drugs has increased due to the discovery of several new antihistaminic compounds which are non-sedating. Some of these new compounds (terfenadine, astemizole, loratadine) are already widely and successfully used against histamine-mediated allergic responses (rhinitis, urticaria), while more novel non-sedating antihistamines are under investigation or in development (acrivastine, mequitazine, epinastine). These 'modern' antihistamines have a degree of efficacy similar to that of most 'classical' H1-antagonists. In addition, they have advantageous features which prevent them from inducing sedative side effects. The mechanisms behind the low incidence of central side effects of these drugs are, however, not entirely clear.

It has been demonstrated that some modern H1-antagonists, i.e. astemizole and terfenadine, have a remarkable specificity for H1-receptors, whereas most classical H1-antagonists are rather aspecific and interact with many other receptors (i.e. adrenergic, serotonergic and cholinergic receptors) (Kaliner *et al.*, 1988). However, this cannot explain the lack of sedation observed with terfenadine and astemizole, since the sedative properties of many other antihistaminic and/or tricyclic psychotropic drugs appear to be associated with blockade of histamine H1-receptors in the brain (Quach *et al.*, 1979; Nicholson *et al.*, 1991).

A more acceptable explanation - and this was claimed for the majority of non-sedating histamine H1-antagonists - is that the lack of central properties can be attributed to a poor penetration into the CNS (i.e., for astemizole (Laduron et al., 1982), loratadine (Barnett et al., 1984), terfenadine (Sorkin and Heel, 1985) and temelastine (Calcutt et al., 1987)). Another - additional - explanation has been given for the non-sedative behaviour of loratadine and mequitazine; for these drugs it has been claimed that they have higher affinity for peripheral versus central histamine H1-receptors (Ahn and Barnett, 1986; Uzan et al., 1979; Barbe et al., 1983). The reason(s) for the differences in receptor affinity between lung and CNS has (have)

not been elucidated (Ahn and Barnett, 1986), but these findings may indicate that subtypes of the histamine H_1-receptor exist.

With the above considerations in mind, it appears that different approaches can be used for the development of new non-sedating histamine H_1-antagonists. The first approach involves the development of drugs which pass the blood brain barrier (BBB) less easy than the classical histamine H_1-antagonists. This is the more common approach since it has been used to develop most of the before-mentioned non-sedating H_1-antagonists.

A second approach is directed towards the development of new classes of non-sedating compounds with additional beneficial properties. Examples resulting from this approach are a new class of histamine H_1-antagonists with H_2-agonistic activity, therewith inhibiting mast cell mediator release (Sterk et al., 1987; Buschauer, 1987), or, currently under investigation, histamine H1-antagonists which contain additional leukotriene LTD_4-antagonistic properties (Zhang et al., 1995).

A third approach - not yet applied - concerns the development of tissue-selective antihistaminic agents based on H_1-receptor heterogeneity. This approach is only meaningful if indeed substantial differences between the antagonistic binding sites of H_1-receptors in the CNS and the periphery exist. Therefore, the feasibility of this approach is investigated in this thesis by screening the affinities of an extensive series of structurally different histamine H_1-antagonists on guinea pig brain and lung receptors (Chapter 3).

Until now, the most effective way to obtain non-sedating H_1-antagonists, has been the first approach, decreasing the CNS penetration potential of antihistamines. Fortunately, the blood brain barrier (BBB) which separates the CNS from the circulating system (blood) is a real barrier for many compounds. It is formed by the special capillaries of the brain, where the endothelial cells have particularly closed tight junctions. In order to cross the BBB, a solute either needs a specific transport mechanism present in the endothelial cells, or it has to diffuse into and across the lipid membranes of the BBB. For most endogenous compounds, passive diffusion over the membranes of the BBB is the only way to reach the CNS. Various factors influence the diffusion rate by which this passive transport into the CNS takes place, for example, pH partitioning (pK_a), oil:water partitioning (log P) and binding to other compartments (i.e., serum protein binding). Chapter 4 of this thesis gives a short overview of some physicochemical parameters which are thought to affect the CNS penetration potential (MW, log P_{oct}, Δlog $P_{oct\text{-}alk}$, Λ_{alkane}, log $D_{oct,pH7.4}$). For an extended series of sedating as well as non-sedating histamine H_1-antagonists, lipophilicity parameters have been measured and discussed in view of existing brain penetration models. Finally, a new qualitative model for the brain penetration of H_1-antagonists is proposed with log $D_{oct,pH7.4}$ and Δlog $P_{oct\text{-}alk}$ as the main factors determining BBB passage (Chapter 4).

Although log $D_{oct,pH7.4}$ and $\Delta log\ P_{oct-alk}$ might be involved in determining the diffusion rate across the BBB directly, these parameters can also be important for binding of a compound to serum proteins. Under certain circumstances, i.e. low diffusion rates across the BBB, serum protein binding may indirectly influence the amount of drug that reaches the brain. Since the degree of serum protein binding presumably plays a role in the incidence of CNS effects, our studies also focused upon serum protein binding of histamine H_1-antagonists. In Chapter 5, the binding of a sedating (mepyramine) and a non-sedating H_1-antagonist (loratadine) to human serum albumin and total serum proteins is compared. In addition, the binding of six non-radiolabeled classical H_1-antagonists to human serum albumin was measured. On the basis of these binding data, the effect of serum protein binding on the brain penetration of histamine H_1-antagonists is discussed.

CHAPTER 3

IS THERE A DIFFERENCE IN THE AFFINITY OF HISTAMINE H_1-RECEPTOR ANTAGONISTS FOR CNS AND PERIPHERAL RECEPTORS ?

AN IN VITRO STUDY

A.M. ter Laak, G.M. Donné-Op den Kelder, A. Bast, H. Timmerman (Eur. J. Pharmacol. 232, 199-205)

Summary

An extended series of structurally different histamine H_1-receptor antagonists is investigated for binding at central and peripheral histamine H_1-receptors in vitro. Antagonist affinities were measured by displacement of [^{3}H]mepyramine from both guinea pig cerebellum and lung membrane suspensions. Single [^{3}H]mepyramine binding sites with identical affinities for [^{3}H]mepyramine were found in both tissues, however the H_1-receptor density was 6-fold lower in lungs than in cerebellum. None of the antagonists tested showed substantial preference for either of the receptors. It is concluded from the displacement data that there is no difference between the antagonist binding sites of cerebellum and lung H_1-receptors.

Introduction

It has been suggested that the sedation produced by classical histamine H_1-receptor antagonists and by some sedative tricyclic psychotropic drugs is associated with blockade of H_1-receptors in the brain. The extent to which these drugs occupy brain H_1-receptors after oral administration in mice is significantly correlated with the sedative properties observed in mice (Hall and Ögren, 1983) and with the sedative properties observed in humans (Quach et al., 1979). The observation that after administration of both enantiomers of chlorpheniramine and of dimethindene sedation in humans is limited to the enantiomer with higher H_1-affinity also strongly suggests that sedation can arise from H_1-antagonism alone (Nicholson et al., 1991). In order to abolish the undesired sedative effect, there are essentially two ways of increasing the selectivity of antihistamines for peripheral H_1-receptors.

First, selectivity for peripheral H_1-receptors can be attained by changing the physicochemical properties of the drugs in order to diminish penetration into the brain, e.g. by altering the log P. A second way to decrease sedative characteristics is to design compounds

that have higher affinity for peripheral H_1-receptors than for central H_1-receptors. Of course, this can only be done if peripheral and central H_1-receptors are different. A somewhat lower affinity for central versus peripheral H_1-receptors has indeed been claimed for mequitazine (Uzan et al., 1979; Barbe et al., 1983) and loratadine (Ahn and Barnett, 1986).

The purpose of the present study was to discover whether peripheral and central histamine H_1-receptors are different. To this end an extended series of existing H_1-receptor antagonists was studied (Fig. 1). Differences in affinity for cerebellum and lung H_1-receptors, as assessed in comparable binding assays, is expected to provide information that is relevant to the design of receptor-selective non-sedating antihistamines.

Materials and Methods

Materials

[^{3}H]mepyramine ([pyridinyl-5-^{3}H]pyrilamine, specific activity 27 Ci/mmol) was obtained from the Radiochemical Centre (Amersham, U.K.). Pyrilamine maleate (mepyramine) and triprolidine HCl were obtained from Sigma Chemical Company (St. Louis, USA. The following drugs were kindly donated by the indicated persons and institutions (unspecified compounds were tested as a free base): chlorpheniramine maleate (R and S) from A. Beld (University of Nijmegen, the Netherlands), cicletanide (+ and -) from the Inst. Henry Beaufour (Le Plessis Robinson, France), dimethindene (R and S) from U. Borchard (University of Düsseldorf, Germany), terfenadine (R and S), promethazine HCl and neobenodine from our own laboratory stock (Zhang et al., 1991), astemizole and levocabastine HCl from Janssen Pharmaceutica NV (Beerse, Belgium), epinastine HCl (WAL801 CL) from Boehringer-Ingelheim (Germany), mianserine HCl from Organon (Oss, the Netherlands), cyproheptadine HCl from MSD (Haarlem, the Netherlands), phenindamine tartrate from Pfizer Ltd. (Sandwich, U.K.), loratadine (SCH29851) and descarboxyethylloratadine acetate (SCH34117) from Schering Co. (Bloomfield, USA), cetirizine HCl from UCB (Braine-d'Alleud, Belgium) and temelastine (SKF93944) from SK&F (Herts, U.K.).

Preparation of membrane suspensions

Membrane suspensions were prepared at 4°C; cerebellum and lung were isolated from adult male type II guinea pigs and stored at -80°C. Thawed cerebellum was homogenised in 50 mM phosphate-buffered saline (PBS) at pH 7.4 (7.25 mM KH_2PO_4, 42.75 mM Na_2HPO_4, 0.9 % NaCl) (20 ml per cerebellum). The homogenate was centrifuged for 1 minute at 260 x *g* to remove cell nuclei and debris. The supernatant was centrifuged for 30 minutes at 20000 x *g*. The resulting pellet was resuspended, homogenised and diluted to 1 mg protein/ml (Bio-Rad

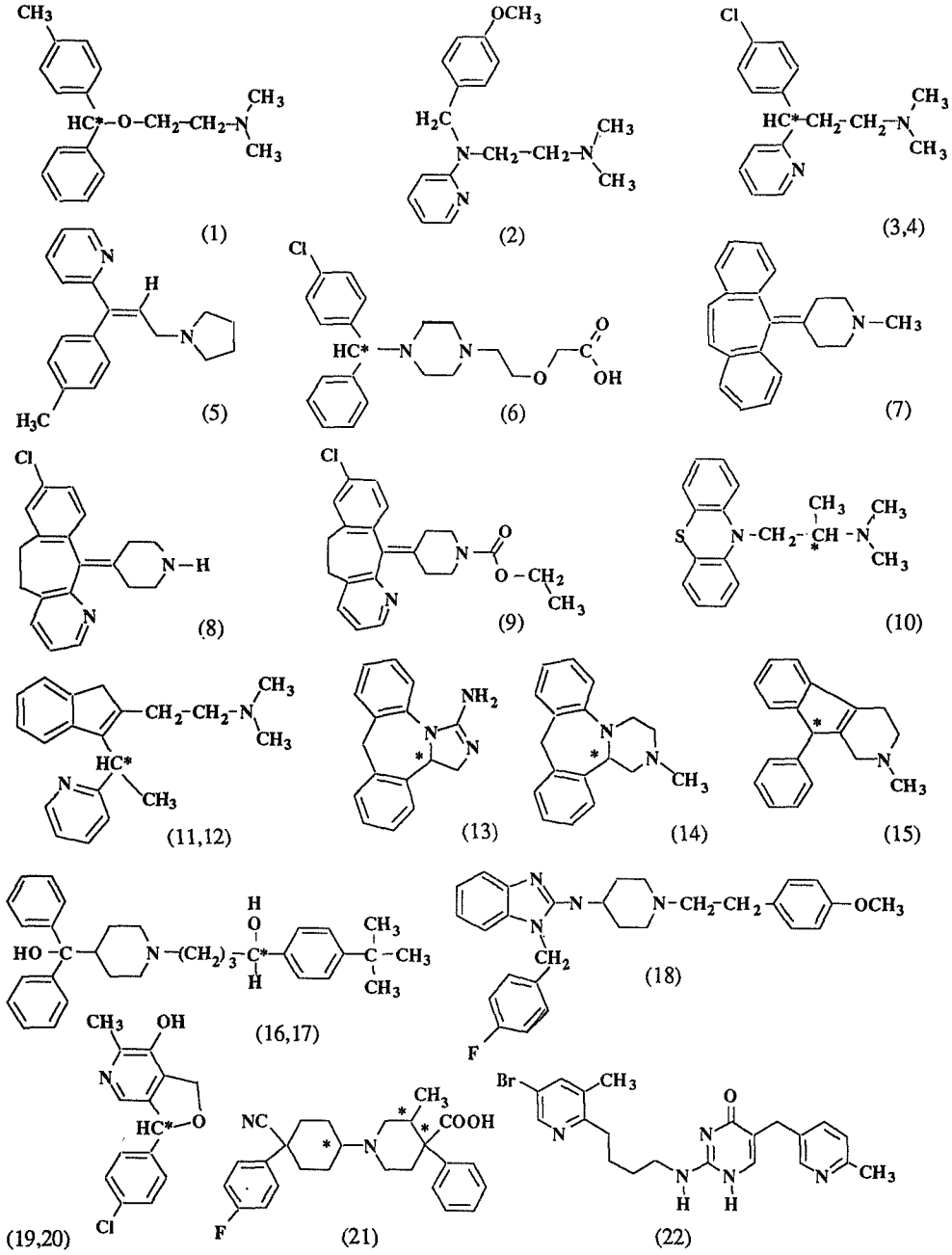

Figure 1. Structural formulas of the H_1-receptor antagonists considered (numbers refer to the pharmacological data listed in Table 1): neobenodine (1); mepyramine (2); chlorpheniramine (S, R) (3, 4); triprolidine (5); cetirizine (6); cyproheptadine (7); descarboethoxyloratadine (8); loratadine (9); promethazine (10); dimethindene (R, S) (11, 12); epinastine (13); mianserine (14); phenindamine (15); terfenadine (S, R) (16, 17); astemizole (18); cicletanide (-, +) (19, 20); levocabastine (21) and temelastine (22).

GmbH protein assay) in PBS pH 7.4 and stored at -80°C. Thawed lungs were minced and homogenised in 10 v/w (ml/g wet weight) 250 mM sucrose, 150 mM sodium perchlorate, 5 mM EDTA, 25 mM imidazole buffer pH 7.4. The homogenate was centrifuged for 10 min at 830 x *g* to precipitate debris and cell nuclei. The pellet was rehomogenised in 5 v/w sucrose buffer and centrifuged again for 10 min at 830 x *g*. The supernatants were combined and centrifuged for 20 min at 23600 x *g*. The resulting pellet was washed twice by resuspension in 50 mM Tris base / HCl pH 7.4 and centrifuged for 20 min at 23600 x *g*. The final pellet was resuspended and diluted to 1.5 mg protein/ml in PBS pH 7.4 and stored at -80°C. All experiments were performed with tissue from one large batch of frozen cerebellum and lung membrane suspension.

Binding assays

All binding experiments were performed under identical assay conditions. All antagonists were dissolved in ethanol (10^{-3} M) and further diluted in PBS pH 7.4. Antagonists were incubated with membrane suspension in 1.0 ml 50 mM phosphate buffer, 0.9% NaCl, pH 7.4 for 2 h at 25°C in Minisorb tubes. Protein concentrations in the final binding assay were different for cerebellum (0.1 mg/ml) and lungs (0.75 mg/ml) due to the lower H_1-receptor concentration in lungs (calculated receptor densities were about 0.6 pmol/mg protein for cerebellum and about 0.1 pmol/mg protein for lungs). The incubation was ended by the addition of 1 ml ice-cold PBS. Membranes were collected on Whatman GF/C filters under vacuum, using a Brandel cell harvester. GF/C filters were presoaked in 0.3% PEI to reduce aspecific binding. Packard Ultima Gold scintillation liquid (4 ml) was added to the filters in Pony vials. Radioactivity was counted in a Packard 1900CA Tricarb liquid scintillation analyser.

Analysis

The K_d of [^{3}H]mepyramine in cerebellum and lungs was determined by Scatchard plot analysis of data from saturation experiments performed in triplicate. Aspecific binding of [^{3}H]mepyramine was measured in presence of 5 mM (-)-cicletanide. Free [^{3}H]mepyramine concentrations were calculated from dpm_{total} - dpm_{bound} for construction of the Scatchard plot.

Binding constants of the H_1-receptor antagonists were measured by displacement of 1 nM [^{3}H]mepyramine. Apparent pK_i values of the antagonists were calculated from the graphically determined IC_{50} value (12 duplicate data points) using the equation: $pK_i = IC_{50} / (1 + L/K_d)$ (Cheng and Prusoff, 1973). pK_i values were measured in triplicate.

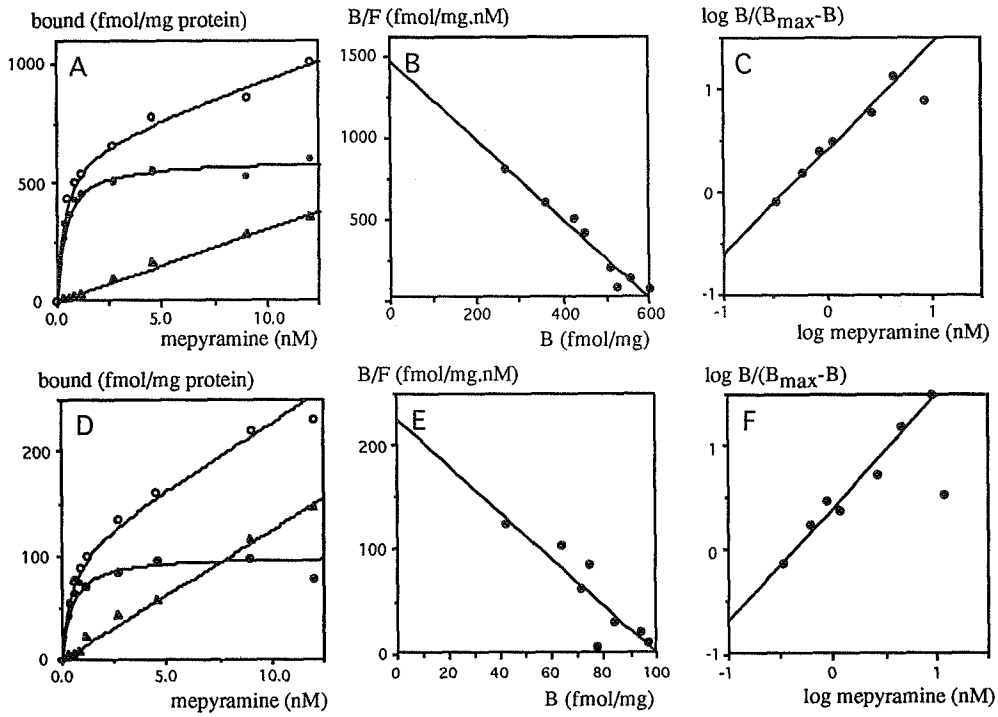

Figure 2. Plots of [^{3}H]mepyramine binding. Specific binding (●) was calculated from total binding (o) and aspecific binding (Δ) for cerebellum (A) and lungs (D). The Scatchard plots for cerebellum (B) and lungs (E) and the corresponding Hill plots (C and F) were calculated from the values of specific [^{3}H]mepyramine binding.

Results

Scatchard plot analyses revealed identical binding constants (K_d) for [^{3}H]mepyramine in cerebellum (0.41 ± 0.04 nM) and lungs (0.44 ± 0.10 nM) with B_{max} values of 597 ± 41 fmol/mg and 100 ± 17 fmol/mg, respectively (Fig. 2). The only difference between the two assays was the final protein content (0.10 mg for cerebellum and 0.75 mg for lungs). This was necessary because of the 6 times lower receptor density in lungs. Hill plot analyses indicated the presence of a single type of binding site in both cerebellum (n_H = 1.01 ± 0.06) and lungs (n_H = 1.09 ± 0.09) (Figs. 2C and 2E).

The displacement of 1 nM [^{3}H]mepyramine by various H_1-receptor antagonists (structural formulas in Fig. 1) was studied under identical assay conditions. A 2-h incubation at 25°C was chosen because of the long dissociation time of certain antagonists. Terfenadine, astemizole, loratadine and cetirizine all have a dissociation half life of more than 90 min (Leysen et al., 1991). For terfenadine, which has a relatively long $t_{1/2}$ of 220 ± 40 min, displacement experiments with cerebellum and with four different incubation times (30, 60, 120 and 240

min) have shown that the equilibrium binding constant can be determined after a 2-h incubation at 25°C (Zhang et al., 1991). However, our binding constant is given as pK_i apparent, because other compounds with an even slower receptor dissociation than terfenadine (e.g. astemizole (Leysen et al., 1991)) may not have reached true binding equilibrium after 2 h. Raising the incubation temperature from 25°C to 37°C to improve binding equilibrium gave unsatisfactory displacement curves because of tissue degradation.

Apparent pK_i values for cerebellum and lung were measured simultaneously with the same series of dilutions. Differences in binding affinity for cerebellum and lung are given as ΔpK_i apparent in Table 1. For 12 of the 22 compounds no significant difference in affinity was found; for the other compounds differences were very small. Figure 3 shows the linear correlation between affinity in the cerebellum and in the lung (slope = 1.02, r = 0.97, n = 22). No antagonist had marked selectivity for lung receptors, for example, neobenodine was only 1.5 times more potent in the lung than in the cerebellum (Table 1). In contrast, several agents appeared to have a slightly higher affinity for the cerebellum than for the lung, e.g. terfenadine, astemizole, cyproheptadine and even loratadine, for which the opposite has been claimed (Ahn and Barnett, 1986).

Discussion

H_1-receptor antagonists can be classified into two major groups, classical and non-classical H_1-receptor antagonists. Recently we reviewed the results of QSAR (quantitative structure-activity relationships) and molecular modeling studies with regard to the structural features of classical H_1-receptor antagonists (Chapter 7; Ter Laak et al., 1992). Classical H_1-receptor antagonists share a common structure consisting of two aromatic rings and a basic nitrogen atom which all contribute to binding to H_1-receptors. These antagonists have been classified into five subclasses according to the group linking the aromatic rings and the amine group. In the present pharmacological study all subclasses of classical H_1-antagonists were represented by one or more compounds (Fig. 1): *diphenhydramines* by neobenodine (p-methyldiphenhydramine) (**1**), *ethylenediamines* by mepyramine (**2**), *aminopropyl compounds* by chlorpheniramine (**3, 4**) and triprolidine (**5**), *cyclizines* by cetirizine (**6**) and *tricyclic compounds* by cyproheptadine (**7**), descarboxyethylloratadine (**8**), loratadine (**9**) and promethazine (**10**). In some of the remaining 'non-classical' H_1-receptor antagonists the presence of two aromatic rings and a basic nitrogen is less evident, e.g. in dimethindene (**11, 12**), epinastine (**13**), mianserine (**14**), phenindamine (**15**), terfenadine (**16, 17**) and astemizole (**18**). In other compounds these structural features are absent, e.g. in cicletanide (**19, 20**), levocabastine (**21**) and temelastine (**22**). The present set of 22 compounds, including four pairs of stereoisomers, is diverse and representative for most H_1-receptor antagonists.

Table 1. Affinity constants of H_1-receptor antagonists, given as apparent pK_i values, measured in triplicate with both cerebellum and lung membranes. For convenience, the differences between cerebellum and lung are shown as ΔpK_i app. (pK_i(cerebellum)-pK_i(lung)).

No.	Compound	N	pK_i app. (cerebellum)	pK_i app. (lungs)	ΔpKi-app.
(1)	neobenodine (RS)	3	7.91 ± 0.13	8.10 ± 0.13	-0.19 ± 0.02
(2)	mepyramine	3	8.94 ± 0.16	8.87 ± 0.15	+0.07 ± 0.08
(3)	chlorpheniramine (S+)	3	8.32 ± 0.07	8.46 ± 0.12	-0.14 ± 0.07
(4)	chlorpheniramine (R-)	3	6.68 ± 0.18	6.76 ± 0.09	-0.08 ± 0.10
(5)	triprolidine (cis/trans)	3	8.78 ± 0.21	8.86 ± 0.28	-0.07 ± 0.09
(6)	cetirizine (RS)	3	7.53 ± 0.10	7.51 ± 0.14	+0.02 ± 0.08
(7)	cyproheptadine	3	9.27 ± 0.31	8.93 ± 0.34	+0.35 ± 0.05
(8)	desc.-loratadine	3	8.39 ± 0.10	8.21 ± 0.09	+0.18 ± 0.16
(9)	loratadine	3	6.81 ± 0.09	6.39 ± 0.09	+0.41 ± 0.17
(10)	promethazine (RS)	3	8.74 ± 0.26	8.70 ± 0.22	+0.04 ± 0.05
(11)	dimethindene (R-)	3	9.21 ± 0.04	9.40 ± 0.11	-0.18 ± 0.13
(12)	dimethindene (S+)	3	7.10 ± 0.24	6.98 ± 0.18	+0.11 ± 0.07
(13)	epinastine (RS)	3	8.85 ± 0.04	8.79 ± 0.22	+0.06 ± 0.18
(14)	mianserine (RS)	3	9.07 ± 0.20	8.87 ± 0.09	+0.19 ± 0.24
(15)	phenindamine (RS)	3	8.20 ± 0.06	8.19 ± 0.09	+0.00 ± 0.08
(16)	terfenadine (S-)	3	6.98 ± 0.22	6.73 ± 0.03	+0.25 ± 0.21
(17)	terfenadine (R+)	3	7.13 ± 0.17	6.82 ± 0.02	+0.32 ± 0.17
(18)	astemizole	3	8.28 ± 0.03	7.81 ± 0.10	+0.46 ± 0.08
(19)	cicletanide (-)	3	7.54 ± 0.04	7.64 ± 0.17	-0.11 ± 0.20
(20)	cicletanide (+)	3	4.37 ± 0.12	4.34 ± 0.13	+0.03 ± 0.24
(21)	levocabastine	3	7.76 ± 0.08	7.67 ± 0.11	+0.09 ± 0.15
(22)	temelastine	3	8.79 ± 0.08	8.91 ± 0.10	-0.12 ± 0.16

It has been claimed that most non-classical non-sedating histamine H_1-receptor antagonists have advantageous physicochemical properties which prevent these drugs from reaching the brain and that they therefore are selective antagonists of peripheral H_1-receptors. This was reported for e.g. cetirizine (Snyder and Snowman, 1987), temelastine (Calcutt et al., 1987), epinastine (Fügner et al., 1988), loratadine (McQuade et al., 1990), terfenadine (McQuade et al., 1990; Leysen et al., 1991), noberastine, astemizole and mequitazine (Leysen et al., 1991). However, ex vivo and in vivo studies have yielded controversial results, because loratadine

and cetirizine do reach the brain according to Leysen et al. (1991), while McQuade et al. (1990) claim that astemizole, mequitazine and cetirizine also penetrate the brain in vivo.

A lower affinity for central versus peripheral histamine H_1-receptors has been claimed to contribute to the peripheral selectivity of certain H_1-receptor antagonists, e.g. mequitazine (Uzan et al., 1979) and loratadine (Ahn and Barnett, 1986). Northern blot analyses with mRNA from a recently cloned H_1-receptor from bovine adrenal medulla showed that this receptor was not present in bovine cardiac atrium and was present in much lower amounts in central cortex compared to lungs (Yamashita et al., 1991). These findings support the existence of H_1-receptor subtypes.

The present study provides data on the relative affinity of many H_1-receptor antagonists for brain and lung histamine H_1-receptors, as assayed under similar conditions.

The identical K_d values for [^{3}H]mepyramine in cerebellum (0.41 nM) and lung (0.44 nM) and the 6 times lower receptor density in lungs are in good agreement with the findings of Leysen et al. (1991). Aspecific binding was measured in the presence of 5 mM (-)-cicletanide as this H_1-receptor antagonist is structurally different from mepyramine and therefore likely to displace only the H_1-specific binding of [^{3}H]mepyramine. When aspecific binding was subtracted from total binding, the calculated Hill coefficients (Figs. 1C and 1F) indicated that a single type of binding site for [^{3}H]mepyramine was present in both cerebellum (n_H = 1.01) and lungs (n_H = 1.09).

Some authors have indicated that two populations of [^{3}H]mepyramine binding sites are present in lung tissue at 25°C (Dini et al., 1991; Carswell and Nahorski, 1982). The higher affinity of loratadine for lung H_1-receptors has also been measured in the presence of a second mepyramine binding site using 2 mM triprolidine to define aspecific binding (Ahn and Barnett, 1986). This second non-specific [^{3}H]mepyramine component in lung tissue is observed when experiments are performed in Tris-HCl buffer and can be suppressed by the presence of sodium ions in the assay buffer (Carswell and Nahorski, 1982). In contrast to Dini et al. (1991) and Ahn and Barnett (1986), we added 0.9% NaCl to our (isotonic) phosphate buffer, which apparently resulted in the observation of (only) one [^{3}H]mepyramine H_1-specific binding component in both cerebellum and lung. It is worth mentioning that the use of isotonic PBS buffer instead of hypotonic buffer may have lead to the formation of sealed and unsealed vesicles, with sealed vesicles being prevalent. We cannot rule out the possibility that a mixture of inside-out and right-side-out vesicles was formed, which would result in at least two compartments and a loss of receptor sites within the sealed inside-out vesicles. However, we found only one [^{3}H]mepyramine binding site in both the cerebellum and lung membrane preparations, with identical K_d values for [^{3}H]mepyramine and a B_{max} ratio between the two tissue preparations comparable to that measured by Leysen et al. (1991) in hypotonic phosphate buffer. These findings suggest that the possible formation of sealed vesicles presents few problems for the measurement of antagonist binding.

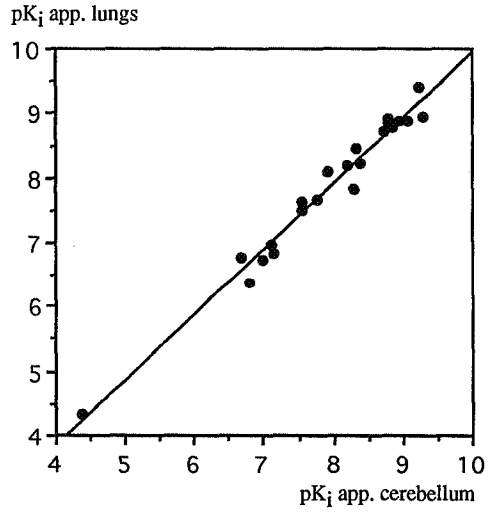

Figure 3. Linear correlation between cerebellum and lung H_1-receptor affinity for all 22 antagonists (slope = 1.02, r = 0.974).

It could be that the second mepyramine binding site reported by others, who used hypotonic buffers (Dini et al., 1991; Carswell and Nahorski, 1982), is not readily accessible within the sealed vesicles in our experiments. The appearance of the additional [^{3}H]mepyramine binding site reported by Carswell and Nahorski, when hypotonic buffer was used could then be explained by the presence of mainly unsealed membranes in their membrane suspension. The K_i values measured in isotonic buffer for non-sedating antihistamines such as terfenadine, astemizole, mequitazine and loratadine (Table 1) were 6 to 16 times higher than the K_i values obtained by Leysen et al. (1991) (2-h incubation), who used hypotonic buffer.

It was reported recently that sodium ions may reduce the affinity of certain antagonists for the H_1-receptor. Treherne et al. (1991) showed that the binding of both [^{3}H]QMDP ((+)N-methyl-4-methyldiphenhydramine, a classical quaternary H_1-receptor antagonist) and [^{3}H]mepyramine is inhibited by a range of mono and divalent cations, but that Na^+ affects the binding of the two radioligands differently. These findings illustrate that even apparently straightforward in vitro binding data depend very much on assay conditions used and that the data may sometimes be of little physiological significance. However, it also shows that it is most important that in vitro binding assays are performed under identical conditions in order to reveal possible differences between, for instance, cerebellum and lung H_1-receptors. In this respect it is worthwhile mentioning that the peripheral H_1-receptor selectivity of mequitazine was based on a comparison of in vitro binding data (cerebellum) with functional in vitro (ileum) and in vivo data (histamine induced hypotension) (Uzan et al., 1979) or on the relative potency of antagonists in different binding assays (Le Fur et al., 1981).

Existing protocols were used (Leysen et al., 1991) to prepare the cerebellum and lung membrane suspensions. Although different buffers were used during the preparation of the two tissue suspensions, the two binding assays are still comparable, because the tissue suspensions are sufficiently diluted with PBS after the last centrifugation step and in the final binding assay.

Data from our displacement studies reveal that the antagonists considered show very little or no significant preference for peripheral versus central H_1-receptors (Table 1). Based on the results obtained with the extended series of structurally diverse antagonists, we conclude that there is no difference between central and peripheral H_1-antagonist receptor binding sites. In three studies (Leysen et al., 1991; Ahn and Barnett, 1986; this study) the relative affinities of loratadine for lung versus brain receptors vary widely (3:1; 1:1; 1:3). These differences can be explained by differences in the assay conditions of the studies. Although the difference in lung and brain receptor affinity measured by Ahn and Barnett was significant in their study (n=6), we conclude from our results that the difference for loratadine, and probably also for mequitazine, is marginal.

Some antagonists showed a slightly higher affinity for cerebellum H_1-receptors than for lung H_1-receptors (e.g. terfenadine, astemizole, cyproheptadine, loratadine, Table 1). Similar small differences have been found for terfenadine and astemizole (but not for loratadine) by Leysen et al. (1991). They proposed that tissue absorption of these lipophilic drugs may diminish free cold drug concentrations and therefore decrease the apparent pK_i value. For example, when 50% cold drug is bound aspecifically to other tissue components than receptors (proteins, membrane constituents), twice as much of the drug is needed to achieve the actual free drug concentration and this results in a 'false' shift in the pK_i value of -0.30 (log 2). We do agree with Leysen et al. that a possible loss of free cold drug, which becomes more significant with higher tissue concentrations (0.75 mg protein for lung versus 0.1 mg for cerebellum) may explain the apparent lower lung H_1-affinity of some compounds.

Although we found no difference between antagonist binding sites of cerebellum and lung H_1-receptors of the guinea pig in vitro, one should keep in mind that there may be physiological differences that affect receptor affinity in vivo, for example, the effect of sodium levels on antagonist binding (Treherne et al., 1991).

We used cerebellum tissue to represent CNS H_1-receptors in contrast with the study of Ahn and Barnett (1986) and Leysen et al. (1991) who used cerebral cortex. Considering the results from northern blot analysis (Yamashita et al., 1991), we cannot exclude the possiblity that the sensitivity of cerebral cortex H_1-receptors is different from that of cerebellum H_1-receptors. However, from our data it is evident that none of the non-sedating H_1-receptor antagonists showed selectivity for peripheral H_1-receptors. It is therefore likely that non-sedating antihistamines lack sedative effects because they do not reach the brain in vivo due to certain advantageous physicochemical properties. Young et al. (1988) observed that the brain penetration of H_2-receptor antagonists correlates with a Δlog P parameter. This Δlog P is defined as the difference between log $P_{octanol/water}$ and log $P_{cyclohexane/water}$ and is considered to reflect the hydrogen-bonding capacity of a drug (Seiler, 1974). For the design of non-sedating agents, it would be interesting to know whether such a correlation also exists for H_1-receptor antagonists.

CHAPTER 4

LIPOPHILICITY AND HYDROGEN BONDING CAPACITY OF H_1-ANTIHISTAMINIC AGENTS IN RELATION TO THEIR CENTRAL SEDATIVE SIDE EFFECTS

A.M. ter Laak, R.S. Tsai, G.M. Donné-Op den Kelder, P.-A. Carrupt, B. Testa and H. Timmerman (Eur. J. Pharm. Sci. 2, 373-384)

Summary

Modern non-sedating histamine H_1-receptor antagonists (e.g. terfenadine, temelastine, cetirizine, astemizole) are considered to be devoid of CNS side effects because, as a result of their physicochemical properties, they do not cross the blood brain barrier (BBB) in sufficient amounts. In the present study lipophilicity parameters considered to be of importance for brain penetration capability (such as log P_{oct}, log $D_{oct,7.4}$, Δlog P and Λ_{alkane}) were determined for a series of structurally different sedating and non-sedating histamine H_1-receptor antagonists. These parameters were obtained from log P_{oct} and log P_{alk} values measured by centrifugal partition chromatography (CPC), a new and efficient method for measuring partition coefficients.

From the obtained lipophilicity data it appears that the (non-)sedative effects of antihistamines cannot be correctly accounted for by brain penetration models that use only H-bonding (Δlog P) or hydration capacity (Λ_{alkane}) as a parameter. Indeed, in this series of usually basic H_1-blockers, ionization also appears to play an important role.

We conclude that sedative effects displayed by antihistamines are better explained by the parameter log $D_{oct,7.4}$, the octanol/water distribution coefficient of both neutral and ionized species at pH 7.4. For neutral organic compounds it was found that brain penetration is highest if they have a log P_{oct} value of approximately 2 ('principle of minimal hydrophobicity', Hansch et al., 1987). Our data suggest that this principle is also applicable to ionizable drugs when log $D_{oct,7.4}$ is used instead of log P_{oct}. A tentative qualitative model for designing antihistamines without CNS side effects is presented.

Introduction

Sedative side effects and brain penetration of histamine H1-receptor antagonists

One major drawback of the classical histamine-H_1 antagonists has been their induction of CNS side-effects (most importantly sedation) at doses lower than needed for optimal therapeutic effect. Various studies suggest that these sedative side-effects are associated with blockade of central histamine-H_1 receptors (Quach et al., 1979; Uzan et al., 1979; Hall et al., 1984; Nicholson et al., 1991). Particularly relevant in this aspect are the studies in man with the enantiomers of chlorpheniramine and dimethindene, sedative effects being shown to be limited to the enantiomers with high histamine H_1-receptor affinity (Nicholson et al., 1991). This strongly suggests that sedation could arise from H_1-receptor antagonism alone. However, antagonism to other CNS receptors such as serotonin, acetylcholine or α-adrenergic receptors by classical and possibly less selective antihistamines could contribute to the sedative effect.

It has been claimed in the literature that non-sedative H_1-blockers such as loratadine (Ahn et al., 1986) and mequitazine (LeFur et al., 1981) have higher affinity for peripheral than for central H_1-receptors. However, this selectivity appears to be far too low to explain the advantageous non-sedating properties of these compounds. Moreover, in a recent study on a series of classical sedating and modern non-sedating antihistamines (including terfenadine, astemizole, loratadine, epinastine, temelastine and cetirizine), no differences were found in the affinity for peripheral and CNS H_1-receptors (Ter Laak et al., 1993). Therefore, it is more likely that the non-sedative behaviour of modern H_1-receptor antagonists is caused by specific molecular properties preventing these molecules from crossing in sufficient amounts the blood-brain barrier (BBB).

Indeed, various studies have indicated that non-sedating antihistamines do not reach the brain or do not occupy CNS H_1-receptors in vivo. This has been demonstrated for terfenadine (Sorkin et al., 1965; Rose et al., 1982; Barnett et al., 1984), loratadine (Barnett et al., 1984), astemizole (Laduron et al., 1982; Barnett et al., 1984), temelastine (Calcutt et al., 1987) and epinastine (Fügner et al., 1988).

It is generally believed that for the passive transport of solutes across bio-membranes, and particularly for crossing the blood-brain barrier, a relatively high lipophilicity is needed. However, preliminary lipophilicity estimates on some sedating and non-sedating antihistamines revealed that lipophilicity conventionally expressed as the partition coefficient in an octanol/water system (log P_{oct}) cannot solely account for differences in CNS penetration behaviour; other factors seem to be involved.

Brain penetration models

In the literature various relationships have been reported which relate lipophilicity and/or molecular size with BBB passage. One of the most common parameters used to explain the brain penetration of neutral organic compounds is log P_{oct}. Levin (1980) derived a quantitative relationship between the permeability coefficient PC (related to CNS entry), log P_{oct} and molecular weight MW for a series of structurally diverse compounds of relatively low molecular weight (MW < 400):

$$\log PC = -4.606 + 0.4115 \log [P_{oct}(MW)^{-1/2}] \quad (n=22, r=0.95) \qquad (1)$$

Hansch and co-workers (1987) improved Eq. 1 to:

$$\log PC = 0.50 \log P_{oct} - 1.43 \log MW - 1.84 \quad (n=23, r=0.96) \qquad (2)$$

but also studied different sets of compounds (hypnotics, aliphatic ethers, imidazolidine derivatives and tricyclic antidepressants) for which in general parabolic equations were derived with an optimal log P_{oct} value of about 2:

$$\log \text{BBB penetration} = a \log P_{oct} - b \log P_{oct}^2 + c \qquad (3)$$

A satisfactory explanation for this parabolic behaviour was given many years ago by the non-steady-state theory of Penniston et al. (1969). In their theoretical multi-compartment model the membrane is simulated as a single compartment of lipid character without specific structural features. The resulting biphasic curves approximate the experimentally observed lipophilicity-penetration relationships extremely well. Most importantly, the validity of the above non-steady-state model was later confirmed experimentally with a physical multi-cell system in a study by Dearden and Patel (1978).

For the particular case of ionizable drugs Hansch et al. (1987) suggested to use the distribution coefficient at pH 7.4 (log D_{oct}) instead of the partition coefficient of the neutral species (log P_{oct}). Log $D_{oct,7.4}$ is a function of the log P and pK_a values of the compound and therefore implicates two molecular features: the percentage of uncharged species of the compound at physiological pH (pK_a) and the ability of this uncharged species to partition into a lipophilic phase (log P_{oct}). For mono-protic bases these two parameters are related to log D_{oct}:

$$\log D_{oct,7.4} = \log P_{oct} - \log (1 + 10^{(pK_a - 7.4)}) \qquad (4)$$

A parabolic equation describing the transport across the blood brain barrier for a series of 14 basic imidazolidines is given by Timmermans et al. (1977):

$$\log (C_{brain}/C_{blood}) = 0.57 \log D_{oct,7.4} - 0.13 \log D_{oct,7.4}^2 - 0.09 \quad (n=14, r=0.987) \text{ with an optimal } \log D_{oct,7.4} \text{ of } 2.16 \qquad (5)$$

The similarity between Eq. 3 and 5 suggests that under physiological conditions the protonated

species of an ionizable drug does not contribute significantly to the partitioning of the drug into and across biomembranes, or to the partitioning into other lipophilic compartments (e.g. non-specific binding to serum proteins such as albumin, α_1-acid glycoprotein or lipoproteins (Christensen and Gram, 1982)).

It was reported only recently that the hydrogen bonding ability of solutes can be a structural determinant for brain penetration. For a series of histamine H_2-antagonists a satisfactory relationship between hydrogen bonding capacity and brain penetration was established by Young et al. (1988). High hydrogen-bonding capacity correlated with low brain penetration capacities according to the equation:

$$\log (C_{brain}/C_{blood}) = - 0.485\ \Delta\log P_{oct\text{-}alk} + 0.889 \quad (n=20,\ r=0.831) \qquad (6)$$

where the parameter $\Delta\log P_{oct\text{-}alk}$ is a descriptor for hydrogen bonding capacity (Seiler, 1974; El Tayar et al., 1992).

Van de Waterbeemd and Kansy (1992) reinvestigated the same series of H_2-antagonists previously studied by Young et al. (1988) resulting in:

$$\log (C_{brain}/C_{blood}) = -0.338\ \Lambda_{alkane} + 0.007\ V_M + 1.730 \quad (n=20,\ r=0.934) \qquad (7)$$

in which V_M presents the molar Van der Waals volume and Λ_{alkane} is a descriptor for hydration capacity, or with Λ_{alkane} alone:

$$\log (C_{brain}/C_{blood}) = -0.208\ \Lambda_{alkane} + 2.301 \quad (n=19,\ r=0.839) \qquad (8)$$

Present study

Based on the indications that the non-sedative behaviour of modern antihistamines is generally accompanied by a low ability to penetrate into the CNS, we decided to determine lipophilicity parameters for a series of 20 structurally different sedating and non-sedating H_1-antihistamines (Fig. 1) in two different solvent/water systems. To achieve this we used centrifugal partition chromatography (CPC), an efficient and highly accurate technique for measuring distribution coefficients in different organic solvent/water systems (El Tayar, 1991). Our study aims at improving the understanding of the influence of lipophilicity (log P, log $D_{7.4}$), hydrogen bond capacities (Δlog P) and/or hydration capacities (Λ_{alkane}) on brain penetration in general but more specifically on the central side effects of histamine H_1-receptor antagonists. Since we intended to study a series of structurally diverse antihistamines and because for most compounds quantitative brain penetration data are not available, quantitative structure-permeation correlations are not possible. Instead, for the purpose of designing non-sedating antihistamines without central side-effects, a generalized qualitative lipophilicity model is presented.

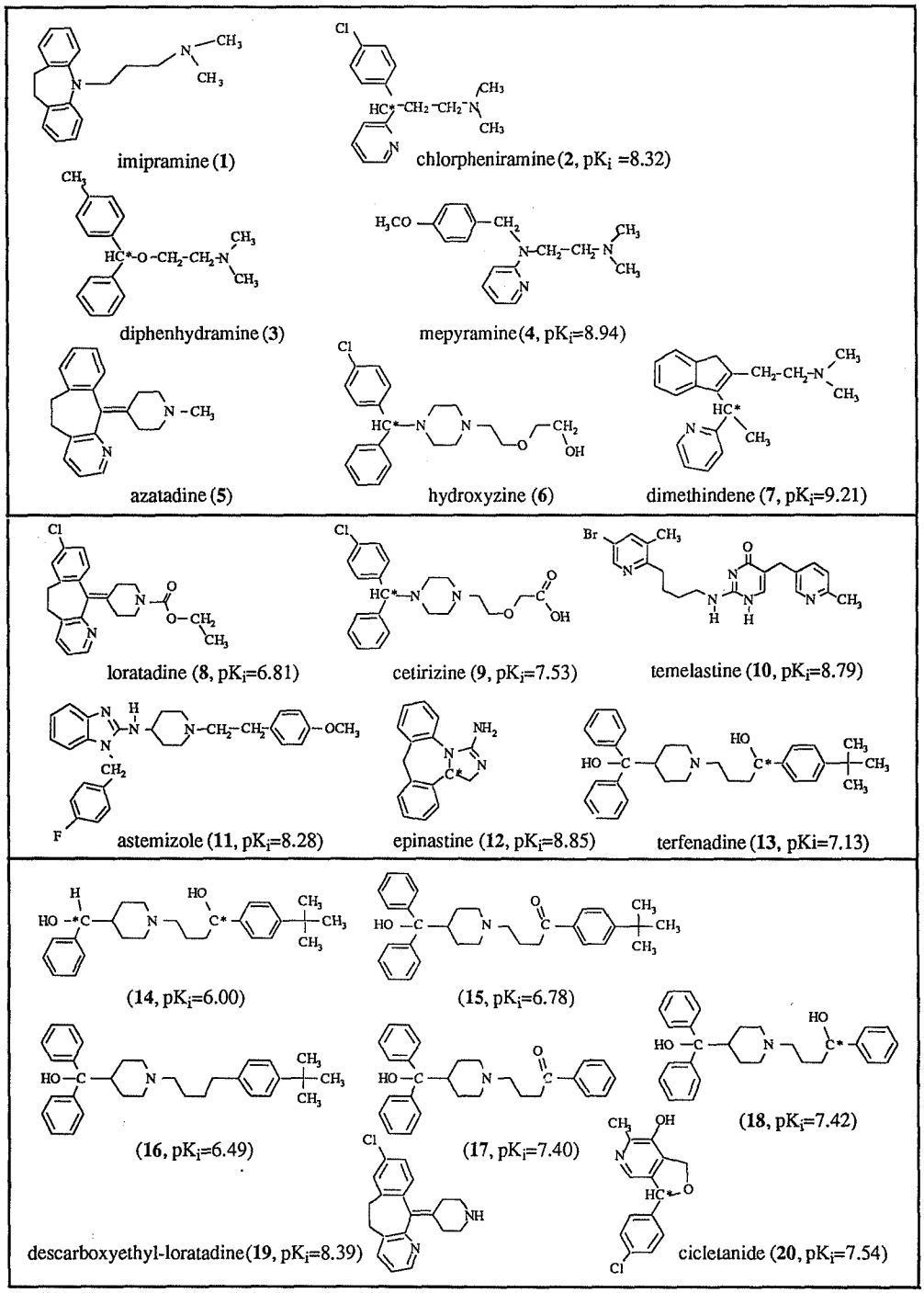

Figure 1. Structural formulas of H_1-antagonists considered in this study. Compounds **1** to **7** are known as H_1-antagonists with sedative side effects. Compounds **8** to **13** are reported as non-sedating H_1-antagonists. For compounds **14** to **20** we have no information on brain penetration. Apparent pK$_i$ values measured *in vitro* on guinea pig cerebellum (Ter Laak et al., 1993) are mentioned between parentheses.

Materials and Methods

Materials

Pyrilamine maleate (mepyramine (**4**)) was obtained from Sigma Chemical Company (St. Louis, USA). The following drugs were kindly donated by the indicated institutions: (S)-(+)-chlorpheniramine maleate (**2**) from A. Beld (University of Nijmegen, Nijmegen, the Netherlands), (-)-cicletanide (**20**) from the Institut Henry Beaufour (Le Plessis Robinson, France), (R)-(-)-dimethindene (**7**) from U. Borchard (University of Düsseldorf, Düsseldorf, Germany), imipramine (**1**), diphenhydramine HCl (**3**), azatadine (**5**), (R)-(+)-terfenadine (**13**) and terfenadine analogues (**14-18**) (Zhang et al., 1993) from our own laboratory stock, astemizole (**11**) from Janssen Pharmaceutica NV (Beerse, Belgium), epinastine HCl (WAL801 CL (**12**)) from Boehringer-Ingelheim (Ingelheim, Germany), loratadine (**8**) (SCH29851) and descarboxyethylloratadine acetate (SCH34117 (**19**)) from Schering Co. (Bloomfield, USA), hydroxyzine.2HCl (**6**) and cetirizine HCl (**9**) from UCB (Braine-d'Alleud, Belgium) and temelastine (**10**) (SKF93944) and icotidine (SKF 93319) from SmithKline Beecham (Welwyn Garden City, U.K.). Analytical grade n-dodecane was purchased from Aldrich-Chemie (Steinheim, Germany), and analytical grade 1-octanol was obtained from Fluka Chemika (Buchs, Switzerland). The aqueous buffers used for CPC measurements were 0.02 M MES-buffer (2-(*N*-morpholino)ethane-sulfonic acid, Calbiochem, La Jolla, California, USA) for pH range 1.5 - 5.0, or 0.02 M MPS-buffer (3-morpholinopropane sulfonic acid, Merck, Darmstadt, Germany) for pH range 5.5 - 7.5. These zwitterionic buffers could minimize the contribution of ion-pairs to the distribution coefficient when the solute is in an ionized state in the aqueous phase.

pK_a measurements

The pK_a values listed for basic compounds **1-6** (the alkylated nitrogens) were taken from the literature (Hansch et al. 1990). Potentiometric titrations of compounds **7**, **9**, **14**, **18**, **19** and **20** were performed with a Metrohm titroprocessor Model 670 (Herisau, Switzerland) using a solute concentration of 10^{-3} - 10^{-4} M in 0.1 M KCl and 0.01 N NaOH as the titrant. The temperature of the titration cell was maintained at 25 ± 0.1 °C, and the cell was refluxed with nitrogen gas. The pK_a values were calculated from a non-logarithmic linearisation of the titration curve (Leeson and Brown, 1966). For three compounds (**14**, **18** and **20**) 2% ethanol had to be added because of their low solubility. For terfenadine (**13**) and its analogues **15-17**, accurate pK_a values were difficult to obtain due to their limited solubility in water. In these cases the pK_a of the least lipophilic but structurally comparable analogue **18** was used to

calculate log P.

For the multiprotic compounds **10**, **11** and icotidine and for the highly basic compound **12**, the pK_a values were determined using the Sirius PCA101 apparatus (East-Sussex, U.K.) equipped with a semi-micro combination pH electrode (Orion 8103SC), a temperature probe, an overhead stirrer, a precision dispenser and a six-way valve for distributing reagents and titrants (0.5 M HCl, 0.1 M KCl and 0.5 M KOH). A weighted sample (1-10 mg) was supplied manually, the diluent and all other reagents added automatically. Bjerrum plots were used to calculate precise pK_a values (Avdeef et al., 1982). The detailed experimental procedures and data analyses have been described elsewhere (Avdeef, 1992). This novel technique appears to overcome the problem of overlapping pK_a values.

The pK_a of loratadine (**8**) was calculated from the log P_{dod} value (2.40) measured by CPC at pH 7.40 and a log D_{dod} value (0.90) measured at pH 3.09 (not in Table 1) via the equation $\log P = \log D + \log (1 + 10^{(pK_a-pH)})$.

Partitioning measurements using centrifugal partition chromatography

Centrifugal partition chromotography (CPC) is a chromatographic technique which uses two poorly miscible liquids as mobile and stationary phases (El Tayar et al., 1991). The partition coefficient in the biphasic system is accurately calculated from the chromatographic retention parameters. The advantages of this method are that it has efficient mechanisms for mixing the two phases and is devoid of a solid support (as in e.g. RP-HPLC) (Ito, 1986). Consequently, the partition coefficient depends only on solute-solvent interactions and is not perturbed by specific interactions with a solid support material.

Partition coefficient meausurements were thus performed with a horizontal flow-through multilayer centrifuge (model CCC1000, Pharma-Tech Research, Baltimore, USA, volume capacity 326 ml) which is of coil planet type and equipped with PTFE-tubing (polytetrafluoroethylene, 3.00 mm I.D., 3.94 mm O.D.). The mobile phase was propelled with a Kontron model 420 HPLC pump and eluated. Absorbtion was detected with a Kontron model 432 UV detector. Dodecane was used for the measurement of log P_{alk} values as in our experience the dodecane/water system does not form air bubbles in the detector cell as often observed with other alkane/water systems. It should be mentioned that differences between log P_{alk} values measured in different alkane/water systems (e.g. cyclohexane, n-heptane or n-dodecane) are negligible (Seiler, 1974). Depending on the estimated value of the partition coefficient, the volume ratio of stationary and mobile phases was adjusted (36:1 - 3:1) by changing the flow rate (0.5-3.0 ml/min) or the rotation speed (800-900 rpm). Chromatograms were recorded with a Hewlett-Packard 3392A integrator. In case of an organic mobile phase, distribution coefficients were calculated from $\log D = \log [(V_T-V_M)/(V_R-V_M)]$, where V_R is the retention volume, V_T the total volume of the column and V_M the volume of the mobile

phase (dead volume). Log D values that can be measured using CPC lie in the range between -3 and +3. Because log D is a function of pH, log P and pK_a, the pH of the aqueous phase can be adjusted so that the log D value is experimentally measurable.

From the pK_a value(s) and the distribution coefficient, the lipophilicty parameters of the neutral species (log P_{oct}, log P_{dod}, Δlog $P_{oct-alk}$) can be calculated. For compounds containing one protonated group at the applied pH (**1-8** and **13-20**) log P is calculated using the standard equation (Eq. 4).

For cetirizine (**9**) which is a zwitterion at pH 7.4, log P of the neutral cetirizine is calculated from the macroscopic acidic and basic pK_a values determined by titration (pK_{a11}=3.66, pK_{a21}=8.21) and from the log D at pH 7.40 using the equation (Tsai et al., 1993):

$$\log P = \log D + \log \{ 1 + 10^{(pK_{a11}-pH)} + 10^{(pH-pK_{a21})} + K_{a11}/K_{a22} \} \quad (9)$$

where K_{a22} is the K_a of hydroxyzine (**6**).

For temelastine (**10**), which is neutral at pH 7.4, log P_{oct} is calculated from the three basic pK_a values in the equation:

$$\log P = \log D + \log \{ 1 + 10^{(pK_{a1}-pH)} + 10^{(pK_{a1}+pK_{a2}-2pH)} + 10^{(pK_{a1}+pK_{a2}+pK_{a3}-3pH)} \} \quad (10)$$

In a similar way the log P_{oct} value of astemizole (**11**) is calculated using:

$$\log P = \log D + \log \{ 1 + 10^{(pK_{a1}-pH)} + 10^{(pK_{a1}+pK_{a2}-2pH)} \}. \quad (11)$$

Since epinastine (**12**) is a strong base (pK_a=11.81), it is assumed that both the ion pair and the neutral form contribute to the distribution of this compound at pH 7.50. The log P_{oct} value of the neutral species is calculated from:

$$\log P = \log \{ D + 10^{(pK_a-pH)} \times (D - P_{ionpair}) \} \quad (12)$$

with the log D_{oct} of epinastine measured at pH 3.6 interpreted as the log P value of the ion pair formed between the protonated species and chloride; this interpretation seems to be valid since at low pH values (3.5-5.5) the measured log D value remains constant (log $P_{ionpair}$ = -1.30, not in Table 1).

For compounds **14** and **18** it was not possible to measure log D_{dod} values with CPC because of their relatively low solubility. For these compounds log D_{dod} values were therefore measured by the traditional shake-flask method with UV detection.

Potentiometric log P determination

For compounds **10**, **11** and **12** log P_{dod} values were measured with the built-in log P option of the Sirius PCA101 instrument (East-Sussex, UK). After the first titration in aqueous solution, a certain amount of dodecane is added and the biphasic solution is "back-titrated". From the difference between the two titration curves the log P_{dod} value can be calculated by simulation procedures (for details, see Avdeef, 1992).

Determination of the molecular van der Waals volume (V_W)

For all compounds, the geometry was fully optimized with the Tripos force field containing electrostatic terms (SYBYL molecular modeling software, version 5.41, Tripos Associate Ltd., St-Louis, Missouri, running on a Silicon Graphics Personal Iris 4D/35 workstation). Molecular volume calculations were performed with the MOLSV program [QCPE, N° 509] using atomic radii described by Gavezotti (1983).

Table 1. pK_a and lipophilicity parameters of H_1-antagonists.

	pK_a	log D_{oct}	log D_{dod}	log P_{oct}	log P_{dod}	Δlog $P_{oct-alk}$	V_W	A_{alk}	log $D_{oct,7.4}$
1 imipramine	9.5	2.35	1.88	4.44	3.98	0.46	293.8	7.41	2.33
2 chlorpheniramine	9.16	1.42	0.32	3.17	2.09	1.08	270.4	8.42	1.40
3 diphenhydramine	8.98	1.60	0.97	3.17	2.56	0.61	268.7	7.89	1.58
4 mepyramine	8.92	1.45	0.47	2.96	2.00	0.96	292.6	9.35	1.43
5 azatadine	9.3	1.70	-0.09	3.59	1.82	1.77	293.5	9.56	1.68
6 hydroxyzine	7.10	0.95 (5.00)	0.91	3.05	1.09	1.96	361.4	12.84	2.87
7 dimethindene	8.45	1.63	0.56	2.70	1.65	1.05	309.7	10.34	1.61
8 loratadine	4.58	1.32 (1.50)	2.40	4.40	2.40	2.00	349.8	11.10	4.40
9 cetirizine	3.66;8.21	1.04	-2.83	4.48	0.61	3.87	361.4	13.32	1.04
10 temelastine	2.7;3.6;5.4	2.66 (5.00)	>3 (2.00)	3.19	1.28	1.91	375.9	13.20	3.19
11 astemizole	5.44;6.71	1.27 (5.00)	>3 (2.00)	3.56	0.95	2.61	438.5	15.88	3.48
12 epinastine	11.5	-0.68(7.50)	>3 (2.00)	3.51	1.76	1.75	236.6	7.48	-0.75
13 terfenadine	8.6	2.11 (5.00)	1.42	5.69	2.63	3.06	492.3	16.23	4.46
14 VUF4585	8.51	1.57 (6.02)	-0.35	4.06	0.79	3.27	418.4	15.29	2.92
15 VUF4590	8.6		2.04		3.25		486.6	15.39	
16 VUF4591	8.6	--	3.20		5.30	--	485.7	13.31	--
17 VUF4592	8.6	1.86 (6.02)	1.03	4.42	2.24	2.18	419.4	13.88	3.19
18 VUF4593	8.58	1.34 (6.02)	-0.19	3.90	1.02	2.88	424.9	15.30	2.69
19 desc.-loratadine	8.65	1.31	-0.81	2.56	0.46	2.10	291.8	10.86	1.29
20 cicletanide	3;11	2.34	-1.76	2.34	-1.76	4.10	228.0	10.68	2.34

oct = octanol / water system; dod = dodecane / water system; log D = distribution coefficient measured at pH 7.4 unless mentioned otherwise between parentheses; log P = partition coefficient of the neutral species; Δlog $P_{oct-alk}$ = log P_{oct} - log P_{dod}; V_W = Van der Waals volume; log $D_{oct,7.4}$ = distribution coefficient in octanol / water at pH 7.4.

Determination of polarity parameters ($\Delta log\ P_{oct\text{-}alk}$ and Λ_{alkane})

The descriptor of hyrogen bonding capacity, the parameter $\Delta log\ P_{oct\text{-}alk}$ (Seiler, 1974), predominantly reflects the hydrogen bond donor capacity of solutes, and, to a lesser extent, their hydrogen bond acceptor basicity (El Tayar, 1992). $\Delta log\ P_{oct\text{-}alk}$ was obtained by simply subtracting the experimentally obtained log P_{dod} from log P_{oct}:

$$\Delta log\ P_{oct\text{-}alk} = log\ P_{oct} - log\ P_{dod} \quad (13)$$

In analogy with previous work (El Tayar et al., 1992), Λ_{alkane} which represents the sum of polar interactions of solutes with water, was calculated with the equation:

$$\Lambda_{alk} = log\ P_{est,alk} - log\ P_{exp,alk} \quad (14)$$

where log $P_{est,alk}$ is defined as the partition coefficient in an alkane/water system of an alkane having the same molecular volume as the investigated compound and the log $P_{exp,alk}$ is the experimental value. The log $P_{est,alk}$ value can be calculated by the following calibration equation, which was derived from the measured partition coefficients of simple alkanes in an alkane/water system and their molecular van der Waals volumes (V_w):

$$log\ P_{est,alk} = 0.0376\ V_w + 0.346 \quad (15)$$

Results and Discussion

Properties of the investigated compounds

Although no consistent quantitative data of brain penetration have been established for the 20 compounds considered in this study (e.g. by *ex vivo* experiments), they can approximately be divided into classical sedating H_1-blockers with high brain penetration capacity and more recently developed H_1-blockers with low brain penetration capacity (Fig. 1). Compounds **1** to **7** are known as H_1-antagonists with pronounced sedative side-effects (Hall and Ögren, 1984;; Roth et al., 1987; Quach et al., 1979; Tozzi, 1974; Pong et al., 1974; Nicholson et al., 1991). Compounds **8** to **13** are reported as non-sedative H_1-antagonists with low brain penetration (Roth et al., 1987; Clissold et al., 1989; Simons, 1992; Calcutt et al., 1987; Laduron et al., 1982; Fügner et al., 1988; Schilling et al., 1990; Sorkin and Heel, 1985). For five terfenadine analogues (**14-18**) (Zhang et al., 1993), compound **19** (Tozzi, 1974) and cicletanide **20** (Schoeffter et al., 1987), no information on sedative side-effects has been reported. In accordance with the above data, Fig. 1 was divided into 3 blocks, namely classical sedating compounds, recently developed non-sedating antihistamines and compounds for which no data on brain penetration or sedative effects are available. The experimental results are presented in Table 1.

Distribution coefficients of compounds 10-12

For compounds **10** to **12** we were not able to measure log D values in the dodecane/water system using the CPC method. With dodecane as mobile phase, the chromatographic peaks eluted with the solvent front even at low pH values where these compounds are almost completely protonated (pH 2.0). These findings indicate that such compounds have unreliably high log P_{dod} values (at least log P_{dod} > 3). However, with the pH-metric method log P_{dod} values were obtained which were surprisingly low (1.28 (**10**), 0.95 (**11**) and 1.76 (**12**), respectively). The observed discrepancy between the two methods in measuring log P_{dod} values for **10**, **11** and **12** are explained by assuming that these compounds have an abnormal partitioning behaviour in the centrifugal force field of CPC and behave as amphiphilic surfactants. The compounds in their protonated state possibly form micelles and partition predominantly into the dodecane phase (Dearden and Bresnen, 1988), or, alternatively, into the interfacial surface area between the two phases. We have used log P_{dod} values measured with the pH-metric method to calculate $\Delta\log P_{oct\text{-}alk}$ and Λ_{alkane} for compounds **10-12**.

Intercorrelation of lipophilicity parameters

Before discussing $\Delta\log P_{oct\text{-}alk}$, Λ_{alkane}, log P_{oct} and log $D_{oct,7.4}$ in relation to the observed CNS effects of antihistamines, we first should pay attention to the intercorrelation coefficients of these lipophilicity parameters (Table 2).

From Table 2 it appears that Λ_{alkane} is correlated with the Van der Waals volume, V_W (r=0.891). A similar correlation between Λ_{alkane} and molar volume (V_M) also exists in the data of Van de Waterbeemd and Kansy (1992) (r=0.744). As correlated parameters should not be used in multivariate analysis, Eq. 8 should be used for the prediction of brain penetration from Λ_{alkane} and not Eq. 7.

Table 2. Intercorrelation matrix of lipophilicity parameters presented in Table 1.

	log P_{oct}	log P_{dod}	Δlog P	V_W	Λ_{alk}	log $D_{oct,7.4}$
log P_{oct}	---					
log P_{dod}	0.511	---				
Δlog P	0.221	0.724	---			
V_W	0.660	0.379	0.407	---		
Λ_{alk}	0.428	0.084	0.683	0.891	---	
log $D_{oct,7.4}$	0.471	0.100	0.266	0.727	0.658	

Table 2 also reveals that hydration capacity Λ_{alkane} is correlated with hydrogen-bond (donor) capacity $\Delta\log P_{oct\text{-}alk}$ (r=0.683). If we leave out the most deviant outlier cicletanide (**20**), the correlation is increased to r=0.821. A similar correlation can be found in the data of El Tayar et al. (1992) (n=118, r=0.923). These correlation data indicate that, although hydration capacity (Λ_{alkane}) and hydrogen-bonding capacity ($\Delta\log P$) are defined differently, they largely describe the same molecular properties, i.e. those related to the hydration process.

Hydrogen bonding capacity ($\Delta\log P_{oct\text{-}alk}$) and brain penetration

$\Delta\log P$ of sedating antihistamines

According to the $\Delta\log P$ model of Young et al.(1988) (see also Eq. 6), one would expect low $\Delta\log P_{oct\text{-}alk}$ values for the classical sedating antihistamines. In a theoretical study of El Tayar et al. (1991) in which $\Delta\log P_{oct\text{-}alk}$ is mainly related to H-bond donor capacity, 75 compounds were studied with zero, one or two hydrogen bond donor groups (e.g. -OH, -NH_2, etc.). The $\Delta\log P_{oct\text{-}alk}$ values were shown to range from -0.79 (n-pentane) to 4.65 (sulphathiazole). In correspondence with these data, most classical H_1-antagonists which lack an H-donor group such as **1** to **4** and **7** have low $\Delta\log P_{oct\text{-}alk}$ values in the range of 0.46 - 1.08. Compounds **2**, **4** and **7** which contain an extra hydrogen-bond acceptor group (an aromatic nitrogen) have slightly higher $\Delta\log P_{oct\text{-}alk}$ values than compounds **1** and **3** which lack such a function. Although azatadine (**5**) also contains an aromatic nitrogen atom and lacks H-donor groups, this compound has a slightly higher $\Delta\log P_{oct\text{-}alk}$ value (1.77) when compared to other more flexible compounds such as **2**, **4** and **7**. The relatively high $\Delta\log P_{oct\text{-}alk}$ of compound **6** (1.96) is explained by the presence of an additional hydroxyl group.

On the whole, the $\Delta\log P_{oct\text{-}alk}$ values (<2) of these sedating H_1-antihistamines are of modest magnitude and are in line with the brain penetration model found by Young et al. (1988).

$\Delta\log P$ of non-sedating antihistamines

Although it is found that sedating antihistamines have moderate $\Delta\log P$ values, the values of the non-sedating antihistamines (**8-13**) demonstrate that a moderate $\Delta\log P_{oct\text{-}alk}$ value does not necessarily imply a high brain penetration capacity. For example, compound **8** has only a marginally higher $\Delta\log P_{oct\text{-}alk}$ value (2.00) than its sedating counterpart **5** ($\Delta\log P_{oct\text{-}alk}$=1.77). Thus the model of Young et al. (1988) cannot explain the low brain penetration capacity of loratadine.

Also the moderate $\Delta\log P_{oct\text{-}alk}$ values of compounds **10**, **11** and **12** (1.91, 2.61 and 1.75, respectively) do not fit the model of Young since the antihypertensive drug clonidine

with a Δlog $P_{oct\text{-}alk}$ value of 2.44 was reported to readily enter the brain (Young et al., 1988). The moderate H-bond donor capacity of compounds **10-12** is due to the presence of nitrogen atoms in the guanidino group, while the remaining part of the molecules contains only H-bond acceptor groups.

Terfenadine (**13**) has a relatively high Δlog $P_{oct\text{-}alk}$ value (3.06), due to the presence of two H-bond donating hydroxyl groups. But again, this value is not high enough to fit the Δlog P model of Young et al. (1988).

Only cetirizine (**9**), which has the highest Δlog $P_{oct\text{-}alk}$ value (3.87) of the studied series of non-sedating compounds, meets the criteria of Young relating a low brain penetration capacity with a high Δlog $P_{oct\text{-}alk}$ value.

In conclusion, it is found that Δlog $P_{oct\text{-}alk}$ does not predict the behaviour of non-sedative H_1-antagonists. Therefore Δlog $P_{oct\text{-}alk}$ is clearly not the only descriptor that determines the (non-)sedative effects of antihistamines. It should be emphasized here that in our study the compounds are structurally and chemically quite diverse and other possibly important physicochemical properties will not be masked in the correlation study. For example, the non-sedating compound loratadine and its sedating counterpart azatadine display only a small difference in Δlog $P_{oct\text{-}alk}$, whereas they have remarkably different pK_a values (4.58 and 9.3 respectively). Also, the non-sedating compound cetirizine exists predominantly as a zwitterion at pH 7.4, while its sedating counterpart hydroxyzine does not. Considering the small differences in Δlog $P_{oct\text{-}alk}$ values, it could be worthwhile trying to explain the different brain penetration of sedating and non-sedating compounds in terms of differences in pK_a(s) and hence log $D_{oct,7.4}$ as will be discussed in a following section.

Δlog P of terfenadine analogues and cicletanide

For terfenadine (**13**) and some of its analogues (**14**, **18**) which all contain two hydrogen-bond donating hydroxyl groups, relatively high Δlog $P_{oct\text{-}alk}$ values were found. The Δlog $P_{oct\text{-}alk}$ value of the analogue lacking one phenyl ring (**14**, 3.29) is not much higher than the value of **13** itself (3.06) or that of **18** (2.88), which lacks the isobutyl group of **13**. Apparently hydrophobic groups have almost no influence on Δlog $P_{oct\text{-}alk}$. In contrast, if one of the H-bond donating hydroxyl groups of compound **18** is replaced by a carbonyl, which is a hydrogen-bond acceptor group, then Δlog $P_{oct\text{-}alk}$ drops by 0.7 units (**17**, Δlog $P_{oct\text{-}alk}$=2.18). The series of terfenadine analogues (**13-18**) shows that, if one wishes to increase the Δlog P of a molecule, H-bond donating hydroxyl groups should be recommended. The non-sedating drug terfenadine (**13**) can essentially be described as an extended classical H_1-antagonist in which two hydroxyl groups have been introduced.

Finally, we mention cicletanide (**20**) which has the highest Δlog $P_{oct\text{-}alk}$ value (4.10) in

our series. This most probably results from the strong H-bond donor capacity of the aromatic hydroxyl group (with a pK_a of approximately 11) and two additional H-bond accepting atoms (the pyridino nitrogen and ether oxygen). According to the model of Young et al. (1988) and based on its high Δlog P value, compound **20** is expected to have low penetration capacity and hence no CNS effects. Interestingly, although cicletanide (**20**) has never been reported as a non-sedating antihistamine, when it was investigated as a hypertensive drug in healthy volunteers, no central side effects were reported (Guinot et al., 1985).

Hydration capacity (Λ_{alkane}) and brain penetration

Equations 7 and 8, derived by Van de Waterbeemd and Kansy, indicate that the hydration capacity parameter Λ_{alkane} can be used for predicting BBB penetration. Indeed, if a solute is heavily solvated in water, as indicated by its high Λ_{alkane}, its passage across hydrophobic membranes could be hindered. The advantage of the parameter Λ_{alkane} over $\Delta\log P_{oct\text{-}alk}$ seems that measurement of a single $\log P_{alk}$ is sufficient to predict brain penetration. However, the relation between Λ_{alkane} and hydration capacity is true only in a limited range, meaning that the Λ parameters should be treated much more cautiously. Moreover, Eqs. 7 and 8 (in which one outlier was deleted) may be misleading due to their poor statistical quality. Table 1 supports these critical arguments, as no obvious relationship seems to be present between Λ_{alkane} and brain penetration

Octanol/water distribution coefficient (log $D_{oct,7.4}$) and brain penetration

Most of the earlier brain penetration models use the octanol partition coefficient $\log P_{oct}$ as a parameter in their studies (Eqs. 1 to 3). From Table 1 it can be seen that the $\log P_{oct}$ values, which are parameters for the neutral species of the series of sedating and non-sedating antihistamines, lie approximately in the same range and cannot explain a difference in sedative effects. However, many of the antihistamines considered in the present study are partially or fully protonated at pH 7.4 (**1-7** and **12-19**), only a few are predominantly present in their neutral form (**8, 10, 11, 20**), whereas one is even present in a zwitterionic form (**9**). It has been suggested by Timmermans et al. (Eq. 9) and Hansch et al. (Eq. 10) that, for the description of CNS entry of ionizable compounds, a parabolic equation depending on the octanol/water distribution coefficient at pH 7.4 ($\log D_{oct,7.4}$) could be used. The parabolic relationships these authors derived have an optimal $\log D_{oct,7.4}$ of approximately 2.

Interestingly, all the sedating antihistamines (**1-7**), have a $\log D_{oct,7.4}$ near 2 (range 1.40 - 2.87). In contrast, the non-sedating antihistamines (**8-13**) except cetirizine (**9**) have either a log $D_{oct,7.4}$ smaller than 0 (-0.75 (**12**)) or higher than 3 (4.40 (**8**), 3.19 (**10**), 3.48 (**11**), 4.46 (**13**)). It is therefore concluded that the sedative properties of all sedating and non-sedating H_1-antihistamines (**1-13**) except cetirizine (**9**) can be understood qualitatively using log

$D_{oct,7.4}$ as a descriptor for brain penetration capacity. We assume that the non-sedating properties of cetirizine (**9**) which has an intermediate log $D_{oct,7.4}$ value (1.04) can be explained by its relatively high Δlog $P_{oct\text{-}alk}$ value only, as discussed in the next paragraph.

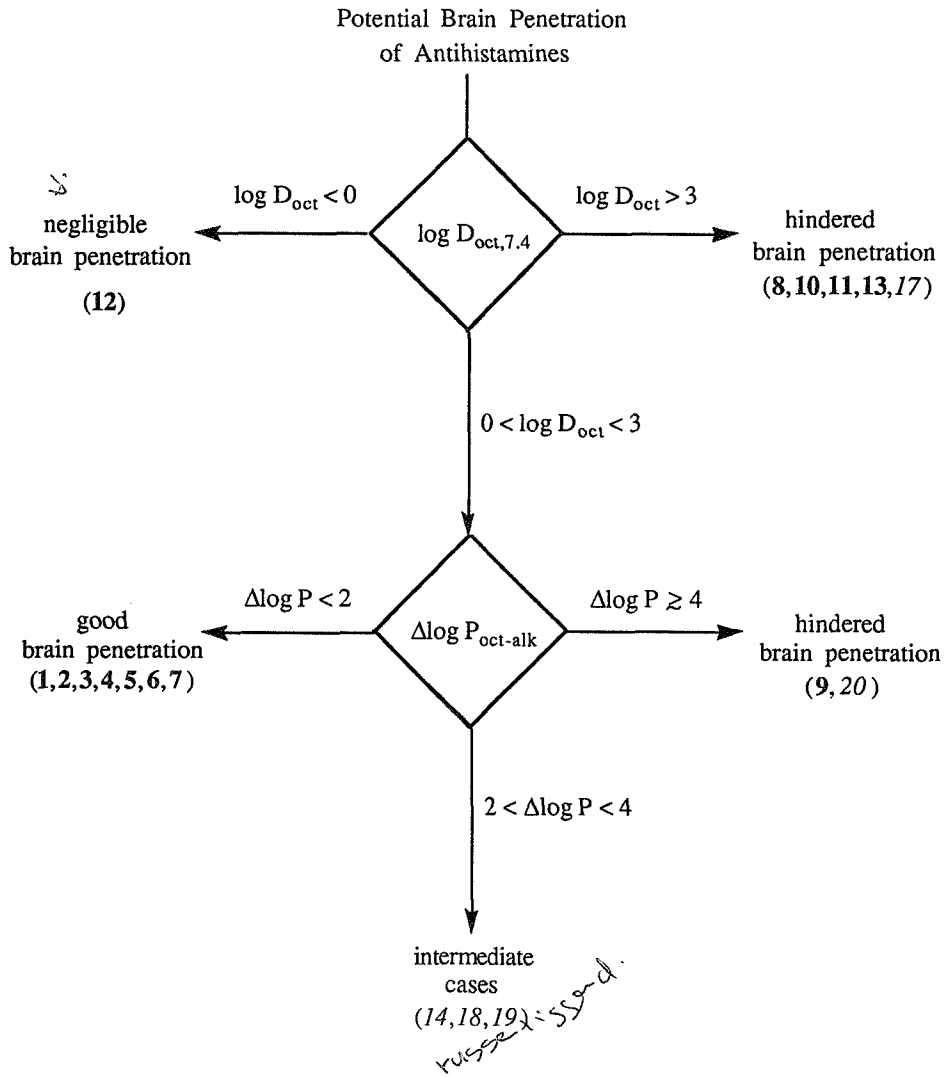

Figure 2. Hypothetical model for the brain penetration capacity of antihistamines. See text for explanation. Numbers given in bold refer to the compounds listed in Table 1 with known (non)-sedative behaviour. Numbers in italic refer to compounds with unknown properties.

Tentative model for the brain penetration capacity of antihistamines

Although $\Delta\log P_{oct\text{-}alk}$ values which seem to explain the brain penetration capacity of histamine H_2-antagonists can hardly explain the central effects of antihistamines, we do not conclude that the $\Delta\log P$ parameter does not affect brain penetration. It is not unlikely that solutes with strong hydrogen bond donor groups (high $\Delta\log P$) such as cetirizine interact with hydrogen bond acceptor groups (ester linkages, phosphate groups, etc.) in lipidic phases. As a consequence of these interactions, diffusion within the lipidic phase is hindered.
In view of the two main physicochemical factors influencing the brain penetration of antihistamines, a semi-quantitative model is formulated in Fig. 2. The potential for brain penetration of antihistamines is at first estimated from their distribution coefficient log $D_{oct,7.4}$. When log $D_{oct,7.4}$ is smaller than 0, brain penetration is negligible. In case log $D_{oct,7.4} > 3$, penetration will be hindered. For compounds with log $D_{oct,7.4}$ values within the range 0 to 3, penetration will occur in case the compound has a weak hydrogen bond donor capacity ($\Delta\log P_{oct\text{-}alk} < 2$). In contrast, compounds like cetirizine with $\Delta\log P_{oct\text{-}alk} >$ or near 4 may have poor penetration capacity due to the perturbation of hydrogen bond formation as suggested by the model of Young et al. (1988). In Fig. 2 the (non)-sedative behaviour of compounds **14** and **17-20** is predicted.

Conclusions

In this study a number of lipophilicity parameters proposed to be of importance for brain penetration have been investigated for a set of sedating and non-sedating histamine H_1-antagonists. The use of hydrogen bond ($\Delta\log P_{oct\text{-}alk}$) or hydration capacities (Λ_{alkane}) for the prediction of brain penetration appears to be non-satisfactory for this series of structurally diverse compounds.

The sedative side effects of the whole series of antihistamines are much better explained by the octanol-water distribution coefficient at pH 7.4, log $D_{oct,7.4}$. We strongly suggest that the principle of minimal hydrophobicity as proposed by Hansch is also applicable to acidic and basic drugs when log $D_{oct,7.4}$ is used in stead of log P_{oct}. Thus, newly to be developed and synthesized non-sedating antihistamines should either have a log D value lower than 0.5 or higher than 3. Table 1 illustrates nicely that a high log D value can be obtained in either of two ways, by increasing lipophilicity (e.g. terfenadine (**13**)) or by reducing the basicity (e.g. loratadine (**8**)) of a molecule that is essentially a typical classical H_1-antagonist. In case a compound has an intermediate log D value (range 0 to 3) a high $\Delta\log P_{oct\text{-}alk}$ is a prerequisite. In a recent study, Young et al. (1993) used the $\Delta\log P_{oct\text{-}alk}$ concept to the design of brain-penetrating H_2-agonists. The H_2-agonists reported in this study had low $\Delta\log P$ values and were found to be only moderately brain penetrating compounds. Because these compounds were basic, it appears that also for these H_2-agonists ionization plays a role in CNS entry.

CHAPTER 5

THE ROLE OF SERUM PROTEIN BINDING IN THE INCIDENCE OF CNS EFFECTS EVOKED BY HISTAMINE H_1-ANTAGONISTS

A COMPARATIVE STUDY ON THE SERUM PROTEIN BINDING OF A SEDATING ([^{3}H]MEPYRAMINE) AND A NON-SEDATING H_1-ANTAGONIST ([^{3}H]LORATADINE)

A.M. ter Laak, G.J. Bijloo, M.J.E. Fischer, G.M. Donné Op den Kelder, J. Wilting and H. Timmerman
(submitted)

Summary

In this study, human serum protein binding, one of the properties which may influence brain penetration of H_1-antagonists, has been investigated by comparing the sedating H_1-antagonist [^{3}H]mepyramine with the non-sedating H_1-antagonist [^{3}H]loratadine. It is shown that human serum albumin (HSA) binding and total serum protein binding of [^{3}H]mepyramine is low at therapeutical levels and at physiological pH (< 30% bound) and strongly depends on the ionization state of this compound (pK_a=8.92). Our results demonstrate that especially the unprotonated form of mepyramine binds to serum proteins. This conclusion is supported by further results from plain HSA binding experiments (this study) on six other unlabeled, 'classical' H_1-antagonists (i.e. diphenhydramine, chlorpheniramine, dimethindene, imipramine, azatadine, descarboethoxyloratadine). On the other hand, the modern non-sedating H_1-antagonist loratadine (log P_{oct}=4.40) binds to a high level to serum proteins at therapeutical levels (> 95% bound). Our results further indicate that the main determinants of HSA binding for H_1-antagonists are lipophilicity and acid-base properties as expressed by log P and pK_a, respectively (both included in the parameter log D_{oct}). However, hydrogen bonding capacity (Δlog P) is not correlated to serum protein binding for the series of H_1-antagonists investigated. We further propose that highly lipophilic, non-sedating H_1-antagonists (i.e., loratadine, terfenadine, astemizole, temelastine) probably have a low extraction ratio in the brain due to the tight lipoid blood brain barrier and a relatively high extraction ratio in the porous peripheral tissues.

Introduction

In the last decades, the therapeutic perspectives of histamine H_1-antagonists have increased with the discovery of new non-sedating compounds (Laduron et al., 1982; Rose et al., 1982; Barnett et al., 1984; Sorkin and Heel, 1985; Calcutt et al., 1987). The difference in the occurrence of side effects between 'classical' sedating and 'modern' non-sedating antihistamines most probably stems from differences in their ability to reach the brain as a result of their physicochemical properties (log P, pK_a) (Ter Laak et al., 1994). In order to avoid passage across the blood brain barrier (BBB), non-sedating antihistamines either need to have a fairly low octanol water distribution coefficient at physiological pH (low fat solubility, log D < 0: cetirizine, epinastine) or a relatively high log D value (low water solubility, log D > 3: loratadine, terfenadine, astemizole, temelastine). In contrast, sedating antihistamines have intermediate log D values (range 1 to 3) (Ter Laak et al., 1994). Also, it has been reported for a series of histamine H_2-antagonists that a high hydrogen bond capacity of a solute (reflected by the ΔlogP parameter of Seiler, 1974; $\Delta\log P = \log P_{oct} - \log P_{alk}$) decreases the ability to penetrate the blood brain barrier (Young et al., 1988 and 1993). Although it appears that BBB passage depends on three parameters (lipophilicity, acid/base properties and hydrogen bonding capacity; Ter Laak et al., 1994), the underlying mechanisms by which these parameters influence pharmacokinetics have not been fully clarified yet. Since it is highly likely that strong serum protein binding hinders brain penetration, we studied the question how the above-mentioned physicochemical parameters are possibly related to serum protein binding. For this study, equilibrium dialysis experiments were performed using low concentrations of free drug (< 1×10^{-5} M). This requires the use of radiolabeled drugs and we therefore decided to compare in detail the serum protein binding of only two radiolabeled antihistamines, [^{3}H]mepyramine, representing a typically basic and sedating H_1-antagonist ($\log D_{pH7.4} = 1.43$), and [^{3}H]loratadine, representing a highly lipophilic non-sedating H_1-antagonist ($\log D_{pH7.4} = 4.40$).

Several protein fractions in the blood are involved in the binding of drugs, such as albumin, α_1-acid glycoproteins (α_1-AGP), γ-globulins and lipoproteins. The most abundant of these proteins is albumin, which is present at a very high concentration of about 40 g/l and makes up 60% of total protein content in the blood. Due to this high concentration, albumin is generally believed to be the most important protein contributing to the binding of drugs. Some studies have shown that this is, however, not always the case. For several basic drugs, the contribution of especially α_1-acid glycoprotein has been shown to be of major importance to the total serum protein binding (Verbeeck et al., 1983; Belpaire et al., 1984; Eap et al., 1990). Therefore, the radiolabeled drugs mepyramine and loratadine were not only investigated for

human serum albumin (HSA) binding, but also for total human serum protein binding, which is also more in line with the *in vivo* situation.

Since it is known that a conformational change in the albumin molecule occurs at around physiological pH (the so-called neutral-to-base (N-B) transition; Wilting et al., 1980, Bos et al., 1989), we also studied pH effects in the range 6.0-9.0. However, since a change in pH may alter the percentage of drug in the protonated form, this will also affect protein binding. In this study such a phenomenon is observed for mepyramine and finds further support by HSA binding experiments on six unlabeled 'classical' H_1-antagonists at three different pH values (pH 6.6, pH 7.4 and pH 8.8) using HPLC detection and relatively high concentrations of free drug (approximately $1x10^{-5}$ M).

Materials and methods

Materials

Descarboethoxyloratadine acetate (SCH34117), loratadine free base (SCH29851) and labeled [^{3}H]loratadine (specific activity 13.0 Ci/mmol) were a gift from Dr. A. Barnett (Schering-Plough Corporation, Bloomfield, New Jersey). [^{3}H]Mepyramine free base (pyridinyl-5-^{3}H-pyrilamine, specific activity 27 Ci/mmol) was obtained from the Radiochemical Center (Amersham, England). Cold mepyramine (pyrilamine maleate) and human serum albumin (HSA) Fraction V powder (A1653) were purchased from Sigma Chemical Company (St. Louis, USA), (+)chlorpheniramine maleate was a gift from A. Beld (University of Nijmegen, Nijmegen, The Netherlands), (-)dimethindene free base was a gift from U. Borchard (Heinrich Heine University, Düsseldorf, Germany), imipramine free base, diphenhydramine HCl and azatadine free base from our own laboratory stock. In order to decrease the amount of bound fatty acid to 0.7-1.0 mol/mol, HSA was deionized before use by passing the solution over a mixed-bed ion-exchange column (Amberlitz IRA 400 and IR 120 in a ratio of 2:1) (Dröge et al., 1982). HSA concentrations were determined using spectrophotometric detection (spec. ext. $E_{1\%,278nm}$=5.8).

Human fresh blood plasm (serum) was provided by the Red Cross Bloodbank Utrecht (The Netherlands). Protein-free ultrafiltrate of human serum was prepared using an ultrafiltration cell (Amicon, type 202, Oosterhout, The Netherlands) provided with membranes (Amicon, type PM10, molecular weight cut-off 5,000). The filtration was carried out with 450 kPa N_2 (g) pressure and was stopped when the volume of the collected ultrafiltrate was about 75% of the initial serum volume.

Equilibrium dialysis / HSA binding / labeled compounds

Equilibrium dialysis studies were performed using a Dianorm Equilibrium Dialyzer (Diachema A.G., Rüschlikon, Switzerland) equipped with 24 Teflon cells consisting of two compartments each having a volume of 1 ml. These compartments are separated by dialysis membranes of hydrated cellulose (Diachema disc membranes, type 10.14, ø 63 mm, molecular-weight cut-off 5,000, from Dianorm, Münich, Germany). The right compartment (V_r) was filled with 1.0 ml phosphate buffer (pH 6.0 and 7.4) or borate buffer (pH 8.8) with an ionic strength of 0.1. The left compartment (V_l) contained 1.0 ml identical buffer containing antihistamine and $6x10^{-5}$ M HSA. The dialysis time was 18-20 h, the temparature 25°C and the rotation velocity of the Dialyzer 8 r.p.m. Labeled bound and free drug were determined using scintillation counting (Packard Tricarb liquid scintillation counter model A-4430).

Equilibrium dialysis / serum protein binding / labeled compounds

In case of serum experiments, one compartment (V_l) is filled with 0.8 ml serum and 0.2 ml buffered drug solution and the other compartment (V_r) with 0.8 ml ultrafiltrate and 0.2 ml buffer. The ionic strengths of serum and ultrafiltrate are usually not in equilibrium, since these experiments showed transport of volume from ultrafiltrate towards the serum compartment (V_l increased from 1.0 to 1.1-1.2 ml and V_r decreased accordingly). Percentages of free and bound drug were corrected for this effect using the ratio between the weighed volumes of both compartments after reaching equilibrium.

Equilibrium dialysis / HSA binding / unlabeled compounds

Experiments with unlabeled drugs were performed with an initial drug concentration of $2x10^{-5}$ M in the left compartment. Final free drug concentrations in the right compartment (V_r) were determined with HPLC using an Asahipak octadecyl polyvinyl alcohol copolymer column (ODP-50, 250x4mm, Hewlett Packard). The system was equipped with a 50 µl injection loop, a Gilson pump model 305, a Gilson 117 UV detector (I=225 or 260 nm) connected to an Apple Macintosh computer and using the HPLC Dynamax® Method Manager (V.1.3.1, Rainin Instrument Co. Inc). The eluent was a buffer/methanol mixture (10 mM Tris buffer, pH 10.0) containing 80% (v/v) methanol with a flow rate set to 0.4 ml/min. Free unlabeled drug in the right compartment after 20 h was measured, respectively, in the presence and in the absence of $6x10^{-5}$ M HSA in the left compartment (V_l). The fraction drug bound to HSA was calculated assuming that non-specific binding to cells and membrane is linearly correlated with concentration.

Calculations

Drug binding of labeled drugs [3H]mepyramine and [3H]loratadine was calculated from the measured and corrected radioactivity in both compartments after equilibrium (after 20 hrs). Non-specific binding to the cellulose membrane and to the cells (in some cases up to 30% of total drug) is automatically excluded in the calculations by measuring total radioactivity added (CPM_{total}). The fraction of free drug is calculated from:

$$\% \text{ free} = (CPM_{right} / CPM_{left}) \times 100 \quad (1)$$

The free drug concentration ($[L]_{free}$) and the concentration of drug bound to the receptor R ([RL]) are calculated from:

$$[L]_{free} = [L]_{ini} \times CPM_{right} / CPM_{total} \quad (2)$$

$$[RL] = [L]_{ini} \times (CPM_{left} - CPM_{right}) / CPM_{total} \quad (3)$$

where $[L]_{ini}$ is the initial concentration of drug in the left compartment and [R] is the total concentration of receptor sites for ligand L on albumin (one mol of albumin may complex more than one mol of ligand) or on serum proteins.

The presence of an unknown number of multiple binding sites on HSA (and also in serum) hinders the computation of accurate binding parameters. Since it is difficult to assign separate binding constants to each binding site, it is more convenient to simply distinguish between saturable (s) and non-saturable (ns) binding, following Lemaire et al.(1982):

$$[RL] = N_1K_1[L]_{free} / (1 + K_1[L]_{free}) + N_2K_2[L]_{free} \quad (4)$$

where N_1 and K_1 are, respectively, the concentration and average binding constant of saturable binding and N_2 and K_2 the concentration and average binding constant of non-saturable binding. If the binding constants (K) and concentration of sites (N) cannot be identified separately, protein binding is presented as the product NK throughout this paper. At low free drug concentrations ($K_1[L]_{free} << 1$), total binding is the sum of saturable and non-saturable binding:

$$[RL] = \{N_1K_1 + N_2K_2\} [L]_{free} = NK[L]_{free} \quad (5)$$

and:

$$\%\text{bound} = [RL] / ([RL]+[L]_{free}) = (NK / (NK + 1)) \times 100 \quad (6)$$

Saturable binding (K_1) was estimated from Scatchard plots (usually within a precision of about 20%; Klotz et al., 1990). Subsequently, binding parameters N_1 and the product N_2K_2

were estimated from nonlinear least squares fitting. Saturation curves were fitted using Eq. 4 and considering a concentration of HSA ($[R]_{total}$) of 5.66 x 10^{-5} M to calculate moles of bound L per mole of albumin (ν):

$$\nu = [RL] / [R]_{total} \quad (7)$$

Effect of protonation

In case of mepyramine, which has a pK_a value of 8.92, protein binding is strongly dependent on the degree of protonation. The total free mepyramine concentration ($[L]_{free}$) consists of free protonated and free unionized species ($[LH^+]$ and $[L]_u$, respectively, Eq. 8), while their equilibrium is determined by the dissociation constant (K_a for a base, Eq. 9):

$$[L]_{free} = [LH^+] + [L]_u \quad (8)$$
$$K_a = [L]_u [H^+] / [LH^+] \quad (9)$$

The concentration of free unionized species therefore depends on pH, the dissociation constant K_a and on the free drug concentration. Combination of Eq. 8 and Eq. 9 leads to:

$$[L]_u = [L]_{free} / (1 + 10^{pKa-pH}) \quad (10)$$

and:

$$[LH^+] = (10^{pKa-pH}) [L]_u \quad (11)$$

In theory, both the unionized species ($[L]_u$) and the ionized species ($[LH^+]$) bind to serum albumin (see Results) and equilibrium binding constants for both species can be defined as:

$$K_u = [RL_u] / N_u[L]_u \quad (12)$$
$$K_i = [RLH^+] / N_i[LH^+] \quad (13)$$

where N_u and N_i are the concentrations of binding sites for the respective species. At low free drug concentrations ($K_1[L]_{free} << 1$), binding of both species is non-saturable and additive:

$$[RL]_{total} = N_uK_u[L]_u + N_iK_i [LH^+] \quad (14)$$

and total binding can be related to one of both species, for example unionized ligand, using Eq. 11:

$$[RL]_{total} = \{ N_uK_u + N_iK_i (10^{pK_a-pH}) \} [L]_u \quad (15)$$

The total concentration of ligand is presented as:

$$[L]_{total} = [RL] + [L]_u + [LH^+] \quad (16)$$

thus, again using Eq. 11:

$$(10^{pK_a-pH}) = \{ [L]_{total} - [RL] - [L]_u \} / [L]_u \quad (17)$$

which can be included into Eq. 15, yielding:

$$[RL]_{total} = \{N_iK_i / (1+N_iK_i) \} [L]_{total} + \{(N_uK_u - N_iK_i) / (1+N_iK_i)\} [L]_u \quad (18)$$

The effect of the N-B transition of HSA on the binding affinity (K) of neutral drugs (i.e., warfarin, diazepam) is usually about a factor 2 to 4 (Wilting et al., 1980a-b) and therefore negligably small with respect to the pH effect on mepyramine binding due to ionization (see Results and Discussion). Thus, assuming that N_uK_u and N_iK_i remain constant over the applied pH range (i.e. neglecting effects of an N-B transition on the drug binding properties of HSA), and at low drug concentrations, a linear relationship between fraction bound (%B) and fraction unionized ligand can be expected (dividing Eq. 18 by $[L]_{total}$):

$$\%B = \{N_iK_i/(1+N_iK_i)\}x100\% + \{(N_uK_u-N_iK_i)/(1+N_iK_i)\} \%F_u \quad (19)$$

An estimation of the values N_iK_i and N_uK_u can be obtained from the intercept and slope of %bound versus %unionized mepyramine measured at different pH values (as in Figs. 2A and 2C).

Thus, under the above assumption, pH dependence of mepyramine binding can be described by the pK_a and the estimated non-saturable binding parameters of ionized and unionized species (combination of Eqs. 11, 14 and 16; see Figs. 2B and 2D):

$$\%B = \frac{[RL]}{[L]_{total}} = \frac{N_iK_i+N_uK_u/(10^{pK_a-pH})}{1+N_iK_i+(N_uK_u+1)/(10^{pK_a-pH})} \times 100\% \quad (20)$$

and the apparent binding of mepyramine at a given pH (NK'; Table 1) is, according to Eqs. 10 and 15:

$$[RL]_{total} = \{ (N_uK_u + N_iK_i (10^{pK_a-pH})) / (1 + 10^{pK_a-pH}) \} [L]_{free} = NK' [L]_{free} \quad (21)$$

Results and Discussion

HSA binding of mepyramine and loratadine

For studying binding characteristics of loratadine and mepyramine to human serum albumin, dialysis experiments were performed using $6x10^{-5}$ M HSA. At pH values well below the pK_a of mepyramine (8.92), low fractions of mepyramine bound to HSA are observed (at pH 6.0 and 7.4, > 90% free mepyramine, Fig. 1A). For binding at these pH values no Scatchard plots could be drawn (Fig. 1B). However, it appears that binding curves are non-linear and saturable at increasing antagonist concentrations (N_1K_1=0.02 at pH 6.0 and N_1K_1=0.09 at pH 7.4, Table 1) (Fig. 1C). At pH 8.8, when mepyramine is partly deprotonated, relatively high fractions of mepyramine bound to HSA are observed (at pH 8.8, > 50% mepyramine bound, Fig. 1A). This binding is almost completely saturable (N_1K_1=1.31) with only a marginal contribution of additional low affinity binding sites on HSA (represented by the parameters for non-saturable binding, N_2K_2=0.04, Table 1).

For mepyramine binding to HSA measured at different pH values, a linear correlation between percentages bound and percentages unionized mepyramine is observed (Fig. 2A). Indeed, assuming that the effect of pH on mepyramine binding is only due to differences in binding affinities of the ionized and unionized species for HSA, such linear correlation can be derived (Eq. 19). Implicitly, we neglected the effect of an N-B transition of HSA on drug binding properties (Eq. 19), since this effect is expected to be much smaller than the pH effect observed for mepyramine. This is supported by literature findings (Wilting et al., 1980a-b) on neutral drugs such as warfarin and diazepam for which no ionization state differences will occur in the pH range 6-9. For these compounds only a small effect of the HSA N-B transition was observed, since at low pH (5) still more than 90% was bound to the protein. In our study at pH 6 only 2% of mepyramine is bound suggesting that this effect is mainly due to deprotonation of the H_1-antagonist. Thus, since the N-B transition is expected to affect mepyramine binding only to a minor extent in the observed pH dependence, we can calculate estimated binding parameters (NK, Eq. 5) for the unionized and ionized species of mepyramine from Fig. 2A using Eq. 19. From this calculation, we find that HSA binding is much stronger for the unionized (N_uK_u=3.22) than for ionized species (N_iK_i=0.007) of mepyramine. The large differences in mepyramine binding at different pH values (NK' values; Table 1) are well explained by the different affinities of ionized (N_iK_i) and unionized (N_uK_u) forms of mepyramine for HSA (Eq. 21).

Table 1. Parameters for [^{3}H]mepyramine and [^{3}H]loratadine binding to non-physiological concentrations of human serum albumin ($6x10^{-5}$ M) at different pH values[a].

HSA BINDING	pH	NK'	N_1K_1 (s)	N_2K_2 (ns)	K_1	N_1	%bound
[^{3}H]mepyramine	6.0	0.02	0.02	0.00			2.0 ± 1.0
	7.4	0.09	0.09	0.00	-	-	8.3 ± 2.8
	8.8	1.35	1.31	0.04	$5.6x10^4$	$2.4x10^{-5}$	57.4 ± 3.2
[^{3}H]loratadine	6.0	2.85	2.55	0.30	$2.8x10^4$	$9.1x10^{-5}$	74.0 ± 1.9
	7.4	4.17	3.62	0.55	$4.0x10^4$	$9.1x10^{-5}$	80.7 ± 1.2
	8.8	6.52	5.78	0.74	$4.9x10^4$	$11.8x10^{-5}$	86.7 ± 1.0

[a]At low concentrations ($K_1[L]_{free}<<1$), total binding is represented by the sum of saturable (s) and non-saturable binding (ns) ($NK=N_1K_1+N_2K_2$; Eq. 4). K_1 and N_1 are the estimated saturable binding constant and the concentration of saturable binding sites on HSA, respectively. K_2 and N_2 the corresponding values for non-saturable sites.

In contrast to mepyramine, loratadine is strongly bound to HSA in the whole range around physiological pH (74%, 81% and 85% loratadine bound at low drug concentrations at pH 6.0, 7.4 and 8.8, respectively, Table 1 and Figs. 1D-F). For this observation, the strongly lipophilic character of loratadine and its low pK_a are responsible: at physiological pH loratadine is not protonated (log P=4.40, pK_a=4.6, Ter Laak et al., 1994). Fitting of the data reveals that the greater part of total loratadine binding to HSA is saturable (N_1K_1, 87-90%) with only a small contribution from unsaturable binding (N_2K_2, 10-13%, Table 1). From the saturation curves, it appears that there are probably two binding sites for loratadine with relatively high affinity (Fig. 1F). This number is, however, only a rough estimate since the unsaturable binding component hinders the precise identification of the number and affinities of all loratadine binding sites on HSA. Alltogether, the percentage of bound loratadine is relatively high in the pH range 6-9. The (relatively small) pH effect can be ascribed to the 'neutral-to-base' (N-B) transition of HSA occurring around physiological pH. Indeed, this N-B transition usually leads to an increased binding of neutral drugs, such as has been reported for warfarin and diazepam (Bos et al., 1989, Wilting et al., 1980[a-b]).

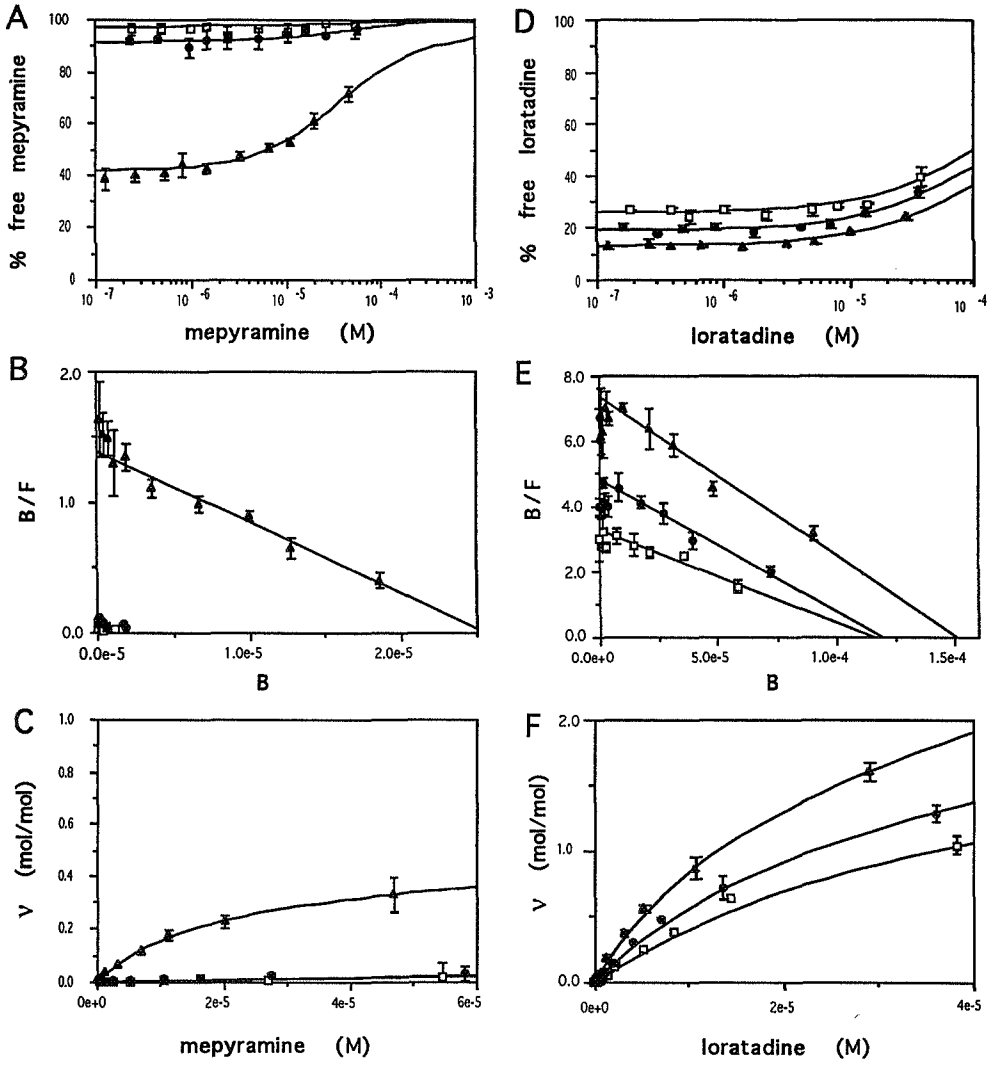

Figure 1. Figures 1A and 1D represent, respectively, curves of %free [^{3}H]mepyramine and %free [^{3}H]loratadine against free drug concentration in the presence of 5.66 x 10^{-5} M (3.8 g/l) HSA at three different pH values (pH 6.0 (□), pH 7.4 (●) and pH 8.8 (▲)). Scatchard plots (B/F versus B, where B=[RL] and F=$[L]_{free}$, Eqs. 2-3) and saturation curves (v versus [L]free, Eqs. 4 and 2) are given for the binding data of mepyramine (Fig. 1B and 1C) and loratadine (Fig. 1E and 1F). Scatchard plots for mepyramine at pH 6.0 and pH 7.4 (Fig. 1B) could not be fitted due to low level of HSA binding. The continuous curves in Figs. 1A, 1C, 1D and 1F are fitted using the estimated binding parameters for saturable (s) and non-saturable (ns) binding given in Table 1 (N_1, K_1, N_2, and K_2).

Table 2. Binding of [^{3}H]mepyramine and [^{3}H]loratadine to total serum proteins measured at different pH values[a].

SERUM BINDING	pH	log D	N_2K_2 (ns)	%bound
[^{3}H]mepyramine	6.40 ± 0.07	0.44	0.17	15 ± 4
	7.52 ± 0.25	1.54	0.34	26 ± 10
	8.33 ± 0.23	2.27	1.94	66 ± 11
[^{3}H]loratadine	6.40 ± 0.07	4.39	19.79	95.2 ± 0.5
	7.52 ± 0.25	4.40	22.92	95.8 ± 0.7
	8.33 ± 0.23	4.40	26.10	96.3 ± 0.5

[a] Log D = log distribution coefficient at the experimental pH. Binding to the pool of serum proteins appeared non-saturable (ns) over six points in the concentration range $5x10^{-7}$-$3x10^{-5}$ M; N_2K_2 (ns) = (apparent) non-saturable binding parameters (Eq. 4); %bound = average percentage of drug bound measured at xix concentrations in three blood plasms (n=18).

Serum binding of mepyramine and loratadine

Dialysis experiments, similar to the above-mentioned with HSA, were performed using fresh blood plasm and ultrafiltrate from three healthy blood donors. Although pH values in serum were originally set to the same values as in the HSA experiments, the final pH deviated from the original one after the long equilibration time (Table 2). It appeared that, in particular the large differences in pH between the different blood plasms (probably due to variations in the buffer strength of the donor blood), were the major cause for a large standard deviation in protein binding, especially in the case of mepyramine (Table 2). In each separate plasm, however, the percentages of free and bound drug appeared to be constant over the drug concentration range investigated ($5x10^{-7}$-$3x10^{-5}$ M). Because of the large total capacity of drug-binding proteins in serum, no saturable binding was observed.

As was to be expected from the experiments with HSA, pH has a large influence on the level of mepyramine binding in serum (15%, 26% and 66% mepyramine bound at pH 6.4, 7.5 and 8.3, respectively; Table 2). A linear correlation between the percentage bound and the percentage free unionized mepyramine is again found when pH corrections for each blood sample are included in the calculations of the percentage free unionized drug (Eq. 10; Fig. 2C). Thus, binding of unionized mepyramine to total serum proteins appears to be in the order of 80 times higher (N_uK_u=8.08) than binding of ionized mepyramine (N_iK_i=0.13). These values explain the large increase in serum binding of mepyramine from N_2K_2=0.17 to N_2K_2=1.94 in the pH range 6.4 to pH 8.3 (Table 2).

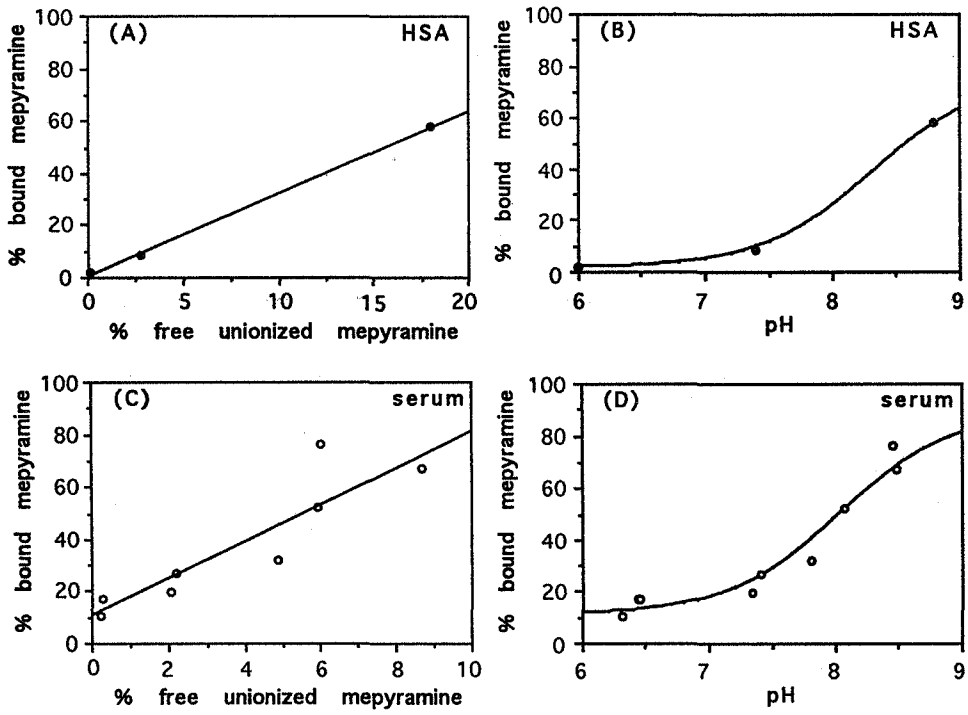

Figure 2. Percentage mepyramine bound versus free unionized mepyramine (Fig. 2A, HSA binding; Fig. 2C, serum binding) and versus pH (Fig. 2B, HSA binding; Fig. 2D, serum binding). Non-saturable binding of unionized (N_uK_u=3.22) and ionized mepyramine (N_iK_i=0.007) to 6 x 10^{-5} M HSA is estimated using Eq. 19 (Fig. 2A; %B=0.7% + 3.18%F_u). Similarly, binding of unionized (N_uK_u= 8.08) and ionized mepyramine binding (N_iK_i= 0.13) to total serum proteins is calculated from Eq. 19 and Fig. 2C (%B = 11.3% + 7.06 %F_u). %Bound mepyramine increases with pH due to the high pK_a value of mepyramine (8.92) (Figs. 2B and 2D, the drawn lines are calculated using Eq. 20).

Again, for loratadine, the effect of pH on serum binding is relatively small (N_2K_2 going from 19.8 to 26.1; Table 2). This pH effect is probably attributable to the N-B transition of HSA, since loratadine itself is neutral around physiological pH. The binding to serum proteins is extremely strong resulting in very high percentages of bound loratadine in serum (95.2, 95.8 and 96.3 %, Fig.1B).

Table 3. Lipophilicity parameters (log P, log D and Δlog P), pK_a values and HSA binding of one non-sedating (**1**, loratadine) and six classical H_1-antagonists (**2-7**). Compound **8** (descarboethoxyloratadine) is a metabolite of **1**.[a]

HSA BINDING		pK_a	log P_{oct}	log $D_{pH7.4}$	Δlog P	log $D_{pH8.8}$ (method)		$\%bound_{pH8.8}$
(1)	[^{3}H]loratadine	4.58	4.40	4.40	2.00	4.40	(scint.)	87 ± 1
(2)	[^{3}H]mepyramine	8.92	2.96	1.43	0.96	2.59	(scint.)	57 ± 3
(3)	imipramine	9.5	4.44	2.33	0.46	3.60	(HPLC)	62 ± 35
(4)	diphenhydramine	8.98	3.17	1.58	0.61	2.73	(HPLC)	65 ± 42
(5)	(-)dimethindene	8.45	2.70	1.61	1.05	2.52	(HPLC)	45 ± 7
(6)	(+)chlorpheniramine	9.16	3.17	1.40	1.08	2.73	(HPLC)	73 ± 20
(7)	azatadine	9.3	3.59	1.68	1.77	2.92	(HPLC)	47 ± 12
(8)	desc.-loratadine	8.65	2.56	1.29	2.10	2.37	(HPLC)	48 ± 9

[a] Note that from sheer necessity, experimental conditions are far from physiological (pH 8.8; see text). Oct = octanol / water system; log P_{oct} = partition coefficient of the neutral species; log $D_{pH7.4}$ = distribution coefficient in octanol/water at pH 7.4; Δlog P = log $P_{octanol/water}$ - log $P_{dodecane/water}$ (data from Ter Laak et al., 1994); log $D_{pH8.8}$ = distribution coefficient in octanol/water at pH 8.8; (scint.) = scintillation counting of radiolabeled free and bound drug; (HPLC) = HPLC determination of unlabeled free drug concentrations; $\%bound_{pH8.8}$ = fraction of the drug bound to $6x10^{-5}$ M HSA at pH 8.8 (n=3). At lower pH values (pH 6.6 and pH 7.4) bound fractions of unlabeled compounds **3-8** were too low and could not be detected with HPLC.

HSA binding of a series of classical H1-antagonists

In the previous paragraphs it was demonstrated that the ionization state of an H_1-antagonist such as mepyramine strongly determines the binding to serum proteins. Many other classical H_1-antagonists are also basic drugs with pK_a values in the range 8-10 (i.e., imipramine, diphenhydramine, dimethindene, chlorpheniramine, azatadine). In order to confirm our findings with mepyramine we measured the binding of unlabeled H_1-antagonists **3-8** to HSA (Table 3).

In the equilibrium dialysis experiments with unlabeled compounds, free drug concentrations were determined with HPLC (Table 3). In order to keep the binding data comparable, we used relatively low concentrations of free drug (approximately 1×10^{-5} M) unfortunately resulting in large standard deviations for the fractions of drug bound (Table 3). As a consequence, no significant binding could be detected at pH 6.6 and 7.4 (not shown). Thus, as already found for mepyramine, there appears to be a strong effect of pH on the binding of compounds **3-8** and, as a consequence, only binding at pH 8.8 could be determined for these unlabeled compounds. These binding data, presented in Table 3 together with their physicochemical parameters, are further discussed in the following paragraphs.

The effect of hydrophobicity (log D) on protein binding

Several years ago, it was shown that hydrophobicity plays an important role in the binding of small organic compounds of miscellaneous structure to albumin (Helmer et al., 1968). For a series of 9 basic beta-adrenergic drugs, a good correlation has been reported between the log octanol-water distribution coefficient at physiological pH (log $D_{oct,7.4}$) and the binding to isolated serum proteins (α_1-AGP, HSA (Fig. 3A), lipoproteins) and total serum proteins (Fig. 3B) (Lemaire and Tillement, 1982).

In their paper Lemaire and Tillement present log distribution coefficients for beta-antagonists measured in an octanol-water system at pH 7.4, as 'log P_{oct}' values. However, it is more appropriate to present them as log $D_{oct,7.4}$ values since 'log P_{oct}' is used for the partition coefficient of the neutral species of a drug, whereas 'log D_{oct}' is a combined measure of both lipophilicity (log P) and pK_a , determining the fraction of drug in the unionized form (Eq. 10). For mepyramine, log D varies depending upon the pH, whereas for loratadine the value does not change (Table 2).

After extrapolation of the apparent binding values presented in Table 1 (NK' values measured with 60 μM HSA) to physiological concentrations of HSA (600 μM), the binding data of mepyramine and loratadine measured at three different pH fall very well within the correlation found for beta-adrenergic compounds by Lemaire and Tillement (Fig. 3A). Interestingly, this suggests that the correlation is valid for log D values, at least up to 4 or 5, and for measurements at pH values other than pH 7.4. The log NK values for mepyramine and loratadine at pH 6.0 and pH 8.8 fall only slightly below and above the line, respectively (Fig. 3A, Table 2). In addition, the binding data of compounds **3-8** measured at pH 8.8 (Table 3) are also in reasonable agreement with this correlation (Fig. 3A).

The good correlation with log D supports our earlier conclusion that it is mainly the unionized form of a basic drug that binds to HSA. Lemaire and Tillement (1982) already stated that binding to HSA is predominantly hydrophobic in nature. Extension of their correlation with our compounds confirms the aspecific nature of hydrophobic interactions with HSA. However, caution is warranted since the correlation, of course, does not prove that all basic compounds bind to the same binding site of HSA.

Lemaire and Tillement (1982) also found a good correlation between lipophilicity and total serum protein binding (Fig. 3B). In general, the binding of beta-adrenergic compounds to serum proteins is very high in comparison with binding to HSA alone (compare log NK values in Figs. 3A and 3B) and it was clearly demonstrated by the authors that this predominantly was a result of strong binding of these drugs to α_1-acid glycoprotein (α_1-AGP).

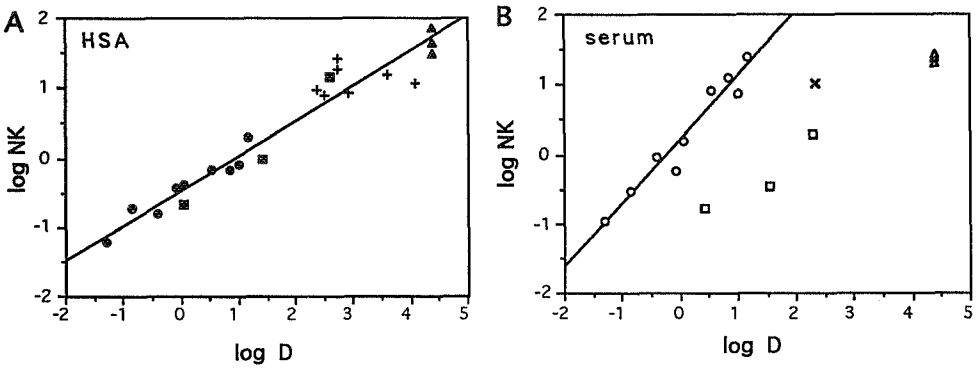

Figure 3. Binding to serum proteins (NK = sum of saturable and non-saturable binding at low antagonist concentrations, Eqs. 5 and 6) is correlated with log D, the log distribution coefficient in octanol/water. Fig 3A: binding of 9 beta-adrenergic antagonists to 600 µM HSA at pH 7.4 (●); data are taken from a study of Lemaire and Tillement (1982); values for mepyramine (■) and loratadine (▲) measured at three different pH values (Table 1), and extrapolated to 600 µM HSA, are presented; similarly, binding data of unlabeled H_1-antagonists **3-8** measured at pH 8.8 (Table 3) are shown (+). Fig. 3B: binding of 9 beta-adrenergic antagonists to total serum proteins (o) (data taken from Lemaire and Tillement, 1982); with respect to this correlation, total serum binding data of mepyramine (□), loratadine (▲) (both this study) and of imipramine (x) (data from Kristensen et al., 1982) are presented.

Our mepyramine and loratadine binding data in serum do not fit in the correlation found for beta-adrenergic drugs. Thus, it may be that mepyramine and loratadine do not bind as strongly to α_1-AGP as the beta-adrenergic compounds do (Fig. 3B), which is remarkable, since it is known that α_1-AGP is especially suited to bind basic compounds. An exception to this rule has, however, also been reported (desipramine, Verbeeck et al., 1983). For the basic drug imipramine we calculated that binding to serum proteins is also relatively low compared to the binding of beta-adrenergic compounds (Fig 3B; NK=8.61, data from Kristensen and Gram, 1982; log $D_{oct,7.4}$=2.33, Ter Laak et al., 1994). Thus, certain basic drugs such as desipramine, imipramine, but also mepyramine and loratadine show relatively low affinities for α_1-AGP. These unexpected results require further studies before reaching a conclusion. However, it might well be that the large differences in Fig. 3B could be explained by different experimental conditions. For example, Lemaire and Tillement used isotonic phosphate buffer in the right dialysis compartment, whereas we applied more physiological conditions (protein-free serum after ultrafiltration). It has also been reported that there are three genetic variants of α_1-AGP with different characteristics of drug binding (Herve et al., 1993). Therefore, it cannot be ruled out that the low serum binding of mepyramine and loratadine is due to variation in α_1-AGP phenotype and/or to variations in the levels of α_1-AGP which may differ considerably between individuals.

inflamed tissue vascular changes occur due to the release of various direct-acting (i.e., histamine, 5-HT, leukotrienes, PAF) or neutrophil-dependent (i.e., LTB_4, TNF-α, IL-8) allergic mediators leading to an increased permeability to plasma proteins and allowing albumin to enter the interstitial fluid (Buckley and Brain, 1994). Thus, as there is no lipoid barrier between HSA in the blood or interstitial fluid (i.e., where > 90% is bound) and H_1-receptors in the tissues, there will be no *diffusion-rate* limitation. Without this limitation, histamine H_1-receptors and serum proteins can freely compete for binding H_1-antagonists. Thus, in spite of the fraction bound to serum proteins, the extraction ratio is high and depends on the total concentration in the blood and the degree of perfusion in the tissue.

Although these considerations explain the observed differences in transport of highly lipophilic drugs to central and peripheral tissues, other phenomena may also play a role. For example, thightly bound drugs may be displaced from serum proteins at the right place and time, i.e. by mediators or by a decrease in pH in inflamed tissue. Although according to our study a decrease in pH would indeed lower the fraction of H_1-antagonist bound to serum proteins, there is, as far as we know, no evidence for a large drop in pH in inflamed tissue.

Conclusion

In summary, we found that classical sedating H_1-antagonists are poorly bound to serum proteins due to a high degree of ionization. On the other hand, we obtained evidence that highly lipophilic non-sedating H_1-antagonists (loratadine, astemizole, terfenadine and temelastine) are strongly bound to serum proteins in the blood. In order to explain the pharmacological action of the latter drugs in peripheral tissues in combination with the lack of central properties, we suggest that highly lipophilic drugs have *diffusion-rate limited* transport across the lipoid BBB and *perfusion-rate limited* transport into peripheral tissues. Serum protein binding and *diffusion-rate limited* transport are both mainly determined by lipophilicity (log P) and degree of protonation (pK_a). Therefore, the parameter log $D_{oct,7.4}$ (in stead of log P_{oct}) yields a first estimate for the brain penetration capacity of a drug. Increased hydrogen bonding capacity (Δlog P), which lowers brain penetration according to the study of Young et al. (1988), does not seem to be correlated with serum protein binding. We therefore suggest that high Δlog P values decrease the diffusion rate across the BBB by a higher degree of hydration of the solute.

SECTION II

MODELING STUDIES ON HISTAMINE H_1-RECEPTOR AGONIST AND ANTAGONIST BINDING SITES

CHAPTER 6

QSAR AND MOLECULAR MODELING STUDIES ON HISTAMINE H1-RECEPTOR ANTAGONISTS

AN INTRODUCTORY REVIEW

A.M. ter Laak, M.J. Van Drooge, H. Timmerman, G.M. Donné-Op den Kelder (Quant. Struct.-Act. Relat. (1992) 11, 348-363)

Summary

In this study quantitative structure-activity relationships (QSAR) and modeling studies of histamine H1-antagonists performed up to the early ninetees are reviewed and discussed. Although some studies have been performed more than 20 years ago they still contain valuable information. First a short introduction to H1-antagonists in general will be given, followed by a discussion of QSAR studies and finally a review of modeling studies. In the past, review articles have been published on H1-antagonists and their structure-activity relationships (Nauta and Rekker, 1978; Casy, 1978; Rekker, 1982; Ganellin, 1982). The aim of this review is to discuss also the recent literature, to combine the results of these recent studies with the older ones and to derive a general interpretation.

Introduction

H1-antagonists

Histamine is a mediator in allergic conditions. In 1933, Fourneau and Bovet observed that a benzdioxane derivative (Fig. 1) could inhibit a bronchial spasm caused by histamine. This was later classified as an antagonism of the H1-receptor. Since the discovery of this first H1-antagonist thousands of compounds have been synthesized and tested for H1-antagonistic activity. This has resulted in a large number of therapeutically applied H1-antagonists, mainly used in allergic diseases.

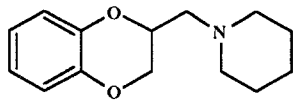

Figure 1. 2-(1-piperidinomethyl)-1,4-benzdioxane, the first compound discovered with H_1-antagonistic activity (Fourneau and Bovet, 1933).

H_1-antagonists can be classified into two major groups, classical and non-classical H_1-antagonists. Classical H_1-antagonists all share a common basic structure shown in Fig. 2. It consists of a basic nitrogen atom (in many cases a dimethylamine or a pyrrolidine function) and two aromatic groups. The aromatic groups and the amine are connected via a linking group, which can take various forms. Some examples and a possible classification of the classical H_1-antagonists was given in Fig. 2.

Because classical H_1-antagonists appeared not to have an optimal therapeutic profile, new H_1-antagonists have been developed. One major disadvantage of classical H_1-antagonists is the induction of sedation which is most probably due to antagonism of H_1-receptors in the brain (Nicholson, 1985; Monti et al., 1986). Two approaches have been followed to develop therapeutically improved H_1-antagonists. In the first place hydrophilic substituent groups have been introduced in classical compounds. Probably because of their decreased penetration of the blood-brain barrier these compounds show a reduced sedative effect. Examples are shown in Fig. 3. On the other hand structurally completely different compounds devoid of the unwanted side-effects of classical H_1-antagonists have been developed. Because of their different chemical structure these compounds were called non-classical compounds. Examples are given in Fig. 4.

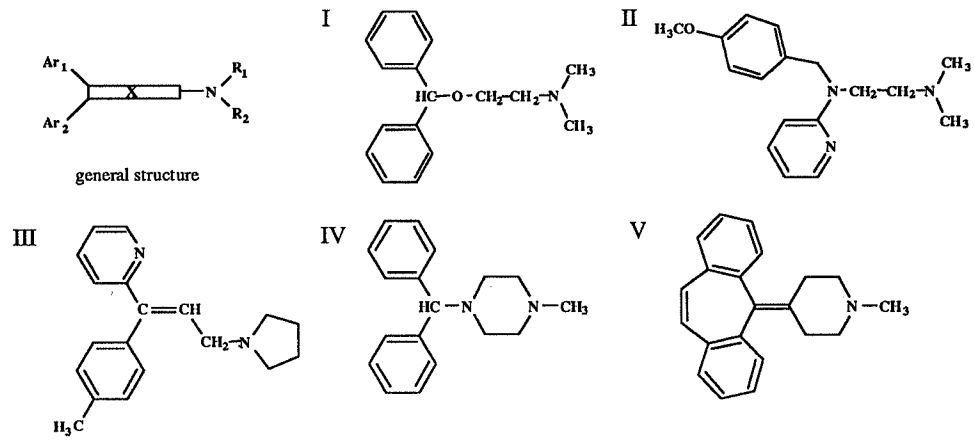

Figure 2. General structure of classical H_1-antagonists (Ar_1 and Ar_2 represent aromatic groups, X is a linking group and NR_1R_2 is a basic amine function) and five examples representing five subclasses: (I) diphenhydramine (diphenhydramines); (II) mepyramine (ethylenediamines); (III) triprolidine (aminopropyl compounds); (IV) cyclizine (cyclizines); (V) cyproheptadine (tricyclic compounds).

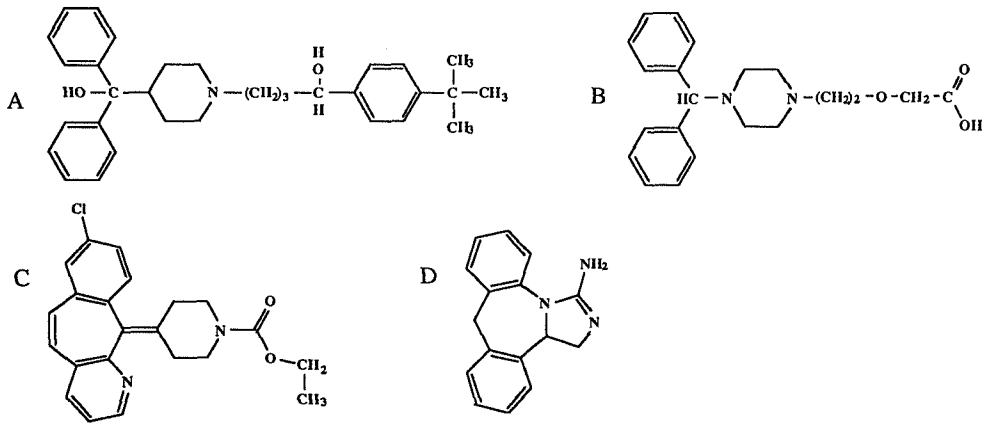

Figure 3. Classical H_1-antagonists with reduced sedating potential: (A) terfenadine; (B) cetirizine; (C) loratadine; (D) epinastine.

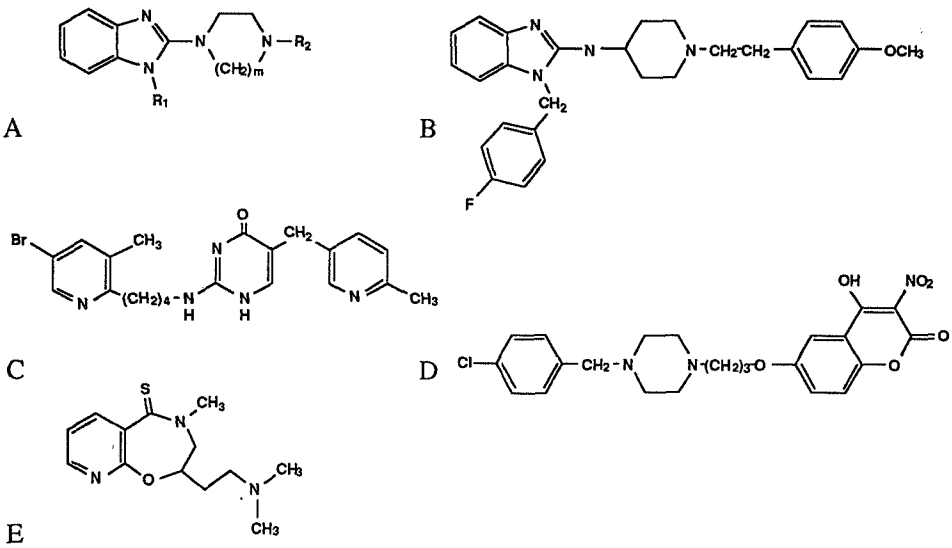

Figure 4. Examples of non-classical H_1-antagonists: (A) 2-(4-substituted-1-piperazinyl)-benzimidazoles (Iemura et al., 1986); (B) astemizole (Laduron et al., 1982); (C) temelastine (Ganellin et al, 1986); (D) nitro-coumarine derivates (Buckle et al., 1984); (E) rocastine (Sleevi et al., 1991).

QSAR

In the following sections QSAR studies will be reviewed. Parallels will be drawn between these studies and, if necessary, their major drawbacks highlighted.
The first QSAR study on H_1-antagonists was published by Kutter and Hansch (1969). From then on a lot of studies were reported. All QSAR studies solely used the multiple regression analysis method (Hansch approach) (Hansch, 1962) and no Free-Wilson analyses (Free and Wilson, 1962) have been carried out. Because the biological activities of a large number of diphenhydramine derivatives became gradually available (reviewed by Harms et al., 1975) many of the published QSAR studies are dealing with this class of H_1-antagonists.

QSAR studies on classical H_1-antagonists

The different role of the two aromatic moieties

On the basis of a study on histamine H_1-antagonists, Kutter and Hansch (1969) emphasized the importance of steric parameters in drug design. The authors investigated a series of diphenhydramines with substitutions in both phenyl rings (Fig.5). The biological parameters were an in vitro activity parameter (antagonism of a standard dose of histamine in guinea pig ileum) and an in vivo parameter (inhibition of histamine response in guinea pig). Electronic (σ) and lipophilic (π) parameters were examined but did not give satisfying equations. Using the, at that time in QSAR research, relatively new steric Taft parameter, E_S, good equations were derived for both in vitro and in vivo data as well as for their combination:

in vitro:

$$\log BR = 0.326\ (\pm 0.09)\ E_S^{o,m} - 0.346\ (E_S p)^2 - 0.189\ E_S p + 0.563\ (\pm 0.43) E_S p' - 1.878\ (\pm 0.65) \quad (1a)$$

$n=30;\ r=0.945;\ s=0.231$

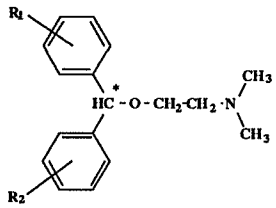

Figure 5. Diphenhydramine, substituted in both phenyl rings (R_1, R_2), investigated by Kutter and Hansch (1969), Rekker (1970) and Harms et al. (1975). C^* is the chiral carbon atom in case $R_1 \neq R_2$.

in vivo: $\log BR = 0.697\ (\pm 0.34)\ E_S^{o,m} - 0.121\ (E_S p)^2 - 0.002\ E_S p + 0.475\ (\pm 0.33)\ E_S p' - 3.781\ (\pm 1.8)$ (1b)
$n=22;\ r=0.914;\ s=0.223$

in vivo / in vitro: $\log BR = 0.358\ (\pm 0.07)\ E_S^{o,m} - 0.216\ (E_S p)^2 - 0.189\ E_S p + 0.482\ (\pm 0.26)\ E_S p' - 2.059\ (\pm 0.47)$ (1c)
$n=52;\ r=0.939;\ s=0.232$

$E_S^{o,m}$ = E_S of ortho and meta substituents in the "most highly substituted ring" ; $E_S p$ = E_S of first para substituent; $E_S p'$ = E_S of second para substituent

From the equal negative steric effect of ortho and meta substitution the authors concluded that probably unfavourable repulsive interactions between receptor and antagonist are involved. Furthermore, mono-para substitution has an activating effect up to an optimum value ($E_S p$ and $(E_S p)^2$), while a second para substituent appears to have a deactivating effect ($E_S p'$). This indicates that para-substitution effects the two rings differently although both effects are mediated sterically. Finally, it is evident that the same physico-chemical parameters determine the in vitro and in vivo activity.

The authors of the above study found E_S and π to be colinear. As all equations using π were less satisfying than those with E_S the authors concluded that the substituents mediate their effect sterically. This point will be discussed in more detail in sections to follow.

The series of compounds for which Eq.1a was derived, was further examined (Rekker, 1970; Harms et al, 1975). Instead of the relatively inaccurate single point activities (log BR values, Eq.1), the more accurate pA_2-values (Ash and Schild, 1966) were used. Also chirality was now taken into account (see Fig. 5). The R-isomer of the para-methyl derivative is 100 times more active than the S-isomer (pA_2 8.7 and 6.8, respectively (Rekker et al., 1972;

'Trans' / 'Cis'

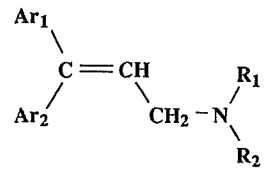

Figure 6. The diaryl aminopropenes investigated by Waringa et al. (1975) and Rekker et al. (1975). Diaryldimethyl-aminopropenes ($R_1 = R_2 = CH_3$) and diarylpyrrolidino-propenes ($R_1R_2=C_4H_8$) were investigated. Ar_1 is 2-pyridyl or phenyl. Ar_2 is pyridyl, (substituted) phenyl or (substituted) benzyl. The position of the aromatic ring is indicated by its orientation (cis or trans) with respect to the amine function.

Harms et al., 1975). Therefore, the authors assumed that also, in case of other mono-para substituted compounds the activity of the racemic mixture is almost entirely due to only one of the two enantiomers. The final equation obtained was (Harms et al., 1975):

$$pA_2 = 0.351\ \Sigma E_S^{o,m} + 0.675\ E_Sp' - 0.456\ (E_Sp)^2 - 3.060\ \sigma'_p + 3.744 \qquad (2)$$

n=16; r=0.960; s=0.294; F=33.1
$t(\Sigma E_S^{o,m}) = 8.05$; $t(E_Sp') = 5.00$; $t((E_Sp)^2) = -9.84$; $t(\sigma'_p) = -5.64$
(one outlier)

$\Sigma E_S^{o,m}$ = sum of E_S-values of ortho and meta substituents of the two rings;
E_Sp' = E_S of para substituent on ring at which para-substitution decreases activity;
E_Sp = E_S of para substituent on ring at which para-substitution increases activity;
σ'_p = resonance parameter introduced by Taft (Hammett σ corrected for inductive effects) for para substituent on ring at which para substitution increases activity.

The steric parameter E_Sp and the resonance parameter σ'_p both describe the para-substituent of one aromatic ring giving rise to a parabolic like curve. The parameter E_Sp' indicates a negative effect of para-substitution on the second aromatic ring.
Eq. 2 supports the conclusions drawn from Eq. 1a, i.e. that para-substitution effects the two rings differently. Although pA_2-values were used and chirality was taken into account, steric parameters still mainly explain the variance in activity of diphenhydramines. Finally, also in this study the parameter π was tested but steric parameters again gave rise to better equations.

The different role of the two aromatic rings was further investigated by Waringa et al. (1974; 1975) within a series of diaryl-aminopropenes (Fig. 6). Para-substitution of the aromatic ring positioned cis with respect to the amine function increases activity, whereas para-substitution in the trans-ring decreases activity (Casy, 1978). Activity appeared to correlate with the hydrophobicity of the cis-aryl ring:

$$pA_2 = 1.160\ D + 1.317\ f_{cis} + 5.062 \qquad (3a)$$

n=11; r=0.990; s=0.223; F=199.3; t(D)=16.7; $t(f_{cis})$=8.2.
D = dummy, differentiates dimethylamines (D=0) from pyrrolidines (D=1)
f_{cis} = *f*-value (hydrophobic fragmental constant) of cis-aryl group

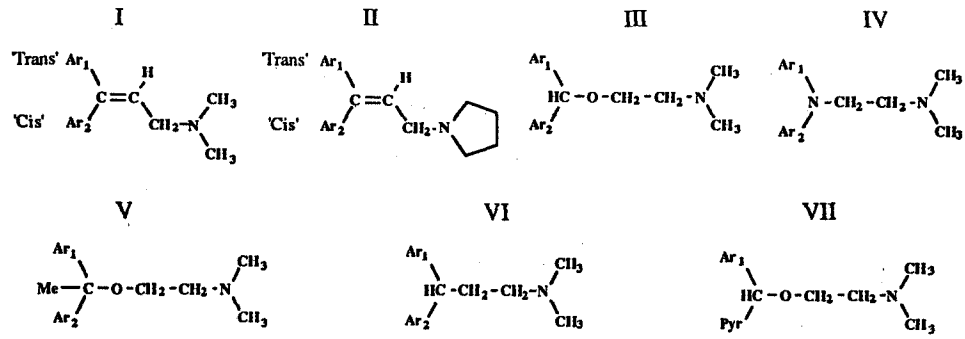

Figure 7. The seven classes of H_1-antagonists investigated by Rekker et al. (1975): (I) 1,1-diaryl-3-N-dimethyl-aminopropenes; (II) 1,1-diaryl-3-N-pyrrolidino-propenes; (III) diphenhydramines; (IV) ethylenediamines; (V) α-methyl-diphenhydramines; (VI) 1,1-diaryl-3-aminopropanes; (VII) aza-diphenhydramines.

Rekker et al. (1975) demonstrated that neither f_{trans} nor [f_{cis} and f_{trans}] resulted in better equations. Furthermore, Rekker et al. extended the class of investigated H_1-antagonists with five other classes (Fig. 7). The classification of the two aromatic rings into a cis- and a trans-ring is straightforward for the aminopropenes (classes I and II, Fig. 7). For the remaining five classes this classification is not that obvious as there is no double bond fixing the position of the aromatic rings relative to the amine function. However, it is known that in these classes mono-para-substitution yields two enantiomers with a difference in activity of about a factor 100. A similar difference is found for the cis- and trans-isomers of the aminopropenes. Therefore, the authors assumed that the more active enantiomer is comparable to a cis-para-substituted aminopropene compound. Thus, the para-substituted ring of the more active enantiomer can be considered as the 'cis'-ring and the non-para-substituted ring as the 'trans'-ring (Fig. 8). Using this classification of the two rings a QSAR equation was developed describing the seven classes of H_1-antagonists. Starting with seven dimethyl-aminopropenes (class I) the other classes were included in a stepwise fashion using dummies D_{II} to D_{VII} resulting in the following equation:

$$pA_2 = 1.243 f_{cis} + 1.187 D_{II} + 0.573 D_{III} + 0.384 D_{IV} + 1.346 D_V + 0.932 D_{VI} + 0.619 D_{VII} + 5.19 \quad (3b)$$

n=37; r=0.932; s=0.332; F=54.4
$t(f_{cis})$=15.9; $t(D_{II})$=6.89; $t(D_{III})$=3.00; $t(D_{IV})$=1.74;
$t(D_V)$=6.31; $t(D_{VI})$=4.43; $t(D_{VII})$=2.92.

As most t-values are larger than 2 the authors concluded that the seven classes of antagonists probably bind to the same receptor site. However, some criticism on the followed approach is justified. First, the authors did not check whether each series of compounds can be described separately with the parameter f_{cis} and that the values for f_{cis} in these separate regression equations are comparable. According to the authors the value for f_{cis} did not change significantly on the stepwise introduction of additional classes of antagonists. Therefore, the integration of seven classes within one equation is probably justified.

Secondly, the compounds investigated appeared to be only a small selection from the compounds for which pA_2-values are reported in literature. From each class 4 to 8 derivatives were selected without mentioning selection criteria. Examining the chosen compounds only little variation in the 'trans'-ring is observed: in 92% of the derivatives the ring is an unsubstituted phenyl or pyridyl ring. Therefore, it is not unexpected that the presence of a parameter describing the 'trans'-ring is not necessary to explain the variance in biological activities. Also, variation in the 'cis'-ring was poor as mainly unsubstituted or para-substituted phenyl or pyridyl derivatives were used. Because of this selective use of derivatives the r-value in Eq. 3b does not give a realistic presentation of the quality of the equation. Also, it is probably not allowed to compare Eq.3 with Eqs. 1a and 2. However, the important conclusion drawn from this study, i.e. that the seven classes of antagonists probably interact with the same receptor site, presumably is valid.

'trans'-ring: para substitution decreases activity

'cis'-ring: para substitution increases activity

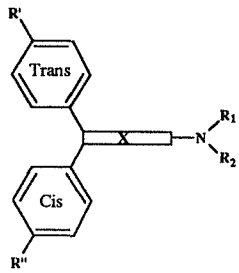

Figure 8. Definition of 'cis'-ring and 'trans'-ring in classical H_1-antagonists. NR_1R_2 and X are the basic nitrogen function and the connecting group as described in Fig. 2, respectively.

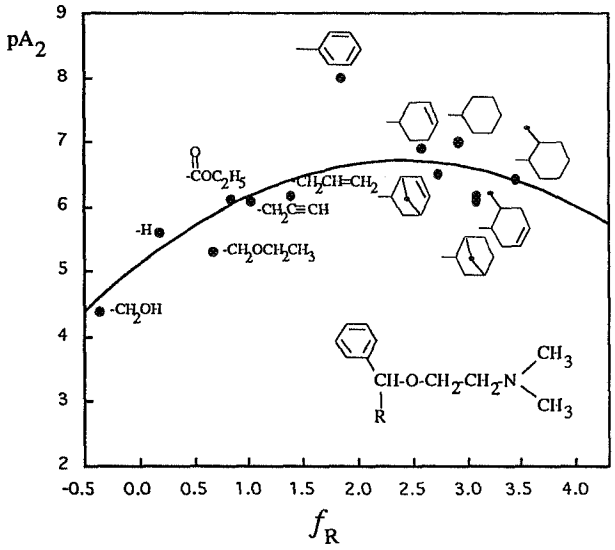

Figure 9. The monophenyl-diphenhydramine derivatives investigated by Rekker (1982) and a graph representing the resulting QSAR equation (Eq. 4).

Classical H1-antagonists with one aromatic group

Eqs. 1a to 3 describe H_1-antagonists with two aromatic groups. Rekker (1982) examined the importance of the parameter f for the H_1-antagonistic activity of a series of diphenhydramine derivatives in which one phenyl group was replaced by non-aromatic substituents (see Fig. 9). It was not mentioned whether besides f also other parameters (e.g. steric parameters) were investigated. The equation derived was:

$$pA_2 = 1.316(\pm 0.532)\, f - 0.272(\pm 0.156)\, f^2 + 5.010(\pm 0.355) \qquad (4)$$

n=12; r=0.894; s=0.351; F=20.0

The above equation indicates the importance of hydrophobic interactions for the monophenyl derivatives of diphenhydramine with the receptor. As diphenhydramine itself appeared to be an outlier, it was concluded that additional interactions are involved, e.g. π-π interactions. When Eqs. 1a and 2 for the diphenhydramines are compared with Eq. 4 for the monophenyl derivatives, it is remarkable that in all equations a quadratic relation is present: [$E_S P$ and $(E_S P)^2$] in Eqs. 1a and 2 and [f and f^2] in Eq. 4. Rekker (1982) proposed that these parameters describe the same aromatic ring because of the observed colinearity between steric and lipophilic parameters in both classes (Hansch, 1962; Kutter and Hansch, 1969). However, after a thorough investigation of literature data evidence was found that these parameters

probably describe non-comparable moieties of the antagonists. The next paragraphs describe this evidence.

In the above mentioned QSAR study on the monophenyl derivatives (Rekker, 1982) the pA_2-values of two additional derivatives are given which, in contrast to the other 12 investigated compounds (described by Eq. 4) have a para-methyl-phenyl group instead of an unsubstituted phenyl ring. This para-substitution raises the activity about tenfold. A similar increase is found on para-substitution of various diphenhydramines (Nauta et al., 1972). Therefore, it is very likely that the phenyl ring in the monophenyl compounds is comparable to the so-called 'cis'-ring of the diphenhydramines on which para-substitution also has a favourable effect (Fig. 8 for definition 'cis'- and 'trans'-ring). This implies that the non-aromatic part (e.g. cyclohexyl) of the monophenyl compounds described by the parameters [f and $f2$] in Eq. 4 is comparable to the so-called 'trans'-ring of the diphenhydramines. As the parameters [E_Sp and $(E_Sp)2$] in Eqs. 1a and 2 describe para-substitution in the so-called "cis-ring" of diphenhydramines, it can be concluded that the terms [f and $f2$] and [E_Sp and $(E_Sp)2$] describe different aromatic rings.

The above discussion indicates that the term [f and $f2$] in Eq. 4 should correspond to parameters describing the diphenhydramine 'trans'-ring variation: E_So,m and E_Sp' (Eqs. 1a and 2). The apparent contradiction between the quadratic dependence on lipophilicity in Eq. 4 and the linear dependence on steric factors in Eqs. 1a and 2 can be explained by a closer examination of the quadratic curve (Fig. 9). In the first phase of the curve hydrophobicity increases activity. This part of the curve describes monophenyl derivatives with non-aromatic aliphatic moieties smaller in size than a phenyl ring. The second phase reveals a decrease in activity upon increasing lipophilicity. This part of the curve describes (substituted) cyclohex(en)yl derivatives which not only are more lipophilic than the aliphatic substituents of the first phase, but also are larger in size than a phenyl group. Eqs. 1a and 2 predict a decrease in activity as a result of any substitution of the 'trans'-phenyl ring (positive coefficients of E_Sp' and E_So,m). Therefore, the negative effect of increasing lipophilicity in Eq. 4 is possibly a steric effect in disguise due to the observed colinearity between the parameters E_S and f. The reverse explanation, that E_Sp' and E_So,m are lipophilic parameters in disguise is less likely as lipophilic parameters were not found to improve Eqs. 1a and 2. The above discussion therefore explains the apparent contradiction between the quadratic dependence on f in Eq. 4 and the linear dependence on steric parameters in Eqs. 1a and 2.

The amine function of classical H1-antagonists

Variation in the basic part of H_1-antagonists has only been studied in a single paper. In 1973 Nauta et al. (1972) published a QSAR study on diphenhydramines with varying amino-groups (Fig. 10). The final equation was:

$$pA_2 = 1.378\ (\pm 0.437)\ D + 2.838\ (\pm 1.086)\ l - 0.419\ (\pm 0.153)\ l^2 - 0.709\ (\pm 0.425)\ \pi_N + - 1.254\ (\pm 0.685)\ \log P - 0.116 \quad (5)$$

n=27; r=0.914; s=0.402; F=26.4; (3 outliers)
D = 1 for para-methyl substitution; otherwise D = 0
l = width of NR_1R_2 moiety
π_N+ = total lipophilicity minus lipophilicity of all substituents on the nitrogen atom
log P = lipophilicity of total compound (experimentally determined)

The favourable effect of mono-para-methyl substitution on H_1-antagonistic activity (positive coefficient of D) was previously found and described in Eqs. 1a-c and 2 ([$(E_SP)^2$, E_SP]). Furthermore, the substituents of the N-atom seem to have an optimal width (l) whereas lipophilicity of the cationic head (π_N+ and log P) increases activity.

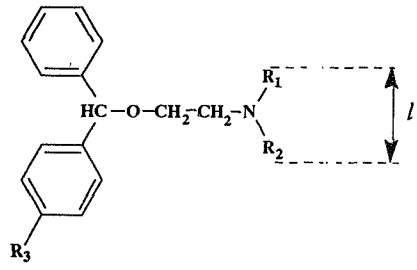

Figure 10. Diphenhydramines used by Nauta et al. (1973) to investigate substitution of the amino function: R_1,R_2 = H, CH_3, C_2H_5, C_3H_7 or $R_1R_2=(CH_2)_n$, n=2-6; R_3 = H or CH_3; l = extension (Å) of the N-substituents in a direction perpendicular to the main axis of the molecule.

QSAR studies on non-classical H_1-antagonists

Introduction

As mentioned in the introduction all classical H_1-antagonists share therapeutical disadvantages. Therefore, new compounds have been and still are being developed. As far as QSAR is concerned studies have been published on octahydropyrazinopyridoindoles (Fig. 11; Saxena et al., 1983; 1990), benzimidazole derivatives (Fig. 13; Iemura and Ohtaka, 1989) with a structural resemblance to astemizole (Fig. 4; Laduron et al., 1982), and isocytosines (Fig. 16; Ganellin et al., 1986). Some of the above compounds display high in vitro activities, yet none of the mentioned structures have been introduced into clinical practice.

Octahydropyrazinopyridoindoles

Saxena et al. (1983) published a QSAR study on a new class of H_1-antagonists, 2-substituted 1,2,3,4,6,7,12,12a-octahydropyrazino-[2',1':6,1]pyrido[3,4-b]indoles (OPPI, Fig. 11A). Various substituents in the phenyl ring were introduced and their influence on H_1-antagonistic activity determined. The compounds were only moderately active, the highest pA_2 being 6.8.

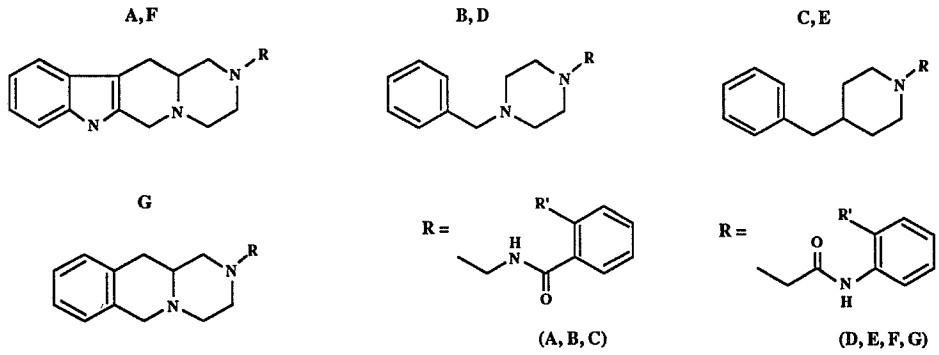

Figure 11. (A, F) 2-substituted 1,2,3,4,6,7,12,12a-octahydropyrazino-[2',1':6,1]-pyrido-[3,4-b]indoles (OPPIs); (B, D) piperazine OPPI derivatives; (C, E) piperidine derivatives; (G) pyrazinoisoquinolines derivatives. Various ortho-substitutions (R') in the aromatic ring of either the [β-(aroylamino)carbonyl]ethyl side chain (A to C) or the [2-[(arylamino)carbonyl]ethyl side chain (D to G) were considered (Saxena et al., 1983; 1990).

The variance in biological activity could not be explained by electronic but by lipophilic parameters instead:

$$\log 1 / IC_{50} = 0.324\ \pi_o + 0.285\ \pi_p + 0.150\ I_o + 0.702 \qquad (6a)$$

n=17; r=0.930; s=0.11; F=27.57; (six outliers)
π_o = π-value of ortho substituent; π_p = π-value of para substituent
I_o = 0 if no ortho substituent is present; otherwise I_o = 1.

Although the correlation is fairly good (r=0.930), there are six unexplained outliers. The importance of lipophilicity at the ortho and para position is evident. As the parameter I_o proved to correlate with steric (e.g. MR_o: r=0.86) and not to lipophilic parameters, some bulk at the ortho position is favourable.

As also in diphenhydramine a positive steric effect of phenyl substitution is observed (Eqs. 1-2, E_sP parameter), Saxena et al. (1983) suggested that the OPPIs bind to the H_1-receptor in a folded conformation in which their phenyl and indole ring occupy similar positions as the two phenyl rings of diphenhydramine (Fig. 12A). Based on the results of this study, the same research group presented a four subsite model for the H_1-receptor (Fig. 12B; Saxena et al., 1985) in which the phenyl and indole rings interact with electronrich hydrophobic groups (sites A and D, resp.), the tertiary nitrogen in the 2-position is responsible for ionic binding (subsite B), and the tertiary N at the 5-position interacts electrostatically with an electronrich group (subsite C). The authors further explored the positive lipophilic effect of the ortho-substituent of the phenyl ring (subsite A). Seven different prototypes (Fig. 11A to F) were synthesized with four to six different ortho-substituents in the phenyl ring. The seven separate QSAR equations correlated with π only. As the slope values were almost identical (0.375 ± 0.045) the authors concluded that the side chain phenyl rings in all these compounds probably occupy the same receptor site A (Fig. 12B). In a more thorough QSAR study on the same compounds Saxena et al. (1990) introduced an indicator variable IA to indicate the presence of the pyrazinopyridoindole skeleton. This indicator variable allowed the combination of the 7 prototypes into one regression equation:

$$\log 1 / IC_{50} = 0.357\ \pi_o + 0.53\ IA - 0.11 \qquad (6b)$$

n=33; r=0.921; s=0.102; F=83.72
π_o = π-value of ortho substituent; IA=1, 0: absence or presence of a pyrazinopyridoindole skeleton

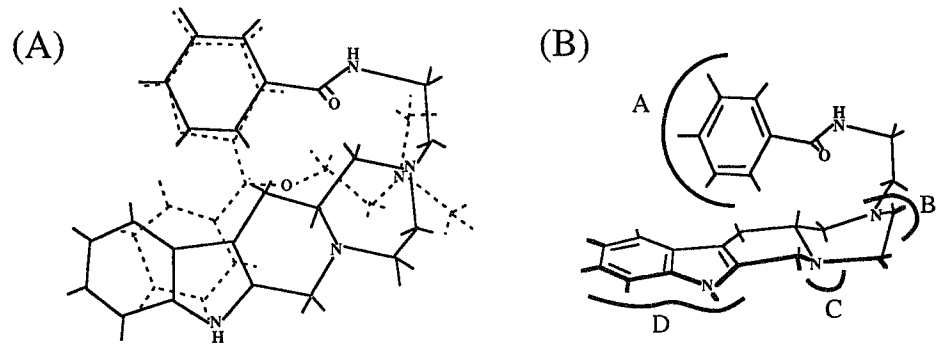

Figure 12. A (left); Superimposition of an OPPI derivative on diphenhydramine as proposed by Saxena et al. (1983). B (right); Four subsite model for the H_1-receptor antagonist binding site (Saxena et al., 1990).

Eq. 6b indicates that subsite C (X=N or CH in Fig.11) is not necessarily essential for activity and that the orientation of the amide fragment modulates activity. Again, the importance of a lipophilic ortho-substituent at the phenyl ring (subsite A) is evident. A significant improvement over Eq. 6b was obtained after inclusion of a steric (MR) and an electronic (σ) parameter although they are of secondary importance for activity:

$$\log 1 / IC_{50} = 0.328\ \pi_o + 0.143\ \sigma_o + 0.013\ MR_o + 0.53\ IA - 0.229 \qquad (6c)$$

n=33; r=0.953; s=0.083; F=68.70

π_o, σ_o, MR_o = π-, σ-, and MR-value of ortho substituent; IA=1, 0: see Eq. 6b

Although Eqs. 6a-c do not contradict the in itself interesting proposition that the OPPIs and derivatives can be superimposed on the diphenhydramines in a folded conformation, the particular conformation suggested by the authors (Fig. 12A) is probably not correct. The positive steric effect in OPPIs (Eq. 6a) results from ortho substitution; in the proposed superimposition of OPPI on diphenhydramine (see Fig. 12A) this ortho position is equivalent to a meta position of diphenhydramine at which substitution was shown to have an unfavourable steric effect (positive coefficient of $E_S^{o,m}$ in Eqs. 1-2). From a further comparison of Eqs. 6a-c with Eqs. 1-2 no indications can be obtained concerning possible equivalent positions in the two classes of compounds. More accurate modeling studies are probably needed to derive the active (possibly folded) structure of these OPPI derivatives.

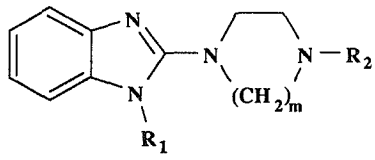

Figure 13. Structure of 2-(4-substituted-1-piperazinyl)-benzimidazoles synthesized and investigated by Iemura et al. (1986; 1989): R_1 = various aliphatic or aromatic groups e.g. $(CH_2)_nCH_3$, $(CH_2)_nPh$, $(CH_2)_nOCH_2CH_3$; R_2 = $(CH_2)_nCH_3$ or $(CH_2)_nPh$ with m=2 (piperazinyl) or m=3 (homo-piperazinyl).

Benzimidazoles

Iemura and Ohtaka (1989) published a QSAR study on fifty 2-(4-substituted-1-piperazinyl)-benzimidazole derivatives (Fig. 13). The most interesting feature of these non-classical H_1-antagonists is that most derivatives contain only one aromatic system (the benzimidazole). Differences in activity caused by changes in R_1 could be explained with steric parameters developed by Verloop (1976):

$$\log 1 / IC_{50} = 1.194(\pm0.252)B_3 + 1.440(\pm0.287)L - 0.098(\pm0.019)L^2 + 0.338(\pm0.231)I + 4.643(\pm1.135) \quad (7)$$

n=50; r=0.912; s=0.329; F=55.63

B_3 = STERIMOL second largest width parameter; L = STERIMOL length parameter; I=0 for m=2; I=1 for m=3

In addition to a quadratic dependence on the length parameter L also the width of the substituent R_1 (B_3) and the ring size of the (homo-)piperazinyl ring (I) are important for H_1-antagonistic activity. The optimal length of the substituents was calculated to be 7.3 Å.

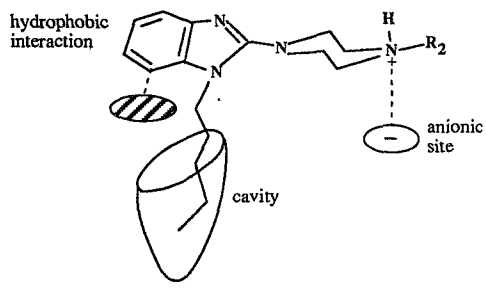

Figure 14. Model of the H_1-receptor antagonist binding site as proposed by Iemura and Ohtaka (1989).

Based on Eq. 7 a model for the H_1-binding site was proposed (Fig. 14) consisting of an anionic site which binds the positively charged (homo)-piperazinyl nitrogen atom, a slit-shaped cavity occupying R_1, and a site which interacts with the benzimidazole and which is perpendicular to the previous site. The benzimidazole ring binds via hydrophobic interactions as also proposed for one of the rings of diphenhydramine (Rekker et al., 1971).

A critical remark can be made with respect to B_3. The values for B_3 either are close to 3.1 Å (14% of the derivatives) or have a value of 1.90 Å (remaining compounds). Clearly, B_3 is not normally distributed.

It is again interesting to compare the results of the above QSAR study (Eq. 7) with the QSAR equations on diphenhydramines (Eqs. 1a, 2) in which steric parameters also were found to be important. As side chain R_1 can be aromatic as well as aliphatic it can be hypothesized that R_1 binds to the same receptor location as one of the diphenhydramine rings. In that case it is possible to draw a parallel between width parameter B_3 (Eq. 7) and the parameter $E_S^{o,m}$ (Eq. 1a, 2). Also the length parameter L and the parameters E_SP or E_SP' are possibly comparable. Eq. 7 does not reveal whether substituent R_1 is equivalent to either the 'cis'- or 'trans'-ring of diphenhydramine. However, preliminary modeling studies indicate that R_1 and the 'trans'-ring are probably equivalent. In that case E_SP' should be equivalent to the second (down-hill) phase of the quadratic curve on L (Fig. 15). The observation that the L-value of a phenyl-ring is 6.3 Å while the optimal value for L in Eq. 7 is 7.3 Å, supports the modeling results.

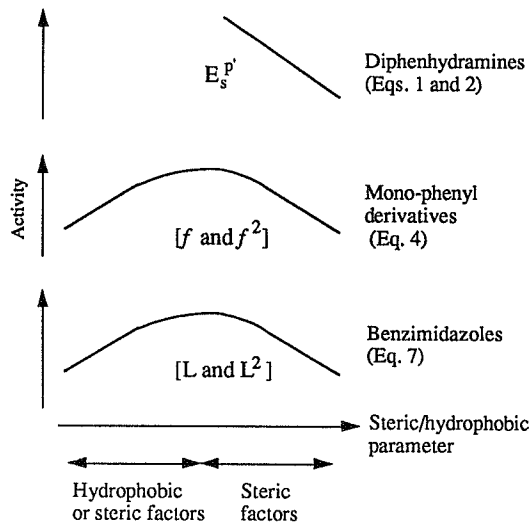

Figure 15. Schematic summary of the parameters in the QSAR equations describing the 'trans'-ring as defined in Fig. 8 or its proposed equivalent: E_SP' for the 'trans'-ring of diphenhydramines (Rekker, 1970; Harms et al., 1975); [f,f^2] for the non-aromatic substituent of mono-phenyl derivatives (Rekker, 1982); [L, L^2] for the R_1-substituent in benzimidazoles (Iemura et al., 1989).

There also is a similarity between Eq. 7 and Eq. 4 for the monophenyl compounds. Similar to the quadratic dependence on the parameter L of side chain R_1 in the benzimidazoles, Rekker derived a quadratic dependence on the lipophilicity of the non-aromatic group in the monophenyl compounds (Fig.15). We already discussed that the non-aromatic substituent of the latter compounds is comparable to the so-called 'trans'-ring of diphenhydramines. Therefore, it is not unexpected that in both the benzimidazoles and the monophenyl compounds an optimal length or lipophilicity for the substituent is found. As colinearity between lipophilicity and steric parameters is often observed, these curves might describe the same effect. We already proposed that the down-hill phase of Eq. 4 might be caused by steric effects; this could be comparable with the down-hill-phase of Eq. 7. This would only leave us with the question whether the up-hill phase in Eqs. 4 and 7 is either a hydrophobic or steric effect.
Summarizing, in three classes of H_1-antagonists, diphenhydramines, monophenyl diphenhydramine derivatives, and benzimidazoles, the so-called 'trans'-ring could be identified (Fig.15). Closer investigations of these and other classes can possibly give more definite answers to the question whether the effects of substitutions in the 'trans'-ring are the result of steric or lipophilic interactions with the receptor or both.

Isocytosines

QSAR studies on 2-(pyridin-2-ylbutylamino)pyrimidin-4(1H)-ones (isocytosines) were described by Blakemore et al. (1983) and Ganellin et al. (1986; 1991). The isocytosine ring (see Fig. 16B-D) was derived from the polar hydrogen-bonding cyanoguanidine group present in the H_2-antagonist cimetidine (Fig. 16A). In a series of 5-substituted isocytosines which were designed as potent H_2-antagonists, oxmetidine (Fig. 16C) was found to have weak H_1-antagonistic activity (pA_2 value of 5.4 in vitro on the guinea-pig ileum). This observation led to the design of compounds with a comparable potency to antagonize histamine at both H_1- and H_2-receptors with a potential therapeutic use in vascular conditions requiring simultaneous blockade of both receptors (Ganellin et al., 1986).

Replacement of the methylenedioxybenzyl moiety of oxmetidine (Fig.16C) with a 3-picolyl (pyridylmethyl) substituent and subsequent replacement of the imidazole with a pyridine was found to enhance H_1-activity and to retain H_2-activity (Fig.16D, Y=R_3=R_5= H, X=S). In two series of substituted pyridine derivatives (Fig.16D, X=CH_2 or S, Y=H) it was shown that H_1-activity is sensitive to the size of the substituent adjacent to the side chain. Furthermore, isocytosines with a methylene linkage (X=CH_2, Fig. 16D) are more potent H_1-antagonists than those with a thioether linkage (X=S, Fig. 16D).

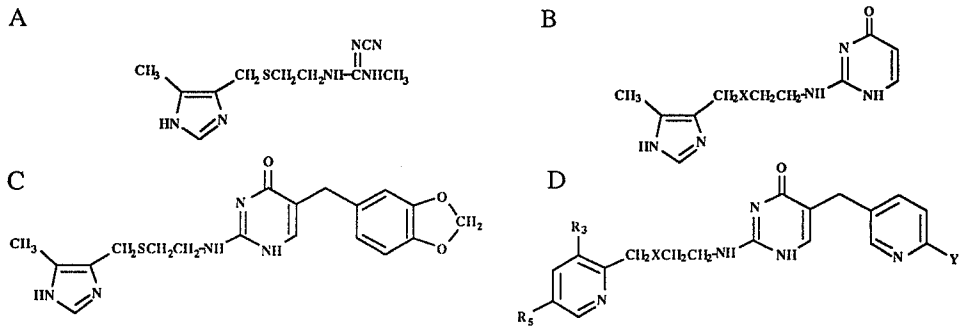

Figure 16. Isocytosines studied by Ganellin et al. (1986; 1991): (A) cimetidine; (B) SK&F 92207; (C) oxmetidine; (D) analogues of icotidine. Icotidine has R_3=OCH_3, R_5=H, X=CH_2 and Y=CH_3. Temelastine has R_3=CH_3, R_5=Br, X=CH_2 and Y=CH_3.

In a more extended series of 3-pyridine derivatives (X=CH_2, Y=CH_3, Fig. 16D) H_1- and H_2-activities were both related to a Verloop parameter *B* representing the size of R3 in the plane of the pyridine towards the side chain. The two activities appear to have different optima with respect to the R3 size, 1.3 Å for H_2- and 2 Å for H_1-activity, respectively (Fig. 17). The two activities become comparable for R3=OCH_3 (SK&F 93319, icotidine).

Although icotidine is quite lipophilic, the compound appeared to have negligible ability to penetrate the brain of animals. This led to a research programme directed to the design of non-sedating H_1-antagonists. The chemical structure of icotidine was altered in order to maximise H_1-receptor and minimise H_2-receptor antagonist activity. A series of 3,5-disubstituted pyridylbutylisocytosines (X=CH_2, Y=CH_3, Fig. 16D) with relatively small substituents (<2.2 Å) was developed for which the following QSAR equation was derived (Ganellin, 1991):

$$\log 1 / C = 5.56 + 1.70\,B + 0.80\,(\sigma_m5 - \sigma_m3) \qquad (8)$$

n=22; r=0.95; s=0.22

B= Steric Verloop parameter describing the size of the R3 substituent in the plane of the pyridine ring towards the methylene side chain (Verloop, 1976).

In this equation, the protection against histamine induced bronchoconstriction in the guinea pig in vivo is expressed as log 1 / C. Apart from a positive steric effect of R3, H_1-activity is enhanced by electron donating R3- and electron withdrawing R5-substituents. The most potent selective H_1-antagonist in this series is 3-methyl-5-bromo-pyridylbutyl-isocytosine, temelastine. This compound displays a pA_2 of 9.6 in the guinea pig ileum *in vitro* and a pA_2 of ca. 5.9 *in vitro*

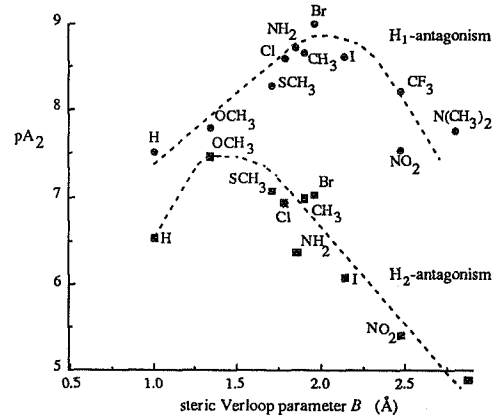

Figure 17. Ganellin et al. (1986) showed that for isocytosines both H_1- and H_2-receptor antagonist activity can be correlated with steric effects of the substituent adjacent to the side chain.

on the guinea pig atrium and hardly penetrates the brain. The high H_1-potency of temelastine is remarkable, as this compound lacks a basic tertiary amino group. The pK_a of the most basic group in temelastine (the 3-picolyl group, Fig. 16D) is 5.9, which is low compared to the pK_a of classical H_1-antagonists ($pKa \approx 9$) (Durant et al., 1985). The low brain penetration of the compound is most likely due to the pronounced hydrogen-bonding capacity of the isocytosine structure, which keeps these compounds out of highly lipophilic tissue regions. Temelastine was investigated in human studies, but found to lack sufficient potency. This might result from a high degree of protein binding found in man (Ganellin et al., 1991).

The positive steric effect of small substituents (size < 2 Å) was also observed in other series of pyridine structures. The most plausible explanation was given by Cooper et al. (1991) who observed that R3-substitution increases the relative population of molecules with the first two methylene bonds of the side chain in a trans / trans conformation. The design of active compounds favouring this conformation confirms Coopers' postulate.

The question arises whether isocytosines and diphenhydramines bind at similar receptor sites. A comparison of QSAR equations derived for the two classes is complicated, because ortho-, meta- and para-positions are not necessarily equivalent. This was already demonstrated for the proposed superimposement of OPPI derivatives on diphenhydramine in which an ortho-position in OPPI is equivalent to a meta-position in diphenhydramine (Fig. 12). Moreover, the QSAR data for the isocytosines and diphenhydramines are too distinct to be helpful in proposing a possible match. For example, the electronic parameter used for the diphenhydramines in Eq. 2 (σ'_p) is different from those used for the isocytosines in Eq. 8 (σ_m5 and σ_m3). Furthermore, the rationale for using a σ_m as an electronic parameter in Eq. 8 is not evident.

Conclusions from QSAR studies

Classical H_1-antagonists are often represented by the general structure given in Fig. 2. This structure is assumed to present their essential functions, i.e. a basic nitrogen atom connected to two aromatic groups. The above reviewed QSAR studies indicate this assumption to be valid. The importance of the basic function is described in terms of the width of the substituents connected to the basic nitrogen and the "lipophilicity" of the nitrogen atom (Eq. 5; Nauta et al., 1972). The importance of the rings is established in Eqs. 1a-3b.

Rekker et al. (1975) demonstrated that at least seven classes of classical H_1-antagonists bind to the same receptor site (Eq. 3b). Saxena et al. (1984; 1990) proposed that the non-classical OPPI derivatives bind in a folded conformation to the same site (Fig. 12A, B). Also the benzimidazole derivatives (Iemura, 1989) can be fitted in a receptor model for classic H_1-antagonists. Therefore, similarities can be expected - and were indeed observed - for the QSARs of classical and non-classical H_1-antagonists. Electronic parameters hardly show up whereas mainly lipophilic and steric parameters explain the variance in biological activity. However, due to the observed colinearity between steric and lipophilic parameters, it is difficult to discover whether for example a decrease in activity is caused by unfavourable steric interactions or by a negative hydrophobic effect.

In the QSARs of the diphenhydramines (Eqs. 1a, 2), their monophenyl derivatives (Eq. 4) and benzimidazoles (Eq. 7), similarities were observed which point to the moieties corresponding to the so-called diphenhydramine 'trans'-ring (Fig. 15). With respect to the 'cis'-ring no conclusions can be drawn. For the isocytosines (Ganellin, 1986; 1991) QSAR data are too limited to indicate a possible superimposition on the classical H_1-antagonists.

Molecular modeling studies on H1-antagonists

Molecular models of the H1-antagonist binding site can aid in the design of new H1-antagonists. These models should be 3-dimensional and explain all classes of antagonists known so far. As long as the 3-D structure of the H1-receptor remains unknown, indirect studies investigating the antagonists are important to achieve this goal. Early models of the binding site were based on modification (SAR) studies of H1-antagonists (i.e., Rekker et al., 1971). Other QSAR studies also led to propositions for the 3D-structure and nature of the binding site (i.e., Fig. 14; Iemura and Ohtaka, 1989). The disadvantage of these models is that they all are based on only one class of H1-antagonists. In contrast, molecular modeling studies can easily be applied to different classes of antagonists at a time. Also, by nature, these studies give more 3-D information.

In the next sections two studies (Kier, 1968; De et al., 1980) will be discussed in which the structures of the agonist histamine and various H1-antagonists are compared. Further discussions will concern modeling studies in which mainly H1-antagonists are compared (Borea et al., 1986; Naruto et al., 1985; Van Drooge et al., 1991; Sleevi et al., 1991). Finally, two modeling studies giving information on the sedative potential of H1-antagonists (Barbe et al., 1983; Pèpe et al., 1989) will be described.

Early modeling studies on H1-antagonists

By carrying out crude quantum chemical calculations (Extended Hückel Theory) Kier (1968) found two preferred conformations for the histamine monocation which are about equal in energy (Fig. 18, conformations 1 and 2, ΔE=0.25 kcal/mol). In conformation 1 (side chain trans) the distance between the protonated nitrogen atom (N^+) and the proximal nitrogen of the imidazole (N_π) is 4.55 Å; in conformation 2 this distance is 3.60 Å. In the potent H1-antagonist triprolidine (Fig. 19A) the N^+ and the pyridine nitrogen atom (X_N) were assumed to fulfil a similar function as the N^+ and N_π atoms of histamine, respectively. UV absorption experiments had shown that the pyridine ring of triprolidine is oriented coplanar with the olefinic bond (Adamson et al., 1957). In this conformation the smallest attainable distance between the N^+ and X_N is 4.8 ± 0.2 Å. Therefore, the biactive conformation of histamine at the H1-receptor was predicted to be conformation 1.

De et al. (1980) followed a similar approach to derive the bioactive conformation of histamine. The authors found 6 minimum energy conformations for histamine in its neutral form with energies within 2 Kcal/mol from each other (ISC-PEM-MO force field) (De and

Figure 18. Using Extended Hückel molecular orbital calculations Kier (1986) found two minimal energy conformations for histamine: conformation 1 with τ_1 = 120° and τ_2 = 180°; conformation 2 with τ_1 = 120° and τ_2 = 300°.

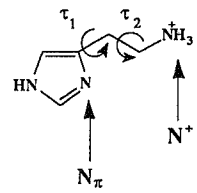

Ghose, 1978). Among these, conformations 1 and 2 found by Kier (1968) were present. The six low-energy conformations of histamine were compared to the minimum energy conformation of two potent H_1-antagonists, diphenhydramine and phenbenzamine (Fig. 19B, C). As their minimum energy conformation was determined by varying only two dihedral angles at a time, lower-energy conformations - and so the real global minimum - might have been missed. The tertiary amine in both antagonists and histamine (N^+) were considered to be equivalent while also the ether oxygen of diphenhydramine (X_O), the aniline nitrogen of phenbenzamine (X_N), and the N_π atom in histamine were assigned similar functions (Fig. 19). In the minimum energy conformation of diphenhydramine the distance between N^+ and X_O was found to be 3.67 Å; in phenbenzamine the corresponding distance between N^+ and X_N appeared to be 3.75 Å. Therefore, the authors concluded that not conformation 1 as postulated by Kier (N^+-N_π distance 4.55 Å), but a conformation similar to conformation 2 (N^+-N_π distance 3.59 Å) is the bioactive conformation of histamine.

The importance of the findings of Kier (1968) and De et al. (1980) with respect to the active conformation of histamine can be doubted. First a remark should be made with respect to the flexibility of the antagonists studied. Today, it is generally accepted that not only the global minimum but also other low-energy conformations can be active at the receptor depending on the free energy of binding. Therefore it is not justified to look at the global minimum only or

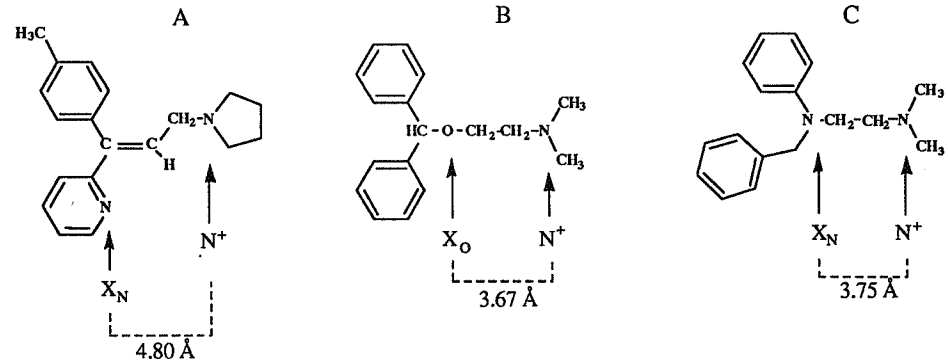

Figure 19. The H_1-antagonists whose structures were compared with minimal energy conformations of histamine. The heteroatom denoted by X was assumed to correspond with the N_π atom of histamine (see Fig. 18). According to Kier (1968) and De et al. (1980) the N^+-X distance is important for activity. Kier found this distance to be about 4.8 Å in triprolidine (A), whereas De et al. (1980) found a value of 3.7 Å in diphenhydramine (B) and phenbenzamine (C).

solely at the planar conformation of triprolidine. Furthermore, in both studies it is assumed that the N_π nitrogen of histamine has a specific role in the interaction with the H_1-receptor and that the pyridine nitrogen in triprolidine, the ether oxygen in diphenhydramine, and the aniline nitrogen in phenbenzamine fulfil a comparable role. Although there is evidence that the N_π atom of histamine has a specific function (e.g. 2-pyridyl-ethylamine has agonistic activity whereas 3- or 4-pyridyl-ethylamine has no significant activity, Leurs et al., 1991), there is no evidence that antagonists must contain a similar functional atom. E.g., replacing the pyridyl in triprolidine with a phenyl hardly influences activity (Ison, 1971; Ganellin, 1982) Furthermore, very potent antihistamines are known (e.g. diaryl-3-amino-propenes) lacking a function comparable to the heteroatoms in the above mentioned molecules (Casy, 1978). Finally, there is no evidence that the agonist histamine and the histamine H_1-antagonists share a common binding site. Therefore, comparing the N^+-N_π distance of histamine with the (N^+-heteroatom) distance of an antagonist to derive the histamine bioactive conformation at the H_1-receptor is not justified.

Comparison of crystal structures

Generally, crystal structure conformations belong to the low-energy conformations accessible in solution or in vacuo. Therefore, investigations on crystal structures can give valuable information, especially if structures of semi-rigid compounds are available. Borea et al. (1986) presented a study regarding the crystal structures of 14 classical H_1-antagonists covering the five classes shown in Fig. 2. The previously described QSAR studies indicated the two aromatic rings and basic nitrogen atom to be involved in receptor binding. Therefore, Borea et al. investigated the relative position of these functional groups in the 14 structures, i.e. the distances d_1 and d_2 between N^+ and the respective centers of gravity of the two rings, and the mutual distance d_3 of these two centers (Fig. 20).

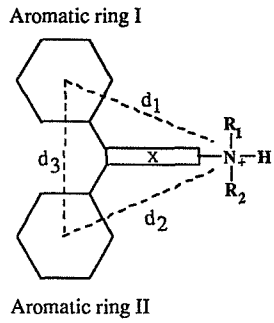

Figure 20. Distances calculated by Borea et al. (1986): d_1 and d_2 are the distances between the protonated nitrogen atom and the centroids of the two aromatic rings; d_3 is the distance between these two centroids.

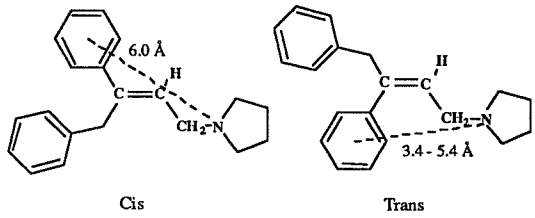

Figure 21. Structures of cis and trans isomers of 1-aryl-1-benzylprop-1-en-3-amines. The difference in activity between both isomers is explained by Borea et al. (1986) with differences in the distance between the nitrogen atom and the centroid of the phenyl ring.

Previously, it had been observed that in crystal structures of several H_1-antagonists (aminopropane derivatives) the distance between the protonated nitrogen (N^+) and the centroid of one of the aromatic rings is about 6 Å (James et al., 1971; 1974; Witiak et al., 1971). Borea et al. observed that in the 14 X-ray structures d_1 and d_3 are remarkably constant, i.e. 6.20 ± 0.15 Å and 4.90 ± 0.24 Å, respectively, whereas d_2 appeared to be more variable ranging from 5.3 to 6.8 Å. According to the authors, the allowed variability of d_2 is in agreement with the observation that in diphenhydramines (Fig. 5) one aromatic ring can be removed without a complete loss of activity (Rekker, 1982). However, on removing this second ring activity drops about 100-fold indicating that it does contribute to receptor binding.

The almost constant d_1 value of 6.2 Å is in agreement with the observation that in the active cis-isomers of 1-aryl-1-benzylprop-1-en-3-amines (Fig. 21) the distance between the aryl group (trans with respect to the amine) and N^+ is about 6Å, whereas in the inactive trans-isomers d_1 ranges between 3.4 and 5.4 Å (depending on the conformation).

A study on crystal structures alone has its limitations. In the report of Borea et al. (1986), a variable d_2 in contrast to an almost constant d_3 was found. This information leads to conflicting conclusions: the invariability of d_3 indicates the importance of the second aromatic group, whereas the variability of d_2 indicates the same ring to be unimportant. This contradiction teaches that a comparison of crystal structures can give misleading information on the importance of certain groups. Molecular modeling studies are needed to derive all low-energy conformations unless the compounds are completely rigid. Borea et al. (1986) considered two antagonists, cyproheptadine and cyclizine (Fig. 2), which the authors assumed to be rigid. However, recent studies indicate that both compounds display some flexibility (Sadek et al., 1990; Van Drooge et al., 1991).

Summarizing, the distance d_1 between one aromatic aromatic ring and N^+ seems to be important in classical H_1-antagonists and should be around 6.2 Å. This confirms the importance of the so-called 'trans'-ring. Conclusions on the relative orientation of the second so-called 'cis'-ring (reflected by d_2 and d_3) are not yet justified.

Receptor mapping studies

Naruto et al. (1985) investigated seven classical H_1-antagonists comprising most classes of Fig. 2. In their study a model of the H_1-receptor is presented based on superimposing functional groups with concomitant energy minimization of the molecules. The two aromatic rings, the protonated nitrogen (N^+) and, if present, a heteroatom in the chain connecting N^+ and the aromatic rings (e.g. ether O in diphenhydramine) were considered to be the functional groups. In addition to these seven antagonists, histamine was fitted having only two functional groups, N^+ and $N\pi$. The molecules were matched in their preferred minimum energy conformation (White force field, Search algorithm). The 3-D arrangement of the four functional groups (two ring systems, N^+ and heteroatom) defines a model for the H_1-receptor binding site.

Although the followed approach seems to be sound, some points of criticism remain. First, the results of the superimposement should have been evaluated, i.e. the compounds should match in a low-energy conformation and the distance between the corresponding functional groups should be acceptably small. Although the first criterium was fulfilled, no information was given on the second one. Secondly, the compounds were superimposed starting from their global minimum conformation so that only conformations similar to this minimum will be found. Thirdly, the two aromatic rings were represented by their centroids only. Therefore, a model in which the two aromatic rings are oriented perpendicular to each other cannot be differentiated from a model in which the two rings run parallel. Furthermore, as also no rigid compounds were studied the pharmacophoric model is far from unique. Finally, there is no evidence that the agonist histamine and the H_1-antagonists share a common binding site.

Recently, Sleevi et al. (1991) derived a probable binding conformation for the antihistamine rocastine (Fig. 4E). A quasi-equatorial boat conformation corresponding to one of the two experimentally determined (NMR) minor contributing conformers matched well with the above mentioned four-element pharmacophore of Naruto et al. (1985). Molecular mechanics calculations (MMX) indicated that the energy of this conformer is only 1.3 Kcal/mol above the global minimum represented by the experimentally determined major conformer in solution. In the superimposement, the pyridine ring of rocastine matches an aromatic ring of the pharmacophore, the ether oxygen overlays the heteroatom and the protonated amine nitrogen is located at the N^+ site.

This match is supported by the available SAR data. As also observed for classical H_1-antagonists, rocastine requires a small tertiary amine substituent for optimal potency. Similarly, replacement of the ether oxygen by either a sulfur, methylene or a methylamino group diminishes activity. Further support was obtained from SAR data on newly prepared

chlorpheniramine analogues. Chlorpheniramine was one of the compounds used to derive the 4-element pharmacophoric model. The increase in potency on introduction of a chloro substituent at the pyridine 7-position of rocastine parallels the SAR associated with the chlorphenyl group of chlorpheniramine.

Although rocastine can be fitted well on the pharmacophoric model of Naruto et al. (1985) and SAR data support this match, the above-mentioned points of criticism on the model of Naruto remain valid. Furthermore, due to the flexibility of the N^+ containing side chain of rocastine, this compound can be fitted on several other models too.

Because of the limitations of the model of Naruto et al. (1985), a reinvestigation on the H_1-antagonist binding site was started within our laboratory (Van Drooge et al., 1991). A thorough literature study was carried out in order to find highly rigid and active H_1-antagonists. Three semi-rigid compounds were found: cyproheptadine, triprolidine and phenindamine (Fig. 22A-C) of which cyproheptadine is the most rigid one. In the studies of Naruto et al. (1985) and Borea et al. (1986), the crystal structure conformation of cyproheptadine, or a very similar one, was assumed to bind at the H_1-receptor. However, the molecule contains some flexiblity in its piperidylene ring (Fig. 22). Besides the chair conformation, also other conformations are possible as recently confirmed by Sadek et al. (1990) with NMR, molecular mechanics and quantum chemical techniques.

In order to determine the bioactive conformation of cyproheptadine (Fig. 22A), phenindamine and triprolidine (Fig. 22B, C) were fitted on low-energy conformations of cyproheptadine. It was concluded that in the receptor-bound conformation the piperidylene ring of cyproheptadine probably has a boat conformation. This contrasts the chair conformation of the crystal structure which was used in the above described studies. Subsequent studies have already shown that various non-classical and/or non-sedative H_1-antagonists (e.g. terfenadine, Fig. 3; astemizole; Fig. 4) can be fitted in this model.

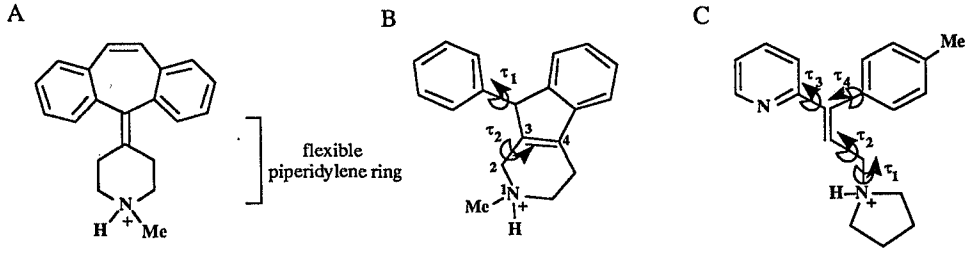

Figure 22. Structures investigated by van Drooge et al. (1991): (A) cyproheptadine; (B) phenindamine; (C) triprolidine. In case of cyproheptadine the flexibility of the piperidylene ring was investigated, whereas in case of phenindamine and triprolidine the flexibility of the marked dihedral angles was investigated.

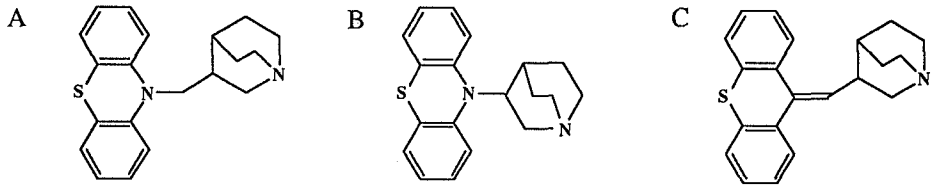

Figure 23. Structures of mequitazine (A), IBF28145 (B) and IBF20007 (C) (Barbe et al., 1983).

Modeling with respect to the sedative potential of H1-antagonists

An important, unwanted side-effect of H_1-antagonists is their sedative activity. Barbe et al. (1983) and Pèpe et al. (1989) performed modeling studies in order to reveal the structural properties determining the sedative properties of H_1-antagonists, since - at the time these studies were performed - it was not clear why some antihistaminic compounds are sedative and others are not.

Barbe et al. (1983) studied the conformational properties of mequitazine and two derivatives (IBF28145 and IBF20007, Fig. 23). Mequitazine, a semi-rigid phenothiazine derivative, has been reported to be a non-sedative H_1-antagonist (Uzan et al., 1979; LeFur et al., 1981). IBF28145 is a reasonably potent, but sedative H_1-antagonist; IBF20007 is only a weak H_1-antagonist but is more sedating than IBF28145. The minimal energy conformations of these three compounds were compared to accessible conformations of other phenothiazines. According to the authors phenothiazines with an extended chain connected to the nitrogen atom of the tricyclic system can access six limit conformations (Galy et al., 1980). It was observed that low-energy conformations of the three above mentioned compounds corresponded to either limit conformation **1**, **3** or both (Fig. 24). Also the crystal structure of the H_1-antagonist chlorpromazine (also a phenothiazine derivative) and the global minimum conformation of mepyramine (Fig. 2) were compared to limit conformations **1** and **3**.

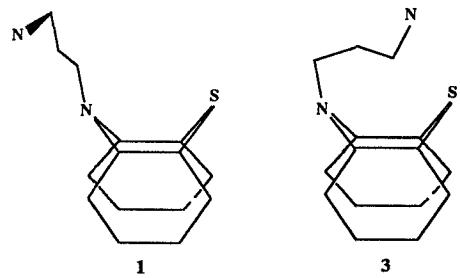

Figure 24. Limit conformations **1** and **3** of phenothiazines. It is suggested by Barbe et al. (1983) that similarity with conformation **1** predicts sedative activity, whereas similarity with conformation **3** predicts H_1-antagonist activity.

It appeared that the specific relative orientation of the nitrogen atom with respect to one aromatic ring in limit conformation **3** is also observed in mequitazine, IBF28145 and mepyramine; the specific orientation of the nitrogen atom with respect to the second aromatic ring in limit conformation **1** is also found in IBF28145, IBF20007, chlorpromazine and mepyramine. The authors therefore hypothesized the existence of a distinct histamine receptor (called 'H3-receptor', although this is not the one named H3-receptor later on by Arrang et al., 1983), which is responsible for sedative activity and to which structures bind if they bear similarity to limit conformation **1**. Regular H_1-antagonistic activity was assumed to result from a similarity to limit conformation **3**. So it was explained why mequitazine only has H_1-antagonistic activity (similarity to only conformation **3**), IBF28145 and mepyramine both have H_1-antagonistic and sedative activity (similarity to both conformations **3** and **1**), and IBF20007 only has sedative activity (similarity to only conformation **1**).

With regard to this modeling study, some critical remarks can be made. Firstly, the authors did not discuss that H_1-antagonistic activity of chlorpromazine could not be predicted correctly (no similarity to conformation **3**). Furthermore, the authors did not mention which conformations of the studied compounds were compared to limit conformations **1** and **3** which makes it difficult to evaluate their results. Finally, the results of Barbe et al. (1983) are in line with the hypothesis in the early eightees that there might exist two subtypes of histamine H_1-receptors. However, other studies (Leysen, 1991; Ter Laak, 1992; Chapter 3) have shown that evidence for this hypothesis is very weak and that probably other factors (i.e., BBB penetration, serum protein binding) determine the sedative effects of H_1-antagonists.

The second study with respect to the sedative potential of H_1-antagonists actually was an indirect study as Pèpe et al. (1989) investigated antidepressant drugs, which predominantly act on certain noradrenergic and serotonergic receptors. The sedative activity of these compounds was explained by action on a histamine receptor.

By superimposing antidepressants on the agonist serotonine two active conformations of serotonine were derived. Since the sedative activity of antidepressants was proposed to be mediated by a histamine receptor (Quach et al., 1979) also the agonist histamine was investigated. It was found that a low-energy conformation of histamine and one of the two active conformations of serotonine had similar molecular electrostatic potentials (MEPs). Therefore, this conformation of histamine was proposed to be the active conformation of histamine at the histamine receptor explaning the sedative potential of antidepressants and possibly also of H_1-antagonists. Because only low-quality energy calculations were used and agonists were compared with antagonists the importance of this study with respect to the sedative potential of H_1-antagonists remains questionable.

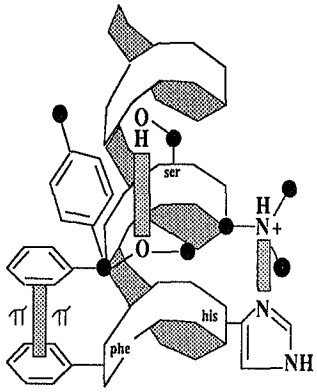

Figure 25. Early H_1-receptor model presented by Rekker et al. (1971). The antagonist diphenhydramine interacts with three amino acids constituting part of an α-helical structure: a Ser interacts with the ether oxygen of the antagonist, a His interacts with the protonated amine nitrogen, and a Phe interacts with the unsubstituted phenyl ring; the second methylated phenyl ring does not interact with the receptor. Histamine was assumed to bind at the same site, its imidazole interacting with the Phe, the protonated amine with the His, and the N_π of the imidazole ring with the Ser. Current views indicate that H_1-receptor agonists and antagonists do not necessarily bind at the same site. Concerning the diphenhydramine-derivatives, QSAR data have been collected providing evidence that both rings interact with the receptor, one of them possibly with a Phe, that the amine interacts with a negative charge on the receptor, and that the ether oxygen is not necessarily stabilized by the receptor (see text).

Conclusions from molecular modeling studies

The deduction of the active conformation of histamine by Kier (1968) and later by De et al. (1980) is based on the unproven idea that H_1-receptor agonists and antagonists bind at the same site and with the same type of functional groups. Also in the early model presented by Rekker et al. (1971) agonists and antagonists were assumed to occupy similar sites. Although the latter model is based on early SAR data on diphenhydramines and contains several contraversional statements compared to those done in later QSAR studies, this work is noticeable in that the authors suggest the ligands to interact with a pseudo receptor which was presented as an α-helical structure (Fig.25). Although at that moment rather speculative, this model is remarkable in view of the current consensus concerning the existence of seven transmembrane α-helical regions in G-protein-coupled receptors (GPCRs).

Since in the theoretical studies of Kier (1968) and De et al. (1980), not all low-energy conformations of the studied antagonists were considered, the importance of either one of the proposed active conformations of histamine can be doubted for this reason. The same criticism applies to the superimposement of crystal structures of rather flexible H_1-antagonists by Borea et al. (1986). However, remarkable consistent distances between proposed functional groups

were found and indicate a probably crucial distance of about 6 Å between the protonated nitrogen and the aryl ring which is likely to be the 'trans'-ring.

Two models (Naruto et al., 1985; Van Drooge et al., 1991) were derived for the histamine H_1-antagonist binding site both using cyproheptadine as a template molecule. However, only the model derived by Van Drooge et al. can possibly claim to be a unique model as only in this case the flexibility of the template and the superimposed molecules was considered. The use of two semi-rigid compounds (phenindamine, triprolidine) appeared to be essential for the deduction of a plausible location of the basic nitrogen. Especially this study of Van Drooge et al. (1991) has laid the foundation for further modeling studies on histamine H_1-antagonists (Chapter 7, this thesis).

CHAPTER 7

THE HISTAMINE H_1-RECEPTOR ANTAGONIST BINDING SITE

A STEREOSELECTIVE PHARMACOPHORIC MODEL BASED UPON (SEMI-)RIGID ANTIHISTAMINES AND INCLUDING A KNOWN INTERACTION SITE ON THE RECEPTOR

A.M. ter Laak, J. Venhorst, G.M. Donné-Op den Kelder and H. Timmerman (J. Med. Chem. (1995) 38, 3351-3360.*

Summary

A new pharmacophoric model for the H_1-antagonist binding site is derived which reveals that a simple atom to atom matching of compounds is not sufficient anymore but that interacting residues from the receptor need to be included. To obtain this model, the bioactive conformations of several (semi-)rigid classical histamine H_1-receptor antagonists have been investigated (cyproheptadine, phenindamine, triprolidine, epinastine, mequitazine, IBF28145 and mianserine). In general, these antihistamines contain two aromatic rings and a basic nitrogen atom. A previously derived pharmacophoric model with the nitrogen position fixed relative to the two aromatic rings no longer appears to be suitable for describing the H_1-antagonist binding site. A procedure is described which allows for significant freedom in the position of the basic nitrogen of the histamine H_1-antagonist. The area accessible to the basic nitrogen is confined to the region accessible to its counterion on the histamine H_1-receptor, i.e. the carboxylate group of Asp^{116}. The basic nitrogen is assumed to form an ionic hydrogen bond with this aspartic acid whose C_α- and C_β-carbons are fixed with respect to the protein backbone. Via this hydrogen bond the directionality of the acidic proton of the antagonist is taken into account. Within our computational procedures an aspartic acid is coupled to the basic nitrogen of each H_1-antagonist considered; the carboxylate group is connected to the positively charged nitrogen via geometric H-bonding restraints obtained from a thorough database search (CSD). Also to the basic nitrogen of the pharmacophore an aspartic acid is coupled (to yield our new template). In order to derive a model for the H_1-antagonist binding site, the aromatic ring systems of the antagonists and template are matched according to a previously described

procedure. Subsequently, the C_α- and C_β-carbons of the aspartic acid coupled to the H_1-antagonists are matched with those of the template in a procedure with allows the antagonist and the carboxylate group to adapt their conformation (and also their relative position) in order to optimize the overlap with the template. A six-point pharmacophore is derived different from the previously determined one, which has stereoselective features and is furthermore able to distinguish between the so-called 'cis'- and 'trans'-rings mentioned in many (Q)SAR studies on H_1-antagonists. Due to its stereoselectivity, the model is able to designate the absolute bioactive configuration of antihistamines such as phenindamine (S), epinastine (S) and IBF28145 (R). A further merit of this study is, that a model is obtained which includes one amino acid from the receptor. Since this amino acid has been identified to be Asp^{116}, tools are now available to dock the antagonists with the aspartic acid coupled to the nitrogen in a homology model of the receptor while matching the coupled aspartate with Asp^{116} of the protein. The most likely (energetically favourable) binding site for the antagonists can then be determined by allowing for rotation around the C_α-C_β bond while leaving the position of C_α and C_β unchanged. Since several homology models can be build for the protein depending on the alignment chosen, the likelihood of the binding site and especially the (dis)agreement with (Q)SAR and biological data will give clues for the most probable 3D-model (i.e. alignment) of the protein (studies in progress). The underlying approach of including known interacting amino acids from the receptor into the pharmacophore is of general importance for verifying protein models with limited reliability such as models derived for G-protein-coupled receptors from bacteriorhodopsin.

Introduction

For several decades almost all compounds with known histamine H_1-blocking activity shared a common chemical structure consisting of two neighbouring aromatic rings and a side chain with a basic nitrogen (see e.g. Fig. 1). Although initially the expectations for the therapeutic use of these so-called 'classical' histamine H_1-antagonists against allergic disorders were very high, the application of these drugs has been rather limited, mainly because of severe central side effects, especially sedation.

In the last decade new H_1-antagonists became available which lack sedative effects, probably due to their limited passage of the blood-brain barrier (Timmerman et al., 1992). The chemical structures of these drugs (e.g. astemizole, temelastine, terfenadine, mequitazine, epinastine, cetirizine and loratadine) often deviate from the basic structure of classical antihistamines. Recently, a study on a series of sedating and non-sedating H_1-blockers demonstrated that non-sedative H_1-antagonists fulfil specific lipophilicity criteria which prevent them from brain penetration (Ter Laak et al., 1994).

For the purpose of rational drug design based on structure-activity information, one is confined to data mainly concerning so called classical antagonists (Ter Laak et al., 1992). QSAR studies indicate that para-substitution with a small lipophilic group (i.e. -CH_3, -Cl) is favourable for only one of the two aromatic rings of classical H_1-antagonists (Fig. 1). Based on a comparison with diphenyl-aminopropene analogues (e.g. triprolidine **3**, Fig. 1) the latter ring is called the 'cis'-ring (Ison et al., 1973). The aromatic character of this ring seems to be indispensable for H_1-activity. In contrast, the second aromatic 'trans'-ring can be replaced by non-aromatic lipophilic groups (e.g. cyclohexyl) without drastic effects on H_1-blocking activity. Obviously, the different receptor environment of the two ring systems is responsible for the stereoselectivity observed for many H_1-antagonists, e.g. the trans-isomer of triprolidine **3** is 1000 times more active than the cis-isomer and the R-isomer of **8** (4-methyl-diphenhydramine, Fig.1) is 100 times more active than the S-isomer (Ison et al., 1973; Harms et al., 1975).

Three-dimensional models describing the structural features of histamine H_1-receptor antagonists are generally based upon the semi-rigid and potent H_1-antagonist cyproheptadine **1** (Borea et al., 1986; Naruto et al., 1985; Van Drooge et al., 1991). Most of the early 3D-models were derived from flexible H_1-antagonists for which only one conformation was considered (crystal structure (Borea et al., 1986) or global minimum (Naruto et al., 1985)). In later years, when lack of CPU time was not so much an issue, Van Drooge et al. derived a five-point pharmacophore by matching low-energy conformations of the semi-rigid and potent H_1-antagonists phenindamine (**2**) and triprolidine (**3**) on six template conformations of cyproheptadine (**1**) (Van Drooge et al., 1991). This non-stereoselective model describes the relative position of two aromatic rings and a basic nitrogen atom derived from **1** with the piperidylene ring in the so-called 'boat3' conformation.

Initially, the present study focused upon the accomodation of (semi)rigid H_1-antagonists in the above mentioned five-point pharmacophore. However, due to unsatisfactorily results we had to establish a new pharmacophore. The final model comprises a residue from the protein (an Asp), contains 6 pharmacophoric recognition points and is stereoselective. These results might have important implications for rational drug design.

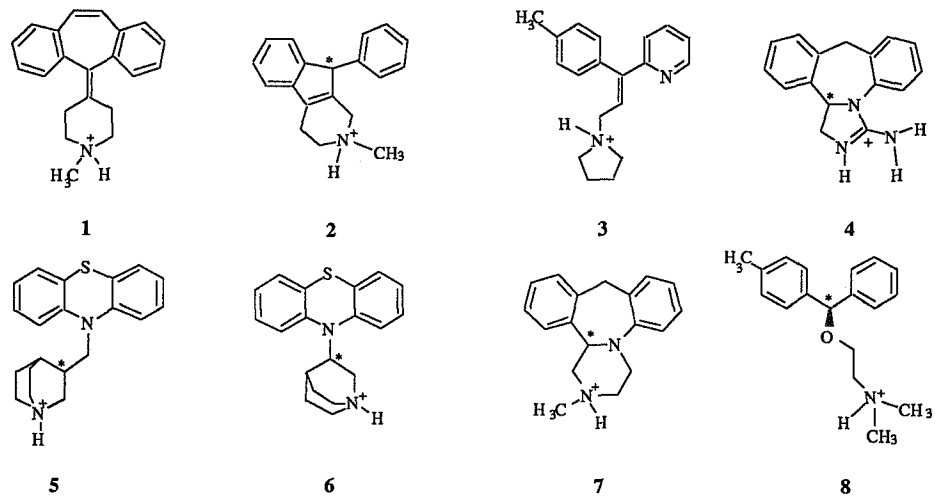

Figure 1. Histamine H_1-antagonists used for the development of the H_1-antagonist binding site model: cyproheptadine (**1**), phenindamine (**2**), trans-triprolidine (**3**), epinastine (**4**), mequitazine (**5**), IBF28145 (**6**), mianserine (**7**) and (R)-4-methyl-diphenhydramine (**8**).

Strategy

Initially, we tried to accomodate (semi-)rigid and potent H_1-antagonists in the five-point pharmacophore derived earlier by Van Drooge et al. (1991) (Fig. 1, compds. **4** to **7**). However, not in all cases the basic nitrogen could be matched with the position of the template nitrogen in the 'boat3' conformation of **1**. Therefore, we allowed for a certain flexibility in the position of the nitrogen. For this purpose, an approach was developed which considers the several interaction possibilities between a basic nitrogen and an aspartic acid in the histamine H_1-receptor. The introduction of an aspartate is based upon the observation that aspartic acids are present within transmembrane domains II and III of the histamine H_1-receptor (Yamashita et al., 1991; Fujimoto et al., 1993; De Backer et al., 1993; Traiffort et al., 1994). A recent site-directed mutagenesis study on the histaminergic H_1-receptor confirms our hypothesis by showing that the aspartate conserved in all aminergic G-protein coupled receptors (Asp^{116}) interacts with the classical H_1-antagonist mepyramine (Ohta et al., 1994). In our strategy we further assume that the 'cis' and 'trans' rings of **1**-**7** have a preferred orientation within the antagonist binding site resulting in a relative position towards the C_α- and C_β-carbons of the aspartate. Furthermore, we implicitly assume that all antagonists considered bind to the same site. These considerations lay the foundation for our model.

In order to derive a new pharmacophoric model for the H_1-antagonist binding site, low energy conformations of compounds **2-7** (Fig. 1) are superimposed on six previously derived low-energy conformations of cyproheptadine (Van Drooge et al., 1991). An aspartate is coupled to the basic nitrogen of each H_1-antagonist and to the template conformations of **1** (Fig. 2A). For this coupling geometric constraints are used obtained from a statistical analysis on the Cambridge Structural Database with respect to the specific type of hydrogen bonding interaction. In a first step the aromatic rings of the antagonist and the template are matched. Subsequently, a 'unique' position for the C_α- and C_β-atoms of the aspartate is derived by allowing for flexibility in the asparate side chain. In this second step the position of the ring systems of the antagonist are fixed relative to those of the pharmacophore while the C_α's and C_β's are being matched (Fig. 2C). An additional advantage of this approach compared to all previous approaches, is that the directionality of the hydrogen bond between the basic nitrogen and the aspartate is automatically taken into account. The stereoselectivity of the model is determined in a final step, where the flexible and stereoselective isomers of **8** are used to designate the 'cis' and 'trans'-ring of our pharmacophoric model. Our approach results in a new and stereoselective pharmacophore defined by the relative positions of the C_α- and C_β-carbons of an aspartic acid of the H_1-receptor (probably Asp^{116}; Ohta et al., 1994) positioned relative to the 'cis'-ring and 'trans'-ring of classical histamine H_1-antagonists.

Methods

Investigated compounds (Fig. 1).

In the present modeling study we consider the (semi-)rigid histamine H_1-antagonists **1-7** and the stereoselective isomers of 4-methyl-diphenhydramine **8**. From displacement experiments with [^{3}H]mepyramine (guinea pig cerebellum membranes, 30 minutes), it is evident that compounds **1-4** and **7-8** are potent H_1-antagonists with apparent pK_i values of 9.27 (**1**), 8.20 (**2**), 8.78 (**3**, cis/trans mixture), 8.85 (**4**), 9.07 (**7**) and 7.91 (**8**, R/S mixture) (Ter Laak et al., 1993). The high potencies of these compounds have also been measured in other, different, and therefore incomparable functional systems, for example pA_2(**1**)=9, pA_2(**2**)=8.8, pA_2(**3**)=9.9, -log(IC_{50})(**4**)=8.8 and pA_2(**8**)=8.7 (in contrast to a value of 6.8 for the S-isomer of **8**) (Trottier and Malone, 1969; Augstein et al., 1972; Harms et al., 1975; Waringa et al., 1975; Fügner et al., 1988). The potencies for **5** and **6** are reported by Barbe et al. (1983) being 7.2 and 7.3, respectively (pED_{50} values measured on guinea pig ileum). However, a binding constant of 8.0 was reported for **5** by Leysen et al. (1991) (displacement of [^{3}H]mepyramine from guinea pig cerebellum membranes after 30 minutes) and even higher pIC_{50} values (up to 9.0) were measured at longer incubation times.

The activities of the potent and (semi-)rigid H_1-antagonists used in this study are measured in different pharmacological systems and should therefore not be compared quantitatively. For this reason no relative weights were given to the compounds during the construction of the present H_1-antagonist model.

Conformational analyses

All calculations on H_1-antagonists **1-8** were performed on the protonated species (Fig. 1). The low-energy conformations of compounds **1** to **3** were obtained from Van Drooge et al. Compounds **4-8** were built using the modeling package ChemX January 1990 (Chemical Design Ltd., Oxford, U.K.). The three possible conformations of the extremely rigid compound **4** were built from scratch and optimized within ChemX. In contrast, the starting conformations of compounds **5-8** were built using crystal structures (complete structures or fragments) from the Cambridge Structural Database (diphenhydramine, code JEMJOA; mianserine, code BUCVAW; phenothiazine group, code MPMPTZ; 3-quinuclidinyl group, code BEWDOW10). Subsequently, MacroModel (Version 2.5) was used for molecular mechanics conformational analyses on compounds **5-8**. If neccesary, the ring closure bond option was used (**5-7**) and a large number of conformations was generated by changing all rotatable bonds with increments of 30°. The conformations were energy optimized with an MM2 force field (NBRF optimization) with the program Batchmin 2.7 in order to obtain the low-energy conformations. The partial charges used in these calculations stem from the classical definition of bond dipoles and thus correspond to the MM2 dipoles exactly. For the dielectric constant a value of 1 was used (BatchMin User Manual Version 4.0, Columbia University, New York).

Fitting procedures

In the present study two different fit procedures were used. The first approach corresponds to the one described earlier in which two neighbouring aromatic rings and a basic nitrogen of an H_1-antagonist are matched with a five-point pharmacophore (Van Drooge et al., 1991). Each aromatic ring is represented by two dummy atoms, 1.8 Å above and below the centroid of the ring. Low energy conformations of compounds **2** to **8** are superimposed on the template conformations of **1** (the pharmacophore) using restrain constants of 10 kcal/(mol.Å2) for the dummies and 100 for the basic nitrogen. The compounds are first matched by allowing for global rotations and translations only (rigid match). In a subsequent step (flexible fit) the internal nonbonded energy of the antagonist is minimized with respect to user-defined *exocyclic* bonds (compound **2**: 1 rotatable bond, **3**: 4 bonds, **5**: 2, **6**: 1 and **8**: 6) and the penalty functions (restraints). *Endocyclic* nitrogen inversion was considered for compounds

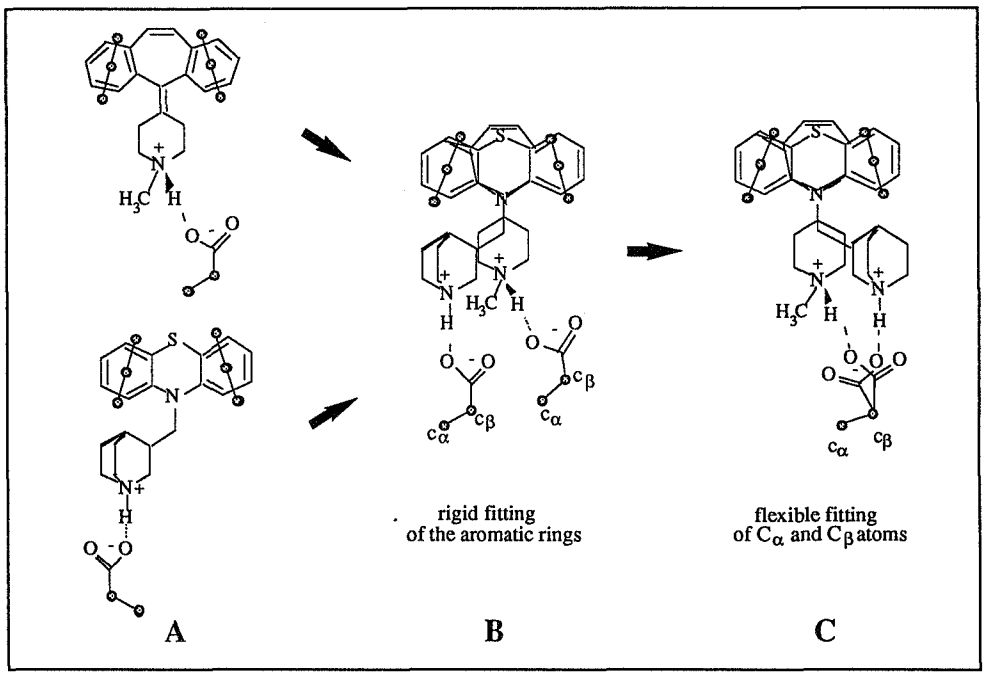

Figure 2. Strategy for fitting histamine H_1-antagonists: (A) an aspartic acid is connected to the protonated amino group of the template (cyproheptadine) and a second H_1-antagonist (here mequitazine) according to geometric constraints obtained from a statistical analysis on CSD data. (B) The aromatic rings are superimposed in a rigid fit. (C) In a flexible fit procedure the C_α- and C_β-atoms of the aspartic acids are matched. The dotted line represents the virtual axis in the N-H···O bond.

4-7. Also the nonplanar ring system(s) of compounds **1**, **2**, **4** and **7** can adopt several distinct low-energy conformations due to variations around *endocyclic* bonds. Therefore, all low energy conformations of compounds **1-2** and **4-7** generated manually or with Macromodel, were considered separately in the above procedure. For compounds **3** and **8** (only exocyclic torsions) only the GES was considered since the restrain constants are high enough to overcome the small energy barriers present.

In the second approach an aspartic acid is coupled to the basic nitrogen of each investigated antagonist and the template conformations of **1** (Fig. 2A). The carboxylate group is connected to the protonated tertiary amino group (all compounds except **4**) according to geometric constraints derived from a statistical analysis (GSTAT88) on 23 structures describing the interaction between a tertiary amino and a carboxylate (Cambridge Structural Database, Oct. 1992; codes BINRIZ, BPAMAL, COYNEJ, CUXKOV, DEBALB, FAKCAV, FUGSAB, FUPDOJ, GEXWOV, JAPCAE, JEGWUN, JIDLAJ, JIFYOM, KEXXUG, KEXYAN, LOXSYC10, MPSIHF, NICSAL,

PRPENG, PYCHMA, SEBROG, TALCOY, VIPRIV, Fig. 3A). X-ray structures were accepted when the N··O distance was smaller than 3.4 Å.

Compound **4** contains a fused guanidino group. A carboxylate is connected using geometric constraints derived from a study on arginine-carboxylate interactions (Allen et al., 1979). The geometry of this bidentate complex (i.e. a methylguanidino-aspartate moiety) was optimized using *ab initio* methods (GAMESS, STO-3G basis set). Although this so-called 'anti II' geometry involves two hydrogen bonds, only one is used to connect the aspartate to the guanidino of **4** (Fig. 3B) (see Discussion). In all cases (**1-8**) a virtual bond was established between the hydrogen donating nitrogen of the antagonist and the hydrogen accepting oxygen of the aspartate in order to allow for rotation around this bond in the flexible fit procedure.

In the first step (rigid fit) the aromatic ring systems are matched defining each ring by two dummies (Fig. 2B). In the subsequent flexible fit, the C_α- and C_β-carbons are matched with restrain constants of 50 kcal/(mol.Å2) (six-point pharmacophore, Fig. 2C). In addition to the above-mentioned user-defined rotatable bonds, also the above *virtual* bond and the C_β-C_γ bond of the aspartate group are allowed to rotate.

Twelve different template conformations of **1** are considered (Table 1). The pharmacophore is asymmetric as the aspartate distorts the mirror symmetry in cyproheptadine. Consequently, both stereoisomers of chiral compounds **2** and **4-8** are considered. The criteria used to accept matching results are: at maximum 0.5 Å for the distances between the centroids of the rings (dI and dII), 0.5 Å for the distances between the basic nitrogens (five-point pharmacophore), at maximum 35° for the angles between the rings (aI and aII) and 0.3 Å for the deviation between C_α's and C_β's (six-point pharmacophore). Final conformations with an energy ($\Delta\Delta H_f$ or ΔE) >10 kcal/mol above GES (global energy structure) were rejected.

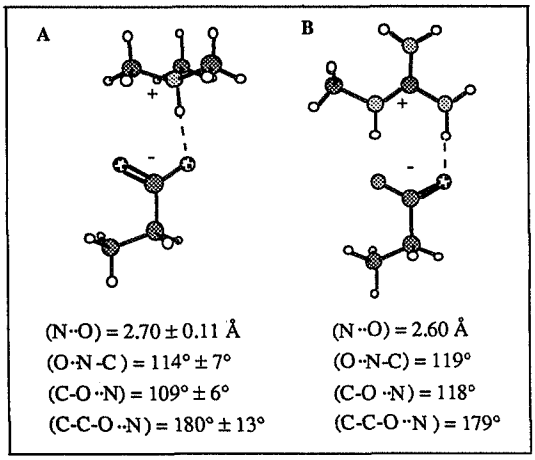

Figure 3. Representation of the applied geometric constraints for the ionic hydrogen bonding interaction between an aspartic acid and (A) a protonated tertiary amino group or (B) a protonated guanidino group. Fig. 3A represents the average hydrogen bond geometry with standard deviations (n=23) from a statistical search (GSTAT88) in the Cambridge Structural Database. Fig. 3B represents an optimized hydrogen bond geometry using ab initio methods (GAMESS, STO-3G basis set).

Energy calculations

All low energy conformations and those obtained after fitting were eventually geometry optimized with the quantum chemical program GAMESS-UK (STO-3G basis set) on an IBM-RISC System 6000 (Dupuis et al., 1980; Guest and Kendrick, 1993). The two aromatic rings, the basic nitrogen and the attached proton were restrained to a fixed position during optimization of the fitted conformation in order to preserve the match with the pharmacophore. A single point SV 4-31G calculation was done to obtain accurate *ab initio* energies. For compounds **1**, **2** and **4** all low energy conformations were refined *ab initio*. For the more flexible compounds **3** and **5-8**, the MM2 global minimum was asumed to yield the *ab initio* global minimum (GES).

The *ab initio* energy difference, (ΔE), between the fitted conformation and the corresponding global minimum was calculated. In contrast to the (semi-)rigid compounds, the GES of the flexible compound **8** contains an intramolecular hydrogen bond. As no information is available on the presence of an internal H-bond in solution, the global energy conformation of **8** is assumed to be the lowest energy conformation without such an H-bond. This energy was used for determining ΔE values.

Table 1. Low energy conformations of cyproheptadine (side views) with their relative ab-initio energies (ΔE) in kcal/mol (GAMESS U.K., SV 4-31G basis set).

	chair1eq	chair2eq	boat3eq	boat4eq	boat5eq	boat6eq
	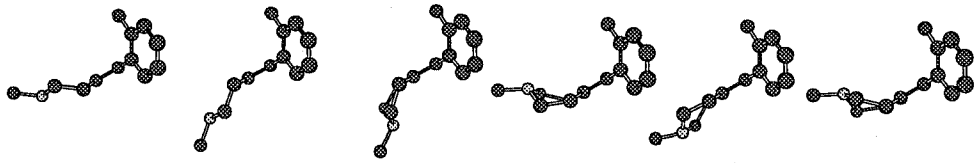					
ΔE	0.00	1.36	6.08	3.35	6.06	3.36
	chair1ax	chair2ax	boat3ax	boat4ax	boat5ax	boat6ax
	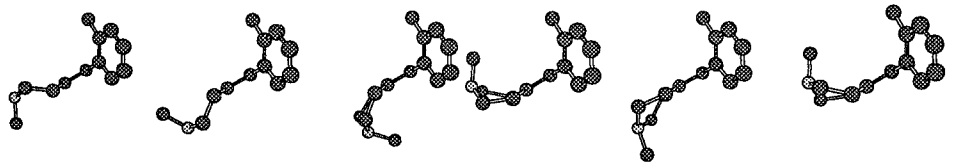					
ΔE	2.42	3.80	8.11	4.99	6.29	4.98

Results and Discussion

Conformational analysis of cyproheptadine (1)

The major reason for using the potent H_1-antagonist **1** as a template molecule is its relative rigidity. The piperidylene ring may attain 2 chair and 4 boat conformations. Including the two different attachments of the N-methyl group being either axial or equatorial, 12 different low-energy conformations are obtained (Table 1). The relative energies of these *ab initio* optimized conformations indicate 'chair1' with the N-methyl group equatorial ('chair1eq') to be the GES; this conformation is also found in X-ray studies on cyproheptadine.HCl (Birknes, 1977). More importantly, ^{1}H-NMR experiments show that 'chair1eq' and 'chair2eq' are the only conformations observed in solution ($CDCl_3$) occuring in a ratio of about 4 : 1 (Sadek et al.,1990). This is in agreement with our data in Table 1.

Consequently, three conformations of **1** were considered as possible templates: the 2 conformations observed in solution ('chair1eq' and 'chair2eq'), and 'boat3eq', since this conformation has earlier been suggested to be the bioactive conformation (Van Drooge et al., 1991).

Conformational analysis of phenindamine (2) and triprolidine (3)

The chiral molecule phenindamine **2** and the non-chiral *trans*-triprolidine **3** are two semi-rigid H_1-antagonists (Van Drooge et al., 1991). It is worthwhile mentioning that the double bond of phenindamine can either be in the piperidyl ring (as in **2**, Fig. 1) or in between the phenyl group and the piperidyl ring (not shown). Thus phenindamine can be isolated in two epimeric forms, their ratio depending on the salt or free base being formed (Branch et al., 1987). The structural formula **2** depicted in Fig. 1 is representative for the commercially available phenindamine tartrate salt and is reported to be the bioactive epimer of phenindamine (Plati and Wenner, 1955). Taking into account the likely epimerization of phenindamine, it is interesting to note that no one has ever separated stereoisomers of **2**. Since no information is available on the absolute configuration of the bioactive epimer **2**, both stereoisomers of **2** were considered in the fitting procedures.

The relative rigidity of **2** is due to the limited flexibility of the fused tetrahydropyridine ring and the presence of only one freely rotatable bond. We found that the tetrahydropyridine ring can adopt two different boat-like conformations which differ only 0.5 kcal/mol in internal energy (*ab initio*, SV 4-31G basis). As the N-methyl group can either be in the favourable equatorial or in the less favourable axial position, 4 local minima are obtained all within 1.8 kcal/mol from the global minimum (Fig. 4).

The conformational analysis for **3** was performed for the *trans*-isomer only as it displays a 1000-fold higher antihistaminic potency than the *cis*-isomer (Waringa et al., 1975). The conformational analysis resulted in a global energy structure (GES) with the α-pyridyl ring and the double bond almost in the same plane (deviation 22°); the substituted phenyl ring is rotated out of this plane by ~ 59° degrees. Considering the many low-energy conformations of **3** (4 rotatable bonds) and low energy barries between the local minima, only the GES was used for flexible fitting purposes. Starting from other low-energy conformations for this specific compound is unlikely to influence the final results.

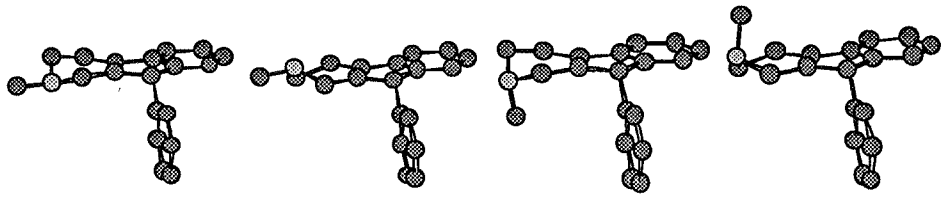

A. 0.00 kcal/mol B. 0.49 kcal/mol C. 1.27 kcal/mol D. 1.82 kcal/mol

Figure 4. The fused tetrahydropyridine ring of phenindamine (2) can adopt two different twisted boat conformations which differ about 0.5 kcal/mol in internal energy (ΔE). The N-methyl group can either be in the preferred equatorial (A and B) or in the axial position (C and D).

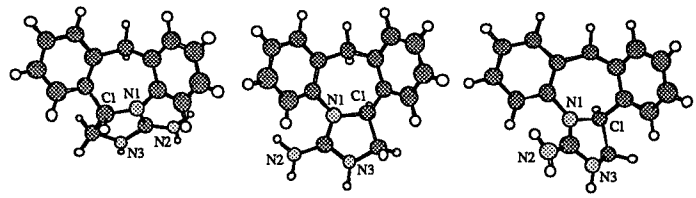

A. 0.00 kcal/mol B. 8.19 kcal/mol C. 8.15 kcal/mol

Figure 5. Three conformations of the protonated S-isomer of epinastine (**4**) with their ΔE values (GAMESS U.K., SV 4-31G basis set). See text for further explanation.

Conformational analysis of epinastine (4), phenothiazine derivatives (5) and (6) and mianserine (7)

Epinastine **4** is a highly rigid and basic compound with a pK_a of ~11 (Ter Laak et al., 1994). All theoretically possible conformations and tautomers of the protonated form were built and optimized. Tautomers with two protons at nitrogen N2 (see Fig. 2) are at least 36 kcal/mol more favourable (SV 4-31G basis set) than tautomers with the acidic proton attached to N1 or N3. Therefore, the tautomer depicted in Fig. 2 is likely to be the bioactive protonated species of **4**. In total, six conformations are possible for **4**: A, B and C for both the S- and R-isomer (Fig. 5). The large *ab initio* energy differences (Table 5) indicate that conformation A is probably active at H_1-receptors. It is important to mention that **4** can be methylated at N3 (thereby replacing the N3-hydrogen) without loosing antihistamininic activity; in fact this compound is 2 times more active than **4** itself (Walther et al., 1990). Based on this observation, the ionic hydrogen bond between **4** and a protein carboxylate is assumed to be formed with N2 and not with N3.

As the tricyclic phenothiazine part of compounds **5** and **6** is symmetric, interconversion of the thiazine ring does not yield different conformations. However, inversion of the ring nitrogen can put the side chain either in an axial or equatorial orientation. The local minima resulting from the conformational analyses show that the equatorial position is energetically more favourable than the axial position (*ab initio* ΔE: 3.40 kcal/mol for **5** and 1.44 kcal/mol for **6**). For fitting purposes, both the equatorial and axial conformers were considered. Since the carbon connecting the tricyclic part with the 3-quinuclidinyl group is chiral, also two stereoisomers were investigated.

Although **7** has no freely rotatable bonds, the molecule is relatively flexible. The fused piperazinyl ring can be oriented either axial or equatorial at both the central chiral carbon and the neighbouring nitrogen (nitrogen inversion). As a consequence, this ring can attain several chair, boat and twisted boat conformations. Conformational analysis yielded six low-energy piperazinyl chair conformations. The GES is a chair with the N-methyl in an equatorial position (SV 4-31G basis set). All low-energy conformations of both stereoisomers were considered in the fitting procedures.

Table 2. Quality of the fits of compounds **2-7** fitted on the 'chair1eq', 'chair2eq' and 'boat3eq' conformations of cyproheptadine [a]

Compound	fitted on 'chair1eq'		fitted on 'chair2eq'		fitted on 'boat3eq'	
	N-N[b] (Å)	ΔE[c] (kcal/mol)	N-N[b] (Å)	ΔE[c] (kcal/mol)	N-N[b] (Å)	ΔE[c] (kcal/mol)
(1) cyproheptadine	--	0.00	--	1.36	--	6.08
(2) phenindamine[a]	0.25	1.82	0.26	2.47	0.17	2.93
(3) triprolidine[a]	0.19	11.61	0.18	10.82	0.08	10.30
(4) epinastine	3.62	0.00	2.57	0.00	1.64	0.00
(5) mequitazine	0.67	0.49	0.04	1.48	0.78	4.63
(6) IBF28145	0.80	5.06	0.94	1.85	0.13	5.43
(7) mianserine	2.35	3.70	1.57	3.70	0.89	6.60

[a] Results for 'chair1eq' and 'chair2eq' are taken from Van Drooge et al. (1991); [b] The distance between the basic nitrogen atoms with respect to cyproheptadine; [c] Ab initio energies of the fitted conformations relative to the global minimum energy (ΔE) (Gamess U.K., SV 4-31G basis set).

Pharmacophores with a fixed position for the basic nitrogen atom

In our present study we found that antihistaminics **4-7** could not be fitted on the previously assumed bioactive 'boat3eq' conformation of cyproheptadine (Van Drooge et al., 1991). Although the aromatic rings of **4-7** match the pharmacophore well, the nitrogens of especially **4**, **5** and **7** hardly match (distance > 0.8 Å ; Table 2). Since we also found that the energy difference between 'boat3eq' and the global minimum 'chair1eq' is substantially higher with *ab initio* methods (ΔE: 6.08 kcal/mol) than with semi-empirical methods (MNDO: $\Delta\Delta H_f$: 2.7 kcal/mol), we questioned the validity of 'boat3' as a possible pharmacophore (Van Drooge et al., 1991).

Based on the above observations, we focused our attention on 'chair1eq' and 'chair2eq', which are found in solution and have the lowest *ab initio* energies. We found that only a limited number of compounds could be fitted on the two five-point pharmacophores represented by 'chair1eq' (compounds **2** and **3**) and 'chair2eq' (compounds **2**, **3** and **5**). In all other combinations (i.e. **4**, **6** and **7** on 'chair2eq', and **4** to **7** on 'chair1eq') the fit of the basic nitrogens was not satisfactorily (N-N distances > 0.5 Å ; Table 2).

In summary, the fit results, partially presented in Table 2, demonstrate that the basic nitrogen of H_1-receptor antagonists does not occupy one particular position in space with respect to the position of the aromatic rings. We therefore conclude that a five-point pharmacophore derived from either 'chair1eq', 'chair2eq', or from 'boat3eq' is not sufficient to describe the histamine H_1-antagonist binding site.

A pharmacophore with a variable position for the basic nitrogen atom

From the results presented in Table 2, we anticipated that the ionic interaction between the basic nitrogen and the H_1-receptor should have a relatively large positional freedom. We therefore introduced an aspartic acid into our model with which the antagonists interact and which represents an aspartic acid from the receptor. A penalty function was put on the position of the C_α and C_β carbons; no restraints were put on the basic nitrogens. This approach results in a six-point pharmacophore, while at the same time sufficient attention is given to the directionality of the acidic proton.

For the construction of the new pharmacophore, the experimentally observed 'chair1eq' and 'chair2eq' were considered as templates. In the two conformations the acidic hydrogens have opposite directions which is illustrated by the different positions of the aspartate in Fig. 6. Since preliminary fitting experiments showed that the acidic hydrogens in 'chair1ax' and 'chair2ax' point approximately in a similar direction as in the above investigated 'chair 2eq' and 'chair1eq' conformation (see Table 1), these axial conformations were not further investigated. It was observed that when more than 3 molecules were fitted simultaneously according to the method described in Fig. 2, the number of restraints prevented the C_α and C_β atoms to converge. Therefore at maximum two compounds out of the series **2-7** were simultaneously fitted on **1**.

Especially in the fits of **4** and **5** on **1**, a clear distinction is present between the quality of the fits on 'chair1eq'and 'chair2eq' (Fig. 6). Within our pre-defined criteria, epinastine **4** does not fit on 'chair1eq' due to the low fit quality of the aromatic rings; the centroids have at best deviations of 0.42 (ring I) and 1.00 Å (ring II), respectively. Moreover, the C_β of the aspartate coupled to **4** could not be superimposed on the C_β of 'chair1eq' (C_β-C_β > 0.8 Å). Also the steric overlap between **4** and 'chair1eq' is low (VDW_{excl}=44.7 Å^3) compared to the overlap between **4** and 'chair2eq' (VDW_{excl}=34.2 Å^3).

Comparable results were found for mequitazine (**5**). Although the rings of **5** fitted well on both templates, the aspartate of **5** did not match the 'chair1eq' aspartate (C_β-C_β > 0.8 Å). Moreover, the 3-quinuclidinyl side chain of **5** is forced to occupy a spatial area different from the one occupied by the piperidylene side chain of the template 'chair1eq' (VDW_{excl}=73.8 Å^3; Fig. 6). In contrast, the fit on the 'chair2eq' aspartate appeared to be much better (C_α-C_α = 0.07 Å, C_β-C_β = 0.15 Å) and resulted in a large steric overlap (VDW_{excl}=8.0 Å^3).

The fit results for both **4** and **5** on **1** indicate that the bioactive conformation of **1** most probably is 'chair2eq'. Low energy conformations of **4** (GES) and **5** (ΔE =1.94 kcal/mol; Table 3) have a good steric overlap with a low-energy conformation of **1** ('chair2eq', ΔE=1.36 kcal/mol) with respect to the aromatic rings and the side chains; moreover the three compounds are able to interact with the same carboxylate group.

Our tentative conclusions are supported by the remarkable good fits of compounds **2, 3, 6** and **7** on the six point 'chair2eq' pharmacophore (Table 3); because of the limited flexibility of **2, 6** and **7**, these results were unexpected. Fig. 7 shows the conformations of **2-7** superimposed on 'chair2eq'. The molecules show a good fit with respect to the aromatic rings, relatively compact steric boundaries of the various side chains and only negligible variations in the position of the C_α and C_β-atoms of the postulated aspartic acid. The model shows that the interacting basic nitrogen occupies largely different positions within the antagonist binding site.

Bioactive conformations of the H1-antagonists

In most cases the energy of the best fitting, presumably bioactive, conformation appeared to be very close to the global or a local minimum (Table 3). For example, the final conformation of phenindamine **2** is a slightly distorted version of conformation C (Fig. 4). An acceptable *ab initio* energy of 3.58 kcal/mol above GES was found.

The internal energy of **3** is high relative to GES (ΔE=7.42 kcal/mol, Table 3). This is caused by the inability of the ChemX force field to treat conjugated systems in an appropriate way. The ChemX molecular mechanics force field easily rotates the aromatic rings out of the plane of the conjugated double bond in order to improve the fit, whereas *ab initio* methods assign relatively high energies to these distorted systems. This phenomenon can also be observed when **3** is fitted on the three different conformations of **1** in the absence of an aspartate (Table 2). Even when the restraints on the basic nitrogen or the aspartate are removed, the ring systems of **3** and **1** are hard to match. This suggests that in order to explain the high antagonistic activity of **3**, we might have to assume that the position of one of the rings might be less restricted than that of the second ring. This suggestion is supported by QSAR studies which indicate that the steric boundaries of the 'trans' ring are relatively undefined compared to those of the 'cis' ring (Chapter 6; Ter Laak et al., 1992). The probably unnecessary forced fit of the 'trans' ring of **3** on the 'trans' ring of **1**, explains the relatively high internal energy of **3**.

As a consequence of the above observations, the orientation of the 'trans' ring in compounds **4** to **7** relative to **1**, might also be too restricted. None the less, the ring systems of **4** to **7** fit extremely well on **1** (Table 3). The lowest fit quality is generally found for the more rigid compounds **4** and **7**. This is probably due to the restriction of the N-H··O hydrogen bond angle and the N-H··O-C dihedral angle to their optimal values of 180° (Fig. 2). Since the actual interaction is probably less restricted, it is to be expected that relative internal energies can be slightly overestimated (in the order of a few kcal/mol).

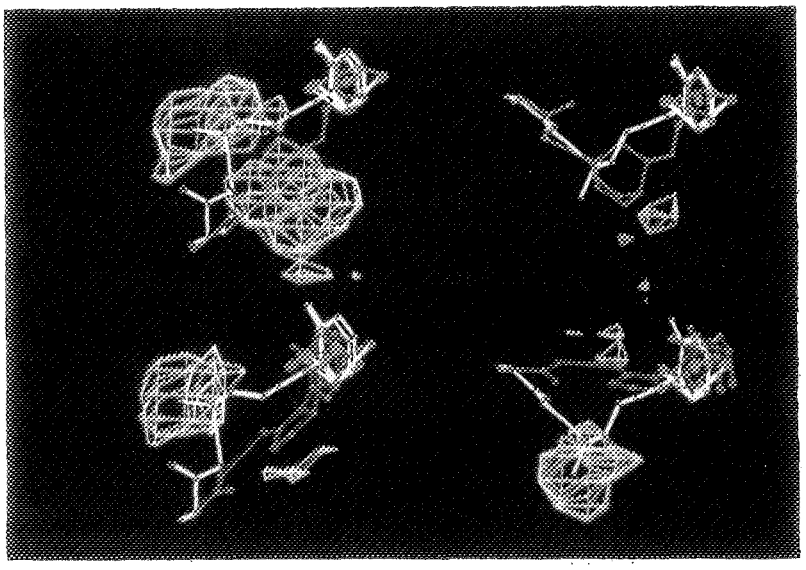

fit of 5

fit of 4

'chair 1eq' 'chair 2eq'

Figure 6. Fits of (R)-mequitazine (**5**, green) and (S)-epinastine (**4**, blue) on two different conformations of the template molecule cyproheptadine (**1**, yellow). Mequitazine (**5**) reveals a much better overlap with 'chair2eq' (upper right) than with 'chair1eq' (upper left) as illustrated by the 'excluded' VDW volumes of the fitted molecules (white). Epinastine (**4**) reveals similar results (lower right and left). Also the quality of the fit for **4** on **1** with repect to the aromatic rings is much better for 'chair2eq' than for 'chair1eq'.

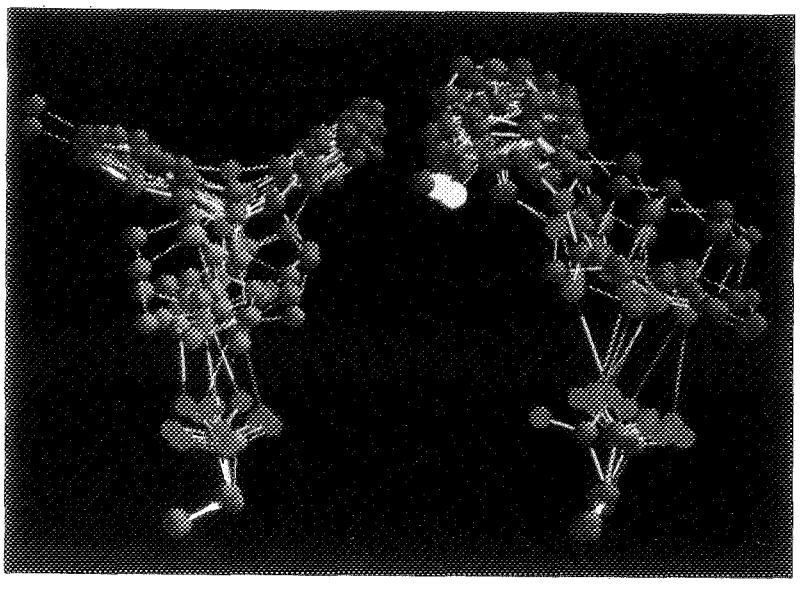

A B

In conclusion, the whole series of (semi-)rigid H_1-antagonists can be fitted well on a 6-point pharmacophore ('chair2eq' coupled to an aspartate) illustrated by high quality fits, low intramolecular energies relative to GES and optimal interaction geometries with an H_1-receptor aspartic acid.

Table 3. Quality of the fits of compounds **2-8** fitted on the 'chair2eq' conformation of cyproheptadine with an aspartate coupled to a basic nitrogen [a]

Compound	dI[b] (Å)	dII[c] (Å)	aI[d] (°)	aII[e] (°)	N-N[f] (Å)	C_α-C_α[g] (Å)	C_β-C_β[h] (Å)	ΔE[i] (kcal/mol)
(1) cyproheptadine	0.00	0.00	0.00	0.00	0.00	0.00	0.00	1.36
(2) phenindamine	0.22	0.37	34.11	4.38	1.16	0.12	0.04	3.58
(3) triprolidine	0.20	0.27	20.29	7.45	1.15	0.09	0.16	7.42
(4) epinastine	0.43	0.29	23.03	31.07	2.04	0.10	0.26	0.00
(5) mequitazine	0.11	0.10	8.41	8.45	0.92	0.07	0.15	1.94
(6) IBF28145	0.24	0.16	17.69	15.75	1.67	0.14	0.20	4.25
(7) mianserine	0.25	0.34	18.31	11.63	1.09	0.33	0.20	2.62
(8) (R)-4-Me-diphenhydramine	0.10	0.09	6.61	6.36	1.11	0.07	0.08	1.88
(8) (S)-4-Me-diphenhydramine	0.16	0.14	5.50	6.17	1.49	0.28	0.25	11.04

[a] All results are with respect to cyproheptadine; [b] Distance between the ring centroids of the 'cis'-rings; [c] Distance between the ring centroids of the 'trans'-rings; [d] Angle between the 'cis'-rings; [e] Angle between the 'trans'-rings; [f] Distance between the basic nitrogens; [g] Distance between the C_α atoms; [h] Distance between the C_β atoms; [i] Ab initio energies of the fitted conformations relative to the global minimum energy (ΔE; GAMESS U.K., SV 4-31G basis set).

Figure 7 (legend). The H_1-antagonists comprising the final H_1-antagonist binding site model; the aspartic acid of the protein is included: red = **1** ('chair2eq'); white = (S)-**2** (Fig. 4); purple = trans-**3**; yellow = (S)-**4** (Fig. 5A); green = (R)-**5** (equatorial); lightblue = (R)-**6** (axial); brown = (R)-**7**; orange = (R)-**8**. (A) 'Front'-view of the model revealing the overlay of the 'cis'-rings (upper-left) and the 'trans'-rings (upper-right) and the fit of the C_α- and C_β-carbon atoms of the aspartate. (B) 'Side'-view (90° rotated) illustrating the variation in the position of the basic nitrogen atom interacting with the aspartic acid.

Definition of the 'cis' and 'trans' ring

One of the aromatic rings of *trans*-triprolidine **3** is substituted with a para-methyl group and has been defined as the 'cis'-ring of H_1-antagonists. We found that the 'cis' and 'trans'-ring of **3** when fitted on **1** cannot be interchanged; in our model, the ring closest to the carboxylate group (smallest distances between the C_α and C_β-atoms of the carboxylate and the centroids of the ring systems) is defined as the 'cis'-ring (Fig. 8).

At this stage of the study, it is important to mention that the model still lacks stereoselectivity, since for none of the chiral compounds (**2** and **4** to **7**) the absolute configuration of the bioactive stereoisomer is known. As a consequence, two pharmacophores are possible: the pharmacophore shown in Fig. 7 and its mirror image.

The pharmacophore with the appropriate stereochemistry can be found by fitting the potent and stereoselective isomers of 4-methyl-diphenhydramine **8** on 'chair2eq'. For both isomers the para-substituted ring was fitted on the 'cis'-ring of 'chair2eq'. Keeping the aromatic rings optimally fitted on the template, only one of the two mirror images of the pharmacophore appeared to be a good template for the most active R-isomer of **8** (1.88 kcal/mol above GES). In contrast, the 100 times less potent S-isomer did not match well with 'chair2eq' unless the side chain was folded (best fit: 11.04 kcal/mol above GES). Fig. 7 and 8 present the pharmacophore in the appropriate configuration. The orientation of the 'cis' and 'trans'-ring of antihistamines with respect to an aspartic acid can therefore be descibed in a three-dimensional and stereoselective pharmacophoric model (Fig. 8).

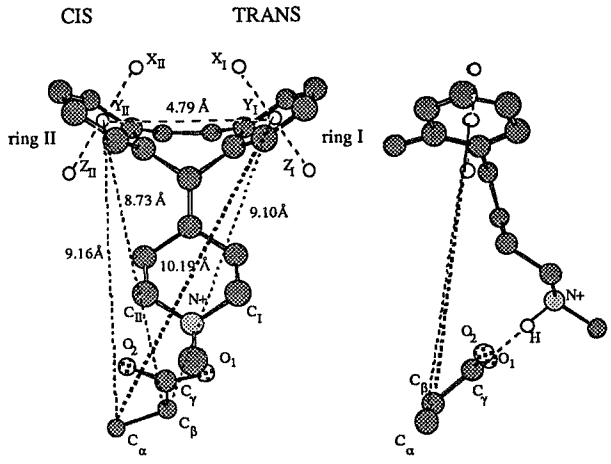

Figure 8. Pharmacophoric model of the histamine H_1-antagonist binding site based on 'chair2eq' of **1** (left: front view; right: side view). Dotted lines connect the C_α and C_β atoms of the aspartate with the centroids of the 'cis'- and 'trans'-ring. The aspartate is defined with respect to cyproheptadine by the distance O_1-N^+ = 2.69 Å , the angles O_1-H-N^+ = 180.0° and O_1-N^+-C_{II} = 114.1° and the dihedral angles $C_\gamma O_1$-N^+-C_I= -177.7°, C_β-$C_\gamma O_1$-N^+ = -179.7° and C_α-C_β-$C_\gamma O_1$= 149.0°.

Qualitative prediction of the stereoselectivity of antihistamines (2), (4) and (6)

Compound **8** made it possible to determine the stereoselectivity of the model; now we can qualitatively predict the absolute configuration of the bioactive stereoisomers of **2**, **4** and **6**. We found that only the S-isomer of **2**, the S-isomer of **4** and the R-isomer of **6** are able to fit the present pharmacophore. The model also designates the phenyl group of phenindamine **2** as the 'cis'-ring. Also the aromatic ring of **4** closest in space to its guanidino group is found to be comparable to the 'cis'-ring (Fig. 8).

Unfortunately, the pharmacophore does not unambiguously predict the stereoselectivity of **5** and **7**. Mequitazine **5** is represented by its R-isomer, whereas the S-isomer fits equally well. This is not surprising, since the chiral center is relatively "far away" from the aromatic ring systems when compared to **6**. Mianserine **7** is represented by its R-isomer, whereas also in this case the miror image (S-isomer) fits equally well. Since in the fits of the R- and S-isomer of **7** the aromatic rings are interchanged, it is not possible to predict the stereoselectivity of **7** and/or designate the putative 'cis' and 'trans'-ring.

The presented pharmacophore enables us to extrapolate the structure activity relationships obtained for classical H_1-antagonists to a 3D-model for (semi)rigid antihistamines. Also less rigid and/or non-classical H_1-antagonists can be fitted in the pharmacophoric model in order to elucidate their stereoselectivity and/or designate their 'cis' and 'trans'-rings. In this way the model will be useful for understanding the binding modes of non-classical antagonists and for the design of new, preferably non-sedating, antihistamines.

Conclusions

A new pharmacophoric model for the histamine H_1-antagonist binding site has been derived which reveals that a simple atom to atom matching of compounds is not sufficient anymore for describing the binding of an extended series of antagonists, but that interacting residues from the receptor need to be included. The new model allows for significant freedom in the position of the basic nitrogen of the histamine H_1-antagonist. The area accessible to the basic nitrogen is confined to the region accessible to its counterion on the histamine H_1-receptor, i.e. the carboxylate group of Asp^{116}. The basic nitrogen is assumed to form an ionic hydrogen bond with this aspartic acid whose C_α- and C_β-carbons are fixed with respect to the protein backbone. Via this hydrogen bond the directionality of the acidic proton of the antagonist is taken into account. A six-point pharmacophore is derived describing the bioactive conformations of cyproheptadine, phenindamine, triprolidine, epinastine, mequitazine, IBF28145 and mianserine.

The merits of this study are:

(1) The pharmacophore is stereoselective and is able to designate the absolute bioactive configuration of antihistamines such as phenindamine (S), epinastine (S) and IBF28145 (R). Since we did not succeed in accomodating the opposite enantiomers of these three compounds, we conclude that the receptor is highly stereoselective for these compounds.

(2) The model is able to distinguish between the so-called 'cis'- and 'trans'-rings mentioned in many (Q)SAR studies on H_1-antagonists.

(3) The bioactive conformation of cyproheptadine is revealed not to be the 'chair1eq' (Naruto et al., 1985; Borea et al., 1986) or 'boat3eq' conformation (Van Drooge et al., 1991), but 'chair2eq'. This has important implications for the docking of cyproheptadine (and other classical H_1-antagonists) into three-dimensional receptor models since the directionality of the proton differs in the three low-energy conformations and cyproheptadine is the basis of our template.

(4) The existence of several low-energy conformations for cyproheptadine indicates that this compound possibly binds to the histamine and muscarine or serotonine receptors in different conformations. This might further explain the different stereoselectivity observed for histamine and muscarine antagonists.

(5) A model is obtained which includes one amino acid from the receptor. Since this amino acid has been identified to be Asp^{116}, tools are now available to dock the antagonists in a homology model of the receptor while matching the aspartate coupled to the basic nitrogen of the antagonist with Asp^{116} of the protein. The most likely (energetically favourable) binding site for the antagonists can then be determined by allowing for rotation around the C_α-C_β bond

while leaving the position of C_α and C_β unchanged. Since several homology models can be build for the protein depending on the alignment chosen (Chapter 8), several possible binding sites will be obtained (one for each 3D-model/alignment). The most probable binding site and therefore the most probable alignment can be attained when the energetics of the binding sites are compared, i.e. does the binding site explain observed biological data such as (relative) affinity values. Furthermore, the properties of the binding site should explain the known (Q)SAR data. These studies will give clues on the most probable 3D-model (i.e. alignment) of the protein. The underlying approach of including known protein interaction sites into the pharmacophore, is of general importance for verifying protein models with limited reliability such as models derived for GPCRs from bacteriorhodopsin. Furthermore, these interaction sites are necessary in case a simple atom to atom matching of compounds is not sufficient anymore to derive a model which can accomodate all investigated compounds. Studies investigating several 3D-models for the H_1-receptor are in progress.

Since our model is able to assign the bioactive stereoisomers of phenindamine (S-isomer), epinastine (S-isomer) and IBF28145 (R-isomer) and further predicts that the receptor binds these enantiomers with high stereoselectivity, we encourage chiral separation of the enantiomers of these compounds for further validation of our model.

CHAPTER 8

MODELING OF THE HISTAMINE H_1-RECEPTOR USING BACTERIORHODOPSIN AS A TEMPLATE

DOCKING OF H_1-ANTAGONISTS INTO VARIOUS H_1-RECEPTOR MODELS

Summary

The first part of this study critically evaluates the use of the 3D structure of bacteriorhodopsin (BR) as a template for G-protein coupled receptors (GPCRs). We demonstrate that results from complete protein models of GPCRs based on BR should be interpreted with care. Nonetheless, H_1-receptor models based on BR have been shown to be relatively successful for the exploration of histamine H_1-agonist binding sites (Chapter 9). In the second part of this study, the histamine H_1-antagonist cyproheptadine (our antagonist template molecule, Chapter 7) is docked into various protein models of the H_1-receptor. Several aromatic amino acid residues are revealed (in domains TM IV and TM VI) which could interact with the aromatic rings of H_1-antagonists. We further found that the positively charged residue Lys^{200} in TM V is suited to interact with a negatively charged carboxylate group present in several non-sedating H_1-antagonists, which form in fact zwitterions. Based upon this observation, zwitterionic compounds may offer advantages as non-sedating H_1-antagonists.

Introduction

Histamine H_1-receptors transduce a primary signal across cell membranes upon stimulation by histamine. Elucidation of the primary amino acid sequence of the histamine H_1-receptor in different species (bovine, Yamashita et al., 1991; rat, Fujimoto et al., 1993; human, De Backer et al., 1993; guinea pig, Traiffort et al., 1994) revealed that the protein is about 480-490 amino acids long and that it is a member of the G-protein coupled receptor superfamily. Receptors of this family transduce their signal via a wide variety of GTP-binding proteins (G-proteins). Upon stimulation of the H_1-receptor, a pertussis toxin-insensitive G-protein (probably a G_q-type protein; Leurs et al., 1995) is activated which results in subsequent stimulation of the

phospholipase C second messenger cascade: phospholipids are degraded to the second messengers inositol-triphosphate (IP_3) and diacylglycerol (DAG), finally resulting in an influx and mobilization of extracellular Ca^{2+} in the cell. The molecular mechanism by which signal transduction takes place is still not elucidated; however, it has been suggested that - upon binding of an agonist - the receptor protein changes its conformation (Weinstein, 1993) and/or translocates protons across the cell membrane (Nederkoorn et al., 1995).

The G-protein coupled receptors (GPCRs) contain seven relatively hydrophobic domains, each 20-25 amino acids long. The three-dimensional structure of GPCRs is probably similar to the structure of the bacterial light-sensitive receptor-protein bacteriorhodopsin (not a GPCR), which also contains seven hydrophobic regions in its primary sequence. Elucidation of the 3D structure of the transmembrane part of bacteriorhodopsin (BR) has revealed that its hydrophobic domains constitute a compact cluster of seven α-helical structures embedded in the hydrophobic cell membrane (Henderson et al., 1990). The recently derived low resolution electron density map of a mammalian GPCR, bovine rhodopsin, has confirmed that the general arrangement of the seven transmembrane domains of GPCRs is similar to the arrangement in BR (Fig. 1) (Schertler et al., 1993). However, soon after, evidence for some (minor) differences in the orientation of helices was obtained (Baldwin, 1993). Despite these small differences, bacteriorhodopsin is often used as a template molecule to build models for GPCRs (i.e., Findlay, 1990; Hibert, 1991) since it is the only seven-helical membrane spanning protein for which a 3D structure is available.

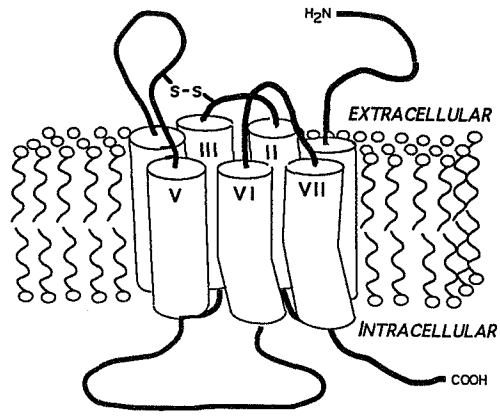

Figure 1. Schematic representation of the 3-D structure of a G-protein coupled receptor embedded in the cell membrane. The N-terminus of the protein is on the extracellular side and the C-terminus on the intracellular side. Three extracellular and three intracellular loops connect the hydrophobic transmembrane domains which form a compact cluster of seven α-helical structures. Conserved cysteine residues probably form a disulfide bond between the first and second extracellular loops.

A recent analysis of the sequence similarities between several aminergic GPCRs has shown that the histamine H_1-receptor is more related to i.e. muscarinergic receptors than to the histamine H_2-receptor (Donnelly, 1994). Moreover, it has been shown that the primary sequence of the histamine H_2-receptor is more homologous to i.e. adrenergic receptors than to the histamine H_1-receptor (Lewell, 1994). Donnelly (1994) concluded that aminergic GPCRs cannot be classified simply in terms of their endogenous ligand. Therefore, it seems likely that the histamine H_1- and H_2-receptors are distantly related proteins for which the binding sites have probably converged in a later step of the evolution (Donnelly, 1994). This observation may have consequences for the design of histaminergic ligands: at least it explains why histamine H_1- and H_2-receptor ligands (both agonists and antagonists) have considerably different structure-activity relationships.

For the purpose of rational design of new selective and potent ligands for the H_1-receptor, the structural information retained in the binding pocket of the receptor is highly required. Therefore, with the primary sequence available, we have built three-dimensional homology models for the histamine H_1-receptor using BR as a template protein. However, during the course of our studies, we found that several critical remarks can be made upon the use of BR as template molecule. These findings are discussed in the first section of this paper, since they are useful for the improvement of GPCR models.

Strategy

In order to obtain insight into the reliability of the results obtained from H_1-receptor modeling, the validity of our template molecule BR is investigated and discussed in Section I. In Section II, various H_1-receptor models - based on different alignments with BR - are evaluated. The H_1-antagonist cyproheptadine is docked into these protein models in order to reveal receptor residues which are possibly important for interactions of classical H_1-antagonists with the receptor. Finally, we also investigated the possible orientation of zwitterionic H_1-antagonists in our protein models, since these compounds are expected to be relatively selective for H_1-receptors.

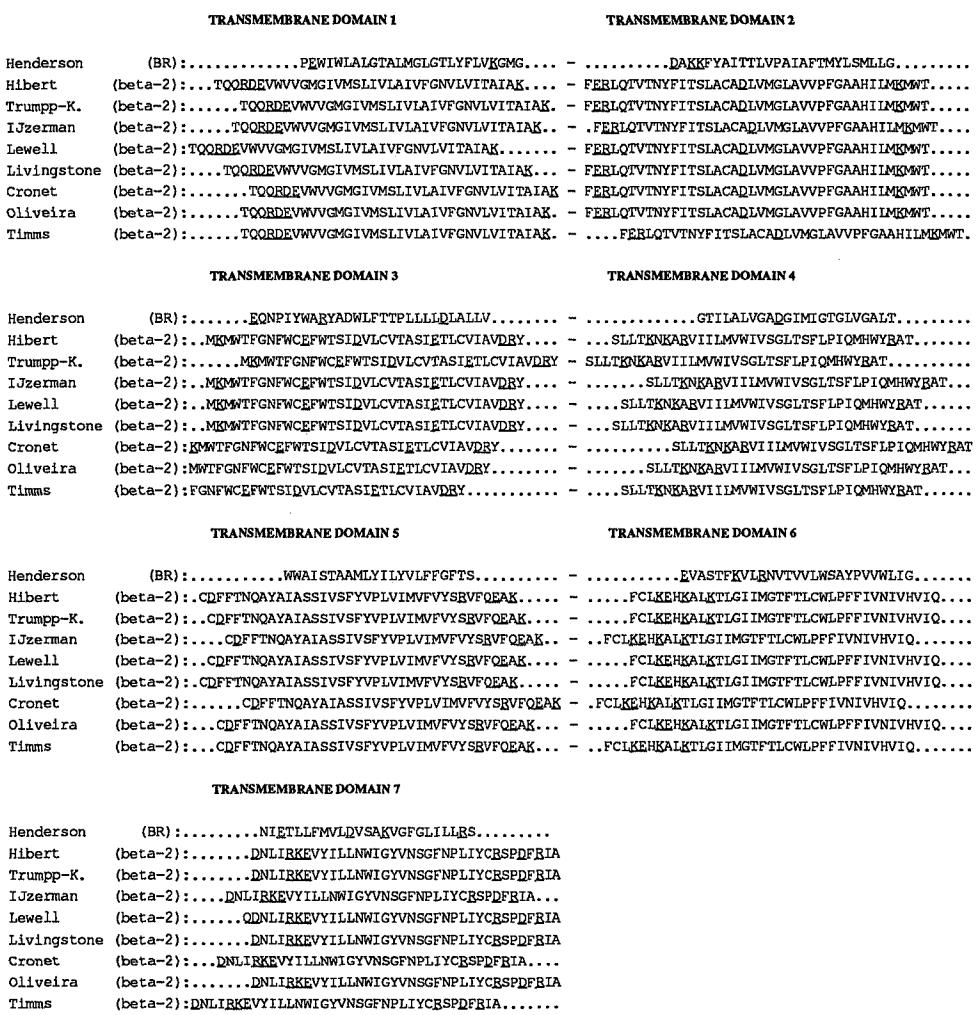

Figure 2. Different research groups use different alignments for homology building of G-protein coupled receptors with bacteriorhodopsin (BR) as a template molecule. Only the amino acid residues of BR for which a three-dimensional structure has been elucidated by Henderson et al. (1990) are shown. For clarity, the aligned GPCR domains are all represented by the primary amino acid sequence of the transmembrane domains of the β_2-adrenergic receptor. However, this was not in all cases the GPCR receptor modelled (Hibert et al. (1991), Trumpp-Kallmeyer et al. (1992) and Oliveira et al. (1993) modelled various aminergic receptors; IJzerman et al. (1992), adenosine receptors; Livingstone et al. (1992), the D_2-receptor; Lewell (1992) and Cronet et al. (1993), the β_2-receptor; Timms et al. (1994), the β_1- and M_2-receptor). Charged amino acids (R, K, D and E) are underlined.

Section I: Modeling of GPCRs based on bacteriorhodpsin

Since 1990, the year in which the 3D structure of BR was elucidated (Henderson et al.), several research groups have used BR as a template molecule to build models of GPCRs; Hibert et al. (1991), Trumpp-Kallmeyer et al. (1992) and Vriend et al. (1993) modelled various aminergic receptors, IJzerman et al. (1992) modelled adenosine receptors, Livingstone et al. (1992) the D_2-receptor, Lewell (1992) and Cronet et al. (1993) the β_2-receptor, Timms et al. (1994) the β_1- and M_2-receptor. The alignments with BR used to build these GPCR models were, however, considerably different (Fig. 2) due to different interpretations and different sources of (pharmacological) information. The present study (Section I) discusses a few different approaches which can be used to construct GPCR models. A multiple sequence alignment of bacterial rhodopsins (not GPCRs) which have a high sequence identity with BR (53-97%) is presented. This alignment gives additional information on the validity of BR as a template molecule for GPCRs. Moreover, it is shown that besides the pharmacological and structural information on a single aminergic receptor, it is also worthwhile to use statistical information from multiple sequence alignments. In Section I, a statistical analysis on the hydrophobicity of 135 aminergic receptors is presented which can be useful for improving the arrangement of transmembrane helices in models of GPCRs.

Section II: Docking of histamine H_1-antagonists

GPCR models are useful to improve the understanding of the structure-activity relationships of these receptors and their ligands. Important interaction sites within the receptor can be identified and the preferred three-dimensional orientation of the functional groups of receptor bound ligands can be determined. When the primary amino acid sequence of the H_1-receptor became available (Yamashita et al., 1991), we redirected our investigations towards protein modeling of the histamine H_1-receptor. Since then, a combination of mutation and receptor modeling studies (Chapter 9) has led to the discovery of different binding sites for H_1-agonists in the H_1-receptor (Leurs et al., 1994, 1995; Ter Laak et al., 1995b). For H_1-antagonists, however, a modeling study on the molecular interactions with the H_1-receptor is relatively complicated. Although the orientation of the aromatic rings of H_1-antagonists can be defined with respect to an aspartic acid of the receptor (Ter Laak et al.,1995a), the directions of other interactions, presumably charge transfer interactions with aromatic residues of the receptor, are still poorly defined (Hunter et al., 1991).

In the present study we docked a previously derived H_1-antagonist pharmacophoric model (cyproheptadine coupled to a receptor aspartate residue, Chapter 7) into different models of the H_1-receptor (Ter Laak et al., 1995a-b). Since there is no consensus on the relative orientation of transmembrane helices in GPCR models, three different alignments from literature were used to build models for the H_1-receptor based on BR (Trumpp-Kallmeyer et al., 1992; Oliveira et al., 1992; Timms et al., 1994). Cyproheptadine (being a representative template molecule for classical H_1-antagonists) is docked into each model knowing that Asp^{116} in TM III (Fig. 5) is involved in the binding of both H_1-receptor agonists as well as antagonists (Ohta et al., 1994). Taking into account the geometric constraints of our small molecule pharmacophore and the flexibility of Asp^{116}, cyproheptadine offers a unique possibility for energy optimization of the ligand-receptor complex. These investigations have led to the observation that various aromatic amino acid residues of the receptor, mainly in transmembrane domains IV and VI, can interact via e.g. charge-transfer interactions with the so-called 'cis' and 'trans'-rings of H_1-antagonists. For the purpose of designing new non-sedating H_1-antagonists, subsequent modeling studies focused on docking of zwitterionic H_1-antagonists (next paragraph).

Docking of zwitterionic non-sedating H_1-antagonists

Decreasing lipophilicity (log $D_{oct,pH7.4}$) is one of the possibilities to prohibit brain penetration and reduce unwanted sedative effects of H_1-antagonists (Ter Laak et al., 1994). For the development of non-sedating H_1-antagonists, the introduction of a negatively charged carboxylate group provides a good possibility to obtain less lipophilic H_1-antagonists. Such zwitterionic compounds will have low log $D_{oct,pH7.4}$ values. Indeed, several existing zwitterionic H_1-antagonists are devoid of unwanted CNS properties and have profound H_1-antagonistic activity (i.e., acrivastine, Leighton et al., 1983; cetirizine, Ramaekers et al., 1992; levocabastine, Stokbroekx et al., 1986). Recently, more research groups have introduced acidic moieties into classical H_1-antagonists such as mianserine and setiptiline (which is the carbon-carbon unsaturated analogue of mianserine), while retaining good H_1-antagonistic activity (Muramatsu et al., 1994). Also, one of the metabolic products of terfenadine contains a carboxylic acid group without losing affinity for H_1-receptors (Garteiz et al., 1982).

The positively charged residue Lys^{200} present in TM V appears to be a unique residue for the histamine H_1-receptor (Leurs et al., 1995; Ter Laak et al., 1995b). This Lys^{200} can establish highly favourable interactions with carboxylate groups. Therefore, we investigated three zwitterionic H_1-antagonists (acrivastine, cetirizine and the major metabolite of terfenadine, Fig. 6) upon the feasibility of such an interaction within the H_1-receptor models.

Methods

Alignments

Primary sequences of bacterial rhodopsins (Fig. 2: bac = PDB:1BRD; arc = S14731; han = A35002; hah = S26161; sen = S09277) were obtained from the PDB and PIR databases using the CAMMSA facilities of the CAOS/CAMM center in Nijmegen, The Netherlands. A multiple sequence alignment of these sequences was obtained with PILEUP using the method of Needleman and Wunsch (1970).

The alignment of 135 aminergic receptors (Oliveira et al., 1993) has been extracted from the file server of EMBL (Heidelberg, Germany). Amino acid types were counted with a spread sheet program (Excel 4.0) to produce hydrophobicity plots (hydropathy indices from Kyte and Doolittle, 1970) and average percentages of charged amino acids at each position in the alignment. A recommended window of 21 amino acids was used to identify the midpoints of transmembrane domains (Engelman, 1986).

Homology building

Coordinates of an H_1-receptor model based on the alignment of Oliveira et al. (1993) were obtained from the EMBL file server (Heidelberg, Germany). Two other H_1-receptor models were built with the standard homology building options of the protein modeling package QUANTA/CHARMm (Quanta 4.0, Molecular Simulations Inc., Burlington, MA, USA). Energy minimizations of the protein models were performed with the CHARMm force field (Version 22). In these procedures, the steepest descent method was used for fast optimization followed by the conjugated gradient method for further and more accurate geometry optimization until the energy convergence criterion (0.10) was reached. Energy optimizations were performed with a distance-dependent dielectric constant, a non-bonded cut-off value of 12 Å and a cut-off value of 4.5 Å for hydrogen bond interactions. The optimization was performed in five phases allowing gradual relaxation of the protein. In the first phase, all atoms were fixed with an harmonic restraint of 100 kcal/(mol.Å2) except for all hydrogen atoms. Subsequently, restraints on atoms of the residue side chains were removed (phase 2), followed by atoms of the helical backbone (phase 3). Harmonic restraints on the backbone atoms were then decreased from 100 kcal/(mol.Å2) to 10 (phase 4) and 0 (phase 5) except for the 14 backbone atoms at both ends of the seven helices.

Docking procedures

H_1-antagonists were docked using the H_1-antagonist pharmacophoric model of Ter Laak et al. (1995a). This model describes the 3D topology of the 'cis' and 'trans' aromatic rings of the 'equatorial chair2' conformation of cyproheptadine with respect to the positions of the C_α and C_β carbon atoms of an aspartate residue from the receptor. The C_α and C_β carbon atoms of the pharmacophore were matched with the corresponding atoms of Asp^{116} in the receptor model. Subsequently, the atoms of Asp^{116} in the protein became redundant and were deleted. Rotation was carried out along the C_α-C_β bond of the replaced Asp^{116} until cyproheptadine was positioned in the receptor in an energetically favourable orientation.

Modeling of zwitterionic compounds

The zwitterionic compounds acrivastine, cetirizine and the acidic metabolite of terfenadine (Fig. 6) were built from scratch and optimized with ChemX (Jan. 1993). The structures were then docked into the H_1-receptor model onto the already present template cyproheptadine according to a previously described fit procedure (Ter Laak et al., 1995a). Cyproheptadine became redundant and was deleted. Subsequently, all freely rotatable bonds in Lys^{200} and in the side chains of the zwitterionic H_1-antagonist were taken into account in an extensive conformational analysis (MacroModel / AMBER force field; Weiner et al., 1986) in order to investigate the feasibility of the proposed interaction.

Results and Discussion

Section I: Modeling of GPCRs based on bacteriorhodopsin

The first and most crucial step in obtaining a GPCR model is to derive an acceptable alignment with BR. Differences in approach and interpretation have led to a wide variety of alignments and GPCR models in literature (Fig. 2). In the following paragraphs, several approaches (i.e., homology, hydrophobicity and geometrical rules) used to derive a feasible arrangement of the transmembrane helices in GPCR models, are discussed.

Homology

The sequence identity between BR and GPCRs is very small (6-11% identity, Hibert et al., 1991) and it can be questioned whether sequence homology alone can be used to construct an acceptable alignment of GPCRs with BR. Therefore we have investigated the homology of bacteriorhodopsin with a variety of 36 different GPCRs (unpublished results of our group). The primary sequence of each hydrophobic domain of these receptors was aligned separately with BR to identify the region with the highest homology score. We observed that the GPCR transmembrane sequences (numbered I to VII, Fig. 1) did not align with the corresponding domains of BR but with other TM domains. Pardo et al. (1992) did similar observations and suggested that exons containing the genetic information of different transmembrane domains could have been shuffled in the proposed evolution of the GPCR gene from BR. However, we found that for each transmembrane domain the obtained alignment is ambiguous; the highest similarity score did not differ significantly from several other scores obtained with slightly different alignments. Thus, we concluded that any alignment of a GPCR with BR based on similarity scores can be misleading since there simply is no sufficient homology. For the purpose of constructing a GPCR model, other information than sequence similarity is needed to obtain the appropriate translational (perpendicular to the membrane) and rotational (along the helical axes) orientation of the seven transmembrane helices within the membrane (next paragraphs).

Translational orientation of membrane helices

One possibilty to identify the relative depth of helices within the membrane is to use information from hydrophobicity plots (Kyte and Doolittle, 1982). However, even hydrophobicity plots obtained with an optimal window lenght of about 20 amino acids (Engelman, 1986) do not always reveal where transmembrane segments start and end, because the peaks are too broad for an unambiguous assignment; the hydrophobic sequence often exceeds the length necessary for spanning the hydrophobic membrane. Moreover, it should be realized that GPCRs are embedded in mammalian cell membranes which are considerably thicker than the bacterial membranes containing BR. The ambiguity of hydrophobic patterns in transmembrane domains is one of the major reasons why various research groups have derived different alignments for the purpose of building GPCR models (Fig. 2).

A second approach to identify the relative depth of helices is to incorporate information from correlated mutations (Oliveira et al., 1993). This approach is based on the assumption that a simultaneous mutation at two residue positions in the amino acid sequence of a GPCR is

(A)

```
                          TM DOMAIN 1                          TM DOMAIN 2
bac     ......QAQT GRPEWIWLAL GTALMGLGTL YFLVKGMGVS DPDAKKFYAI TTLVPAIAFT MYLSMLLGYG LTMVPFGG.............
arc     LQAGFDLLND GRPETLWLGI GTLLMLIGTF YFIARGWGVT DKEAREYYAI TILVPGIASA AYLAMFFGIG VTEVELASG...........
han     QRELFEFVLN DPLLASSLYI NIALAGLSIL LFVFMTRGLD DPRAKLIAVS TILVPVVSIA SYTGLASGLT ISVLEMPAGHFAEGSSVMLG
hah     GAQSAAAVRE NALLSSSLWV NVALAGIAIL VFVYMGRTIR PGRPRLIWGA TLMIPLVSIS SYLGLLSGLT VGMIEMPAGH.........
sen     .........M DAVATAYLGG AVALIVGVAF VWLLY.RSLD GSPHQSALAP LAIIPVFAGL SYVGMAYDIG TVIV.............

                    TM DOMAIN 3          TM DOMAIN 4                    TM DOMAIN 5
bac     ....EQNPIY WARYADWLFT TPLLLLDLAL LVDADQGTIL ALVGADGIMI GTGLVGALTK .VYSYRFVWW AISTAAMLYI LYVLFFGFTS
arc     ....TVLDIY YARYADWLFT TPLLLLDLAL LAKVDRVTIG TLIGVDALMI VTGLIGALSK .TPLARYTWW LFSTIAFLFV LYYLLTSLRS
han     GEEVDGVVIM WGRYLTWALS TPMILLALGL LAGSNATKLF TAITFDIAMC VTGLAAALTT SSHIMRWFWY AISCACFLVV LYILLVEWAQ
hah     ALAGEMVRSQ WGRYLTWALS TPMILLALGL LADVDLGSLF TVIAADIGMC VTGLAAAMTT SALLFRWAFY AISCAFFVVV LSALVIDWAA
sen     ....NGNQIV GLRYIDWLVT TPILVGYVGY AAGASRRSII GVMVADALMI AVGAGAVVTD ..GTLKWALF GVSSIFHLSL FAYLYVIFPR

                          TM DOMAIN 6                          TM DOMAIN 7
bac     KAESMRPEVA STFKVLRNVT VVLWSAYPVV WLIGSEGAGI .VPLNIETLL FMVLDVSAKV GFGLILLRSR AIFGEAEAPE PSAGDGAAAT SD..
arc     AAAKRSEEVR STFNTLTALV AVLWTAYPIL WIVGTEGAGV .VGLGIETLA FMVLDVTAKV GFGFVLLRSR AILGETEAPE PSAGADASAA D...
han     DAK..AAGTA DMFNTLKLLT VVMWLGYPIV WALGVEGIAV .LPVGVTSWG YSFLDIVAKY IFAFLLLNYL TSNESVVSGS ILDVPSASGT PAID
hah     SAS..SAGTA EIFDTLRVLT VVLWLGYPIV WAVGVEGLAL VQSVGVTSWA YSVLDVFAKY VFAFILLRWV ANNERTVAVA GQTLGIMSSD D...
sen     VVPDV.PEQI GLFNLLKNHI GLLWLAYPLV WLFGPAGIGE .ATAAGVALT YVFLDVLAKV PYVYFFYARR RVFMHSESPP APEQATVEAT AAD.
```

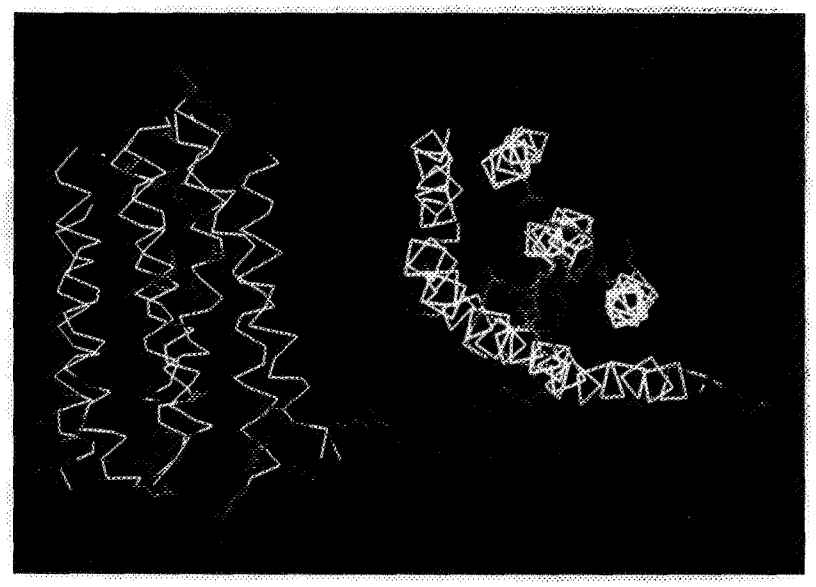

(B) (C)

Figure 3. (A) Multiple sequence alignment of the amino acid sequences of five bacterial rhodopsins from the PDB (bac = bacteriorhodopsin (Halobact. hal.); arc = archaerhodopsin (Halobact. sp.); han = halorhodopsin (Natronobact. ph.); hah = halorhodopsin (Halobact. hal.); sen = sensory rhodopsin (Halobact. hal.)). Charged residues (R, K, D, E) are underlined. (B) Side view of the overlap of five bacterial rhodopsin models (bac, arc, han, hah and sen) based on the three-dimensional structure of bacteriorhodopsin (Henderson et al., 1990). The seven transmembrane domains are represented by the backbone atoms of amino acids homologous to the elucidated residues in bacteriorhodopsin (yellow). For clarity, side chains of only charged amino acid residues (positively charged R and K, red; negatively charged D and E, blue) are shown. (C) View from the extracellular side illustrating the preference for an inward orientation of charged amino acid residues present in the transmembrane part of bacterial rhodopsins.

more likely to occur when the two residues are neighbours in the receptor protein. With this method several residues which are presumably close to each other in GPCRs were identified (Oliveira et al., 1993).

Rotational orientation of transmembrane helices

Correlated mutations are also more likely to occur to amino acids pointing towards the interior of the receptor. Residues which are conserved among the various GPCRs are more likely to point to the interior than the others, since these 'internal' residues probably play a role in ligand binding and signal transduction of the receptor protein. Residues which point to the exterior membrane environment, are often not conserved and of hybrophobic character.

Based on the latter observation, Cronet et al. (1993) derived so-called "environmental preference parameters" for each type of amino acid allowing to orientate the helices of seven-helical transmembrane proteins. For this purpose, the authors constructed a multiple sequence alignment of four bacterial rhodopsins (not GPCRs) having high sequence identity with BR (53-97% identity). From this multiple sequence alignment and the information from the 3D structure of BR, a scoring table was derived which describes the preference of each amino acid type to occur at a certain helix angle (from inside (towards the receptor core) to outside (towards the membrane environment)). This scoring table was then used to optimize the rotational orientation of the helices of the β_2-adrenergic receptor (Cronet et al., 1993).

Similar to the study of Cronet et al., we constructed a multiple sequence alignment of five closely related bacterial rhodopsin sequences (Fig. 3A). We anticipated that by building homology models of these proteins based on BR, we would obtain more useful structural information than from the three-dimensional structure of BR alone. An important feature, which became evident from both the alignment (Fig. 3A) and the superpositioning of the homology models (Fig. 3B) of bacterial rhodopsins, is that the intra- and extracellular loops contain many randomly positioned (nonconserved) charged amino acid residues (R, K, E, D). Indeed, especially positively charged residues, often located near the bounderies of transmembrane segments, are known to be involved in specifying the topology of membrane proteins (Dalbey, 1990). The transmembrane domains of the bacterial rhodopsins, on the other hand, hardly contain any charged residues. However, in case they are present, they are usually conserved (Fig. 3A) and point to the interior of the receptor (Fig. 3C).

The 3D structure of BR elucidated by Henderson et al. (1990) is generally assumed to represent the seven transmembrane domains of BR. However, we conclude that the template BR most probably also represents parts of the intracellular loops; at the lower ends of the helices of the superimposed bacterial rhodopsins, many nonconserved charged residues are present pointing towards the exterior of the protein, presumably into the intracellular aqueous environment. Especially the start of TM II (DAKK) and the beginning of TM VI (KVLR) of BR (Fig. 3A) are often wrongly assigned to be hydrophobic TM domains; many research groups are misled and align the hydrophobic domains of GPCRs with these intracellular regions of BR (Fig. 2).

In summary, the homology built models of a number of bacterial rhodopsins provide us with more structural information on seven-helix bundles than does the 3D structure of bacteriorhodopsin alone. Based upon these homology models, we conclude that the 3D structure of BR does not solely represent transmembrane domains but also parts of the intracellular loops.

The above considerations have shown that statistical information from multiple sequence alignments may provide interesting structural information. Therefore, we performed a simple statistical analysis on an extensive alignment of 135 aminergic receptors available from the EMBL file server (Oliveira et al., 1993). We calculated the average hydropathy index (Fig. 4A) and the average occurrence of charged residues (Fig. 4B) at each position in the alignment. Assuming that the arrangement of helices is conserved among the subfamily of aminergic GPCRs, the extreme values indicate the midpoints of the transmembrane domains. These extremes are much better observed in this analysis than in a usual hydrophobicity plot of only one sequence. Both the hydropathy indices and the charged residues indicate approximately the same residues as midpoints of the TM domains (Fig. 4A-B). Although we did not incorporate the results from this statistical analysis in our receptor modeling studies so far simply because they became available when our other studies had already been performed; we intend to use them in future studies and suggest these data in general to be useful for improving the orientation of transmembrane helices in future models of aminergic GPCRs.

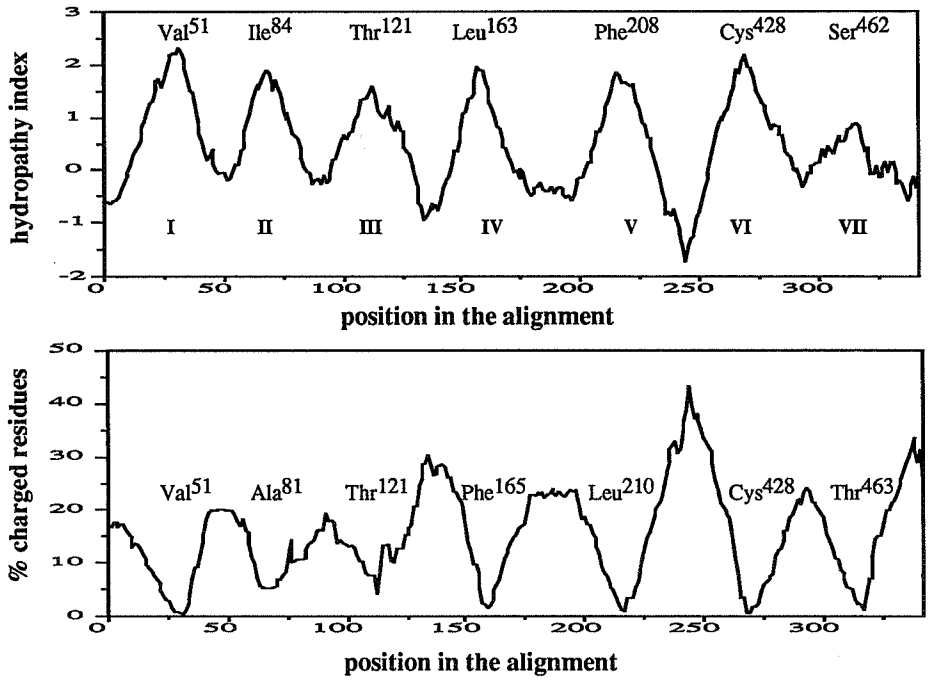

Figure 4. Statistical analysis on the multiple sequence alignment of 135 aminergic G-protein coupled receptors obtained from the TM7 file server in Heidelberg, Germany. Parts of the intra- and extracellular loops are omitted from the alignment (Oliveira et al., 1993). The hydrophobicity plot (above) presents the average hydropathy index at each position in the alignment using a window of 21 residues (Kyte and Doolittle, 1982). The percentage of charged amino acids (R, K, E, D) at each position in the alignment of the 135 aminergic GPCR sequences (window=21) is given in the lower panel. Residues of the guinea-pig H_1-receptor (Fig. 5) which correspond to the presumed midpoints of the transmembrane domains (extreme values) are given.

Section II: Docking of cyproheptadine

Cyproheptadine was docked into three models of the histamine H_1-receptor in order to determine the most probable binding site of histamine H_1-antagonists (see also 'Methods'). Cyproheptadine could not be fitted into the model based on the alignment of Trumpp-Kallmeyer et al. (1992) since the orientation of Asp^{116} in this model does not allow for an acceptable orientation of the antagonist within the protein. In contrast, cyproheptadine could be docked in the two receptor models based on Oliveira (1992) and Timms (1993). After rotation over the C_α-C_β bond of the aspartate (see Methods) only one unique orientation was found in both models, in which the aromatic rings of the antagonist are located in between transmembrane domains III, IV, V and VI and are surrounded by several aromatic residues from the receptor. These orientations were used to start further energy optimizations. As a result, considerably different positions for the aromatic rings of cyproheptadine in the two receptor models were found. These large differences appear to be due to the different relative location and orientation of Asp^{116}.

In Timms' H_1-receptor model, the 'cis'-ring of cyproheptadine points to the inner core of the receptor and is located in the proximity (within 5 Å) of two phenylalanines in TM VI (Phe^{435} and Phe^{436}) and a tryptophane in TM IV (Trp^{167}). The 'trans' aromatic ring is found near only one aromatic residue, Trp^{174} (TM VI) (Table 1) (for residue numbering, see Fig. 5). These findings are in agreement with structure-activity-relationships; for the 'cis'-ring, charge

Table 1. Amino acid residues which are in the proximity of -and possibly interact with- the 'cis' and 'trans' aromatic rings of histamine H_1-antagonists docked into H_1-receptor models either based upon the alignment used by Timms et al. (1993) or by Oliveira et al. (1993). Residues are numbered according to the primary sequence of the guinea pig histamine H_1-receptor (Traiffort et al., 1994; Fig. 5). The corresponding transmembrane domains are given between parentheses.

(alignment: Timms et al., 1993)		(alignment: Oliveira et al., 1993)	
'cis'-ring	'trans'-ring	'cis'-ring	'trans'-ring
Trp^{167} (IV)	Trp^{174} (IV)	Trp^{161} (IV)	Trp^{167} (IV)
Phe^{435} (VI)			Phe^{433} (VI)
Phe^{436} (VI)			Phe^{436} (VI)

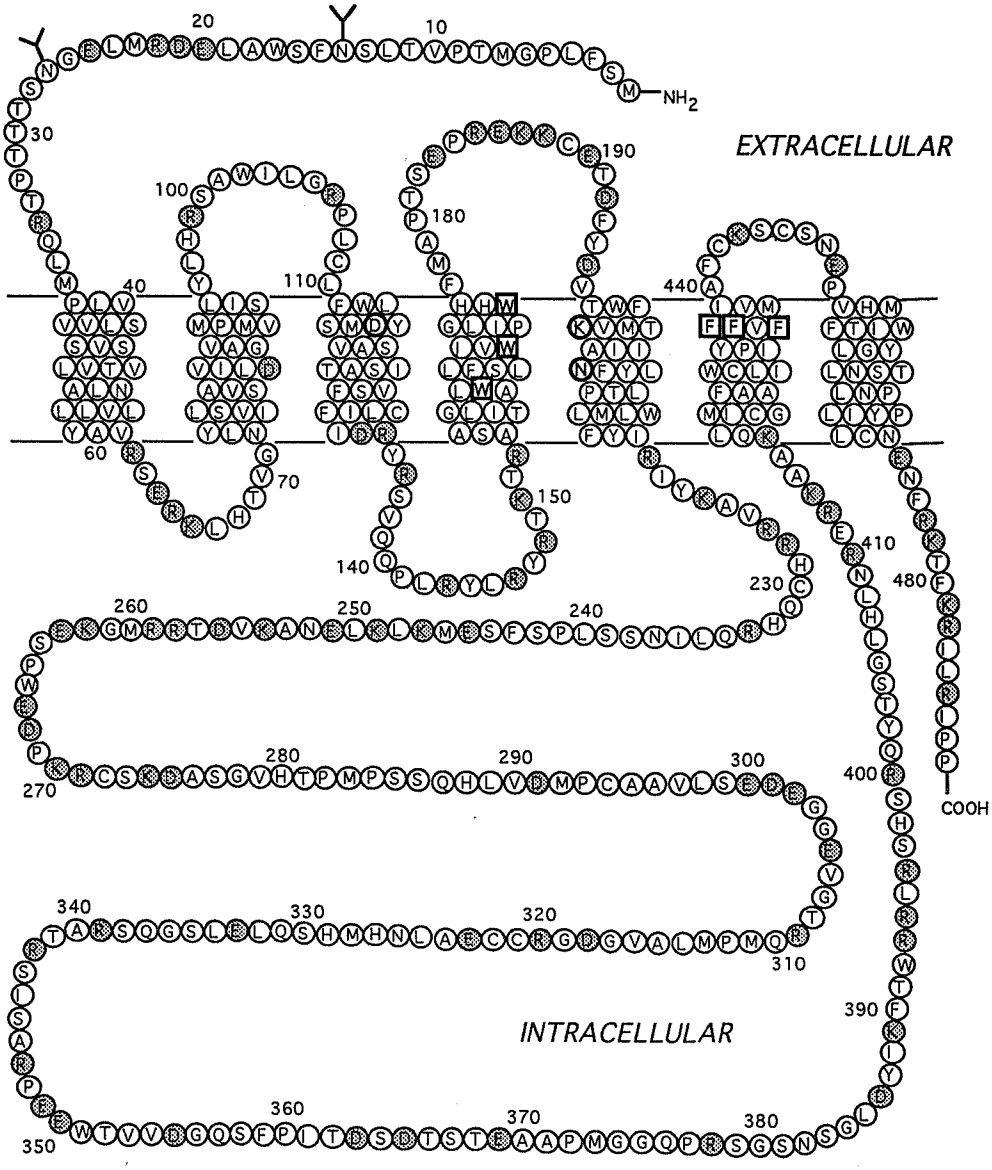

Figure 5. Schematic representation of the histamine H_1-receptor using the primary amino acid sequence and numbering from guinea-pig (Traiffort et al., 1994). Shaded circles indicate charged amino acid residues. Bold circles indicate residues which, according to site-directed mutagenesis studies, are involved in receptor activation by agonists (Ohta et al., 1994; Leurs et al., 1994;1995). Bold squares indicate aromatic residues in TM IV and VI which, according to present modeling studies, are supposed to interact with the aromatic rings of histamine H_1-antagonists (see Table 1).

transfer interactions have been proposed to be important while for the 'trans'-ring mainly hydrophobic interactions were thought to be important (Ter Laak et al., 1992; Chapter 6).

In contrast, in Oliveira's H_1-receptor model, the 'cis'-ring is situated near one aromatic residue Trp^{161} (TM IV), while the 'trans'-ring is close to residues Phe^{435}, Phe^{436} (TM VI) and Trp^{167} (TM IV). Clearly, there are large differences between the proposed binding sites in the two models (Table 1). This finding demonstrates again the strong influence of the alignment on the three-dimensional features of the ligand binding site and should warn GPCR modelers who focus on very detailed geometric aspects of their receptor models.

Therefore, with regard to the positions of the 'cis' and 'trans'-rings in the receptor (determining the stereochemistry of H_1-antagonists) a decisive conclusion can, as yet, not be drawn. However, the present modeling study is able to indicate residues which may in future studies, for example by site-directed mutagenesis, be proven to be involved in H_1-antagonist binding. Interestingly, many of these residues, i.e. Trp^{167}, Trp^{174}, Phe^{435} and Phe^{436} (Table 1) are unique for the H_1-receptor since they are not present at corresponding positions in most other aminergic GPCRs. Since these residues are also absent in the muscarinic M_1-receptor (which also binds cyproheptadine with high affinity) it is likely that the receptor-bound conformation of cyproheptadine in the muscarinic M_1-receptor is different from that in the histamine H_1-receptor.

Docking of zwitterionic H_1-antagonists

Three zwitterionic compounds were docked into both H_1-receptor models (Timms and Oliveira) on top of the template molecule cyproheptadine (i.e., Fig. 6A). By performing a simple conformational analysis giving rotational freedom to Lys^{200} in TM V and to the side chains of the zwitterionic compounds (which are not defined within the pharmacophoric model), the feasibility of an interaction between Lys^{200} and the carboxylate group of the H_1-antagonists was investigated. Interestingly, in Oliveira's model, such an interaction was possible for all three zwitterionic antihistamines investigated (Fig. 6B-C). In contrast, in the model of Timms, this interaction appeared impossible in the case of acrivastine.

These findings indicate that Lys^{200} (being a unique residue for the H_1-receptor) may be involved in the binding of zwitterionic H_1-antagonists. Recently, this suggestion has found further support, since the affinity of (D)-cetirizine appeared to be 6-fold lower for the mutant Lys^{200}Ala H_1-receptor (195 ± 5 nM) than for the wild type H_1-receptor (32 ± 8 nM) (Leurs et al., unpublished results). Furthermore, affinities of other classical H_1-antagonists which lack

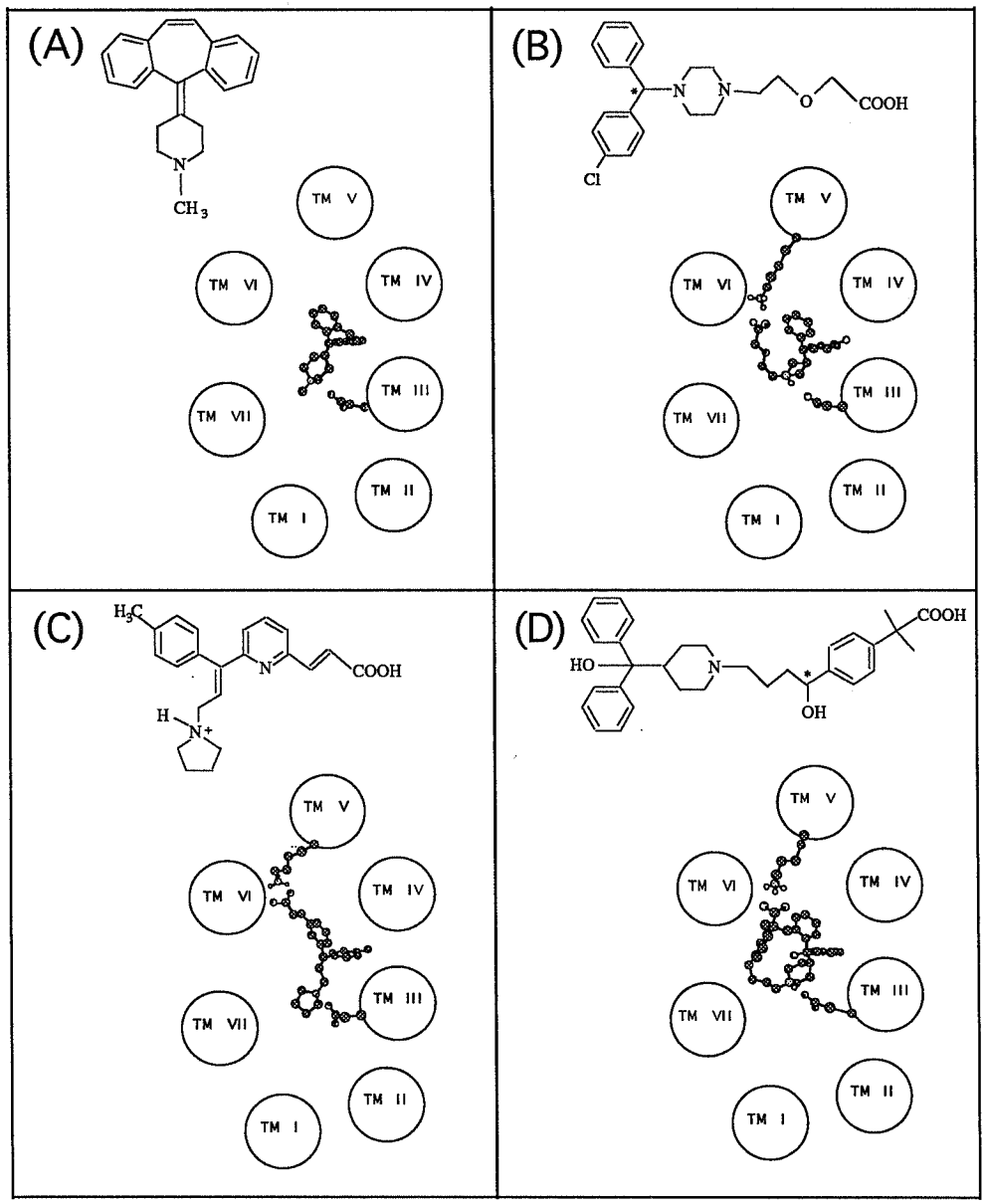

Figure 6. Schematic representation of the orientation of cyproheptadine (A) and three zwitterionic H_1-antagonistic compounds docked into the histamine H_1-receptor model based upon the alignment of Oliveira et al. (1993). The carboxylate groups of cetirizine (B), acrivastine (C) and the major metabolite of terfenadine (D) interact with the cationic ammonium group of Lys^{200} present in TM V. Carbon, hydrogen, nitrogen and oxygen atoms are represented by grey, white, black and dotted circles, respectively.

such a negatively charged group, such as (D)- and (L)-chlorpheniramine, were unaffected by this mutation (Leurs et al., unpublished results). Thus, it may be concluded that an interaction between the acidic group of cetirizine and Lys^{200} is favourable for receptor affinity of this compound. Further pharmacological studies, for example with acrivastine, may provide further evidence and yield more information on the orientation of histamine antagonists in the H_1-receptor. In addition, the development of zwitterionic H_1-antagonists is highly recommended: zwitterionic H_1-antagonists cannot only be expected to be devoid of sedating properties, they may also be relatively potent and selective compounds for the histamine H_1-receptor.

Conclusions

From the data presented it is evident that before using bacteriorhodopsin as a template molecule to build GPCR models, several problems considering the alignment procedure have to be considered. Until now, the choice of an acceptable alignment remained fairly arbitrary. We have also shown that the coordinates of BR by Henderson et al. (1990) do not necessarily represent residues of the hydrophobic transmembrane domains. Therefore, for modeling studies on aminergic GPCRs, it is advised to arrange the seven-helix bundles according to the presumed midpoints of the TM domains obtained from a statistical analysis of 135 aminergic GPCRs presented in this study (Fig. 4).

Despite the drawbacks of BR as a template molecule, we docked the histamine H_1-antagonist cyproheptadine into various homology models of the H_1-receptor. As expected, the alignment chosen appeared to be very important in determining the characteristics of the antagonist binding site, since distinct differences were found between the orientations of cyproheptadine in two different protein models. In both models, the aromatic rings of cyproheptadine appear to interact with aromatic residues from TM IV and TM VI. Four of these residues (Trp^{167}, Trp^{174}, Phe^{435} and Phe^{436}) are unique for the H_1-receptor and may be interesting candidates for future mutagenesis studies.

Finally, our modeling studies show that Lys^{200} in TM5 may be involved in binding zwitterionic H_1-antagonists. Recently, this was confirmed for cetirizine in preliminary binding experiments on the Lys^{200}Ala mutant H_1-receptor. Since Lys^{200} is unique for the H_1-receptor, the development of zwitterionic compounds as selective non-sedating H_1-antagonists is highly recommended.

CHAPTER 9

MODELING AND MUTATION STUDIES ON THE HISTAMINE H_1-RECEPTOR AGONIST BINDING SITE REVEALING DIFFERENT BINDING MODES FOR H_1-AGONISTS

ASP^{116} (TM III) HAS A CONSTITUTIVE ROLE IN RECEPTOR STIMULATION

A.M. ter Laak, H. Timmerman, R. Leurs, P.H.J. Nederkoorn, M.J. Smit, G.M. Donné-Op den Kelder (J. Comp.-Aided Mol. Design (1995) 9, 319-330)

Summary

A modeling study has been carried out in which the binding of histamine (His), 2-methyl-histamine (2-MeHis) and 2-phenyl-histamine (2-PhHis) at two postulated agonistic binding sites on the fifth transmembrane domain (TM V) of the histamine H_1-receptor was investigated. For this purpose a conformational analysis study was performed on three particular residues of TM V, i.e. Lys^{200}, Thr^{203} and Asn^{207}, for which a functional role in binding has been proposed. The most favourable results were obtained for the interaction between His and the Lys^{200} / Asn^{207} couple. Therefore, Lys^{200} was subsequently mutated and converted to an Ala resulting in a 50-fold decrease of H_1-receptor stimulation by histamine. Alltogether the data suggest that the Lys^{200} / Asn^{207} couple is important for activation of the H_1-receptor by histamine. In contrast, analogues of 2-PhHis seem to belong to a distinct subclass of histamine agonists and an alternative mode of binding is proposed in which the 2-phenyl ring binds to the same receptor location as one of the aromatic rings of classical histamine H_1-antagonists. Subsequently, the binding modes of the agonists His, 2-MeHis and 2-PhHis and the H_1-antagonist cyproheptadine were evaluated in three different seven α-helical models of the H_1-receptor built in homology with bacteriorhodopsin, but using three different alignments. Our findings suggest that the position of the carboxylate group of Asp^{116} (TM III) within the receptor pocket depends on whether an agonist or an antagonist binds to the protein; a conformational change of this aspartate residue upon agonist binding is expected to play an essential role in receptor stimulation.

Introduction

Of the many histamine analogues that have been tested on H_1-receptors, histamine (**1**, Fig. 1) itself appears to be among the most potent and effective H_1-agonists (Cooper et al., 1990). Potent and highly selective histamine H_1-agonists belong to the class of 2-phenyl-histamine analogues: compounds **11b** and **11c** (Fig. 1) have H_1-agonistic activities of 129 % and 112 % relative to histamine, respectively (Koper et al., 1990; Zingel et al., 1990; 1993).

In general, several 5-membered rings (i.e. **2-3**, **8-10**, Fig. 1), and even six-membered rings such as in 2-pyridyl-ethylamine (2-PEA, **4**) can replace the imidazole ring of histamine while retaining H_1-agonist activity (Cooper et al., 1990). Crucial for agonistic activity appears to be a proximal basic nitrogen (N^{π}) which is found in all H_1-agonists with an activity > 0.1% of histamine (compare **4** with **5** and **6**, Fig.1). Moreover, this proximal nitrogen cannot be methylated without total loss of activity (compare **1** with **7**, Fig. 1). Therefore, the bioactive form of histamine at H_1-receptors is most likely the N^{τ}-H tautomer in which the N^{π} is freely accessible.

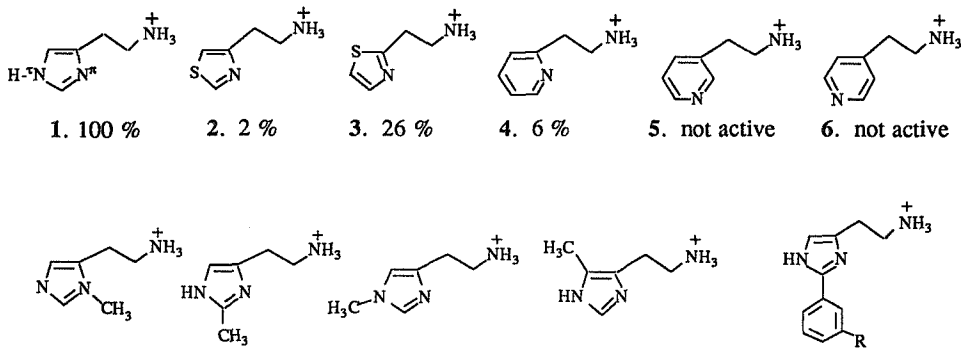

Figure 1. A selection of compounds illustrating some aspects of the structural properties neccesary for H_1-receptor activation (see text). Agonist activities measured on the guinea pig ileum of compounds **2-10** relative to histamine (=100 %) are taken from Cooper et al. (1990). Relative activities of **11a-c** are taken from a study by Zingel and Schunack (1993). Compounds **1**, **3**, **4**, **8** and **11c** have recently been tested on two mutant H_1-receptors (Thr^{203}->Ala^{203} and Asn^{207}->Ala^{207}; Leurs et al., 1994). Histamine (**1**), 2-methyl-histamine (**8**) and 2-phenyl-histamine (**11a**) are investigated in the present theoretical study.

Substitution in the imidazole ring at the 2-position with alkyl groups higher than methyl (**8**) is highly unfavourable for H_1-receptor activity, probably due to steric effects (Leurs et al., 1994). Therefore, at first sight, it is surprising that aromatic groups are tolerated at this position (i.e. **11a-c**). However, recent site-directed mutagenesis studies of our group reveal that 2-phenyl histamine analogues form a distinct subclass of histamine agonists, since they appear to interact differently with Asn^{207} in TM V (Leurs et al., 1994).

The aspartic acid in transmembrane domain 3 (TM III) which is conserved in all aminergic receptors (Asp^{116} in the guinea pig H_1-receptor (gpH_1R); Traiffort et al., 1994), has been shown to be essential for agonist and antagonist binding at histamine H_1-receptors (Ohta et al., 1994). For G-protein coupled receptors (GPCRs) which bind aminergic ligands, it is generally accepted that this aspartate interacts with the positively charged basic group of the ligand. In contrast, receptor specificity appears to be defined by residues in other TM domains, especially those in TM V as has been suggested by mutagenesis studies on the hamster β_2-adrenergic (Ser^{204} and Ser^{207}; Strader et al., 1989) and the canine H_2-histaminergic receptor (Asp^{186} and Thr^{190}; Gantz et al., 1992). Therefore, we decided to identify the corresponding functional residues in TM V of the H_1-receptor responsible for binding of the imidazole ring of histamine in its N^{τ}-H tautomeric form. Interaction between the imidazole ring and the H_1-receptor is likely to be optimal in case both the N^{τ}-H and the N^{π} functional groups can form hydrogen bonds with protein residues. Possible hydrogen bond donor and acceptor functionalities in TM V are Asn^{207}, as a H-bond accepting moiety for the N^{τ}-proton and either Thr^{203} or Lys^{200}, as a H-bond donor to N^{π}. The presence of Lys^{200} in this region of TM V is remarkable, since in all other aminergic GPCRs no charged residues are observed in the corresponding TM domain (Fig.2). In the primary amino acid sequence of the histamine H_1-receptor a third hydrogen bond donor residue (Thr^{212}) is observed in the proximity of Asn^{207} (Fig. 2). However, Thr^{212} is found at the opposite site of the TM V α-helix with respect to the above-mentioned residues Lys^{200}, Thr^{203} and Asn^{207} (as an indication, $C\beta(Thr^{203})$-$C\alpha(Thr^{203})$-$C\alpha(Thr^{212})$-$C\beta(Thr^{212})$=151°). Since, based on sequence homology with the β-adrenergic receptor and the histamine H_2-receptor, Thr^{212} can be expected to be absent from the receptor binding pocket and to point towards the membrane environment, we did not further consider Thr^{212} in our modeling study.

A severe disadvantage of GPCR modeling studies using the cryomicroscopy structure of bacteriorhodopsin (Henderson et al., 1990) as a template is the known low homology between the TM domains of GPCRs and bacteriorhodopsin (6-11% identity). This low homology has resulted in largely different alignments used by various research groups (Chapter 8). It is therefore evident that the choice of an alignment for GPCR homology building remains fairly

							*			*			*															
HIS1	194	Y	N	V	T	W	F	K	V	M	T	A	I	I	N	F	Y	L	P	T	L	L	M	L	W	F	Y	A	K	I	222
HIS2	177	Q	V	N	L	V	Y	G	L	V	D	G	L	V	T	F	Y	L	P	L	L	V	M	C	I	T	Y	Y	R	I	205
ADR-β1	219	V	T	N	R	A	Y	A	I	A	S	S	V	V	S	F	Y	V	P	L	C	I	M	A	F	V	Y	L	R	V	247
ADR-β2	194	F	T	N	Q	A	Y	A	I	A	S	S	I	V	S	F	Y	V	P	L	V	I	M	V	F	V	Y	S	R	V	222
ADR-β3	199	A	S	N	M	P	Y	V	L	L	S	S	S	V	S	F	Y	L	P	L	L	V	M	L	F	V	Y	A	R	V	227
ADR-α1a	207	T	E	E	V	G	Y	A	I	F	S	S	V	C	S	F	Y	L	P	M	A	V	I	V	V	M	Y	C	R	V	235
ADR-α2	191	N	D	Q	K	W	Y	V	I	S	S	C	I	G	S	F	F	A	P	C	L	I	M	I	L	V	Y	V	R	I	217
DOP1	189	S	L	S	R	T	Y	A	I	S	S	S	V	I	S	F	Y	I	P	V	A	I	M	I	V	T	Y	T	R	I	219
DOP2	185	A	N	P	A	F	V	V	Y	S	S	I	V	S	F	Y	V	P	F	I	V	T	L	L	V	Y	I	K	I	Y	213
DOP4	188	E	D	R	D	Y	V	V	Y	S	S	V	C	S	F	F	L	P	C	P	L	M	L	L	L	Y	W	A	T	F	216
5HT1a	190	S	K	D	H	G	Y	T	I	Y	S	T	F	G	A	F	Y	I	P	L	L	L	M	L	V	L	Y	G	R	I	218
ACM2	181	F	S	N	A	A	V	T	F	G	T	A	I	A	A	F	Y	L	P	V	I	I	M	T	V	L	Y	W	H	I	209
ACM3	190	L	S	E	P	T	I	T	F	G	T	A	I	A	A	F	Y	M	P	V	T	I	M	T	I	L	Y	W	R	I	218
ACM4	226	L	S	N	P	A	V	T	F	G	T	A	I	A	A	F	Y	L	P	V	V	I	M	T	V	L	Y	I	H	I	254
ACM5	188	L	S	E	P	T	I	T	F	G	T	A	I	A	A	F	Y	I	P	V	S	V	M	T	I	L	Y	C	R	I	216

Figure 2. Multiple sequence alignment of the fifth transmembrane domain (TM V) for a representative set of aminergic GPCRs. Numbers refer to the first and last amino acid residue of the row. In all catecholaminergic receptors (ADR, DOP) conserved Ser residues are found in TM5. Their positions correspond with Thr^{203} and Asn^{207} in the guinea pig histamine H_1-receptor and Asp^{186} and Thr^{190} in the canine H_2-receptor. Lys^{200} is found in the histamine H_1-receptor in a region of the TM V domain where no charged residues are observed in all other aminergic GPCRs. Histaminergic receptors, HIS1 = PIR2:JX0287 (guinea pig), HIS2 from Gantz et al. (1992, canine). Adrenergic receptors (human), ADR-β_1 = PIR2:A39911, ADR-β_2 = PIR2:A28405, ADR-β_3 = PIR2:A41348, ADR-α_{1a} = PIR1:JH0447, ADR-α_2 = PIR2:A34169. Dopaminergic receptors (human), DOP1 = PIR1:DYHUD1, DOP2 = PIR1:DYHUD2 , DOP4 = PIR1:DYHUD4. Serotoninergic receptors (rat), $5HT_{1a}$ = PIR1:JH0315. Acetylcholinergic-muscarinergic receptors (human), ACM2 = PIR2:S10126, ACM3 = PIR2:S10127, ACM4 = PIR2:S10128 , ACM5 = PIR2:JT0530.

arbitrary. As yet there is no consensus on the relative orientation of the GPCR α-helices. Therefore, docking studies must be interpreted with caution, especially when the interaction between (usually small) agonists and residues in different TM domains is investigated.

In view of these drawbacks we have chosen a simplified strategy and focussed in detail on the possible interactions of histaminergic ligands with only one TM domain (TM V). The influence of other domains than TM V on agonistic action was temporarily neglected and TM V was treated as a separate entity (an oligopeptide containing 10 residues). An extensive conformational analysis of the three candidate residues Lys^{200}, Thr^{203} and Asn^{207} was performed and their interaction with the imidazole ring of His (**1**), 2-MeHis (**8**) and 2-PhHis (**11a**) studied.

Subsequently, stable agonist-oligopeptide complexes were selected for investigating agonist-TM V interactions in complete 3D-models of the H_1-receptor. Three different alignments were evaluated (Trumpp-Kallmeyer et al., 1992; Timms et al., 1992; Oliveira et al., 1993). In each receptor model and for several TM V-agonist complexes the feasibility of the interaction between the protonated ethylamine side chain of the agonist and Asp^{116} in TM III was investigated. For this purpose, the oligopeptide backbone atoms of these complexes were matched with the backbone atoms of the 10 corresponding residues in the 3D-model of the protein, thus representing the binding mode of the agonist having previously determined optimal interactions with TM V.

In order to reveal whether distinct differences are present between the agonistic and antagonistic binding sites on the H_1-receptor, the H_1-antagonist cyproheptadine was docked into the three different receptor models. The bioactive conformation of this compound was obtained from a previous study on the H_1-antagonistic binding site in which a stereoselective pharmacophore was derived by superimposing seven (semi-)rigid and potent antihistamines (Chapter 7). This H_1-antagonist pharmacophore is represented by two aromatic rings and the positions of the C_α and C_β-carbons of the aspartate from TM III (Asp^{116}) to which the basic nitrogen of antagonists is bound (Fig.7A).

During the course of our study it became apparent that the 2-phenyl ring of 2-PhHis is important for receptor affinity. Interestingly, the so-called 'cis' aromatic ring of H_1-antagonists plays a similar role (Chapter 6). Therefore, in our attempt to find an alternative binding mode for 2PhHis analogues, the 2-phenyl ring of **11c** was matched with the 'cis'-ring of the H_1-antagonist pharmacophore, which indeed led to the identification of an acceptable alternative agonist binding mode for 2-PhHis analogues.

Methods

Conformational analysis

The histamine H_1-receptor was constructed from the PDB-structure of bacteriorhodopsin according to the alignment of Trumpp-Kallmeyer et al. (1992) and minimised with QUANTA/CHARMm V.22.0. (Quanta 4.0, Molecular Simulations Inc., Burlington, MA, USA). Subsequently, 10 residues from TM V (Phe-Lys-Val-Met-Thr-Ala-Ile-Ile-Asn-Phe) were extracted as an α-helical oligopeptide with neutral N- and C-termini and used for further investigations.

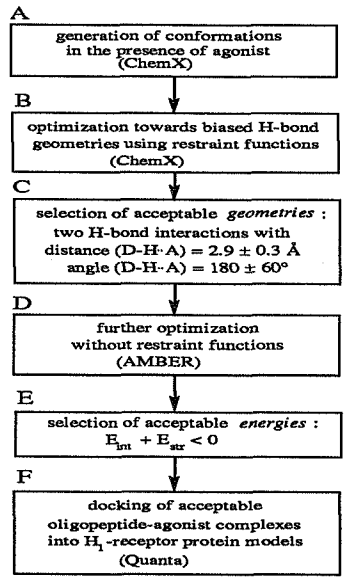

Figure 3. Schematic representation of the methods used to obtain stable complexes of histamine analogues with residues in TM V of the histamine H_1-receptor: (A) Conformations are generated for the oligopeptide as described in the text in the presence of agonist. (B) The orientation of the imidazole is optimized with respect to the oligopeptide (Fig. 4) using X-ray database results (Ippolito et al., 1990). (C) Complexes are selected using predefined criteria for proper H-bonds after which they are further optimized in AMBER (D) and selected upon their final energy (E). The remaining complexes are incorporated into complete 3D-protein models and the agonist binding sites investigated (F) (see text for further details).

In order to investigate all acceptable interactions between the residues in TM V and an imidazole ring, it is neccesary to use adequate energy functions for hydrogen bonded interactions. However, the available hydrogen bonding functions of ChemX ($V_{hb}=C/r^A - D/r^B$) or AMBER (angle-independant (10,12)-Lennard-Jones) do not account adequately for the directionality of hydrogen bonds. CHARMm does include directionality in its hydrogen bonding function ($E_{hb}= [(A/r_{AD}^6)-(B/r_{AD}^4)] \times \cos^m(\Theta_{AHD}) \times \cos^n(\Theta_{AAAH}) \times sw(r_{AD}^2,r_{on}^2,r_{off}^2) \times sw(\cos^2(\Theta_{AHD}),\cos^2(\Theta_{on}),\cos^2(\Theta_{off}))$), but to our experience this function leads to geometries (i.e. $\Theta_{C=O..H}$ being 180°) which are not in agreement with protein X-ray data (Ippolito et al., 1990). In order to prevent the conformation analyses and the subsequent ChemX optimization on three residues of TM V (Lys^{200}, Thr^{203} and Asn^{207}) in the presence of agonist to yield a large number of geometries with improper hydrogen bonds, we biased the directionality of the proposed hydrogen bonds with restraint functions on pre-defined dummy atoms. For further optimization and calculation of interaction energies we used the AMBER force field (Kollman's united and all atom force field with additional parameters for organic functionality; Weiner et al., 1986) since it is especially parametrised for the simulation of proteins.

Overall, a strategy was developed in which the geometries of oligopeptide-agonist complexes were generated with ChemX (Fig. 3A-B) and those with proper hydrogen bond angles and torsion angles were selected (Fig. 3C) for further optimization and calculation of the interaction energies with AMBER (Fig. 3D-E). These methods are described in more detail in the following paragraph.

The possible interaction sites of His (**1**), 2-MeHis (**8**) and 2-PhHis (**11**) with residues in TM V were represented by either the Asn^{207}/Thr^{203} couple (Fig. 4A) or the Asn^{207}/Lys^{200} couple (Fig. 4B). These two interaction sites were investigated separately. For each of these two couples a large number of conformations (324 and 8748, respectively; Table 1) was generated with ChemX (Jan. 1993) in the presence of agonist, while the atoms of the oligopeptide backbone and the remaining side chains remained unchanged (Fig. 3A and 4). The stepwise increment for the in Fig.4 indicated torsion angles was either 180° (2 steps for sp2-sp2 atom bonds), 60° (6 steps for sp2-sp3 atom bonds) or 120° (3 steps for sp3-sp3 atom bonds) yielding the likely number of local minima for these bonds.

Dummy atoms are connected to the H-bond donor or acceptor functions of the imidazole ring of the agonists (X1 and X2) and the three amino acid residues (X3-X5) and put at those positions were the counter donor- or acceptor-atoms are expected according to a protein X-ray database search (Ippolito et al., 1990). Subsequently, four penalty functions were used (restraint constant k=100 kJ/A2) to minimize the distance between the dummies and their counter atoms. These penalty functions are considered as restrain forces ($F_r=k.(l-l_0)$) during optimization of the ChemX VDW energy (ChemX Reference Guide, 1993). The ChemX VDW energy neglects bond and angle strain energy terms, and uses only torsion, nonbonded, electrostatic and hydrogen bonding energy terms ($E_{VDW} = V_{tor}+V_{nb}+V_{el}+V_{hb}$). Thus, the orientation and the position of the agonist relative to the respective couple and the torsion angles of the two considered residues (Lys/Asn or Thr/Asn; arrows, Fig.4) are optimized (Fig. 3B).

Low energy TM V-ligand conformations (energy less than 50 kJ/mol from the lowest energy) were selected with two H-bonds between the imidazole ring and oligopeptide residues fulfilling the following criteria: distances (D-H··A)=2.9±0.3 Å and angles (D-H··A)=180±60° (Fig. 3C). The selected structures were further optimized with AMBER (derivative convergence < 0.005 kJ/Å.mol) using the PR Conjugate Gradient (PRCG) method in BatchMin V.4.5 / MacroModel V.2.5 releasing all restraints except on the oligopeptide backbone. In these calculations structures were optimized with a constant dielectric treatment (ε=1), the standard united-atom AMBER charge set and Kollman's 6,12-Lennard Jones hydrogen bonding treatment (Batchmin User Manual V4.0, Colombia University, New York).

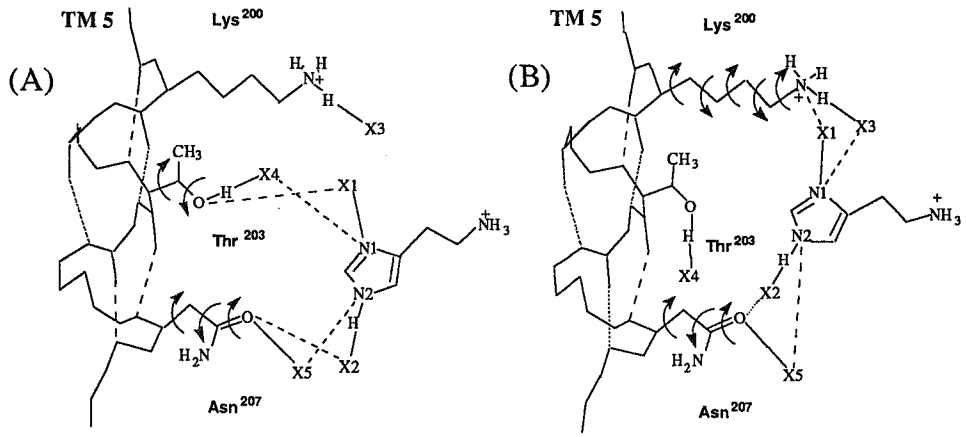

Figure 4. In order to study all possible interactions with histamine, conformational analysis studies were performed on Lys^{200}, Thr^{203} and Asn^{207} present in TM V of the histamine H_1-receptor. In our hypothesis either the Thr^{203}/Asn^{207} couple (A) or the Lys^{200}/Asn^{207} couple (B) can be expected to interact with the imidazole ring of histamine analogues. Different conformations were generated for the putative interacting residues by adequately chosen torsion angle increments along several rotatable bonds (arrows) (Fig. 3A). Appropriate X-ray hydrogen bond geometries are mimicked by dummy atoms on the imidazole ring (X1 and X2) and the proposed interacting residues (X3-X5). In the minimization procedure (Fig. 3B), four restraint functions are put on the distances between the dummy atoms and their counter atoms (dashed lines).

The AMBER global energy structure of the oligopeptide in the absence of agonist was obtained from a conformational analysis in MacroModel V.2.5 by rotation along the indicated oligopeptide bonds (arrows, Fig. 4) using torsional increments as before in the presence of agonist. The global energy structures of the agonists itself (His, 2-MeHis and 2-PhHis) were obtained using increments of 60 degrees for the rotatable bonds of the ethylamine side chain.

Energy calculations

The AMBER interaction energy (E_{int}) of the optimized agonist-oligopeptide complex is calculated by:

$$E_{int} = E_{comp} - E_{olig} - E_{ago} \qquad (1)$$

where E_{comp} is the energy of the optimized complex and where E_{olig} and E_{ago} are the energies of the separated oligopeptide and agonist in the complex, respectively.

The strain energy imposed on the residues of the oligopeptide while interacting with the ligand is calculated by:

$$E_{str} = E_{olig} - E_{olig,GES} \quad (2)$$

where $E_{olig,GES}$ is the energy of the global minimum structure of the oligopeptide in the absence of agonist. Upon the agonist no strain energy is induced since the ethylamine side chain is kept in a fixed extended local minimum conformation.

The interaction energy of the oligopeptide-ligand complex should at least compensate the strain energy imposed on the oligopeptide residues by the agonist. Therefore 'stable' complexes are assumed to be represented by negative ΔE values:

$$\Delta E = E_{int} + E_{str} = E_{comp} - E_{ago} - E_{olig,GES} \quad (3)$$

Receptor docking

Three different H_1-receptor models, which differ in the relative orientation of their seven TM helices, were built from the cryomicroscopy structure of bacteriorhodopsin (PDB-code:1brd). Two models were built in analogy with the alignment of Trumpp-Kallmeyer et al. (1992) and Timms et al. (1992), respectively, using the homology building options of QUANTA Version 3.3. A third H_1-receptor model was obtained from the 7TM file server of EMBL (Heidelberg, Germany; Oliveira et al., 1993). Prior to docking procedures, these transmembrane seven-helical bundles were optimised with CHARMm V. 22.0. The oligopeptide backbone atoms of selected TM V-agonist complexes (previous paragraph) were fitted onto the backbone atoms of the 10 corresponding residues in TM V using ChemX fit procedures; subsequently, the duplicate TM V residues were removed.

In order to investigate the antagonist binding site in the H_1-receptor, the previously determined cyproheptadine-aspartate complex (Chapter 7) was docked into the protein in such way that the aspartate of the complex matched Asp^{116} of the model (fitting C_α and C_β atoms). The superfluous aspartate is subsequently removed, Asp^{116} is then rotated around its C_α-C_β bond in order to establish a favourable orientation for the coupled antagonist. The unique antagonist-protein model with minimal steric hindrance is energy optimized with CHARMm V. 22.0 (Fig.7C).

Mutation studies

Recently, our group characterized the wild-type H_1-receptor and two mutants (Thr^{203}->Ala and Asn^{207}-Ala) stably transfected into Chines Hamster Ovary (CHO) cells pharmacologically (Leurs et al., 1994). In the present study new results are presented concerning the mutation of Lys^{200} (to Ala) (Leurs et al., submitted). This gpH_1-receptor mutant was successfully expressed in CHO cells and tested according to procedures described earlier (Leurs et al., 1994).

Results and Discussion

Interactions of agonists with the Thr^{203}/Asn^{207} couple

The conformation analysis on the Thr^{203}/Asn^{207} couple yielded 324 conformations (N_{start}; Table 1A) in the presence of either agonist His (Fig.4A), 2-MeHis or 2-PhHis. Optimization with ChemX led to respectively 26, 19 and 9 conformations with acceptable H-bond geometries (N_{ChemX}; Table 1A). After further minimization with AMBER with restrain functions only on the backbone, 11, 2 and 1 conformations with satisfactory hydrogen bond interactions (Thr-O-H..Nπ / Nτ–H..O=Asn) remained, respectively (N_{AMBER}). Only for His three 'stable' ($\Delta E < 0$) complexes could be formed (N_{stable}; Table 1A), although the energy gain from these interactions is low ($\Delta E > -1.35$ kcal/mol; Table 1). Moreover, the strain energies imposed on the side chains in order to establish these interactions and which are probably partly due to a loss of the internal H-bond between Thr^{203} and the protein backbone, are generally high ($E_{Str} \approx$ 7-20 kcal/mol; Table 1A). For these reasons a strong and also selective binding of the agonist imidazole ring by Thr^{203} and Asn^{207} seems unlikely.

Interactions of agonists with the Lys^{200}/Asn^{207} couple

Several stable complex formations result from the conformation analysis study on the Lys^{200}/Asn^{207} couple in the presence of each investigated agonist (Fig. 4B). For this pair of residues, a large number of conformations was generated (N_{start}=8748; Table 1B) merely due to the many rotatable bonds in Lys^{200}. After optimization with AMBER, a large number of complexes was observed with satisfactory H-bonds for all three agonists (63, 53 and 42 for His, 2-MeHis and 2-PhHis, respectively; Table 1B). All complexes were stabilised by two presumably essential H-bonds (Lys-ε-N^+-H..Nπ and Nτ–H..O=Asn). A large number of these complexes (15, 12 and 18, respectively; Table 1B) were assigned 'stable'.

Table 1. Theoretical results on the interaction between H_1-agonists and TM V of the histamine H_1-receptor [a]

(A)	number of (remaining) conformations Thr^{203}/Asn^{207}						
	N_{start}	N_{ChemX}	N_{AMBER}	N_{stable}	E_{int}	E_{str}	ΔE (kcal/mol)
His	324	26	11	3	-8.03	6.68	-1.35
2-MeHis	324	19	2	0	-11.18	14.66	+3.48
2-PhHis	324	9	1	0	-12.39	19.73	+7.34
(B)	number of (remaining) conformations Lys^{200}/Asn^{207}						
	N_{start}	N_{ChemX}	N_{AMBER}	N_{stable}	E_{int}	E_{str}	ΔE (kcal/mol)
His	8748	67	63	15	-11.08	4.70	-6.38
2-MeHis	8748	67	53	12	-14.11	6.54	-7.57
2-PhHis	8748	56	42	18	-15.46	7.67	-7.79

[a] Results of the conformational analyses on the Thr^{203}/Asn^{207} (A) and the Lys^{200}/Asn^{207} (B) couple in the presence of histamine (His, **1**), 2-methyl-histamine (2-MeHis, **3**) or 2-phenyl-histamine (2-PhHis, **11a**). N_{start} presents the number of conformations generated with ChemX in the presence of ligand (Fig. 3A). N_{ChemX} is the number of conformations with acceptable H-bond interactions (geometric criteria; see Fig. 3C) between the agonist imidazole and the protein residue couple (2 H-bonds). These were obtained after ChemX optimization of the N_{start} conformations in the presence of agonist (Fig. 3B) and with penalty functions on the appropriate donor, acceptor and dummy atoms (as in Fig. 4A-B). N_{AMBER} indicates the number of conformations of the oligopeptide-ligand complex with acceptable H-bond interactions after AMBER optimization of the N_{ChemX} conformations. N_{stable} represents the peptide-agonist complexes which fulfil the criterium: $\Delta E < 0$, where ΔE indicates the stability of the complex (see Eqs. 1-3). Only for the complex with the lowest ΔE value, the corresponding E_{int}, E_{str} and ΔE values are given.

Interestingly, in all 'stable' complexes, the imidazole ring of the agonist is found to bind to a conformation of TM V which is very similar to the GES of the oligopeptide in the absence of agonist. The GES is a structure in which the Thr^{203} side chain is hydrogen bonded to the backbone carbonyl of Lys^{200} while the conformation of the Lys^{200} side chain is mainly determined by two H-bonds, one to the hydroxyl oxygen of Thr^{203} and one to its own backbone carbonyl (see Fig. 5A). The amine of Asn^{207} also interacts via an H-bond with its own backbone carbonyl. Since the charged amino group of Lys^{200} is bend in the direction of Asn^{207}, these residues constitute a perfect binding site for the imidazole ring (Fig. 5). The strain energy which is imposed upon the residues upon agonist-binding largely results from breaking of an internal H-bond (Lys^{200}). This energy is different for His (+4.70), 2-MeHis (+6.54) and 2-PhHis (+7.67) (Table 1B). However, in all cases this strain energy is greatly surpassed by the H-bond interaction energy of the complexes as demonstrated by negative energy balances (ΔE = -6.38, -7.57 and -7.79 kcal/mol, respectively; Table 1B).

It is worthwhile mentioning that some important differences in the geometries of these three complexes were observed, although in each case two hydrogen bonds could be established between the agonist and the Lys/Asn couple. Histamine and 2-MeHis appear to interact in an orientation perpendicular to the α-helix backbone of TM V (Fig. 5B) preventing that large substituent groups at the 2-position can be accomodated in this binding mode. As a consequence 2-PhHis is pushed away from the backbone resulting in a sideways orientation of the imidazole ring (in parallel with the backbone) and the phenyl ring binding in the free space close to Ala^{205} (see also *ligand docking* of 2-PhHis).

The above results indicate that for the three agonists studied, the Lys/Asn couple constitutes a more likely binding site than the Thr/Asn couple.

Interpretation of binding and functionality of wild-type and mutant H_1-receptors

Previously, our group reported pharmacological data on the wild-type H_1-receptor and two mutants with alterations in TM V (Thr^{203}->Ala and Asn^{207}->Ala; Leurs et al., 1994). Whereas the Thr^{203} mutation had almost no effect on agonist action, the Asn^{207} mutation resulted in a severe loss of affinity and functional activity in the case of His (**1**) and 2-MeHis (**8**) (Table 2). Since the Asn^{207} mutation had only a small effect on the affinity of agonists that lack an N^{τ}-atom (**3** and **4**), it was concluded that the N^{τ}-proton interacts with Asn^{207}(Leurs et al., 1994).

The question concerning the residue serving as an H-bond donating residue to the N^{π}-atom present in all potent H_1-agonists remained however unsolved. The results of Leurs et al. (1994) showed that Thr^{203} is unlikely to be involved in binding the N^{π}-atom of histamine. In the present modeling study we confirm that a strong and simultaneous binding of Thr^{203} and Asn^{207} to the imidazole ring is unlikely indeed, as the highest observed energy yield for such an interaction is only -1.35 kcal/mol (in case of histamine; Table 1).

On basis of our current results, Lys^{200}, being a strong H-bond donating residue, was mutated to an Ala causing a 5-fold decrease in histamine affinity and an even higher decrease in the functional EC_{50}-value (50-fold; Table 2). These observations are in full agreement with our modeling investigations which reveal that the Lys^{200}/Asn^{207} residue pair in TM V is especially suited to bind an imidazole ring (energy gain: 6-8 kcal/mol; Table 1B; Fig. 5). We therefore conclude that Lys^{200} interacts specifically with the N^{π}-atom of histamine. This is further supported by a 15-fold decrease in EC_{50}-value of the agonist 2-pyridyl-ethylamine (2-PEA (**4**); Fig.1) upon mutation of Lys^{200} (Table 2).

Table 2. Affinity and activity of H_1-agonists on wild-type and mutant H_1-receptors [a]

	K_i-value (mM)			EC_{50} (mM)		
A	Wild Type	Thr^{203} ->Ala	Asn^{207} ->Ala	Wild Type	Thr^{203} ->Ala	Asn^{207} ->Ala
His (**1**)	12	26	>1000	3.9	7.5	>1000
2-PEA (**4**)	38	44	129	-	-	-
2-MeHis (**8**)	42	25	>1000	-	-	-
m-Br-2-PhHis (**11c**)	0.67	0.44	4.3	0.56	0.53	6.6
B	Wild Type	Lys^{200} ->Ala		Wild Type	Lys^{200} ->Ala	
His (**1**)	30	150		1.2	63	
2-PEA (**4**)	69	86		23	340	
2-MeHis (**8**)	98	60		8.5	16	
m-Br-2-PhHis (**11c**)	0.87	2.2		0.59	0.56	

[a] (A) Earlier pharmacological data of four histamine H_1-agonists measured on wild-type and two mutant H_1-receptors (Thr^{204}->Ala and Asn^{207}->Ala) from Leurs et al. (1994). (B) New pharmacological data on wild type and the Lys^{200}->Ala mutant H_1-receptor (Leurs et al., submitted). Binding constants (K_i-values; displacement of 1.5 nM [^{3}H]-mepyramine) were measured on stably transfected H_1-receptors in CHO cells (A) or transiently in HEK-293 cells (B). Functional EC_{50} values were obtained by measuring [^{3}H]IP_x production in CHO cells. Bold numbers refer to the structural formulas in Fig. 1.

Close inspection of the agonist-oligopeptide complexes reveal that the orientation of 2-MeHis in the binding pocket is similar to the one of His including two hydrogen bonds with the Lys^{200}/Asn^{207} couple (ΔE values are -6.38 and -7.57 kcal/mole for His and 2-MeHis, respectively, Table 1B). This interaction is supported by the strong effect of the Asn^{207} mutation on the agonist binding of 2-MeHis. However, the effect of the Lys^{200} mutation is marginal, which is rather unexpected (EC_{50} changes from 8.5 to 16 μM). It is likely that 2-MeHis is orientated differently from His, in a way in which the H-bond with Asn^{207} is still possible, but in which the H-bond with Lys^{200} is lost. The oligopeptide model system, but the complete H_1-receptor models (see below) as well, were unable to reveal any cause for this reorientation. Possibly, the position of Asp^{116}, which interacts with the ethylamine side chain, is not 'correct' in the used protein models due to deficiencies in homology building based on bacteriorhodopsin (see below).

Although 2-PhHis can be accommodated in the Lys/Asn pocket via two hydrogen bonds, the mutation data (Table 2, **11c**) indicate this orientation to be wrong, since both the Lys and

Asn mutation have negligible effects. Therefore, in the complete protein models (see below), a different binding mode for 2-PhHis analogues was sought outside both the Lys/Asn and also the Thr/Asn site.

Ligand docking in H1-receptor models

Complete receptor models were constructed in order to further identify the possible binding modes of the three agonists (**1, 8, 11a**) and also to answer the question whether an ionic H-bond can be established with the third interacting H-bond accepting residue Asp^{116} in TM III. Three different alignments with bacteriorhodpsin were used, yielding three H_1-receptor models in which the oligopeptide-agonist complexes were docked (see Methods). Based on these results the alignment of Trumpp-Kallmeyer et al. (1992) was rejected since the agonists were penetrating the backbone of TM VI and/or pointing to the apparent membrane environment. In the two remaining models the distance between the carboxylate oxygen of Asp^{116} and the position of the basic nitrogen of the agonist appeared to be relatively large: 4-5 Å in Oliveira's model (Fig. 6A,B) and 6-7 Å in Timms' model (not shown), whereas an optimal distance for an ionic hydrogen bond (N^+-O^-) is about 2.9 Å (Ippolito et al., 1990). These results indicate a probable incorrectness of GPCR modeling based on a light-induced non-GPCR (see also Introduction and Chapter 8). The distance between TM III and TM V, and possibly also their relative orientation, deviates from the structural features of bacteriorhodopsin. This is supported by recent findings in the electron microscopy structure of the GPCR bovine rhodopsin in which the relative orientations of the TM domains deviate slightly from those in bacteriorhodopsin (Schertler et al., 1993). Since all three agonists could be accommodated in the two protein models with interactions as found in the oligopeptide model system, the results of the mutation studies with 2-MeHis (Lys^{200} mutation; see above) can only be explained by considering possible deficiencies in the relative orientations of TM domains.

The binding mode of 2-PhHis derived from the oligopeptide model system is also feasible within the two protein models. However, its side chain approaches Asp^{116} from an angle quite different (Fig. 6B) from the one of 2-MeHis or His (Fig. 6A), which influences the orientation and position of the carboxylate. Since the mutation data are not consistent with the binding mode of 2-PhHis as presented in Fig. 6B, we conclude that the presented orientation of the basic nitrogen and Asp^{116} might be unfavourable for agonist action. Therefore, another binding mode was searched for in which binding of Asp^{116} to 2-PhHis occurs in a way similar to the binding of (2-Me)His. Inevitably, this must lead to a binding mode in which the imidazole ring of 2-PhHis occupies a different receptor site than those of His and 2-MeHis. Furthermore, the 2-phenyl ring should preferably be at a receptor site which explains the enhanced affinity of 2-PhHis compared to His in the wild type receptor.

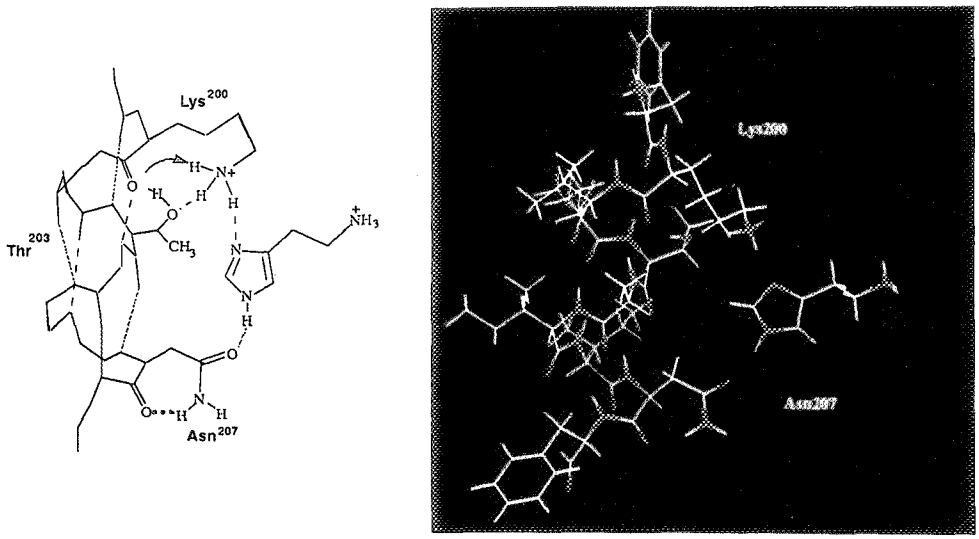

Figure 5. Schematic (left) and computer graphics (right) representation of the interaction of histamine with Lys^{200} and Asn^{207} in TM V. The oligopeptide remains close to its GES; the hydrogen bond between the ε-amino group of Lys^{200} and its backbone carbonyl is broken (arrow) and two hydrogen bonds with the imidazole ring are established (one with Lys^{200} and one with the carbonyl of Asn^{207}).

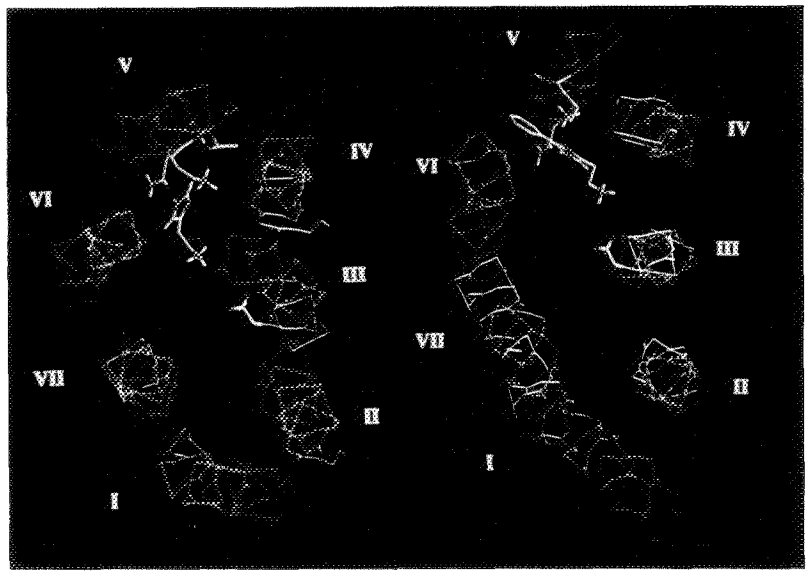

Figure 6. Computer graphics representations of histamine (A: left) and 2-phenyl-histamine (B: right) docked into the histamine H_1-receptor model of Oliveira et al. (1993). The orientations of His and 2-PhHis with respect to TM V are a direct result of the AMBER optimisation. The imidazole ring of 2-PhHis (B: right) lies in parallel with the backbone of TM V and its ethylamine side chain approaches Asp^{116} from a different angle than in the case of His (A:left). This mode of binding for 2-PhHis (B: right) is rejected based on mutation data (see text).

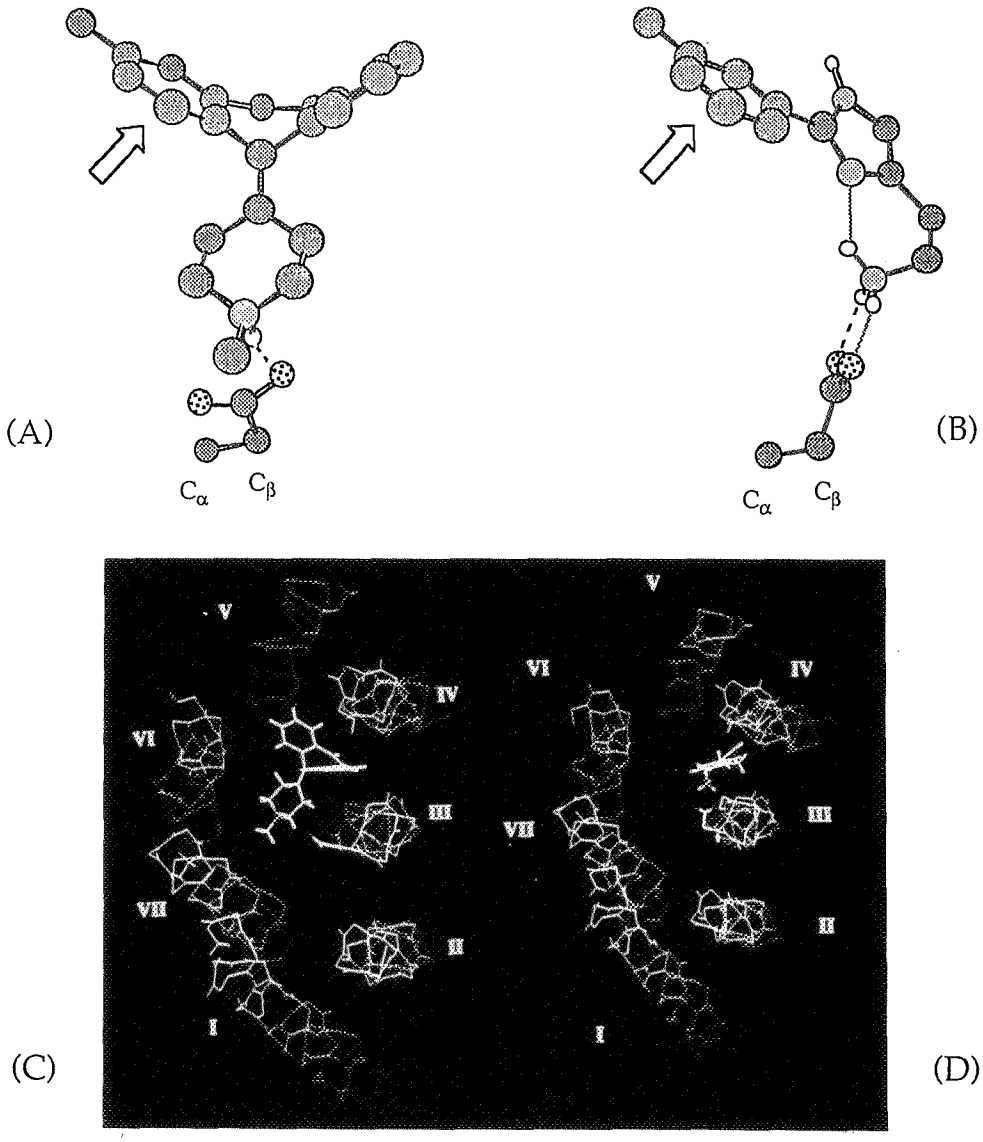

Figure 7. Speculative fit of 2-phenyl-histamine analogue **11c** (B) onto the H_1-antagonist pharmacophore (A) (see Chapter 7). The 2-phenyl ring of **11c** is fitted onto the so-called 'cis'-ring of the antagonist pharmacophore (arrow). For the 'cis'-ring a small lipophilic para-substituent (i.e. CH_3 or Cl) is favourable for affinity; consequently this group is matched with the favourable meta-Br substituent of **11c**. Optimization of **11c** with respect to the aspartate in structure 7A (fixed C_α and C_β atoms) results in the formation of an internal hydrogen bond in **11c** and a conformational change of the aspartate (Fig.7B). Both the antagonist pharmacophore (cyproheptadine, A) and the 2-phenyl-histamine analogue (B) were docked into the H_1-receptor model based upon the alignment of Oliveira et al. (1993) (Fig. 7C and D, respectively).

Considering the above data, we anticipated the possibility that the binding site for 2-PhHis is similar to the binding site of H_1-antagonists. Recently, the H_1-antagonist pharmacophore was derived (Chapter 7) consisting of two aromatic ring systems, the so-called 'cis' and 'trans' ring, and the C_α and C_β atoms of an aspartic acid (Asp^{116}). The ring system is fixed with respect to the aspartate (Fig. 7A). The 'cis' ring preferably should be aromatic while a small lipophilic para-substituent enhances affinity. Remarkably, in case of 2-PhHis a small lipophilic (*meta*-)substituent (**11b-c**) also increases affinity. To investigate whether the H_1-agonist 2-PhHis could possibly occupy the H_1-antagonist binding site, the agonist was matched with the H_1-antagonist cyproheptadine coupled to an aspartate (Fig. 7A). The two aromatic ring systems and lipophilic substituents important for affinity were superimposed. While restraining the 2-phenyl ring at the position of the H_1-antagonist 'cis' ring, the GES of **11c** was optimized with AMBER with respect to the fixed aspartate. Following this procedure, an unexpected result was obtained. It appeared that the 2-PhHis analogue **11c** interacts with Asp^{116} in an acceptable 'folded' conformation in which the ethylamine side chain forms an internal H-bond with the imidazole ring (Fig. 7B). The geometry of **11c** in this conformation is almost identical to that of the GES (also a 'folded' conformation) with an intramolecular energy of 0.82 kcal/mol above the GES. Remarkably, the conformation of Asp^{116} interacting with 2-PhHis (Fig. 7B) is quite different from its conformation when binding with the H_1-antagonist cyproheptadine (Fig. 7A). This suggests that 2-PhHis analogues stabilize a different conformation of Asp^{116} than H_1-antagonists do (see also next section).

In order to further investigate the binding modes of cyproheptadine (representing the antagonist binding mode) and the agonist 2-PhHis within the protein, the H_1-antagonist (Fig. 7A) was docked into Oliveira's protein model in a unique orientation (Fig. 7C; see Methods). Subsequently, 2-PhHis was docked according to the fit onto the H_1-antagonist pharmacophore (Fig. 7D). The aromatic 'cis'-ring is now found in the proximity of Trp^{161} (TM IV) which is conserved within the cationic neurotransmitter GPCR subfamily and which could possibly bind the aromatic ring by means of aromatic-aromatic interactions (Hunter et al., 1991).

Fig. 7C shows that the relatively large bulk volume of the antagonist can only be accomodated within the receptor pocket when Asp^{116} points in the direction of TM VI. In contrast, upon binding of 2-PhHis (Fig. 7D), Asp^{116} attains a different conformation and is oriented in the direction of TM V. This latter finding is in agreement with the earlier proposed binding modes for the agonists His and 2-MeHis in Fig. 6A in which the interactions between the agonists and the three residues Asp^{116}, Lys^{200} and Asn^{207} can only take place when Asp^{116} of TM III attains a conformation in which it points in the direction of TM V (Fig. 6A). Therefore, we conclude that the orientation of the agonist 2-PhHis, as suggested by the fit onto

the antagonist pharmacophore (Fig. 7A-B), is possible in the evaluated 3D-receptor model. In addition, our findings suggest that the conformation of Asp116 is different for binding to agonists or antagonists. This observation may have important implications for the unraveling of activation mechanisms in GPCR models (next section).

The role of Asp116 in the activation mechanism of aminergic GPCRs

Asp116 which is highly conserved in aminergic GPCRs, is generally seen as the main anchoring point for agonist and antagonist binding. Residues in other TM domains (especially TM V) appear to be involved in determining the selectivity of these receptors for their endogenous agonists, e.g. in adrenergic and/or dopaminergic receptors two serines interact with the agonist catechol moiety (Strader et al., 1989), an Asp and Thr residue in the histamine H_2-receptor (Gantz et al., 1992) and a Lys and Asn residue in the H_1-receptor interact with the agonist imidazole ring (this study). The question can be raised, however, whether activation of aminergic receptors is induced by the amine side chain or by the ring system of the agonist. It is remarkable that all aminergic agonists are relatively small molecules with short side chains and that all postulated binding modes for e.g. histamine and catecholamines suggest that they have some kind of bridging function between TM III and TM V. Considering the relatively large gap between TM III and TM V, it seems likely that the above agonist interactions can only be established if Asp116 attains a conformation in which it points in the direction of TM V (as in Fig. 6A). Basic H_1-antagonists such as cyproheptadine are likely to interact with the same aspartic acid in TM III (Ohta et al., 1994), but it appears that they stabilize a different conformation of Asp116 (Fig. 7C).

Since it is not possible to attain a general mechanism for receptor stimulation via the variable part of aminergic ligands (eg. histamine, (nor-)adrenaline, dopamine, serotonin, acetylcholine, muscarine), it makes sense to assign a key-role to the conserved Asp116 in TM III. Our findings suggest that the induction of a conformational change in Asp116 by an agonist could be a general and crucial step in aminergic receptor stimulation. As a prerequisite for an activated receptor state, rearrangement of Asp116 could fit in any of the various concepts of GPCR stimulation that have been proposed in literature: conformational changes in the intracellular loops due to rearrangement of the seven-helix bundle (Hibert et al., 1991), the so-called 'arginine switch' mechanism (Oliveira et al., 1994) or ligand mediated proton transfer mechanisms (Timms et al., 1994; Donné-Op den Kelder, 1994; Nederkoorn et al., 1995). The binding modes of H_1-receptor agonists and antagonists as indicated in our model mean that in attempts to unravel the activation mechanism of GPCRs a crucial role should be considered for Asp116.

Conclusions

In the present study we combined results from site-specific mutagenesis studies on the histamine H_1-receptor with findings from different molecular modeling approaches such as conformation analyses, pharmacophore fitting and receptor docking studies. From our findings the following conclusions emerge:

(1) The conformational analyses on specific residues of TM V of the histamine H_1-receptor demonstrate that residues Lys^{200} and Asn^{207} constitute a selective and energetically favourable binding site for the imidazole ring of histamine. This conclusion finds support from the severe decrease in activity of histamine for the Lys^{200}->Ala and Asn^{207}->Ala H_1-receptor mutants.

(2) In all three investigated H_1-receptor models, TM III and TM V are at least 1 Å too far apart to optimally establish the three proposed H-bond interactions between residues Asp^{116}, Lys^{200}, Asn^{207} and the agonist histamine (or 2-MeHis). This may either be due to the use of bacteriorhodopsin (not a GPCR) as a template molecule or to the chosen alignment which positions TM III in a certain orientation with respect to TM V. With regard to this latter point, TM III and TM V have the best relative orientation in the H_1-receptor model based on the alignment of Oliveira et al. (1993).

(3) The imidazole ring of 2-phenyl-histamine seems to play a minor role in agonist binding. Based on the fit of 2-phenyl-histamine onto an H_1-*antagonist* pharmacophore, the 2-phenyl-ring of 2-PhHis interacts with the same receptor site as the so-called 'cis'-ring of H_1-*antagonists*; an internal hydrogen bond between the amine function and the proximal nitrogen atom is essential for stabilizing this particular binding mode of 2-PhHis.

(4) The different conformations of Asp^{116} in TM III observed in our modeling studies upon H_1-agonist or H_1-antagonist binding indicate that this aspartate may play a key-role in receptor stimulation. To accomodate H_1-antagonists, Asp^{116} attains a conformation in which it points in the direction of TM VI (possibly representing the resting state of the aminergic GPCR). Upon binding of small agonists such as histamine, Asp^{116} changes its conformation and points in the direction of TM V which contains residues responsible for the observed selectivity i.e. Lys^{200} and Asn^{207} (yielding the activated state of the GPCR). In this way, Asp^{116} is assigned a crucial function in triggering GPCR stimulation.

SECTION III

SUMMARY AND CONCLUSIONS

CHAPTER 10

SUMMARY AND CONCLUSIONS

Summary

The studies described in this thesis aim to develop ways for the rational design of new 'non-sedating' H_1-antagonists. Based on suggestions in literature that central histamine H_1-receptors are not identical to peripheral H_1-receptors, it was thought possible to develop non-sedating histamine H_1-antagonists which block selectively peripheral H_1-receptors while leaving central H_1-receptors unaffected. However, early on in our studies, no significant differences were found between the affinity for guinea pig cerebellum (CNS) and lung (peripheral) H_1-receptors for a series of twentytwo structurally diverse histamine H_1-antagonists (*Chapter 3*). These results clearly contradict the any how meager evidence in literature on the existence of central and peripheral subtypes of the H_1-receptor. As a consequence, the search for selective non-sedating antihistamines which reach selectivity by differences in pharmacodynamic rather than pharmacokinetic properties was stopped.

A next option to obtain non-sedating H_1-antagonists is to prevent these compounds from reaching the central nervous system (CNS), the site where blockade of H_1-receptors induces the observed side effects. The extent to which an antihistaminic drug is able to cross the blood-brain barrier (BBB) and penetrate into the CNS is determined by its specific physicochemical properties. Properties such as lipophilicity, degree of ionization and the ability to form hydrogen bonds, were measured for a series of sedating and non-sedating antihistamines (*Chapter 4*). The results suggest that log $D_{oct,pH7.4}$ (the octanol/water distribution coefficient at physiological pH, which automatically includes the degree of ionization of the drug) rather than log P_{oct} (the octanol/water partition coefficient of a neutral drug) should be used to estimate the brain penetration of ionizable drugs. In this thesis, a new approach to predict the brain penetration of antihistamines is presented including Hansch's principle of minimal hydrophobicity; we predict that brain penetration is highest for drugs with a log $D_{oct,pH7.4}$ value around 2, and hindered for drugs with very high (> 3) or very low (< 0) log $D_{oct,pH7.4}$ values. Furthermore, a high capacity of a given drug to form hydrogen bonds (Δlog P > 4) hinders brain penetration as well. Another factor which may affect the ability of a drug to reach the CNS is the level of serum protein binding in the blood. In *Chapter 5*, serum protein

binding of a series of six moderately lipophilic, sedating H_1-antagonists and one highly lipophilic non-sedating H_1-antagonist (loratadine) was investigated. In contrast to suggestions in literature, hydrogen bonding capacity (Δlog P) did not appear to be correlated with serum protein binding. It was shown that classical basic antihistamines have a relatively low level of serum protein binding due to a high degree of ionization. On the other hand, highly lipophilic non-sedating antihistamines bind very strongly to serum proteins. In order to explain the pharmacological action of highly lipophilic non-sedating antihistamines, it is suggested that for these compounds transport across the BBB is *diffusion-rate* limited and restricted by the low free fraction of drug in the blood, whereas transport to peripheral tissues (lacking a real barrier) is *perfusion-rate* limited and not determined by serum protein binding.

The rational design of new H_1-antagonists requires of course detailed knowledge of structural properties important for receptor binding. *Chapter 6* of this thesis provides a review of literature studies on the structure-activity relationships of histamine H_1-antagonists. The general structure of classical histamine H_1-antagonists is described by three pharmacophoric groups, i.e. two aromatic rings and a positively charged basic nitrogen atom. For one aromatic ring (the 'cis'-ring) charge transfer interactons are thought to be important for receptor binding, whereas for the second aromatic ring (the 'trans'-ring), the contribution of hydrophobic interactions is probably more important. The three-dimensional arrangement of the two aromatic rings with respect to the basic nitrogen atom has been investigated in various molecular modeling studies in literature. We matched the energetically acceptable conformations of seven relatively rigid and potent histamine H_1-antagonists onto each other (*Chapter 7*). We found that the basic nitrogen atom of the H_1-antagonists cannot be defined at one particular position with respect to the aromatic rings. Since the positively charged basic nitrogen atom of H_1-antagonists is thought to interact with a negatively charged aspartate residue of the histamine H_1-receptor, we included an aspartic acid into our molecular model, thereby allowing variation in the position of the amino function of the antagonist. With this new approach, a pharmacophoric model for the histamine H_1-antagonist binding site was constructed, which includes all existing rigid antihistaminic compounds with high quality fits, low conformational energies and an optimal ionic hydrogen bond interaction with an aspartate residue of the receptor. This new model has the additional advantage that the presence of the aspartate residue introduces chirality; consequently, it is the first three-dimensional model which is able to predict the stereoselectivity of chiral histamine H_1-antagonists.

Useful information on the structural requirements of potent H_1-antagonists is also retained in the 3-D structure of the histamine H_1-receptor protein. Until today, the construction of an H_1-receptor protein model can, however, only be based on the elucidated 3-D structure of a poorly related bacterial protein, bacteriorhodopsin. In *Chapter 8*, the many problems which

have to be considered when building such a G-protein coupled receptor model are discussed. We found that bacteriorhodopsin can be a misleading template for building G-protein coupled receptor models. Still, upon docking our previously derived antagonist model, we were able to indicate amino acid residues in the H_1-receptor protein which are likely to interact with the 'cis'- and 'trans'-rings of the antagonists (*Chapter 8*). It was also found that the negatively charged carboxylate group of certain zwitterionic H_1-antagonists (i.e., cetirizine, acrivastine) is able to establish favourable charge-charge interactions with the positively charged amino acid Lys^{200} present within the H_1-receptor binding pocket. *Chapter 9* describes further investigations on the receptor binding modes of histamine H_1-agonists. From the molecular modeling and site-directed mutagenesis studies presented, we conclude that the binding of histamine is established via hydrogen bond interactions with amino acid residues Asp^{116}, Lys^{200} and Asn^{207} in the histamine H_1-receptor. Surprisingly, it was found that the receptor binding mode of 2-phenyl-histamine analogues - selective H_1-agonists with a potency ≥ His - is different from that of histamine. Based on a good match of this H_1-agonist with the previously derived H_1-antagonist pharmacophore, it is suggested that the aromatic ring of 2-phenyl-histamine binds to the same receptor site as the 'cis'-ring of histamine H_1-antagonists. Finally, our receptor modeling studies revealed that the conformation of Asp^{116} in transmembrane domain III of the histamine H_1-receptor is different when interacting with agonists or with antagonists. Based upon this observation, it is suggested that an agonist-induced conformational change of Asp^{116} is a crucial step in H_1-receptor stimulation.

Samenvatting

Antihistaminica (histamine H_1-receptor antagonisten) blokkeren de werking van histamine op de histamine H_1-receptoren van de gladde spieren in de bronchi, de vaatwanden, het maagdarmkanaal, de blaas, de baarmoeder en de capillairen (haarvaten). Ook de overdadige en schadelijke werking van histamine, die optreedt bij bepaalde allergische aandoeningen, kan geremd worden door antihistaminica. Deze stoffen zijn daarom zeer bruikbaar als geneesmiddel tegen allergische aandoeningen zoals hooikoorts, asthma, urticaria (netelroos) en conjunctivitis (bindvliesontsteking). De oudere 'klassieke' antihistaminica hebben echter het grote nadeel dat zij zeer vaak bijwerkingen vertonen, met name sedering (slaperigheid, sufheid). Met name deze bijwerkingen zijn tot op heden een belangrijke belemmering gebleken voor de veelvuldige toepassing van 'klassieke' antihistaminica als geschikte anti-allergiemiddelen. De laatste tien jaar worden de 'klassieke' sederende antihistaminica echter geleidelijk van de markt verdrongen door nieuwe 'niet-sederende' antihistaminica (astemizole, terfenadine, loratadine), die in veel mindere mate bijwerkingen vertonen.

De studies, die zijn beschreven in het eerste deel van dit proefschrift (Section I), verschaffen meer inzicht in de moleculaire eigenschappen die van belang zijn voor het verkrijgen van nieuwe niet-sederende histamine H_1-antagonisten. Zo leek het aanvankelijk mogelijk om niet-sederende H_1-antagonisten te ontwerpen, die selectief de perifere histamine H_1-receptoren in het lichaam blokkeren, maar die geen affiniteit hebben voor H_1-receptoren in het centrale zenuwstelsel (CZS) (daar waar de bijwerkingen worden geïnduceerd). Deze benadering kon echter vroegtijdig worden gestopt, aangezien werd vastgesteld dat histamine H_1-receptoren in het centrale zenuwstelsel identiek zijn aan perifere H_1-receptoren (*Hoofdstuk 3*). Het rationeel ontwerp van niet-sederende H_1-antagonisten kan daarom niet worden gebaseerd op het bestaan van histamine H_1-receptor subtypes (verschillen in farmacodynamiek), maar moet vooral worden gezocht in stoffen die het CZS niet of nauwelijks kunnen binnendringen. Een gelukkige bijkomstigheid is dat het transport van een stof vanuit het bloed naar het CZS in veel gevallen wordt bemoeilijkt door de aanwezigheid van de bloed-hersen barrière. De fysisch-chemische stofeigenschappen, die het transport van een antihistaminicum door de bloed-hersen barrière mogelijkerwijze beïnvloeden, zijn onderzocht in *Hoofdstuk 4*. Aan de hand van een serie reeds bestaande sederende en niet-sederende antihistaminica is een nieuw kwalitatief model opgesteld, waarmee de mate van CNS penetratie van een geneesmiddel voorspeld kan worden op basis van gemeten fysisch-chemische eigenschappen van de stof. Ook een hoge mate van binding aan serum eiwitten in het bloed kan

de CNS penetratie van een H_1-antagonist belemmeren. In *Hoofdstuk 5* is de binding van één niet-sederende (loratadine) en zes klassieke sederende H_1-antagonisten aan humane serum eiwitten bestudeerd en beschreven. Tevens wordt in dit hoofdstuk het mogelijke effect van serum eiwit binding op het (gunstige) farmacologische profiel van zeer lipofiele niet-sederende antihistaminica bediscussieerd.

Het tweede deel van dit proefschrift (Section II) betreft onderzoek naar de structuur-eigenschappen van stoffen die de histamine H_1-receptor kunnen stimuleren (H_1-agonisten) of blokkeren (H_1-antagonisten) met behulp van verscheidene CADD (Computer-Aided Drug Design) technieken. *Hoofdstuk 6* geeft een overzicht van bestaande literatuur studies waarin structuur-activiteits relaties en/of de moleculaire modelering van H_1-antagonisten zijn beschreven. In *Hoofdstuk 7* is - op basis van zeven relatief rigide moleculen met hoge H_1-antagonistische activiteit - een drie-dimensionaal model opgesteld voor de histamine H_1-antagonist bindingsplaats. Dit model beschrijft de optimale orientatie van twee aromatische ringen (aanwezig in vrijwel alle klassieke H_1-antagonisten) ten opzichte van een (hypothetisch) aminozuur uit de histamine H_1-receptor (een negatief geladen aspartaat). Aangezien dit nieuwe model chiraal is (niet identiek aan zijn spiegelbeeld) verschaft het de mogelijkheid om kwalitatief de stereoselectiviteit van chirale H_1-antagonisten te voorspellen.

Voor het rationeel ontwerpen van H_1-agonisten en H_1-antagonisten is ook het verkrijgen van informatie uit de drie-dimensionale structuur van de H_1-receptor zeer zinvol. Alhoewel de 3-D structuur van het H_1-receptor eiwit niet bekend is, kan een hypothetisch 3-D model worden gebouwd op basis van de bekende structuur van een ander (bacterieel) membraaneiwit (bacteriorhodopsine). Zowel histamine H_1-antagonisten (*Hoofdstuk 8*) als H_1-agonisten (*Hoofdstuk 9*) kunnen worden ingepast ('gedockt') in een dergelijk H_1-receptor model, waarna vervolgens de belangrijke interacties met de histamine H_1-receptor kunnen worden bestudeerd en beschreven. In combinatie met mutatie studies werden drie aminozuren in de histamine H_1-receptor gevonden (Asp^{116}, Lys^{200} en Asn^{207}) die van belang zijn bij de receptor stimulatie door de endogene H_1-agonist histamine. Daarentegen lijken 2-phenyl-histamine analoga (ook potente H_1-agonisten) op een geheel eigen wijze met de H_1-receptor te interacteren (*Hoofdstuk 9*). Gebaseerd op een verrassende fit van 2-phenyl-histamine op het eerder afgeleide H_1-antagonist model (*Hoofdstuk 7*), werd gevonden dat een conformatie verandering van Asp^{116} in de H_1-receptor een belangrijke rol zou kunnen spelen bij stimulatie van de receptor door agonisten.

REFERENCES

Adamson, D.W., Barett, P.A., Billinghurst, J.W. and Jones, T.S.G. (1957) Aminoalkyl tertiary carbinols and derived products. Part V. Antihistamines. The stereochemistry of cis- and trans-3-phenyl-3-pyridylallylamines *J. Chem. Soc.* **2**, 2315-2326.

Ahn, H.-S. and Barnett, A. (1986) Selective displacement of [^{3}H]mepyramine from peripheral vs. central nervous system receptors by loratadine, a non-selective antihistamine *Eur. J. Pharmacol.* **127**, 153-155.

Arrang, J.M., Garbarg, M. and Schwartz, J.C. (1983) Auto-inhibition of brain histamine release mediated by a novel class (H_3) of histamine receptor, *Nature* **302**, 832-837.

Ash, A.S.F. and Schild, H.O. (1966) Receptors mediating some actions of histamine *Br. J. Pharmacol.* **27**, 427-436.

Augstein, J., Ham, A.L. and Leeming, P.R. (1972) Relationship between antihistamine and antidepressant activity in hexahydroindenopyridines *J. Med. Chem.* **15**, 466-470.

Avdeef, A., Kearney, D.L., Brown, J.A. and Chermotti, A.R. (1982) Bjerrum plots for the determination of systematic concentration errors in titration data *Anal. Chem.* **54**, 2322-2326.

Avdeef, A. (1992) pH-metric log P. Part 1. Difference plots for determining ion-pair octanol / water partition coefficients of multiprotic substances *QSAR* **11**, 510-517.

Baldwin, J.M. (1993) The probable arrangement of the helices in G-protein coupled receptors *EMBO J.* **12**, 1693-1703.

Barbe, J., Andrews, P.R., Lloyd, E.J., Brouant, P., Soyfer, J.C., Galy, J.P. and Galy, A.M. (1983) Individualisation des supports structuraux des actions sédative et anti-H_1 *Eur. J. Med. Chem.* **18**, 531-534.

Barnett, A., Iorio, L.C., Kreutner, W., Tozzi, S., Ahn, H.S. and Bulbenkian, A. (1984) Evaluation of the CNS properties of SCH29851, a potential non-sedating antihistamine *Agents and Actions* **14**, 590-597.

Belpaire, F.M. and Bogaert, M.G. (1989) Binding to albumin and alpha-1 acid glycoprotein as a source of variability in drug disposition, In: Breimer, D.D., Crommelin, D.J.A. and Midha, K.K. (Eds.) *Topics in Pharmaceutical Sciences, Proc. 49th Int. Congr. Pharmaceut. Sci. of F.I.P.*, Fédération Internationale Pharmaceutique, The Hague, pp 563-571.

Birknes, B. (1977) The structure of an antihistamine: cyproheptadine hydrochloride sesquihydrate *Acta Cryst.* **B33**, 687-691.

Black, J.W., Duncan, W.A.M., Durant, G.J., Ganellin, C.R. and Parsons, M.E. (1972) Definition and antagonism of histamine H2-receptors, *Nature* **236**, 385-390.

Blakemore, R.C., Brown, T.H., Cooper, D.G.. Durant G.J., Ganellin, C.R., Ife, R.J., Parsons, M.E. Rasmussen, A.C., and Sach, G.S. (1983) Pyridine-containing isocytosines as combined H_1/H_2 histamine receptor-antagonists (poster), *186th National American Chem. Soc. Meeting*, Washington, USA.

Branch, S.S., Casy, A.F., Hussain, R. and Upton, C. (1987) The structure of phenindamine base and salts in the solute state *J. Pharm. Pharmacol.* **40**, 83-84.

Borchard, U., Hafner, D. and Heise, R. (1985) H_1-antagonistic actions of (+) and (-) dimethindene *Naunyn-Schmiedebergs Arch. Pharm.* **330**, Abstract 42.

Borea, P.A., Bertolasi, V. and Gilli, G. (1986) Crystallographic and conformational studies on histamine H_1-receptor antagonists. IV. On the stereochemical vector of antihistaminic activity *Arzneim. Forsch. / Drug. Res.* **36** (I), 895-899.

Bos, O.J.M., Labro, J.F.A., Fischer, M.J.E., Wilting, J., and Janssen, L.H.M. (1989) The molecular mechanism of the neutral-to-base transition of human serum albumin *J. Biol. Chem.* **264**, 953-959.

Bovet, D. and Staub, A.-M. (1937) *C. R. Seances Soc. Biol. Ses. Fil.* **124**, 547-554.

Bovet, D. (1959) Isosterism and competitive phenomena in drugs *Science* **129**, 1255-1264.

Buckle, D.R., Outred, D.J., Smith, H. and Spicer, B.A. (1984) N-benzylpiperazino derivatives of 3-nitro-4-hydroxycoumarin with H_1-antihistamine and mast cell stabilizing properties *J. Med. Chem.* **27**, 1452-1457.

Buckley, T. and Brain, S.D. (1994) In: Page, C. (Series Ed.) and Brain, S.D. (Ed.) *The Handbook of Immunopharmacology. Immunopharmacology of the microcirculation*, Academic Press, London (UK), pp 63-75.

Buschauer, A. (1987) Synthesis and pharmacological activity of substituted imidazolyl- and thiazolylmethylthioethylguanidines *Arzneim. Forsch.* **37** (9), 1003-1007.

Calcutt, C. R., Ganellin, C.R., Jackson, B., Leigh, B.K., Owen, D.A.A. and Smith, I.R. (1987) Evidence for low brain penetration by the H_1-receptor antagonist temelastine *Eur. J. Pharmacol.* **133**, 65-74.

Casy, A. F. (1978) Chemistry and structure-activity relationships of synthetic anti-histaminics. Chemistry of anti-H_1 histamine antagonists, In: Rocha e Silva, M. (Eds.) *Handbook of experimental pharmacology Vol. XVIII (2)*, Springer Verlag, Berlin, pp 175-214.

Casy, A.F. (1989) Antihistaminic Drugs, In: Smith, F.D. (Ed.) *Handbook of Stereoisomers: Therapeutic Drugs*, CRC Press, Boca Raton, p 149.

ChemX (1993) *Reference Guide July '93*, Chemical Design Ltd, Oxon, England.

Cheng, Y.-C. and Prusoff, W.H. (1973) Relationship between the inhibition constant (K_i) and the concentration of inhibitor which causes 50 per cent inhibition (IC_{50}) of an enzymatic reaction *Biochem. Pharmacol.* **22**, 3099-3108.

Clissold, S.P., Sorkin, E.M. and Goa, K.L. (1989) Loratadine. A preliminary review of its pharmacodynamic properties and therapeutic efficacy *Drugs* **37**, 42-57.

Cooper, D.G., Young, R.C., Durant, G.J. and Ganellin, C.R. (1990) Histamine receptors, In: Hansch, C., Sammes, P.G. and Taylor, J.B. (Eds.) *Comprehensive Medicinal Chemistry (Vol. 3)*, Pergamon Press, Oxford, pp 323-421.

Cooper, D.G., Durant, G.J., Ganellin, C.R., Ife, R.J. Meeson, M.L. and Sach, G.S. (1991) Structure-activity studies of pyridinylalkylisocytosine H_1-receptor antihistamines and identification of an active conformation *Il Farmaco* **46** (**1**), 3-20.

Cronet, P., Sander, C. and Vriend, G. (1993) Modeling of transmembrane seven helix bundels *Protein Engeneering* **6**, 59-64.

Cramer III, R.D., Patterson, D.E. and Bunce, J.D. (1988) Comparative molecular field analysis (CoMFA). 1. Effect of shape on binding of steroids to carrier proteins *J. Am. Chem. Soc.* **110**, 5959-5967.

Dalbey, R.E. (1990) Positively charged residues are important determinants of membrane protein topology *TIBS* **15**, 253-257.

Dale, H.H. and Laidlow, P.P. (1910) The physiological action of β-iminazolylethylamine *J. Physiol.* **41**, 318-344.

Dale, H.H. and Laidlow, P.P. (1911) Further observations on the action of β-iminazolylethylamine *J. Physiol.* **43**, 182-198.

De Backer, M.D., Gommeren, W., Moereels, H., Nobels, G., Gompel, P.V., Leysen, J.E. and Luyten, W.H.M.L. (1993) Genomic cloning, heterologous expression and pharmacological characterization of a human histamine H_1-receptor *Biochem. Biophys. Res. Comm.* **197**, 1601-1608.

De, A.U. and Ghose, A.K. (1978) Exploration of cancer receptor site(s): Part II - Theoretical proof by ISC-PEM-MO for the interstrand guanine binding of DNA by nitrogen and sulfur mustards through their minimum energy conformations-cum-preferred conformations *Indian J. Chem.* **16B**, 1104-1110.

De, A.U., Ghose, A. K., Bhattaacharyya, S. and De, A. (1980) Exploration of histamine receptor geometry: Part I - minimum energy-cum-preferred conformations of histamine *Indian J. Chem.* **19B**, 787-795.

Dearden, J.C. and Patel, K.D. (1978) Use of a physical multi-cell model to confirm theoretical predictions of biphasic structure-activity relationships *J. Pharm. Pharmacol.* **30**, 51p.

Dearden, J.C. and Bresnen, G.M. (1988) The measurements of partition coefficients *QSAR* **7**, 133-150.

Dini, S., Caselli, G.F., Ferrari, M.P., Giani, R. and Clavenna, G. (1991) Heterogeneity of [^{3}H]-mepyramine binding sites in guinea pig cerebellum and lung *Agents and Actions* **33**, 181-184.

Donné-Op den Kelder, G.M., Nederkoorn, P.H.J. and Timmerman, H. (1994) Signal transduction via G-protein coupled receptors: the ternary complex (HR*G) acts as a secondary proton pump and a GTP synthase, In: *Trends in QSAR and Molecular Modeling '94*, J.R. Prous Science Publishers, in press.

Donnelly, D., Findlay, J.B. and Blundell, T.L. (1994) The evolution and structure of aminergic G-protein coupled receptors *Receptors and Channels* **2**, 61-78.

Dröge, J.H.M., Janssen, L.H.M. and Wilting, J. (1982) A comparative study on some physico-chemical properties of human serum albumin samples from different sources *Biochem. Pharmacol.* **31**, 3775-3779.

Dupuis, M., Spangler, D. and Wendoloski, J. (1980) In: *NRCC Software Catalog, Vol 1, Program No. QG01 (GAMESS).*

Durant, G.J., Ganellin, C.R., Griffiths, R., Harvey, C.A., Owen, D.A.A. and Sach, G.S. (1985) Some newer H_1-receptor histamine antagonists *Adv. Biosci.* **51**, 3-11.

Eap, C.B., Cuendet, C. and Baumann, P. (1990) Binding of d-methadone, l-methadone and dl-methadone to proteins in plasma of healthy volunteers: Role of the variants of α_1-acid glycoprotein *Clin. Pharmacol. Ther.* **47**, 338-346.

El Tayar, N., Testa, B. and Carrupt, P.-A. (1992) Polar intermolecular interactions encoded in partition coefficients: an indirect estimation of hydrogen-bond parameters of polyfunctional solutes *J. Phys. Chem.* **96**, 1455-1459.

El Tayar, N., Tsai, R.-S., Vallat, P., Altomare, C. and Testa, B. (1991) Measurement of partition-coefficients by various centrifugal partition chromatographic techniques *J. Chrom.* **556**, 181-194.

Engelman, D.M., Steitz, T.A. and Goldman, A. (1986) Identifying nonpolar transbilayer helices in amino acid sequences of membrane proteins *Ann. Rev. Biophys. Biophys. Chem.* **15**, 321-353.

Findlay, J. and Eliopoulos, E. (1990) Three-dimensional modelling of G protein linked receptors *TiPS* **11**, 492 499.

Fourneau, E. and Bovet, D. (1933) The "sympatholyic" action of a new derivative of dioxane *Arch. Int. Pharmacodyn.* **46**, 178-191.

Free, S.M. and Wilson, J.W. (1964) A mathematical contribution to Structure-Activity studies *J. Med. Chem.* **7**, 395-399.

Fügner, A., Bechtel, W.D., Kuhn, F.J. and Mierau, J. (1988) In vitro and in vivo studies of the non-sedating antihistamine epinastine *Arzneim. Forsch. / Drug Res.* **38**, 1446-1453.

Fujimoto, K., Horio, Y., Sugama, K., Ito, S., Liu, Y.Q. and Fukui, H. (1993) Genomic cloning of the rat histamine H_1-receptor *Biochem. Biophys. Res. Comm.* **190**, 294-301.

Galy, A.-M., Levayer, C., Galy, J.-P. and Barbe, J. (1980) Multiconformational pattern of biological actions of phenothiazinic drugs: S.A.R. of two N-alkylpyrrolidyl derivatives as solutes, In: Usdin, E., Eckert, H. and Forrest, I.S. (Eds.) *Phenothiazines and structurally related drugs: basic and clinical studies*, Elsevier, New York, pp 21-24.

Ganellin, C.R. (1982) Chemistry and structure-activity relationships of drugs acting at histamine receptors, In: Ganellin, C.R. and Parsons, M.E. (Ed.) *Pharmacology of histamine receptors*, Wright - PSG, Bristol, pp 10-102.

Ganellin, C.R., Blakemore, R.C., Brown, T.H., Cooper, D.G., Durant, G.J., Harvey, C.A., Ife, R.J., Owen, D.A.A., Parsons, M.E. Rasmussen, A.C. and Sach, G.S. (1986) Icotidine: An antagonist of histamine at boh H_1 and H_2 receptors *New England Reg. Allergy Proc.* **7**, 126-133.

Gantz, I., Munzert, G., Tashiro, T., Schaffer, M., Wang, L., DelValle, J. and Yamada, T. (1991) Molecular cloning the human histamine H_2-receptor *Proc. Natl. Acad. Sci. USA* **88**, 429-433.

Gantz, I., DelValle, J., Wang, L., Tashiro, T., Munzert, G., Guo, Y., Konda, Y. and Yamada, T. (1992) Molecular basis for the interaction of histamine with the histamine H_2-receptor *J. Biol. Chem.* **267**, 20840-20843.

Garteiz, D.A., Hook, R.H., Walker, B.J. and Okerholm, R.A. (1982) Pharmacokinetics and biotransformation studies of terfenadine in man *Arzneim.Forsch./Drug Res.* **32 (II)**, 1185-1190.

Gavezotti, A. (1983) The calculation of molecular volumes and the use of volume analysis in the investigation of structured media and of solid-state organic reactivity *J. Am. Chem. Soc.* **105**, 5220-5225.

Guest, M.F. and Kendrick, J. (1993) In: *GAMESS User Manual, an Introductory Guide*, Daresbury Laboratories, Daresbury (U.K.).

Glasson, S., Zini, R., D'Athis, P., Tillement, J.-P. and Boissier, J.R. (1980) The distribution of bound propranolol between the different human serum proteins *Mol. Pharmacol.* **17**, 187-191.

Guinot, P. and Frölich, J.C. (1985) Study of the effects of cicletanine on prostanoids *Arzneim.-Forsch.* **35**, 1714-1716.

Haaksma, E.E.J., Leurs, R. and Timmerman, H. (1990) Histamine receptors: subclasses and specific ligands *Pharmac.Ther.* **47**, 73-104.

Hall, H. and Ögren, S.-O. (1984) Effects of antidepressant drugs on histamine-H_1 receptors in the brain *Life Sci.* **34**, 597-605.

Halpern, B.N. (1942) Les antihistaminiques de synthèse, essais de chimiothérapie des états allergiques *Arch. Int. Pharmacodynamie* **68**, 339-345.

Hansch, C., Maloney, P.P., Fujita, T. and Muir, R.M. (1962) Correlation of biological activity of phenoxyacetic acids with Hammett substituent constants and partition coefficients *Nature* **194**, 178 -180.

Hansch, C., Björkroth, J.P. and Leo, A. (1987) Hydrophobicity and central nervous system agents: on the principle of minimal hydrophobicity in drug design *J. Pharm. Sci.* **76**, 663-687.

Hansch, C., Sammes, P.G. and Taylor, J.B. (1990) Cumulative subject index and drug compendium, In: Drayton, C.J. (Ed.) *Comprehensive Medicinal Chemistry*, Pergamon Press, Oxford.

Harms, A.F., Hespe, W., Nauta, W.Th., Rekker, R.F., Timmerman, H. and De Vries, J. (1975) Diphenhydramine derivatives: Through manipulation toward design, In: Ariëns, E.J. (Ed.) *Drug Design, Vol. VI*, Academic Press, New York, pp 2-80.

Helmer, F., Kiehs, K. and Hansch, C. (1968) The linear free-energy relationship between partition coefficients and the binding and conformational perturbation of macromolecules by small organic compounds *Biochemistry* **7**, 2858-2863.

Henderson, R., Baldwin, J., Ceska, T.H., Zemlin, F. , Beckmann, E. and Downing, K. (1990) Model for the structure of bacteriorhodopsin based on high resolution electron cryomicroscopy *J. Mol. Biol.* **213**, 899-929.

Herve, F., Gomas, E. Duche, J.-C. and Tillement, J.-P. (1993) Evidence for differences in the binding of drugs to the two main genetic variants of human α_1-acid glycoprotein *Br. J. Clin. Pharmacol.* **36**, 241-249.

Hibert, M.F., Trumpp-Kallmeyer, S., Bruinvels, A. and Hoflack, J. (1991) Three-dimensional models of neurotransmitter G-binding protein-coupled receptors *Mol. Pharmacol.* **40**, 8-15.

Hunter, C.A., Singh, J. and Thornton, J.M. (1991) π-π Interactions: the geometry and energetics of phenylalanine - phenylalanine interactions in proteins *J. Mol. Biol.* **218**, 837-846.

Iemura, R., Kawashima, T., Fukuda, T., Ito, K. and Tsukamoto, G. (1986) Synthesis of 2-(4-substituted-1-piperazinyl)benzimidazoles as H_1-antihistaminic agents *J. Med. Chem.* **29**, 1178-1183.

Iemura, R. and Ohtaka, H. (1989) Quantitative structure-activity relationships of H_1-antihistaminic benzimidazole derivatives *Chem. Pharm. Bull.* **37**, 967-972.

IJzerman, A.P., Van Galen, P.J.M. and Jacobsen, K.A. (1992) Molecular modeling of adenosine receptors *Drug Design and Discovery* **9**, 49-64.

Ippolito, J.A., Alexander, R.S. and Christianson, D.W. (1990) Hydrogen bond stereochemistry in protein structure and function *J. Mol. Biol.* **215**, 457-471.

Ison, R.R., Franks, F.M. and Soh, K.S. (1973) The binding of conformationally restricted antihistamines to histamine receptors *J. Pharm. Pharmacol.* **25**, 887-894.

Ito, Y. (1988) Principles and instrumentation of countercurrent chromatography, In: Mandava, N.B. and Ito, Y. (Eds.) *Countercurrent chromatography: theory and practice*, Marcel Dekker, New York.

James, M.N.G. and Williams, G.J.B. (1974) The crystal and molecular structure of the antihistaminic drug tripolidine hydrochloride monohydrate *Can. J. Chem.* **52**, 1880-1888.

Janssens, F., Torremans, J., Janssen, M., Stokbroekx, R.A., Luyckx, M. and Janssen, P.A.J. (1985) New antihistaminic N-heterocyclic 4-piperidinamines. 1. Synthesis and antihistaminic activity of N-(4-piperidinyl)-1H-benzimidazol-2-amines *J. Med. Chem.* **28**, 1925-1933.

Janssens, F., Torremans, J., Janssen, M., Stokbroekx, R.A., Luyckx, M. and Janssen, P.A.J. (1985) New antihistaminic N-heterocyclic 4-piperidinamines. 2. Synthesis and antihistaminic activity of 1-[(4-fluorophenyl)methyl]-N-(4-piperidinyl)-1H-benzimidazol-2-amines *J. Med. Chem.* **28**, 1934-1943.

Janssens, F., Torremans, J., Janssen, M., Stokbroekx, R.A., Luyckx, M. and Janssen, P.A.J. (1985) New antihistaminic N-heterocyclic 4-piperidinamines. 3. Synthesis and antihistaminic activity of N-(4-piperidinyl)-3H-imidazo[4,5b]pyridin-2-amines *J. Med. Chem.* **28**, 1943-1947.

Kaliner, M.A. and Check, W.A (1988) Non-sedating antihistamines *Allergy Proc.* **9** (No.6), 649-663.

Kier, L.B. (1968) Molecular orbital calculations of the preferred conformations of histamine and a theory of its dual activity, In: Kier, L.B. (Ed.) *Histamine molecular orbital calculations*, Springer Verlag, Berlin, pp 441-445.

Klotz, I.M. (1990) Ligand-protein binding affinities, In: Creighton, T.E. (Ed.) *Protein function, A practical approach*, IRL Press, Oxord University Press, Oxford, pp. 25-54.

Koper, J.G., Van der Vliet, A., Van der Goot, H. and Timmerman, H. (1990) New selective histamine H_1-agonists *Pharmaceutisch Weekblad Scientific Edition* **12** (6), 236-239.

Kristensen, C.B. and Gram, L.F. (1982) Equilibrium dialysis for determination of protein binding of imipramine - evaluation of a method *Acta. Pharmacol. Toxicol.* **50**, 130-136.

Kutter, E. and Hansch, C. (1969) Steric parameters in drug design. Monoamine oxidase inhibitors and antihistamines *J. Med. Chem.* **12**, 647-652.

Kyte, J. and Doolittle, R.F. (1982) A simple method for displaying the hydropathic character of a protein *J. Mol. Biol.* **157**, 105-132.

Laduron, P.M., Janssen, P.F.M., Gommeren, W. and Leysen, J.E. (1982) In vitro and in vivo binding characteristics of a new long-acting histamine H_1-antagonist, astemizole *Mol. Pharmacol.* **21**, 294-300.

Leeson, L.J. and Brown, M. (1966) Some observations on non-logarithmic titration curves for the determination of dissociation constants and purity *J. Pharm. Sci.* **55**, 431-433.

LeFur, G., Malgouris, C. and Uzan, A. (1981) Effect of mequitazine, a non-sedative antihistamine on brain H_1 receptors *Life Sci.* **29**, 547-552.

Leighton, H.J., Butz, R.F. and Findlay, J.W.A. (1983) A potent antihistamine with low sedation potential *Pharmacologist* **25**, 163-164.

Lemaire, M. and Tillement, J.-P. (1982) The binding characteristics of some adrenergic beta-receptor antagonists to human serum proteins *Biochem. Pharmacol.* **31** (3), 359-365.

Leurs, R., Van der Goot, H. and Timmerman, H. (1991) Histaminergic agonists and antagonists; recent developments, In: Testa, B. (Ed.) *Advances in Drug Research*, Academic Press, London, pp 217-304.

Leurs, R., Smit, M.J., Ter Laak, A.M. and Timmerman, H. (1994) Site-directed mutagenesis of the histamine H_1-receptor reveals a selective interaction of asparagine^{207} with a subclass of H_1-receptor agonists *Biochem. Biophys. Res. Comm.* **201**, 295-301.

Leurs, R., Smit, M.J., Timmerman, H. (1995) Molecular pharmacological aspects of histamine receptors *J. Pharmacol. Ther.* **66**, in press.

Leurs, R., Smit, M.J., Meeder, R., Ter Laak, A.M. and Timmerman, H. (1995) Lysine^{200} located in the fifth transmembrane domain of the histamine H_1-receptor interacts with histamine but not with all H_1-agonists *Biochem. Biophys. Res. Comm.*, in press.

Levin, V.A. (1980) Relationship of octanol/water partition coefficient and molecular weight to rat brain capillary permeability *J. Med. Chem.* **23**, 682-684.

Lewell, X.Q. (1992) A model of the adrenergic beta-2 receptor and binding sites for agonist and antagonist *Drug Design and Discovery* **9**, 29-48.

Lewell, X.Q. (1994) *Symposium on Membrane Protein Models; Experiment, theory and speculation*, Leeds (poster).

Leysen, J.E., Gommeren, W. and Van Gompel, P. (1988) The dissociation rate of unlabeled drugs from receptor sites: a poorly investigated, yet important aspect in receptor research. Studies on the serotonin-S_2 receptor *J. Receptor Res.* **8**, 547-559.

Leysen, J.E., Gommeren, W., Janssen, P.F.M. and Janssen, P.A.J. (1991) Comparative study of central and peripheral histamine-H_1 receptor binding in vitro and ex vivo of non-sedating antihistamines and of noberastine, a new agent *Drug Development Research* **22**, 165-178.

Livingstone, C.D., Strange, P.G. and Naylor, L.H. (1992) Molecular modelling of D_2-like dopamine receptors *Biochem. J.* **287**, 277-282.

McQuade, R.D., Richlan, K., Duffy, R.A., Chipkin, R.E. and Barnett, A. (1990) In vivo binding properties of non-sedating antihistamines to CNS histamine receptors *Drug Develop. Res.* **20**, 301-306.

Monti, J.M., Pellejero, T. and Jantos, M. (1986) Effects of H_1- and H_2-receptor agonists and antagonists on sleep and wakefulness in the rat *J. Neurol. Transm.* **66**, 1-11.

Muramatsu, H., Sawanishi, H., Iwasaki, N., Kakiuchi, M., Ohashi, T., Kato, H. and Ito, Y. (1994) Studies on zwitter-ionization of Drugs. III. Synthesis and pharmacological activities of *N*-alkylcarboxylic acid derivatives of 1,2,3,4,10,14b-hexahydro-dibenzo[*c,f*]-pyrazino[1,2-*a*]azepine and 2,3,4,9-tetrahydro-1*H*-dibenzo[3,4:6,7]-cyclohepta[1,2-*c*]pyridine *Yakugaku Zasshi* **114**, 54-62.

Naruto, S., Motoc, I. and Marshall, G.R. (1985) Computer-assisted analysis of bioactivity. I. Active conformation of histamine H_1-receptor antagonists *Eur. J. Med. Chem.* **20**, 529-532.

Nauta, W.Th., Bultsma, T., Rekker, R.F. and Timmerman, H. (1973) Structure Activity Relationship : A series of compounds related to diphenhydramine, In: Pratesi P. (Ed.) *Special Contributions, Medicinal Chemistry, Milaan 1972*, London Butterworths, Londen, pp 125-137.

Nauta, W.Th. and Rekker, R.F. (1978) Chemistry and structure-activity relationships of synthetic anti-histaminics. Structure-activity relationships of H_1-receptor antagonists, In: Rocha e Silva, M. (Eds.) *Handbook of experimental pharmacology Vol. XVIII (2)*, Springer Verlag, Berlin, pp 215-246.

Nederkoorn, P., Donné-Op den Kelder, G.M. and Timmerman, H. (1995) Does the ternary complex act as a secondary proton pump and a GTP synthase ? *TiPS* **16**, 156-161.

Needleman and Wunsch (1970) A general method applicable to the search for similarities in the amino acid sequence of two proteins *J. Mol. Biol.* **48**, 443-453.

Nicholson, A.N. and Stone, B. (1982) Performance studies with the H_1-histamine receptor antagonists, astemizole and terfenadine *Br. J. Clin. Pharmacol.* **13**, 199-202.

Nicholson, A.N. (1985) Central effects of H_1 and H_2 antihistamines, In: Wauquier, A. (Ed.) *Sleep: Neurotransmitters and Neuromodulators*, Raven Press, New York, pp 211-220.

Nicholson, A.N., Pascoe, P.A., Turner, C., Ganellin, C.R., Greengrass, P.M., Casy, A.F. and Mercer, A.D. (1991) Sedation and histamine H_1-receptor antagonism: studies in man with the enantiomers of chlorpheniramine and dimethindene *Br. J. Pharmacol.* **104**, 270-276.

Ohta, K., Hayashi, H., Mizuguchi, H., Kagamiyama, H., Fujimoto, K. and Fukui, H. (1994) Site-directed mutagenesis of the histamine H_1-receptor: roles of aspartic acid^{107}, asparagine^{198} and threonine^{194} *Biochem. Biophys. Res. Comm.* **203**, 1096-1099.

Oliveira, L., Paiva, A.C.M. and Vriend, G. (1992) A common motif in G-protein coupled transmembrane seven helix receptors *7TM* **1**, 13-26.

Oliveira, L., Paiva, A.C.M. and Vriend, G. (1993) A common motif in G-protein coupled transmembrane seven helix receptors *J. Comp.-Aided Mol. Design* **7**, 649-658.

Oliveira, L., Paiva, A.C.M., Sander, C. and Vriend, G. (1994) A common step for signal transduction in G-protein coupled receptors *Trends Pharmacol. Sci.* **15**, 170-172.

Pardo, L., Ballesteros, J.A., Osman, R. and Weinstein, H. (1992) On the use of transmembrane domain of bacteriorhodopsin as a template for modeling the three-dimensional structure of guanine nucleotide-binding regulatory protein coupled receptors *Proc. Natl. Acad. Sci.* **89**, 4009-4012.

Penniston, J.T., Beckett, L., Bentley, D.L. and Hansch, C. (1969) Passive permeation of organic compounds through biological tissue: a non-steady state theory *Mol. Pharmacol.* **5**, 333-341.

Pèpe, G., Reboul, J.-P. and Oddon, Y. (1989) Relation between psychotic or sedative activity of tricyclic antidepressant drugs and noradrenaline and serotonin receptor characteristics from conformational and molecular electrostatic potential analysis *Eur. J. Med. Chem.* **24**, 1-13.

Plati, J.T. and Wenner, W. (1955) Pyrindene derivatives. II. The chemistry of 2-methyl-9-phenyl-2,3,4,9-tetrahydro-1-pyridindene *J. Org. Chem.* **20**, 1412-1424.

Pong, S.F. and Huang, C.L. (1974) Comparative study on distribution, excretion, and metabolism on hydroxyzine-^{3}H and its methiodide-^{14}C in rats *J. Pharm. Sci.* **63**, 1527-1532.

Quach, T.T., Duchemin, A.M., Rose, C. and Schwartz, J.C. (1979) In vivo occupation of cerebral histamine H_1 receptors evaluated with [^{3}H]mepyramine may predict sedative properties of psychotropic drugs *Eur. J. Pharmacol.* **60**, 391-396.

Rafferty, P. and Holgate, S.T. (1988) Anti-allergic drugs, In: Barnes, P.J., Rodger, I.W. and Thomson, N.C. (Eds.) *Asthma, basic mechanisms and clinical management*, Academic Press, London.

Ramaekers, J.G., Uiterwijk, M.M.C. and O'Hanlon, J.F. (1992) Effects of loratadine and cetirizine on actual driving and psychometric test performance, and EEG during driving *Eur. J. Clin. Pharmacol.* **42**, 363-369.

Rekker, R.F., Timmerman, H., Harms, A.F. and Nauta, W.Th. (1971) The antihistaminic and anticholinergic activities of optically active diphenhydramine derivatives *Arzneim. Forsch./ Drug Res.* **21**, 688-691.

Rekker, R. F. T., H., Harms, A.F. Nauta, W.Th. (1972) Changes in antihistaminic and anticholinergic activities of diphenhydramine derivatives on quaternalization and the role of an asymmetric centre. *Chim. Ther.* **7**, 279-282.

Rekker, R.F., Nauta, W.Th., Bultsma, T. and Waringa, C.G. (1975) Integrated QSAR of H_1-receptor antagonists *Eur. J. Med. Chem.* **10**, 557-562.

Rekker, R.F. (1979) *Symposium on the design of bioactive compounds, Royal Netherlands Chemical Society*, The Hague, The Netherlands.

Rekker, R.F. (1982) The predictive merits of antihistamine-QSAR studies, In: Keverling-Buisman, J.A. (Ed.) *Strategy in drug research*, Elsevier, Amsterdam, pp 315-335.

Riley, J.F. and West, G.B. (1953) The presence of histamine in tissue mast cells *J. Physiol.* **120**, 528-537.

Rose, C., Quach, T.T., Llorens, C. and Schwartz, J.C. (1982) Relationship between occupation of cerebral H_1-receptors and sedative properties of antihistamines *Arzneim. Forsch. / Drug Res.* **32**, 1171-1173.

Roth, T., Rhoers, T., Koshorak, G., Sicklesteel, J. and Zorick, F. (1987) Sedative effects of antihistamines *J. Allergy Clin. Immunol.* **80**, 94-98.

Rowland, M. and Tozer, N.T. (1980) In: Rowland, M. and Tozer, N.T. (Eds.) *Clinical pharmacokinetics: Concepts and applications*, Lea and Febiger, Philadelphia, pp 34-47.

Sadek, M., Craik, D.J., Hall, J.G. and Andrews, P.R. (1990) Conformational analysis of cyproheptadine hydrochloride *J. Med. Chem.* **33**, 1098-1107.

Saxena, A.K., Dhaon, M.K., Ram, S., Saxena, M., Jain, P.C., Patnaik, C.K. and Anand, N. (1984) Synthesis and QSAR in 2-substituted 1,2,3,4,6,7,12,12a-octa-hydropyrazino[2',1':6,1]pyrido[3,4-b]indoles. A new class of H_1-antagonists *Indian J. Chem.* **22B**, 1224-1232.

Saxena, M., Agarwal, S.K., Patnaik, G.K. and Saxena, A.K. (1990) Synthesis, Biological Evaluation and QSAR analysis of {B-[aroylamino]ethyl-piperazines and -piperidines and {B-[[aroylamino]-carbonyl]ethyl-piperazines and -piperidines, pyrazino-pyroindoles and pyrazino-isoquinolines, A new class of potent antihistamines *J. Med. Chem.* **33**, 2970-2976.

Schertler, G.F.X., Villa, C. and Henderson, R. (1993) Projection structure of rhodopsin *Nature* **362**, 770-772.

Schilling, J. C., Adamus, W.S. and Kuthan, H. (1990) Antihistaminic activity and side effect profile of epinastine and terfenadine in healthy volunteers *Internat. J. Clin. Pharmacol., Ther. and Tox.* **28**, 493-497.

Schoeffter, P., Ghysel-Burton, J., Cabanie, M. and Godfraind, T. (1987) Competitive and stereoselective histamine H_1-antagonistic effect of cicletanide in guinea-pig isolated ileum *Eur. J. Pharmacol.* **136**, 235-237.

Seiler, P. (1974) Interconversion of lipophilicity from hydrocarbon-water systems into the octanol-water systems *Eur. J. Med. Chem.* **9**, 473-479.

Sleevi, M.C., Cale, Jr., A.D., Gero, T.W., Jaques, L.W., Welstead, W.J., Johnson, A.F., Kilpatrick, B.F., Demian, I., Nolan, J.C., and Jenkins, H. (1991) Optical isomers of rocastine and close analogs: synthesis and H_1 antihistaminic activity of its enantiomers and their structural relationship to the classical antihistamines *J. Med. Chem.* **34**, 1314-1328.

Sorkin, E.M. and Heel, R.C. (1985) Terfenadine. A review of its pharmacodynamic properties and therapeutic efficacy *Drugs* **29**, 34-56.

Sterk, G.J., Koper, J., Van der Goot, H. and Timmerman, H. (1987) Studies on histaminergic compounds VIII. A new series of compounds showing H_1-antagonistic and H_2-agonistic properties; synthesis, in vitro pharmacology and structure-activity relationships *Eur. J. Med. Chem.* 22, 491-498

Stokbroekx, R.A., Luychx, M.G.M., Willems, J.J.M., Janssen, M., Bracke, J.O.M.M., Joosen, R.L.P. and Van Wauwe, J.P. (1986) Levocabastine (R50547): the prototype of a chemical series of compounds with specific H_1-antihistaminic activity, *Drug Development Research* **8**, 87-93.

Strader, C.D., Candelore, M.R., Hill, W.S., Sigal, I.S. and Dixon, R.A.F. (1989) Identification of two serine-residues involved in agonist activation of the beta-adrenergic receptor *J. Biol. Chem.* **264**, 13572-13578.

Ter Laak, A.M., Van Drooge, M.J., Timmerman, H. and Donné-op den Kelder, G.M. (1992) QSAR and molecular modeling studies on histamine H_1-receptor antagonists *QSAR* **11**, 348-363.

Ter Laak, A.M., Donné-Op den Kelder, G.M., Bast, A. and Timmerman, H. (1993) Is there a difference in the affinity of histamine H_1-receptor antagonists for CNS and peripheral receptors ? *Eur. J. Pharmacol.* **232**, 199-205.

Ter Laak, A.M., Tsai, R.S., Donné-op den Kelder, G.M., Carrupt, P.-A., Testa, B., and Timmerman, H. (1994) Lipophilicity and hydrogen bonding capacity of H_1-antihistaminic agents in relation to their central sedative side effects *Eur. J. Pharmac. Sci.* **2**, 373-384.

Ter Laak, A.M., Venhorst, J., Donné-op den Kelder, G.M. and Timmerman, H. (1995a) The histamine H_1-receptor antagonist binding site. A stereoselective pharmacophoric model based upon (semi-)rigid H_1-antagonists and including a known interaction site on the receptor *J. Med. Chem.* **38**, 3351-3360.

Ter Laak, A.M., Leurs, R., Smit, M.J., Nederkoorn, P.H.J., Timmerman, H. and Donné-op den Kelder, G.M. (1995b) Modeling and mutation studies on the histamine H_1-receptor agonist binding site revealing different binding modes for H_1-agonists; Asp^{116} (TM3) has a constitutive role in receptor stimulation *J. Comp.-Aided Mol. Design* **9**, 319-330.

Ter Laak, A.M., Bijloo, G.J., Fischer, M.J.E., Donné-Op den Kelder, G.M., Wilting, J. and Timmerman, H. (1995c) The role of serum protein binding in the incidence of CNS effects evoked by histamine H_1-antagonists. A comparative study on the serum protein binding of a sedating ([^{3}H]mepyramine) and a non-sedating H_1-antagonist ([^{3}H]loratadine), submitted.

Timmerman, H. (1992) Factors involved in the incidence of central nervous system effects of H_1-blockers, In: Church, M.K. and Rihoux, J.-P. (Eds.) *Therapeutic Index of antihistamines*, Hogrefe and Huber Publishers, Lewiston NY, pp 19-31.

Timmermans, P.B.M.W.M., Brands, A. and Van Zwieten, N.S. (1977) Lipophilicity and brain disposition of clonidine and structurally related imidazolidines *Arch. Pharm.* **300**, 217-226.

Timms, D., Wilkinson, A.J., Kelly, D.R., Broadley, K.J. and Davies, R.H. (1992) Interactions of Tyr^{377} in a ligand-activation model of signal transmission through beta1-adrenoreceptor alpha-helices *Int. J. Quant. Chem: Quant. Biol. Symp.* **19**, 197-215.

Timms, D., Wilkinson, A.J., Kelly, D.R., Broadley, K.J. and Davies, R.H. (1994) Ligand-activated trans-membrane proton transfer in β_1-adrenergic and m_2-muscarinic receptors *Receptors and Channels* **2**, 107-119.

Tozzi, S. (1974) Pharmacology of azatadine, a potential anti-allergy drug *Agents and Actions* **4**, 264-270.

Traiffort, E., Leurs, R., Arrang, J.M., Tardivel-Lacombe, J., Diaz, J., Schwartz, J.-C. and Ruat, M. (1994) Guinea pig histamine H_1-receptor. I. Gene cloning, characterization, and tissue expression revealed by in situ hybridization *J. Neurochem.* **62**, 507-518.

Treherne, J.M., Stern, J.S., Flack, W.J. and Young, J.M. (1991) Inhibition by cations of antagonist binding to histamine H_1-receptors: differential effect of sodium ions on the binding of two radioligands *Br. J. Pharmacol.* **103**, 1745-1751.

Trottier, R.W. and Malone Jr., M.H. (1969) Comparative in vitro evaluation of cryogenine, cyproheptadine, and diphenhydramine as antagonists of furtrethonium, histamine, and serotonin *J. Pharm. Sci.* **58**, 1250-1256.

Trumpp-Kallmeyer, S., Hoflack, J., Bruinvels, A. and Hibert, M. (1992) Modeling of G-protein-coupled receptors: application to dopamine, adrenaline, serotonin, acetylcholine, and mammalian opsin receptors *J. Med. Chem.* **35**, 3448-3462.

Tsai, R.-S., Carrupt, P.-A., El Tayar, N., Giroud, Y., Andrade P., Testa, B., Bree, F. and Tillement, J.P. (1993) Physicochemical and structural properties of non-steroidal anti-inflammatory oxicams *Helv. Chim. Acta* **76**, 842-854.

Urry, D.W., Peng, S.Q., Parker, T.M., Gowda, D.C. and Harris, R.D. (1993) Relative significance of electrostatic- and hydrophobic-induced pK_a shifts in a model protein: the aspartic acid residue *Angew. Chem. Int. Ed. Engl.* **32**, 1440-1442.

Uzan, A., LeFur, G. and Malgouris, C. (1979) Are antihistamines sedative via a blockade of brain H_1 receptors *J. Pharm. Pharmacol.* **31**, 701-702.

Van der Waterbeemd, H., and Kansy, M. (1992) Hydrogen-bonding capacity and brain penetration *Chimia* **46**, 299-303.

Van Drooge, M.J., Donné-op den Kelder, G.M. and Timmerman, H. (1991) The histamine H_1-receptor antagonist binding site. Part I: active conformation of cyproheptadine *J. Comp.-Aided Mol. Design* **5**, 357-370.

Verbeeck, R.K., Cardinal, J.-A., Hill, A.G. and Midha, K.K. (1983) Binding of phenothiazine neuroleptics to plasma proteins *Biochem. Pharmacol.* **32**, 2365-2570.

Verloop, A., Hoogenstraaten, W. and Tipker, J. (1976) Development and application of new steric substituent parameters in drug design, In: Ariëns, E.J. (Ed.) *Drug Design Vol. VII*, Academic Press, New York, pp 165-207.

Walther, G., Daniel, H., Bechtel, W. D. and Brandt, K. (1990) New tetracyclic guanidine derivatives with H_1-antihistaminic properties. Chemistry of Epinastine. *Arzneim. Forsch. / Drug Res.* **40** (I), 440-446.

Waringa, C.G., Rekker, R.F. and Nauta, W.Th. (1975) 1,1-Diaryl-3-aminopropenes and some related compounds *Eur. J. Med. Chem.* **10** (4), 349-352.

Weiner, S.J., Kollman, P.A., Nguyen, D.T. and Case, D.A. (1986) An all atom force field for simulations of proteins and nucleic acids *J. Comp. Chem.* **7**, 230-252.

Weinstein, H. (1993) Computational simulations of molecular structure, dynamics and signal transduction In: Bonati, L., Cosentino, U., Lasagni, M., Maro, G., Pitea, D. and Schiraldi, A. (Eds.) *Biological systems: mechanistic implications for ecological physical chemistry*, Elsevier: Amsterdam, pp 1-16.

Wilting, J., Van der Giesen, W.F., Janssen, L.H.M., Weideman, M.M., Otagiri, M. and Perrin, J. (1980) The effect of albumin conformation on the binding of warfarin to human serum albumin *J. Biol. Chem.* **255**, 3032-3037.

Wilting, J., 't Hart, B. and De Gier, J.J. (1980) The role of albumin conformation in the binding of diazepam to human serum albumin *Biochim. Biophys. Acta* **626**, 291-298.

Witiak, D.T., Muhi-Eldeen, Z., Mahishi, N., Sethi, O.P. and Gerald, M.C. (1971) L(S)- and D(R)-3-amino-1-phenylpyrrolidines. Stereoselective antagonists for histamine and acetylcholine receptors in vitro *J. Med. Chem.* **14**, 24-30.

Yamashita, M., Fukui, H., Sugama, K., Horio, I., Ito, S., Mizuguchi, H. and Wada, H. (1991a) Expression cloning of a cDNA encoding the bovine histamine H_1-receptor *Proc. Natl. Acad. Sci.* **88**, 11515-11519.

Yamashita, M., Ito, S., Sugama, K., Fukui, H., Smith, B., Nakanishi, K. and Wada, H. (1991b) Biochemical characterization of histamine H_1-receptors in bovine adrenal medulla *Biochem. Biophys. Res. Comm.* **177** (3) , 1233-1239.

Yamazaki, M., Fukuoka, H., Nagata, O., Kato, H., Ito, Y., Terasaki, T. and Tsuji, A. (1994) Transport mechanism of an H_1-antagonist at the blood brain barrier: transport mechanism of mepyramine using the carotid injection technique *Biol. Pharm. Bull.* **17**, 676-679.

Yamazaki, M., Terasaki, T., Yoshioka, K., Nagata, O., Kato, H., Ito, Y. and Tsuji, A. (1994) Carrier-mediated transport of an H_1-antagonist at the blood brain barrier: Mepyramine uptake into bovine brain capillary endothelial cells in primary monolayer cultures *Pharmaceutical Res.* **11**, 975-978.

Yamazaki, M., Terasaki, T., Yoshioka, K., Nagata, O., Kato, H., Ito, Y. and Tsuji, A. (1994) Carrier-mediated transport of an H_1-antagonist at the blood brain barrier: A common transport system of H_1-antagonists and lipophilic basic drugs *Pharmaceutical Res.* **11**, 1516-1518.

Young, R.C., Mitchell, R.C., Brown, T.H., Ganellin, C.R., Griffiths, R., Jones, M., Rana, K.K., Saunders, D., Smith, I.R., Sore, N.E. and Wilks, T.J. (1988) Development of a new physiological model for brain penetration and its application to the design of centrally acting H_2-receptor histamine antagonists *J. Med. Chem.* **31**, 656-671.

Young, R.C., Ganellin, C.R., Griffiths, R., Parsons, M.E., Mitchell, R.C., Saunders, D. and Sore, N.E. (1993) An approach to the design of brain-penetrating histaminergic agonists *Eur. J. Med. Chem.* **28**, 201-211.

Zhang, M.Q., Ter Laak, A.M. and Timmerman, H. (1991) Optical isomers of the H_1 antihistamine terfenadine: synthesis and activity *Bioorg. and Med. Chem. Letters* **1** (8), 387-390.

Zhang, M.Q., Ter Laak, A.M. and Timmerman, H. (1993) Structure-activity relationships within a series of analogues of the histamine H_1-antagonist terfenadine *Eur. J. Med. Chem.* **28**, 165-173.

Zhang, M.Q., Walczynski, K., Ter Laak, A.M. and Timmerman, H. (1994) Optically active analogues of ebastine: synthesis and effect of chirality on their antihistaminic and antimuscarinic activity *Chirality* **6**, 631-641.

Zingel, V., Elz, S. and Schunack, W. (1990) Histamine analogues. 33rd communication: 2-phenylhistamines and high H_1-agonistic activity *Eur. J. Med. Chem.* **25**, 673-680.

Zingel, V. and Schunack, W. (1993) Agonisten des Histamin-H_1-Rezeptors. Strucktur und Pharmakologie *Pharmazie* **48**, 483-493.